



HAL
open science

Study of marrow microenvironment and focal adherences in myelodysplastic syndromes and leukemias

Carmen Mariana Robu

► **To cite this version:**

Carmen Mariana Robu. Study of marrow microenvironment and focal adherences in myelodysplastic syndromes and leukemias. Human health and pathology. Université Jean Monnet - Saint-Etienne; Universitatea de medicina si farmacie "Grigore T. Popa" (Iasi, Romania), 2012. English. NNT : 2012STET001T . tel-00955168

HAL Id: tel-00955168

<https://theses.hal.science/tel-00955168>

Submitted on 4 Mar 2014

HAL is a multi-disciplinary open access archive for the deposit and dissemination of scientific research documents, whether they are published or not. The documents may come from teaching and research institutions in France or abroad, or from public or private research centers.

L'archive ouverte pluridisciplinaire **HAL**, est destinée au dépôt et à la diffusion de documents scientifiques de niveau recherche, publiés ou non, émanant des établissements d'enseignement et de recherche français ou étrangers, des laboratoires publics ou privés.

University of Medicine and Pharmacy Gr. T. Popa Iași, Romania

University Jean Monnet Saint-Etienne, France

Faculty of Medicine

A thesis submitted for the degree of Doctor of Philosophy

Discipline: Molecular and Cellular Biology

Carmen-Mariana AANEI

March 12, 2012

<p>STUDY OF MARROW MICROENVIRONMENT AND FOCAL ADHERENCES IN MYELODYSPLASTIC SYNDROMES AND LEUKEMIAS</p>
--

Thesis supervisors:

Professor Dr. Eugen CARASEVICI

Professor Dr. Lydia CAMPOS-GUYOTAT

Members of the Jury:

Prof. Dr. Marc BERGER

Prof. Dr. Victor CRISTEA

Prof. Dr. Denis GUYOTAT

Prof. Dr. Minodora DOBREANU

Professor Dr. Lydia CAMPOS-GUYOTAT

Professor Dr. Eugen CARASEVICI

Rapporteur

Rapporteur

Examiner

Examiner

Thesis Supervisor

Thesis Supervisor

TITRE DE LA THÈSE EN FRANÇAIS

ÉTUDE DU MICROENVIRONNEMENT MÉDULLAIRE ET DES COMPLEXES D'ADHÉRENCE FOCALE DANS LE MYÉLODYSPLASIES ET LÉUCÉMIES

RESUMÉ DE LA THÈSE EN FRANÇAIS

Les syndromes myélodysplasiques (SMD) sont considérés comme des maladies clonales des cellules souches hématopoïétiques (CSH). Le microenvironnement joue un rôle important par ses contacts direct avec les cellules progénitrices hématopoïétiques (CPH).

Notre objectif était d'évaluer les défauts de croissance des cellules stromales mésenchymateuses (CSM) dans les MDS, d'explorer les molécules d'adhérence impliquées, et d'effectuer des corrélations avec leurs dysfonctionnements de croissance et les anomalies des CPH.

Les CSM de MDS sont intrinsèquement pathologiques, montrant une baisse continue de la prolifération pendant 14 jours de culture et une capacité clonogénique réduite. Ces anomalies sont corrélés à une diminution des molécules d'adhérence CD44 et CD49e. Par ailleurs, le potentiel clonogénique des CPH est contrôlé par des mécanismes d'adhérence dépendant du stroma, CD49e pouvant être une des molécules impliquées.

L'analyse en immunofluorescence des protéines d'adhérence focale (FA), paxilline et pFAK [Y³⁹⁷], et des deux protéines régulatrices, HSP90αβ et p130CAS permet l'identification d'anomalies qualitatives et quantitatives. Une expression accrue de paxilline, pFAK et HSP90αβ et leur forte co-localisation nucléaire dans les CSM d'anémie réfractaire avec excès de blastes (AREB) sont corrélées avec un avantage prolifératif et un impact négatif sur la capacité clonogénique de CPH.

Ces résultats ouvrent des possibilités intéressantes : la signalisation via les protéines FA pourrait être impliquée dans les interactions HPC-MSc ; par ailleurs, FAK étant une protéine cliente d'HSP90, les inhibiteurs d'HSP90 sont une potentielle thérapie adjuvante dans les myélodysplasies.

TITRE DE LA THÈSE EN ANGLAIS

STUDY OF MARROW MICROENVIRONMENT AND FOCAL ADHERENCES IN MYELODYSPLASTIC SYNDROMES AND LEUKEMIAS

RESUMÉ DE LA THÈSE EN ANGLAIS

Myelodysplastic syndromes (MDS) are regarded as clonal disorders of haematopoietic stem cells (HSC). Recent evidence demonstrates that stromal microenvironment, in addition to HSC defects, plays a particular role via its direct contact with haematopoietic precursor cells (HPC). This thesis aims at evaluating the putative growth deficiencies of mesenchymal stromal cells (MSC) from MDS individuals compared with normal controls, exploring their adhesion profile, assessing the adhesion process-involved molecular substrates, and establishing correlations with their growth patterns and HPC dysfunctions. Functional assays revealed that MSC from MDS are intrinsically pathological, show a continuous decline of proliferation over a 14-day culture and a reduced clonogenic capacity in the absence of signals from HPC. MSC growth defects significantly correlate with decreased CD44 and CD49e expression. Moreover, stroma-dependent adhesion mechanisms control HPC clonogenic potential and CD49e might be one of the molecules involved in this process. Qualitative and quantitative abnormalities of focal adhesion (FA) proteins paxillin and pFAK [Y³⁹⁷] and of two regulatory proteins, HSP90αβ and p130CAS were identified via immunofluorescence analysis. Paxillin, pFAK [Y³⁹⁷] and HSP90αβ increased expression, besides its stronger nuclear colocalization in MSC from RAEB correlates with a consistent proliferative advantage and has a negative impact on HPC clonogenic capacity. These results open interesting opportunities, e.g. HPC-to-MSc interactions involve FA proteins signalling, and, as FAK is an HSP90αβ-client protein, it may enhance the utility of HSP90αβ inhibitors as adjuvant therapy in MDS.

ACKNOWLEDGEMENTS

Firstly, I would like to express my gratitude to the jury members who made me the honour to judging this work:

*I thank **Prof. Dr. Marc Berger** and **Prof. Dr. Victor Cristea** for their agreement to review my work as rapporteurs and to **Prof. Dr. Denis Guyotat** and **Prof. Dr. Minodora Dobreanu** as examiners.*

*Thereafter I would like to thank my supervisor, **Prof. Dr Lydia Campos Guyotat**, for giving me the opportunity to carry out this project in her lab, for her helpful comments on my thesis, and for her patience.*

*I owe my deepest gratitude to **Prof. Dr. Denis Guyotat** for the interesting conversations, detailed review and for thoughtful comments.*

Thanks to all the people who have made the time I have spent in Saint Etienne fun and memorable.

It has been great! Many thanks for keeping me sane and on the right track!

*Special thanks go out to **Annie** for her assistance with cell cultures and immunofluorescence staining, to **Salima** and **Caroline** for cytometry assistance, to **Department of Genetics, Nathalie, Béatrice, Jacques, and Sylviane** for their assistance in fluorescence microscopy and FISH technique, and to **BioMol Department, Eliane** (for the folk dances), **Elisabeth**, and **Françoise** for their help in extraction and quantification of DNA, RNA.*

*Thanks also to all biologists of Haematology Lab (CHU St Etienne), **Christian Vasselon, Pascale Flandrin-Gresta, Nathalie Nadal, Françoise Solly** for the interesting scientific discussions that we had.*

*Not at least, I would like to thank to **Maryse** for her patience and for the enormous amount of work, which she made with administrative papers and reagents orders.*

*I am also pleased to acknowledge the expertise of **Jean-François Mayol** in the MSC functional assays and of **Claude Lambert** in cell sorting.*

*I would also like to thank to **Professor Eugen Carasevici** and to the other members of **Haematology and Immunology laboratories, “St Spiridon” Hospital, Iasi** because they gave me the opportunity to work and to learn with them. Specially thanks to **Dr. Florin Zugun-Eloae** for his patience, interesting conversations and technical support.*

*I would like to thank to members of the **Service Hématologie Clinique, Institut de Cancérologie de la Loire**, and to **Haematology Department of Saint Spiridon Hospital**, for their constant assistance with cells prelevements and for their permanent enthusiasm for science.*

*I acknowledge the financial support of the “**Ligue Départementale contre le Cancer de la Loire**”, and “**Association Les Amis de Rémi**” (France).*

*Thanks to my **family** for all the support and advice you have given me over the last few years - I could not have done it without you, and I will endeavour to see more of you now!*

*Thanks to **Constantin** for his love, support, patience and understanding, for helping me put things into perspective on occasion, and for being my light at the end of the tunnel.*

*Finally, apologies to the many **friends** whom I have been ignoring, but who have nevertheless been there whenever I needed some moral support.*

Table of Contents

ABSTRACT	<i>i</i>
ACKNOWLEDGEMENTS	<i>ii</i>
GLOSSARY OF ABBREVIATIONS	<i>vii</i>
TABULAR LISTING OF FIGURES AND TABLES	<i>ix</i>
FIGURES	<i>ix</i>
TABLES	<i>x</i>
BIBLIOGRAPHICAL PART	
Chapter I - Preliminary Basis: The Bone Marrow Haematopoietic Niche	1
I-1. Embryogenesis and early stem cell development	1
I-2. Haematopoiesis	3
I-2.1. Overview	3
I-2.2. HSC Plasticity	6
I-2.3. Haematopoiesis regulation networks	7
I-2.4. Epigenetic mechanisms regulating normal haematopoiesis	10
I-2.4.1. DNA methylation	12
I-2.4.2. Histone acetylation and deacetylation	13
I-2.5. Haematopoiesis Functional Assays	14
I-3. Bone marrow microenvironment or stroma	19
I-3.1. Overview	19
I-3.2. Histology of the Bone Marrow	19
I-3.3. Mesenchymal Stromal Cells	28
I-3.3.1. Terminology	28
I-3.3.2. Cytomorphology and cytomorphometry	29
I-3.3.3. Cytochemistry	31
I-3.3.4. Phenotype	32
I-3.3.5. Schematic model depicting mesenchymal stromal cell proliferation and differentiation	34
I-3.3.6. Plasticity of Mesenchymal Stromal Cells	36
I-3.3.7. MSCs create their own niches <i>in vitro</i> cultures	36
I-3.3.8. Isolation and <i>in vitro</i> expansion of Mesenchymal Stromal Cells	38
I-3.3.9. Functional assays for Mesenchymal Stromal Cells	41
I-3.4. Mechanisms of action of stromal cells on haematopoiesis	42
I-4. Conclusion	45
Chapter II- The Myelodysplastic Syndromes	46
II-1. The Myelodysplastic Syndromes: Introduction	46
II-2. Clonal hematopoiesis in Myelodysplastic Syndromes	46
II-3. Aetiology and pathophysiology of Myelodysplastic Syndromes	49
II-3.1 Aetiology of MDS	49
II-3.2 Pathophysiology of MDS	49
II-4. Cytogenetic and Molecular abnormalities	55
II-4.1 Cytogenetic Abnormalities	55
II-4.2 Molecular Abnormalities	56
II-5. Classification	59
II-6. Prognostic	61
Chapter III- Focal adhesion proteins	62
III-1. Introduction	

III-2. The components of focal adhesions	63
III-2.1 Adhesion receptors	63
III-2.2 Focal Adhesion Kinase (FAK) Protein	64
III-2.3 FAK-protein binding partners	65
III-3. FAK functionality in cells	66
III-3.1 Motility	66
III-3.2 Invasion and metastasis	66
III-3.3 Survival	67
III-3.4 Proliferation	67
III-3.5 Angiogenesis	67
III-4. FAK in tumorigenesis	68
III-4.1 FAK levels affect carcinogenesis	68
III-4.2 FAK phosphorylation in cancer	68
III-4.3 Model of the possible contributions of FAK in cancer development	69
III-4.4 FAK expression in haematological malignancies	70
III-5. FAK targeted therapy	71
Chapter IV- Heat shock proteins	72
IV-1. Introduction	72
IV-2. Heat shock protein 90 structure and functional features related to the conformational structure	72
IV-3. HSP90 in tumorigenesis	73
IV-4. HSP90 as a drug target	75
EXPERIMENTAL PART	
I. Overview to Experimental Part	76
II. Materials and Methods	78
II-1. Patients and healthy donors	78
II-2. Cell Cultures	80
II-2.1. Culture-Expanded Mesenchymal Cells	80
II-2.2. Lab-Tek Cultures	81
II-2.3. Human Haematopoietic Colony-Forming Cell Assays	81
II-3. Morphologic and morphometric analysis	81
II-3.1. Stroma Layers Stain	81
II-3.2. Evaluation of stroma layer composition	82
II-3.3. Morphometrical evaluation of stromal cells from primary cultures	82
II-4. Flow cytometry	82
II-4.1. Cell Preparation	82
II-4.2. Antibody staining	82
II-5. Cell Selection	83
I-5.1. EasySep Immunomagnetic Selection Procedure	83
II-6. Immunofluorescence	85
II-6.1. Cytospin Preparation	85
II-6.2. Culture Slides Preparation	85
II-6.3. Antibody Staining of Slides	85
II-6.4. Relative Fluorescence Measurements	86
II-6.5. Protein Clustering Analysis	86
II-6.6. Cell cycle and Apoptosis evaluation using DAPI Nuclear Counterstain	86
II-6.7. Confocal microscopy	87
II-7. Functional Assays	87
II-7.1. Proliferation Tests	87
II-7.2. Clonogenicity Tests	87
II-8. Data standardization and statistical interpretation	87

III. Experimental Results	
III.1. Intrinsic growth deficiencies of mesenchymal stromal cells in myelodysplastic syndromes	89
III.1-1. Relevance of morphological and morphometric evaluation of BM stromal cells from MDS settings vs. normal counterpart	91
III.1-2. BM stromal cells phenotype (MDS vs. Normal controls)	92
III.1-3. Growth particularities of BM MSCs selected from MDS vs. normal	92
III.2. Focal adhesion protein abnormalities in myelodysplastic mesenchymal stromal cells	94
III.2-1. Focal adhesion proteins evaluation in MSCs selected from MDS settings vs. normal bone marrows	96
III.2-2. Role of Paxillin-pFAK [Y³⁹⁷]-HSP90 signalling pathway in MSCs proliferation	97
III.2-3. The impact of increased expression of pFAK [Y³⁹⁷] in MSC on MSC-HPC relationship	98
III.3. Heat-Shock-Protein (HSP)-90 is overexpressed in high-risk myelodysplastic syndromes and associated with higher expression and activation of Focal Adhesion Kinase (FAK)	99
GENERAL DISCUSSION	100
1. Myelodysplasia could be also a disease of stroma?	101
2. The phenotypic characterization of the MSC niche in <i>in vitro</i> primary cultures	102
3. What would be the phenotypic features of MDS cultures?	104
4. MSC growth deficiencies in MDS are directly correlated with diminution of adhesion markers expression	105
5. The diminution of adhesion markers expression on MSC surface interfere with HSC clonogenicity	106
6. Molecular mechanisms whereby the FA proteins can contribute to the increased proliferation of MSCs selected from RAEB settings	106
7. Molecular mechanisms whereby pFAK expression can influence the clonogenicity of haematopoietic precursors (HPC)	108
PERSPECTIVES	111
CONCLUDING REMARKS	113
REFERENCES	114
ANNEXES	
Annex 1 - HSP90 is overexpressed in high-risk myelodysplastic syndromes and associated with higher expression and activation of FAK	145
Annex 2 - Flow cytometry-based quantification of cytokine levels in plasma and cell culture supernatants – study application of the bone marrow (BM) microenvironment in acute myeloid leukemia (AML)	146
Annex 3 - Congenital Acute Leukemia with Initial Indolent Presentation - A Case Report	147

GLOSSARY OF ABBREVIATIONS

Osteoblasts (osteobl)
Osteoclast (osteocl)
Bone-lining cells (blc)
Haematon Units (HU)
Buffy coat (BC)
Endothelial progenitor cells (EPCs)
Haematopoietic stem cells (HSC)
Induced Pluripotent Stem cells (iPS)
Common lymphoid progenitors (CLP)
Common myeloid progenitors (CMP)
Granulocyte / macrophage progenitor (GMP)
Megakaryocyte / erythroid progenitor (MEP)
Mesenchymal stromal cells (MSC)
Long Term Culture-Initiating Cell Assay (LTC-IC cultures)
Cord blood (CB)
Spleen colony forming cell (CFU-S)
Urokinase plasminogen activator receptor (UPAR)
T cell receptor (TCR)
Neural stem cells (NSC)
Basic helix-loop-helix (bHLH) transcription factors family
Stem cell leukaemia (SCL) transcription factor
T cell acute lymphoblastic leukaemia (T-ALL)
Leukaemia inhibitory factor (LIF)
Bone morphogenetic protein (BMP)
Vascular endothelial growth factor (VEGF)
Colony-forming unit-erythroid (CFU-E)
Burst-forming unit-erythroid (BFU-E)
Colony-forming unit-granulocyte, macrophage (CFU-GM)
Colony-forming unit-granulocyte, erythroid, macrophage, megakaryocyte (CFU-GEMM)
Colony-forming unit-megakaryocyte (CFU-Mk)
Spleen colony forming unit (CFU-S)
Adventitial reticular cells (ARCs)
Low-affinity nerve growth factor receptor (LNGFR)
Stromal cell-derived factor-1 (SDF-1)
Chemokine (C-X-C motif) ligand 12 (CXCL12)
Osteoprotegerin (OPG)
Rapidly self-renewing cells (RS-MSCs)
Slowly replicating cells (SR-MSCs)
Periodic acid Schiff (PAS)
Doubling time (DT)
Very small embryonic-like (VSEL) stem cells
Parathyroid-related peptide receptor (PTH1R)
Protein kinase A (PKA)
Angiopoietin 1 (ANG-1)
Vascular cell adhesion molecule 1 (VCAM 1)
Platelet endothelial cell adhesion molecule-1 (PECAM-1/CD31)
Acute myeloid leukaemia (AML)
Myelodysplastic syndromes (MDS)
Refractory anaemia (RA)
Refractory anaemia with ringed sideroblasts (RARS)

Refractory anaemia with excess of blasts (RAEB)
Refractory anaemia with excess of blasts in transformation (RAEB-t)
MDS-related acute myeloid leukaemia (AML)
Atypical chronic myeloid leukaemia (aCML)
Protection of telomeres protein 1 (POT1)
Telomeric repeat binding factor (TRF1)
Interphase fluorescent in situ hybridization (FISH)
Single nucleotide polymorphism array-based karyotyping (SNP-A)
Oligonucleotide array-based comparative genomic hybridization (CGH-A)
Extracellular matrix (ECM)
p130 Crk-associated substrate (CAS)
Histone acetyltransferases (HATs)
Histone deacetyltransferases (HDACs)
DNMT (DNA (cytosine-5-)-methyltransferase))

TABULAR LISTING OF FIGURES AND TABLES

FIGURES

Figure 1. Schematic representation of stem cell hierarchical tree
Figure 2. Schematic diagram of haematopoietic maturation stages
Figure 3. Self-renewal and differentiation in human haematopoiesis
Figure 4. Schematic diagram depicting potential mechanisms involved in adult HSC-NSC plasticity
Figure 5. Transcription factors implicated in haematopoietic lineage development
Figure 6. Extrinsic factors implicated in the fate of HSC and other haematopoietic progenitors
Figure 7. Mechanisms involved in disabling the pluripotency genes
Figure 8. Effects of DNA methylation on gene expression
Figure 9. Human haematopoietic CFC assays in MethoCult® media: Procedure diagram
Figure 10. Representative pictures for human haematopoietic colonies (Giemsa stain)
Figure 11. Representative image for CAFC assays
Figure 12. Histology of the bone marrow
Figure 13. Morphological similarities between BM MSCs with long projections and ARCs
Figure 14. Model of adipocyte differentiation from ARCs
Figure 15. Bone marrow stromal cells
Figure 16. MSCs morphology and morphometry
Figure 17. Schematic model of mesengenic process
Figure 18. Schematic model depicting the changing properties of human MSCs expanded in culture
Figure 19. Multilineage differentiation potential of MSCs
Figure 20. Molecular interactions between HSCs and osteoblasts at the endosteal HSC niche
Figure 21. The hematopoietic stem cell microenvironment
Figure 22. Mechanism leading to clonal expansion in bone marrow failure
Figure 23. The nature of haematopoietic clonality in MDS
Figure 24. Schematic representation of the multiple-step molecular pathogenesis of RARS-T
Figure 25. Cell adhesion model
Figure 26. Schematic diagrams of FAK structure
Figure 27. FAK phosphorylation regulates downstream signalling pathways
Figure 28. Model of the possible contributions of FAK in carcinogenesis
Figure 29. Structure of HSP90 dimer
Figure 30. Model of the possible contributions of HSP90 in carcinogenesis
Figure 31. Experimental strategy of STRO-1 / CD73 Immunomagnetic Selection
Figure 32. Experimental strategy of MSCs selection and functional assays
Figure 33. Representative examples for stromal cells cultures at week 4 in RPMI-1640
Figure 34. Experimental strategy of focal adhesion proteins evaluation on CD73⁺ MSCs Lab-Tek cultures
Figure 35. Correlations between paxillin expression and the proliferation rates of CD73⁺ selected MSCs
Figure 36. pFAK [Y³⁷⁹] expression in MSC vs. the clonogenic potential of HPCs selected from same cases
Figure 37. Model of FAK signalling pathways possibly involved in intrinsic proliferation of MSCs
Figure 38. Model of the possible contributions of FAK expression to the influence of MSCs on the clonogenicity of haematopoietic precursors

TABLES

Table 1 Citations in PubMed as of 17 August 2011
Table 2 Phenotypic characterization and expression of growth factors of human MSCs
Table 3 Inductive factors for <i>in vitro</i> mesenchymal lineage differentiation
Table 4 Myelodysplastic Syndromes pathophysiology
Table 5 Invariant balanced and unbalanced chromosomal abnormalities detected by metaphase karyotyping and FISH
Table 6. Recurrent gene mutations in MDS and MDS/AML settings
Table 7 Peripheral blood and bone marrow findings in MDS (The 2008 revision of WHO classification)
Table 8 IPSS Prognostic Score System
Table 9 Focal adhesion components
Table 10 Clinical and laboratory characteristics of MDS patients and control subjects studied
Table 11 Antibody clones, isotype and source

BIBLIOGRAPHICAL PART

Chapter I – Preliminary Basis: The Bone Marrow Haematopoietic Niche

I-1. Embryogenesis and early stem cell development

Stem cells are undifferentiated cells defined by their ability at the single cell level to both self-renew and differentiate in order to produce mature progeny cells, including both non-renewing progenitors and terminally differentiated effector cells.

Stem cells have been classified by their developmental potential as: **totipotent** (able to give rise to all embryonic and extra-embryonic cell types, such as trophoctodermal cells, which give rise to the subsequent cell lineages that produce the placental tissues and components of the yolk sac), **pluripotent** (able to give rise to all cell types of the embryo proper), **multipotent** (able to give rise to a subset of cell lineages), **oligopotent** (able to give rise to a more restricted subset of cell lineages than multipotent stem cells), and **unipotent** (able to contribute only one mature cell type) (Figure 1). **Pluripotent** embryonic stem (ES) cells were first isolated by *in vitro* cell culture derived from the inner cell mass (ICM) of blastocysts [1]. *In vivo*, the ES cells create the three embryonic germ layers: ectoderm (believed to give rise to skin and neural lineages), mesoderm (believed to generate blood, bone, muscle, cartilage, and fat), and endoderm (believed to contribute at tissues of the respiratory and digestive tracts) [1].

Recently, a new category of cells, *in-vitro*-reprogrammed induced pluripotent stem cells (iPS) were generated from human somatic cells using the four transcription factors (Oct4, also called Oct3/4 or Pou5f1, SOX2, NANOG, and LIN28), which can reprogramme a somatic genome back into an embryonic epigenetic state [2], [3], [4]. These induced pluripotent human stem cells have normal karyotypes, express telomerase activity, cell surface markers and genes that characterize human ES cells, and maintain the developmental potential to differentiate into all three primary germ lines [2]. Noteworthy is that the iPS production can be suppressed by the p53-p21 pathway [3].

The common marker of multiple stem cell populations is the high level activity of ATP binding cassette (ABC) transporter proteins, and although the biological significance of this property is unclear, it has been useful in the enrichment of stem cells from multiple tissues by virtue of their enhanced efflux of the fluorescent dye Hoechst 33342 (the so-called “side population”, SP cells) [1]. In addition, other metabolic markers / dyes such as rhodamine123 (which stains mitochondria), Pyronin-Y (which stains RNA), and BAAA

(indicative of aldehyde dehydrogenase enzyme activity) are imprints of the functional stem cell activity [5].

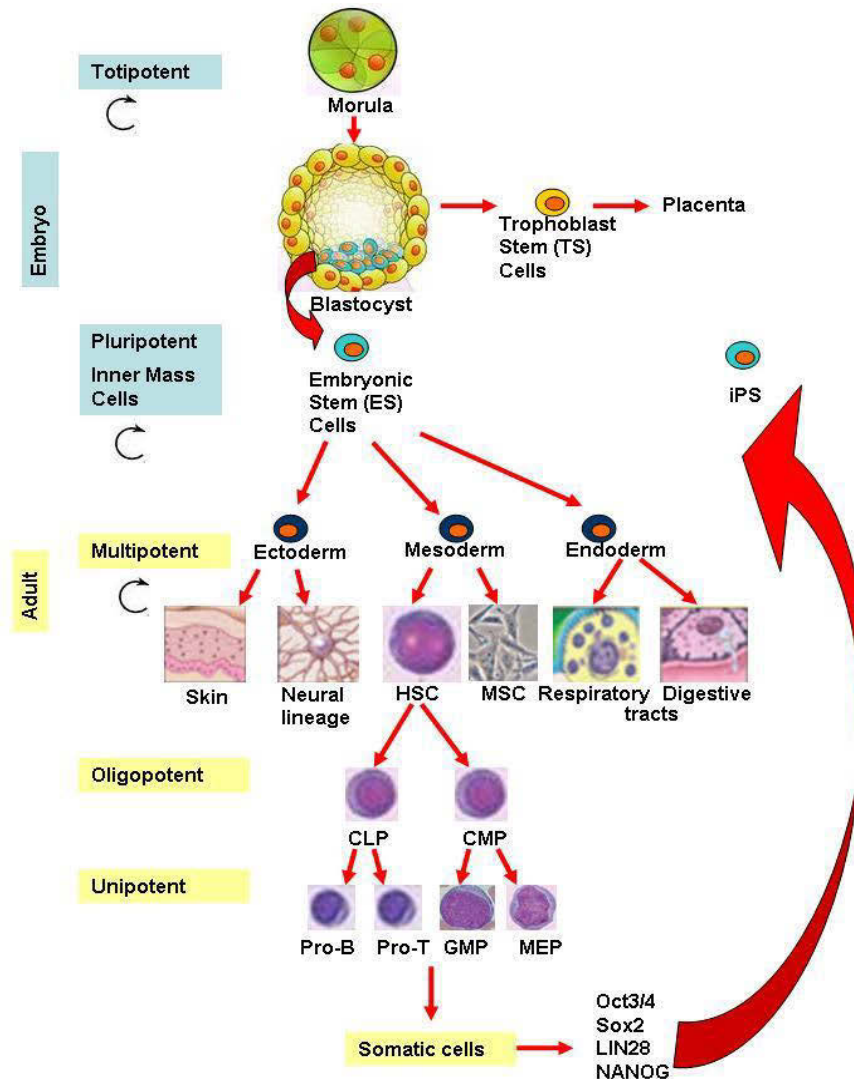


Figure 1. Schematic representation of stem cell hierarchical tree

iPS: induced Pluripotent Stem cells; *HSC*: haematopoietic stem cells; *CLP*: common lymphoid progenitors; *CMP*: common myeloid progenitors; *GMP*: granulocyte / macrophage progenitor; *MEP*: megakaryocyte / erythroid progenitor; *MSC*: mesenchymal stromal cells. Adapted from: Wagers A. J. & Weissman I. L., *Cell* 2004, and Junying et al, *Science* 2007

I-2. Haematopoiesis

I-2.1. Overview

Haematopoiesis is a multiple-step process, in which a relatively small population of haematopoietic stem cells (HSC) give rise, after a sequentially maturation stage, to all types of blood cells (Figure 2) [6].

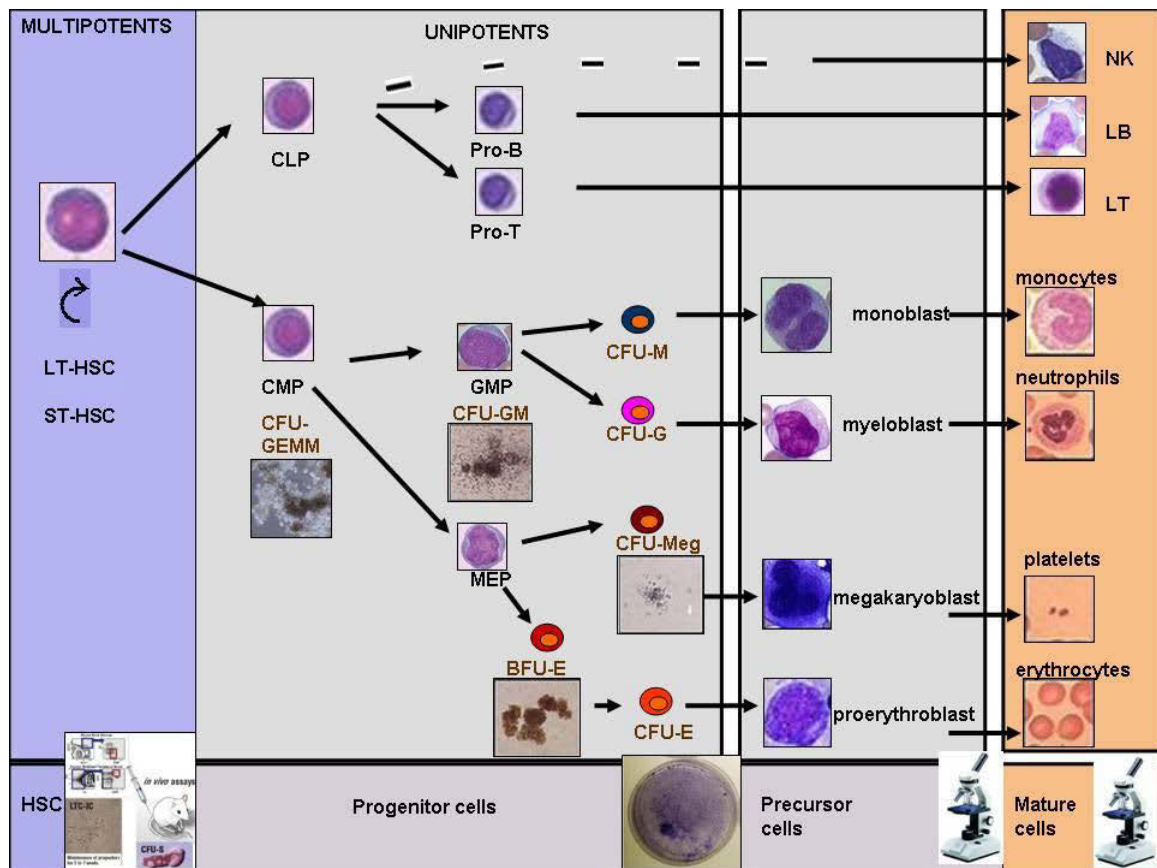


Figure 2. Schematic diagram of haematopoietic maturation stages

The different cells identified have been clustered into three families according to the type of assay which served for their identification: in vivo transplantation assay or cytometry selection and Long Term Culture-Initiating Cell Assay (LTC-IC cultures) (the left panel), in vitro colony assays in methylcellulose culture system (middle panel), and morphological classification (right panel). Adapted from: Domen J., Wagers A. & Weissman I. L., Stem Cell Information 2011

The HSC is currently best characterized as a **multipotent** stem cell population [1]. The HSC pool represents only 0.05% of the whole bone marrow [7] and is able to maintain haematopoiesis over a lifetime based on its two fundamental features, slow division and high self-renewal rate [6]. A possible explanation for these slow division kinetics might be to reduce the risk of mutagenesis and defects during cell division [8], and it is also a prerequisite

for maintaining haematopoiesis during a life-time, otherwise the stem cell pool might be rapidly depleted [6].

The phenotype recognized for the HSC highly enriched mouse population, which includes all multipotent progenitors, is Thy-1.1^{low}Sca-1^{hi}Lineage (Lin)^{-/low} [7].

In humans, a small subset of HSC is capable of long-term repopulation upon transplantation (LT-HSC). These cells can be enriched by their immunophenotype as CD34⁺CD38⁻Thy-1⁻Rh123^{low} [9], they are usually dividing very slowly, provide a multilineage haematopoietic engraftment ability [10], and the next compartment comprises short-term repopulating stem cells (ST-HSC) that sustain haematopoiesis only for a limited several-week span (i.e., 4-10 weeks) after transplantation and these may correspond to a CD34⁺CD38⁻ phenotype [6], [7]. The progenitor cells (such as CMP) are included in the CD34⁺CD38⁺ cell fraction. In the later stages, CD34 expression is absent and lineage specific markers are expressed [6].

Recent evidence also indicates the existence of a CD34⁻ HSC, which seems likely to be quiescent, capable to convert into CD34⁺ phenotype upon activation with 5-fluorouracil (5-FU) or after culture and, after transplantation, could revert into CD34⁻ phenotype again [9]. Recent experiments using CD34⁻ cord blood cells that are in the G₀ state show that these cells have more than 1000-fold potential to form GM-CFC, a 250-fold higher BFU-E forming capacity, and 600-fold higher expansion potential compared to G₁ cells [9], [11]. Moreover, these most primitive HSC show marrow repopulating ability, resistance of 5-FU, and low retention of rhodamine-123 (Rh123) [9], [12].

The dual function of self-renewal and differentiation is regulated by asymmetric cell divisions, where one daughter cell retains the stem cell function, whereas the other differentiating cells become a faster proliferating precursor cell [6], [13]. Alternatively, cells can undergo symmetric divisions to produce either two identical, self-renewing cells, or two differentiated daughter cells [6], [13]. The pool of HSC and progenitor cells is regulated by a feedback mechanism that is related to the number of mature cells in the blood (Figure 3) [6].

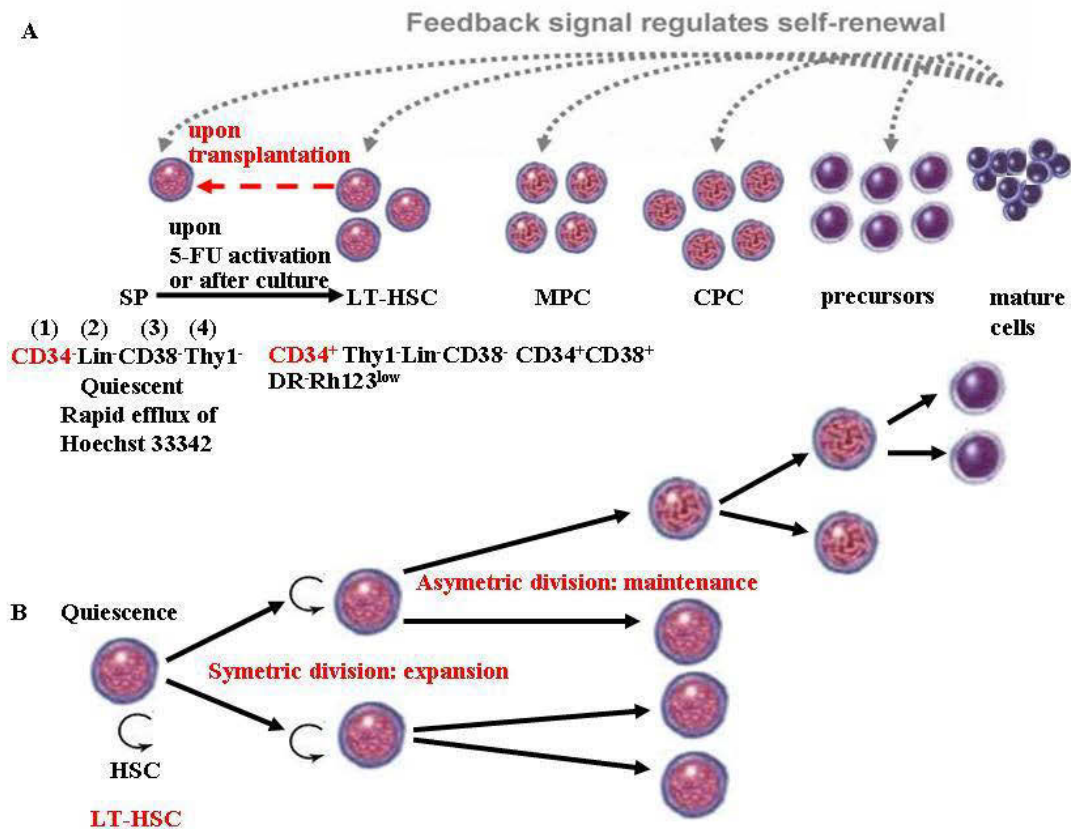


Figure 3. Self-renewal and differentiation in human haematopoiesis

Haematopoietic differentiation is a multiple-step process. A small group of long term repopulating haematopoietic stem cells (LT-HSC) replicates very slowly. The downstream compartments are increasingly committed to a specific lineage and have a fate-rate replicating capacity. Some of the progeny have to self-renew to keep the pool of haematopoietic stem and progenitor cells. The percentages of self-renewal versus differentiation are regulated by a feedback mechanism that is related to the number of mature cells in the blood (A). The stem cells can divide by either asymmetric or symmetric modes of division, and the balance between these two modes is controlled to produce appropriate numbers of stem cells and differentiated daughters (B). SP: side-population, 5-FU: 5-fluorouracil, DR: class II human leukocyte antigens molecules, Rh123: rhodamine-123 MPC: multipotent progenitor cells, CPC: committed progenitor cells. Adapted from: Marciniack-Czorchra A., Stiehl T., Wagner W., Aging 2009

⁽¹⁾ CD34 is a cell surface glycoprotein and functions as a cell-cell adhesion factor. It may also mediate the attachment of stem cells to bone marrow extracellular matrix or directly to stromal cells. In experiments on mice, CD34 has proved useful to distinguish between HSCs with long-term marrow repopulating ability (CD34^{low/-} c-kit⁺ Sca-1⁺ Lin⁻), named also (CD34^{low}-KSL), and the progenitors with short-term reconstitution capacity (CD34⁺ c-kit⁺ Sca-1⁺ Lin⁻) or (CD34⁺-KSL). The CD34^{low}-KSL cells express only the following genes GATA-2, IL-1R alpha, IL-2R gamma, AIC-2B (colony stimulating factor 2-receptor, beta, low-affinity [granulocyte-macrophage]), c-kit, EPO-R, and c-mpl. In contrast, the CD34⁺-KSL express all the cytokine receptor genes, which have specificity for haematopoietic lineage, except IL-2R beta, IL-7R alpha, and IL-9R alpha. Clonal culture analysis showed that CD34^{low}-KSL cells were more potent in proliferation and multilineage differentiation capacities than CD34⁺-KSL cells. Moreover, the clone-sorted CD34^{low}-KSL and CD34⁺-KSL, cultured in the presence of SCF, IL-3, and EPO showed that CD34^{low}-KSL cells required much more time to undergo the first cell division than CD34⁺-KSL. Taken together, these data support the claim that CD34^{low}-KSL cells are at a higher rank in

haematopoietic hierarchy than CD34⁺KSL cells [14]. In humans, CD34 marker could differentiate two populations of HSC: the CD34⁻ are quiescent cells, which possess colony-forming potential in short-term assays, maintain long-term colony forming potential in *in vitro* cultures and allow the differentiation of blood cell lineages; and the CD34⁺ HSC which preserve all these features, but provide the major contribution to haematopoietic engraftment in NOD / SCID mice [9], [10].

(2) Lin^{-/low} signify that HSCs are negative for the markers that are used for detection of lineage commitment [7].

(3) CD38 is a nonlineage-restricted type II transmembrane glycoprotein, which serves as an ectoenzyme catalyzing the synthesis and hydrolysis of cyclic ADP-ribose. The enzymatic functions of CD38 contribute to an array of its immunoregulatory functions. Ligation of CD38 with agonistic antibodies induce diverse effects in haematopoietic cells ranging from growth stimulation to induction and prevention from apoptosis, induction of cytokines production, activation of kinases, and phosphorylation of certain proteins. The CD38 antigen was found to have a rather unique distribution pattern, being predominantly expressed by progenitors, and early haematopoietic cells, then lost during maturation, and re-expressed during cell activation. The expression of membrane CD38 is modulated by certain physiological and pharmacological agents such as cytokines, and lectins [15].

(4) Thy-1 (CD90) expression is restricted to, on average, 1-4% of human foetal liver, cord blood (CB), and bone marrow, and binding to these cells types is essentially restricted to a very small subset of lymphoid cells and approximately 25% of CD34⁺ cells. The function of Thy-1 on HSCs is unknown, but it has been postulated to be involved in cellular recognition, adherence, and cell activation due to its involvement in the release of intracellular Ca²⁺ and phosphorylation of cytoplasmic proteins. Thy-1 may be important in stromal adherence, possibly providing a growth inhibitory signal. The lower expression of Thy-1 on circulating CD34⁺ cells from umbilical CB may result from a reduced requirement for adherence [16].

I-2.2. HSC Plasticity

Recent evidence has largely hailed the possibility to “transdifferentiate” the plastic bone marrow or circulating stem cells to non-haematopoietic tissue [17]. Transdifferentiation describes the conversion of a cell of one tissue lineage into a cell of an entirely distinct lineage, with concomitant loss of the tissue-specific markers and function of the original cell type, and acquisition of markers and functions of the transdifferentiated cell type [1]. The lineage conversion can occur directly, by activating an otherwise dormant differentiation programme to alter the lineage specificity of the cell (Figure 4A) or could occur via de-differentiation of a tissue-specific cell to a more primitive, multipotent cell and subsequent re-differentiation along a new lineage pathway (Figure 4B) [1].

The lineage conversion between HSC and neural stem cells (NSC) has been accepted so far. Thus, Sigurjonsson *et al.* proved that CD34⁺ HSC from adult human donors could produce neurons efficiently if they are introduced into the lesions of spinal cord of the developing chicken embryo [18]. Moreover, Bjornson *et al.* showed that genetically labelled NSC, after transplantation into irradiated hosts, could produce a variety of blood cell types, including myeloid and lymphoid cells as well as early haematopoietic cells [19].

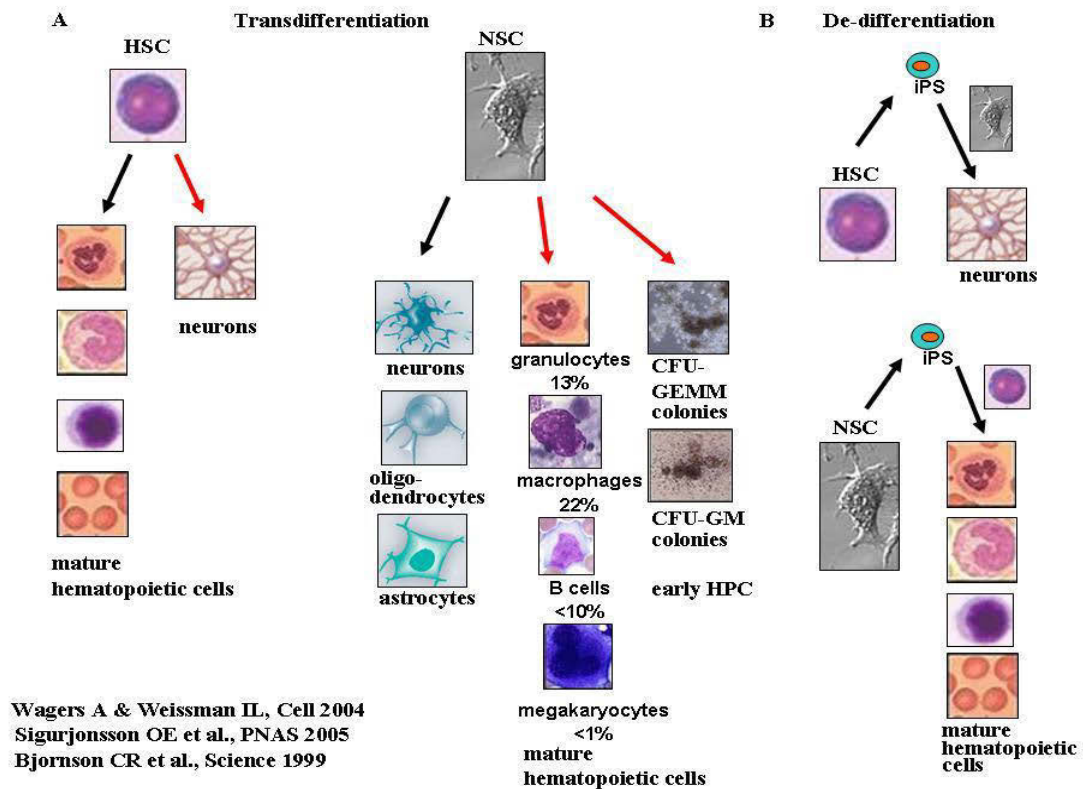


Figure 4. Schematic diagram depicting potential mechanisms involved in adult HSC-NSC plasticity. Adapted from: Wagers A. J. & Weissman I. L., Cell 2004

I-2.3. Haematopoiesis regulation networks

The production of differentiated haematopoietic cells is tightly regulated by intrinsic (Figure 5) and extrinsic factors (Figure 6) [20].

Intrinsic regulators

The multipotent haematopoietic cells, prior to differentiation, express genes associated with the erythroid lineage (β globin), and with the myeloid lineage (myeloperoxidase) at low levels, the myeloid transcription factors (PU.1 and C/EBP α), lymphoid (GATA-3), and myeloid receptors such as c-fms, the G-CSF receptor and the alpha chain of the GM-CSF receptor. These observations are consistent with the concept of multilineage priming in stem cells. In this context, lineage commitment requires not only that the appropriate gene expression programme is enhanced, but also that alternate lineages are repressed [20]. Imbalances of this equilibrium induce the disease. For example, the ectopic activation of PU.1 expression in the erythroid lineage inhibits erythroid differentiation and causes

erythroleukaemia. The misexpression of the stem cell leukaemia (SCL) transcription factor in T lineage cells conduces to thymocyte differentiation arrest and T-cell leukaemia. The absence of E2A and Pax5 transcription factors disturb the development of committed pro-B cells [20].

To summarise, HSCs express lineage affiliated genes, which are enhanced or repressed upon the degree of maturation [21]. The haematopoietic transcription factors drive cell fate acting cooperatively, as the SCL transcription complex, antagonistic, i.e. the GATA-1 / PU.1, GATA-1 / FOG, or SCL-E2A in the lymphoid lineages, as well as the auto-regulatory pathways [20]. The transcriptional regulation is sensitive to intrinsic perturbations. For example, the E2A transcription factor is essential to B lineage development (commitment and proper B-cell differentiation), and the E2A locus is often concerned by chromosomal translocations in B-cell leukaemias [22]. In the thymus, E2A collaborates with HEB, another basic helix-loop-helix (bHLH) transcription factor, to drive thymocyte differentiation. The oncogenes that are involved in T cell acute lymphoblastic leukaemia (T-ALL) have been shown to directly associate with E2A and HEB in thymocytes, and to inhibit their transcriptional proprieties [23]. Moreover, there are evidences that the B- versus T-cell fate is dependent on the level of E2A activity, B-cell commitment being more sensitive to E2A dosage than T-cell lineage commitment [20].

Other examples include inactivating mutations of GATA-1 in megakaryoblastic leukaemia [24] and of PU.1 in acute myeloid leukaemia (LAM) [25]. In addition, the early lineage commitment is sensitive to PU.1 dosage governing B cell as well as macrophage developments. Thus, low levels of PU.1 are compatible with B-cell fate, while high PU.1 levels is specific to macrophage switch [26]. Moreover, high levels of PU.1 favour the macrophage fate over the granulocyte fate [27].

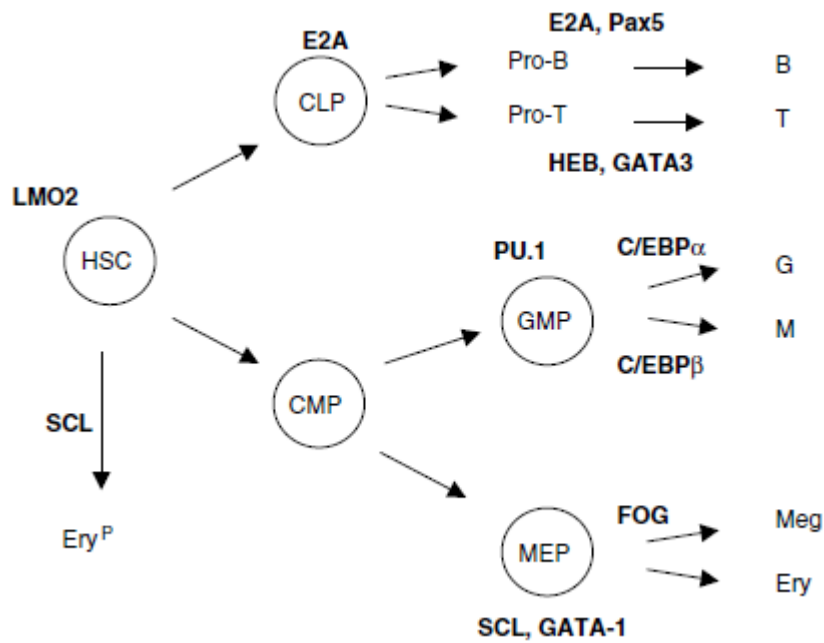


Figure 5. Transcription factors implicated in haematopoietic lineage development

LMO2: LIM-only protein, **E2A:** Ebox binding protein, **SCL:** stem cell leukaemia, **HEB:** HeLa Ebox Binding protein, **EBF:** early B cell factor, **GATA-1/2/3:** GATA binding protein, **C/EBP α and β :** CAAT/enhancer binding protein, **Pax5:** paired domain protein, **FOG:** Friend of GATA, **From: Hoang T., Oncogene 2004**

Extrinsic regulators

Environmental signalling could occur through direct HSC-MSC interaction, or through the action of soluble mediators (Figure 6). In the absence of these signals, haematopoietic cells undergo a default pathway of apoptosis [20]. Thus, there are soluble factors that could contribute to the decision between self-renewal and differentiation. For example, leukaemia inhibitory factor (LIF) through LIF-STAT3 contributes together with bone morphogenetic protein (BMP)-Smad pathway to the decision of maintaining the totipotency of ES *in vitro*, or, to adopting a neural fate [28]. Other cytokines have a regulator role of haematopoietic cell differentiation through the alteration of transcription factor dosage, thereby shifting the transcription network towards a particular pathway [20]. For example, the dosage of GM-CSF influences the choice between a macrophage and a granulocyte fate, by regulation of PU.1 expression in multipotent CMP, and in committed myeloid progenitors (GMP) [20]. Similarly, the G-CSF receptor induces granulocyte differentiation through upregulation of transcription factor C/EBP α [29] and by altering the ratio of C/EBP α versus PU.1 in favour of the granulocyte lineage [27]. Furthermore, the vascular endothelial growth factor (VEGF) has proved to have an anti-apoptotic role during the development of the

primitive erythroid lineage, and this effect is mediated the SCL transcription factor [30]. Similarly, c-kit through Jak-STAT signalling pathway suppress apoptosis in haematopoietic cells [31]. Moreover, c-kit prevents progression in the B lineage at the level of transition from pro-B to pre-B by down-regulation of E12 transcription factor, a product of the E2A locus [32]. In conclusion, the combinatorial interaction between cell-extrinsic cues and cell-intrinsic processes consolidates the lineage choice and drive cells to differentiation and maturation pathways.

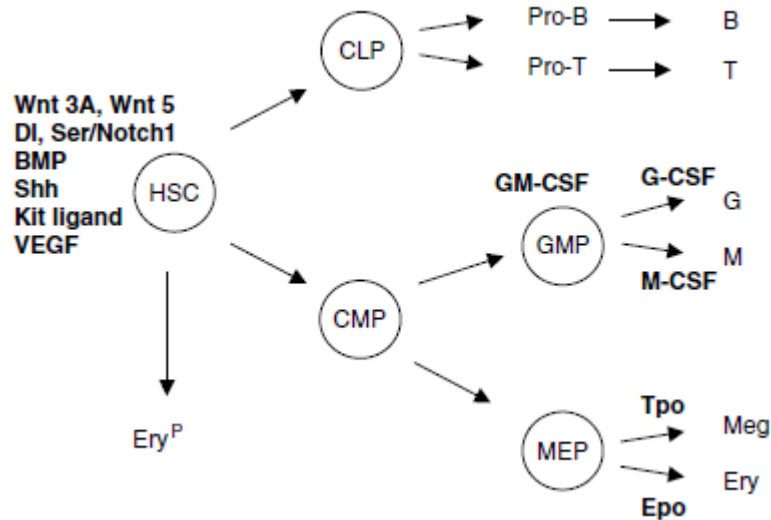


Figure 6. Extrinsic factors implicated in the fate of HSC and other haematopoietic progenitors

Wnt: Wnt signalling protein, *DL, Ser*: Delta, serrate (Notch ligands), *BMP*: bone morphogenic protein, *Shh*: Sonic Hedgehog, *VEGF*: Vascular endothelial growth factor, *SF*: Steel factor, *KL*: Kit ligand, *SCF*: Stem cell factor, *LIF*: Leukaemia inhibitory factor, *GM-CSF*: Granulocyte/macrophage colony stimulating factor, *G-CSF*: Granulocyte colony stimulating factor, *M-CSF*: Macrophage colony stimulating factor, *Tpo*: Thrombopoietin, *Epo*: Erythropoietin. **From: Hoang T., Oncogene 2004**

I-2.4. Epigenetic mechanisms regulating normal haematopoiesis

The molecular processes governing hematopoiesis involve the interplay between lineage-specific transcription factors, listed above, and a series of epigenetic tags, including DNA methylation and covalent histone tail modifications [33]. The DNA in eukaryotic chromatin is packed by histones into arrays of repeating units called nucleosomes. Each nucleosome contains a nucleosome core, where the DNA is wrapped around a histone octamer, consists of (H3)₂-(H4)₂ tetramer and two dimers H2A-H2B, and a stretch of relatively unconstrained DNA called the linker DNA. The nucleosome cores occlude the DNA from many DNA-

binding factors, playing a significant role in chromatin packing and gene regulation. In addition, the post-translational modifications of chromatin (such as acetylation, phosphorylation, methylation, ubiquitination, polyADP-ribosylation), commonly known as “histone code”, are capable of affecting its structure and gene transcription, and are catalysed by opposing families of enzymes, allowing the developmental potential of HSCs to be dynamically regulated. Thus, during development, in normal conditions, cells undergo a process whereby they lose pluripotency and become committed to a more-restricted cell type. This pathway involves three steps of chromatin remodelling: first, transcriptional repressors are recruited to OCT4; second, heterochromatin is generated by the methylation of H3K9 and the subsequent binding of heterochromatin protein 1 (HP1) to this histone modification; and third, the underlying DNA is methylated [34] (Figure 7). Although the histone modification takes place as a secondary event, the repressive chromatin structure is easily reversed by altering the cell environment, and only the DNA methylation can ultimately stabilize OCT4, bringing it in the inactive state [34].

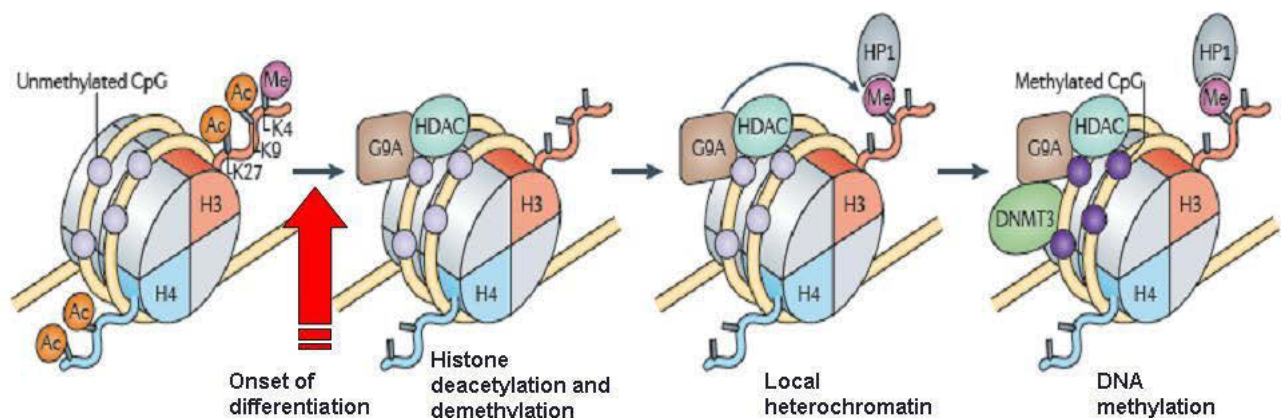


Figure 7. Mechanisms involved in disabling the pluripotency genes

In ES cells, pluripotency genes — such as octamer-binding transcription factor 4 (OCT4; named also OCT3 or POU5F1) and NANOG — have unmethylated CpG islands, and the histones that package these genes have specific modifications, including acetylation of histones H3 and H4 and methylation of histone H3 lysine 4 (H3K4). With the onset of differentiation, histone methyltransferase G9A (also known as EHMT2) is recruited, together with a histone deacetylase (HDAC), and this causes deacetylation of local histones and demethylation of H3K4. In the next step, G9A catalyses the methylation of H3K9, and this modification serves as a binding site for the heterochromatin protein 1 (HP1), thus generating a form of local heterochromatin. Finally, G9A recruits DNA methyltransferase 3A (DNMT3A) and DNMT3B, which mediate de novo methylation of the underlying DNA. Ac, acetyl; Me, methyl. From: Cedar H. & Bergman Y., Nature Reviews. Immunology 2011

I-2.4.1. DNA methylation

DNA methylation in vertebrates occurs in the cytosine residues of CG dinucleotides, and this process is associated with transcriptional silencing. This silencing can be achieved by either repressing the binding of transcription factors (Figure 8A) or by recruiting proteins that specifically bind to methylated CGs (methyl-CG-binding proteins, e.g., MeCP2), which can further recruit histone deacetyltransferases (HDACs) and corepressors (Figure 8B) [35]. This process is catalysed by a family of enzymes including DNMT1, which preferentially targets hemi-methylated DNA and is required for “maintenance” methylation during DNA replication; and DNMT3A and DNMT3B which are required for de novo methylation [33]. In addition, the 5-methylcytosine dioxygenase TET proteins promote DNA demethylation in mammalian cells through a process that requires the base excision repair pathway [34]. Recent evidence shows that DNA methylation has a direct role in regulating HSC self-renewal and commitment to lymphoid versus myeloid cell fates [34]. Meis homeobox 1 (Meis1), involved in haematopoiesis lineage development, is unmethylated in multipotent progenitor cells (MPPs), but seems to progressively become hypermethylated and transcriptionally silenced during differentiation progresses [34].

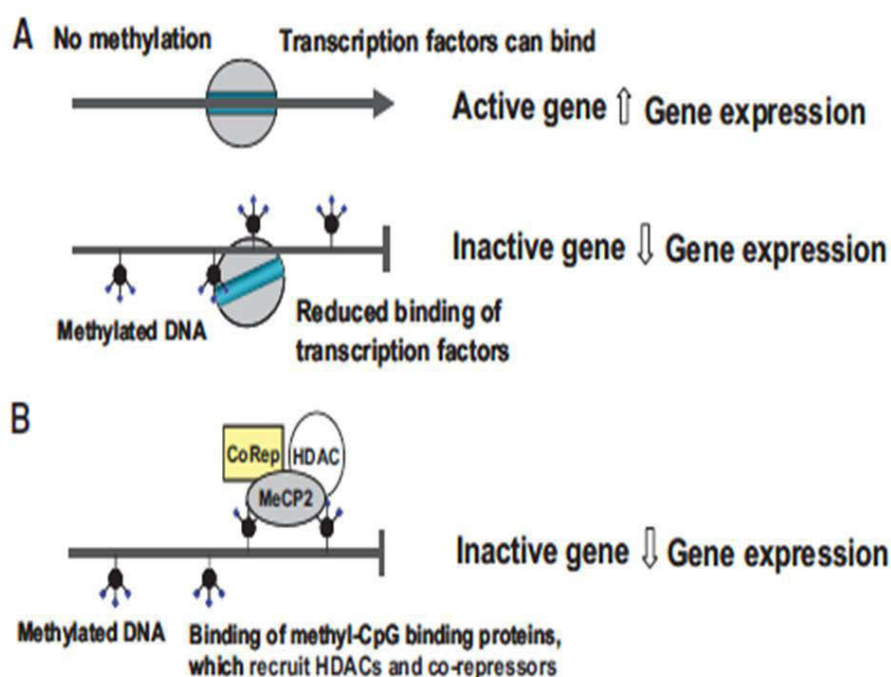


Figure 8. Effects of DNA methylation on gene expression

From: Ling C. & Groop L., Diabetes 2009

On the other side, many genes in HSCs or MPPs are initially methylated and thereafter undergo to selective demethylation in a lineage-specific manner. For lymphoid lineage, these

genes include *Lck*, which undergoes demethylation in T cells and encodes a SRC family kinase that is responsible for initiating signalling downstream of the T cell receptor, and POU domain class 2-associating factor 1 (*Pou2af1*), that encodes a B cell-specific co-activator and undergoes demethylation in B cells. In granulocyte-macrophage progenitors, the genes that undergo specifically demethylation are myeloperoxidase (*Mpo*), and CXC-chemokine receptor 2 (*Cxcr2*) [34].

I-2.4.2. Histone acetylation and deacetylation

Acetylation is the result of equilibrium between two opposing activities: histone acetyltransferases (HATs) which acetylate the lysine residues on histones and loosen up histone-DNA interactions to allow gene expression, and histone deacetylases (HDACs) that catalyze removal of acetyl groups from lysine residues and strengthen up histone-DNA interactions to prevent gene expression. Acetylation of core histones has been correlated with cellular processes, including chromatin assembly, DNA repair, and recombination (reviewed by Gregoretta I. V.) [36]. The ability of histone acetylation to regulate gene expression occurs via the direct effect of chromatin structure modification, which serves to neutralize the charge between histone tails and the DNA backbone, and also by serving as a docking site for regulatory factors [33]. Moreover, many HDACs are at least partially cytoplasmic; some fractions of these proteins can act on non-histone substrates, including the cytoskeletal protein tubulin and transcription factors (i.e. p53) [36].

During hematopoiesis, lineage-restricted transcription factors regulate specific gene-expression patterns by recruiting HAT or HDAC complexes to the promoters of target genes. For example, during erythropoiesis, erythroid-specific transcription factors including GATA-1, which is essential for red lineage maturation and survival, directly recruit HAT-containing complexes to the β -globin locus to stimulate transcriptional activation. Specifically, GATA-1 recruits CREB-binding domain (CBP) to the β -globin gene locus, resulting in the acetylation of histones H3 and H4, and facilitating high-globin gene expression. GATA-1 itself is also acetylated on conserved lysine residues by CBP, which leads to enhance its transcriptional activity [33].

I-2.5. Haematopoiesis Functional Assays

Functional tests used to explore haematopoiesis have been conceivable to identify and evaluate separately the various classes of haematopoietic progenitors. Thus, the standardized short-term colony assays quantify the lineage-committed myeloid precursors, but identification of primitive cells, having the ability to repopulate durably myeloid and lymphoid lineages and preserving the self-renew capacity, still largely depends on *in vivo* assays. Whatever the assay, should measure two cardinal parameters: cell proliferation (measured by the number of cells produced), and the differentiation potential (estimated by the number of different lineages represented in its progeny) [37].

In vitro assays

Short-term in vitro assays

The prototypes of the short-term assays are *semi-solid colony assays*, or *CFC assays*, which identify and quantify lineage-restricted progenitors in well-standardized conditions (according to the manufacturer's instructions; see www.stemcell.com/technical/manuals.asp).

The individual progenitors, called colony-forming cells (CFCs), cultured in a suitable semi-solid matrix, such as methylcellulose or collagen supplemented with nutrients and cytokines, proliferate during 14 to 16 days at 37°C to form discrete cell clusters or colonies with specific characteristic (composition, size, colour, disposition) (Figure 9).

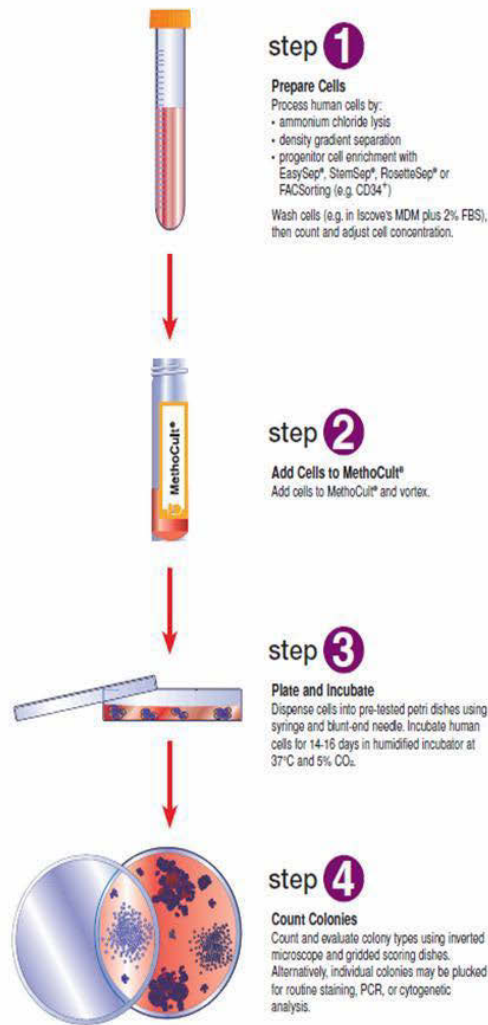


**Figure 9. Human haematopoietic CFC assays in MethoCult® media:
 Procedure diagram**

*From: Human Colony-Forming Cell Assay Using MethoCult®,
 Technical Manual, Stem Cell Technologies, Catalog #28404, 2004*

Colony evaluation and enumeration can be done *in situ* by light microscopy or by plucking individual colonies and then staining the cells using cytochemical and immunocytochemical methods. The classes of human haematopoietic progenitors detected using MethoCult® media include (Figure 10):

CFU-GEMM: Colony-forming unit-granulocyte, erythroid, macrophage, megakaryocyte reflect a multipotential progenitor that produces colonies, which contain erythroblasts and cells of at least two other recognizable lineages. Due to their primitive nature, CFU-GEMM tend to produce large colonies of >500 cells (Figure 10 A).

CFU-GM: Colony-forming unit-granulocyte, macrophage. The colonies contain at least 20 granulocyte cells (CFU-G), macrophages (CFU-M) or cells of both lineages (CFU-GM) (Figure 10 B). CFU-GM colonies arising from primitive progenitors may contain thousands of cells in single or multiple clusters (Figure 10 C).

BFU-E: Burst-forming unit-erythroid. It produces a colony containing >200 erythroblasts in a single cluster or in multiple ones and can be sub-classified based on the number of cells / cell clusters per colony. BFU-E is more immature progenitors than CFU-E and requires EPO and cytokines with burst-promoting activity such as Interleukin-3 (IL-3) and Stem Cell Factor (SCF) for optimal colony growth (Figure 10 D).

CFU-E: Colony-forming unit-erythroid. It produces 1-2 cell clusters containing a total of 8-200 erythroblasts. CFU-Es are mature erythroid progenitors that require erythropoietin (EPO) for differentiation (Figure 10 E).

CFU-Mk: Colony-forming unit-megakaryocyte (Figure 10 F). These colonies contain 3 or more megakaryocytic cells. Although megakaryocytic progenitors can be cultured in methylcellulose-based medium containing the appropriate growth factors, it is difficult to distinguish CFU-Mk based on cellular and colony morphology (Figure 10 G). Therefore, the manufacturer recommends that CFU-Mk be enumerated in collagen-based, MegaCult®-C following staining of megakaryocytes in dehydrated gels by immunocytochemical staining [38].

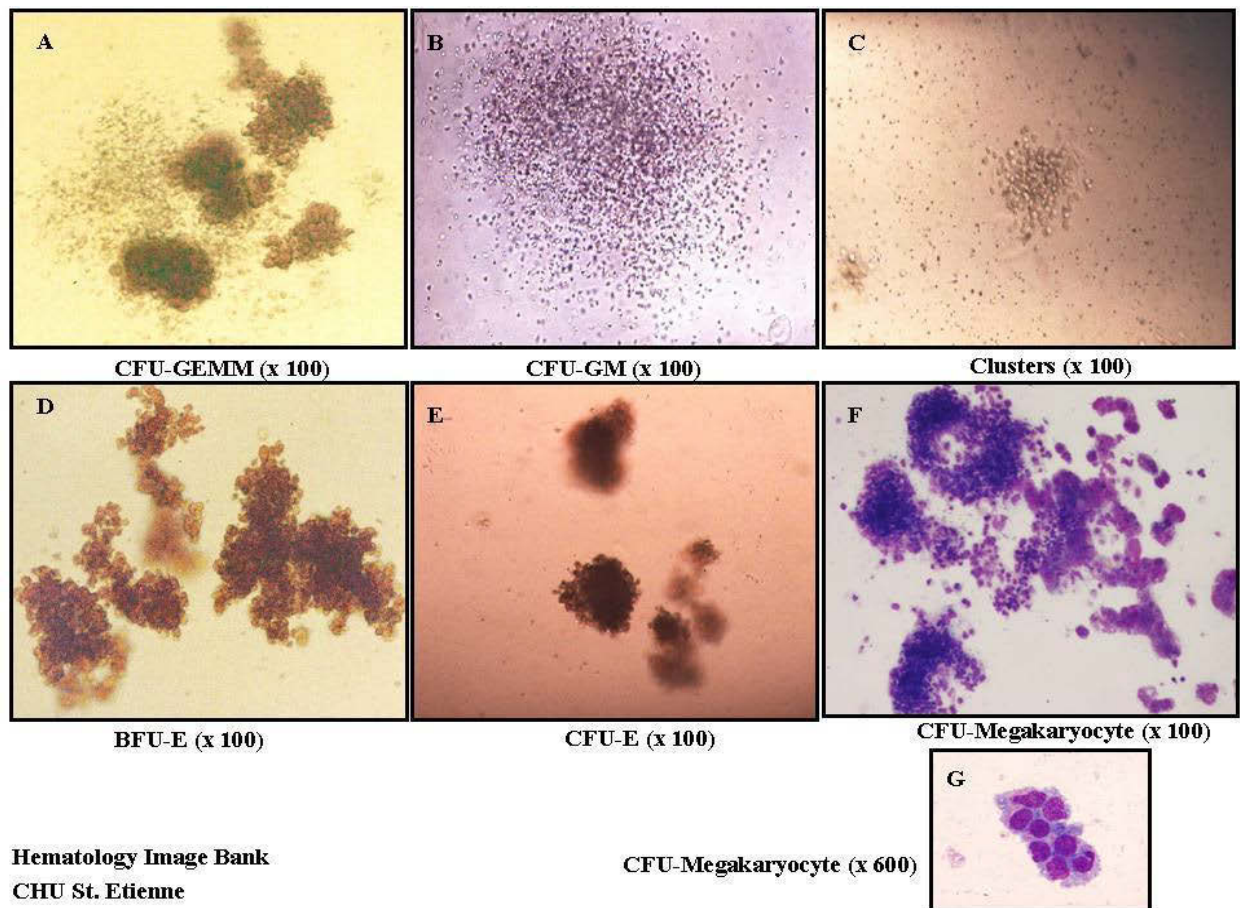


Figure 10. Representative pictures for human haematopoietic colonies (Giemsa stain)

Frequencies of CFC among human $CD34^+$ bone marrow cells average 15% in the $CD34^+CD38^+$ fraction, and 5% in the more immature $CD34^+CD38^-$ population, respectively. [37].

Short-term colony assays are not adequate for the detection of more immature progenitors because the lifespan of these cells in viscous medium (methylcellulose, agar, or plasma clot) does not extend beyond 3 weeks, which is too short a span for stem cells to produce a differentiated progeny, and it cannot be renewed. The semi-solid cultures could be employed to evaluate the myeloid precursors. Surprisingly, the colony assays for lymphoid progenitors have not been well-defined [37].

CFCs can proliferate and generate colonies in liquid cultures, too, in the presence of the same cytokines, but identification of their progeny will require flow cytometry analysis and the benefit of an easy scoring of several progenitors in the same dish would be lost [37].

Long-term assays

In vitro long-term assays for HSCs include Long-Term Culture-Initializing Cell (LTC-IC) assay and Cobblestone Area Forming Cell (CAFC) one. LTC-IC assays are based on the ability of HSCs, but not more mature progenitor cells, to form and maintain a population of progenitor cells with clonogenic potential over at least a five-week culture period [5]. Most human LTC-IC is CD34⁺ CD38^{low/-} [37].

CAFC assays measure the ability of the most primitive progenitor cells (*in vivo* repopulating cells, HSCs, and day 12 CFU-S) to grow under stromal cell layer where they proliferate cyclically and release their progeny (CFC and differentiated cells) in the non-adherent fraction (Figure 11) [5], [37]. These cells could be maintained for several months in mice and 8 to 10 weeks in humans [37].



Hematology Image Bank
CHU St. Etienne

Figure 11. Representative image for CAFC assays

Cobblestone area-forming cell (CAFC) integrates tightly in the adherent layer where they cyclically proliferate and release their progeny during 8-10 weeks (Magnification, x 1000)

I-3. Bone marrow microenvironment or stroma

I-3.1. Overview

The bone marrow microenvironment is an ensemble of structures, which provide the basic framework, nutritional supply, the waste removal system for haematopoiesis, and the specialized support of self-renewal and differentiation for the haematopoietic precursors.

This system belongs to the vascular network, bone marrow innervation, bone marrow (BM) stroma, and extracellular matrix.

The **marrow vasculature** consists principally of a network of sinuses that originate at the endosteum from cortical capillaries and terminate in collecting vessels that enter the systemic venous circulation [39]. The marrow does not have lymphatic drainage [40].

Bone marrow innervation occurs with myelinated and non-myelinated nerves that enter through the nutrient canals. Some innervation also occurs through epiphyseal and metaphyseal foramina. Nerve bundles follow the arterioles with branches serving the smooth muscle of the vessels or, occasionally, terminating in the haematopoietic tissue amongst haematopoietic cells. [40].

I-3.2. Histology of the Bone Marrow

The bone marrow in adults is found within the cancellous bone of the axial skeleton, girdle bones, and some areas of the metaphyses [41].

It consists of **haematopoietic tissue islands** surrounded by **vascular sinuses** interspersed within a meshwork of **trabecular bone**.

Trabecular bone is enclosed by a complex layer of diverse cells:

- **osteoblasts**,
- **osteoclasts**,
- and flat, simple or two-layered, **nonactivated bone-lining cells (BLCs)** [40].

The trabecular surfaces are covered by a layer of endosteal cells. Occasional multinucleate osteoclasts are also a normal finding at trabecular margins [42].

The inner surface of the bone cavities and the outer surface of the cancellous bone spicules within the cavities are covered by an endosteal lining consisting of **a single layer of flat “bone-lining cells”** supported by a thin layer of reticular connective tissue, **osteoblasts** and **osteoclasts** (Figure 12) [40].

HISTOLOGY OF THE BONE MARROW

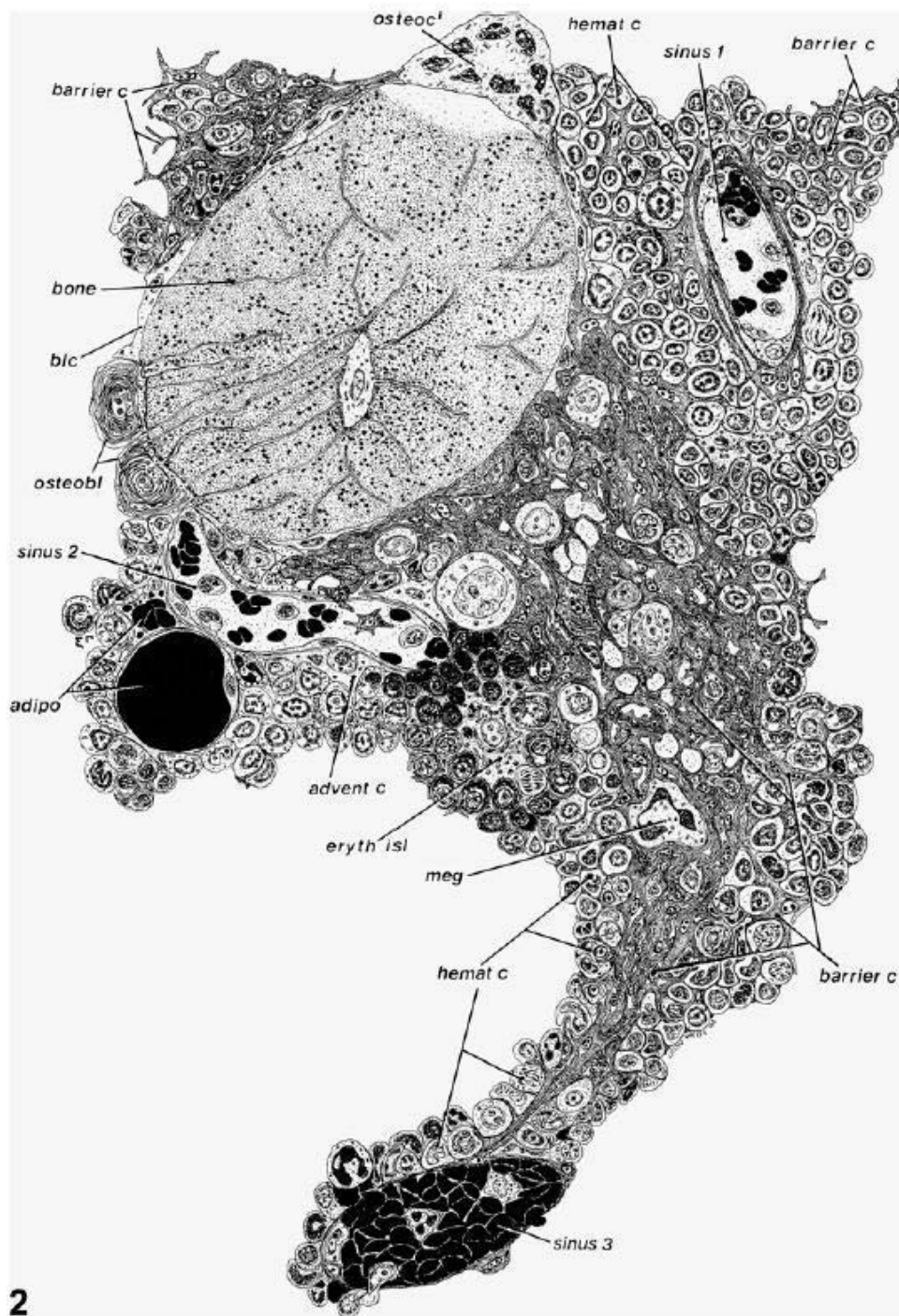


Figure 12. Histology of the bone marrow

Osteoc: osteoclasts, *hemat c*: haematopoietic cells, *barrier c*: barrier cells, *blc*: bone-lining cells, *osteobl*: osteoblasts, *adipo*: adipocytes, *advent c*: adventitial reticular cells, *eryth isl*: erythroblastic islands, *meg*: megakaryocytes. *From: Weiss L. & Geduldig U., Blood 1991*

The sinuses (vascular spaces) of the marrow are thin-walled, lined with **flat specialized endothelial cells**, which prevent the premature escape of immature cells into the peripheral blood. The basal lamina of venous sinuses is incomplete and in combination with a thin or not basement membrane, allowing mature cells to pass through the wall of the sinuses [40], [43].

Haematopoietic tissue islands (Haematon Units / Buffy coat) are composed from haematopoietic cells in interaction with the bone marrow microenvironment to form the so-called **bone marrow haematopoietic stem cell niches**.

Haematopoietic stem cells and lineage-restricted progenitor cells (HPCs) are not randomly distributed in the BM, but there are localized according to their differentiation stage. The majority of true HSCs are found at the endosteum in contact with osteoblasts, whereas more committed progenitors accumulate in the central BM [44]; erythropoiesis takes place in distinct anatomical units (erythroblastic islands), granulopoiesis occurs in less distinct foci, and megakaryopoiesis occurs adjacent to the sinus endothelium [40]. The barrier cells hold many haematopoietic cells, notably putative stem cells and differentiating megakaryocytes. The massed barrier cells are disposed in a crescent, progressing deep into the marrow. Barrier cells, especially in haematopoietic zones containing very early differentiating stages, may insinuate long, slender processes between and around endothelium and adventitial tunics. The blood-marrow barrier is thereby augmented, impeding emigration and immigration of circulating cells, preventing the premature release of immature haematopoietic cells to the circulation as well. In contrast, profiles of vascular sinuses can be made entirely of a simple layer of barrier cells stretched quite thin, except at the perikaryon. These lie in haematopoietic zones containing late differentiating forms ready for delivery to the circulation, their wall being crossed by blood cell-filled apertures. They are structurally suited to facilitate delivery of blood cells to the circulation [40].

Stromal Cells includes all cell types that are located between the outer surfaces of marrow blood vessels and the bone surfaces that encase the haematopoietic space and tissue [45]. The stromal cells compose the supportive tissues of the bone marrow [42].

In this family are included:

- **Westen-Bainton cells / adventitial reticular cells / stromal fibroblasts / barrier cells / pericytes** (modified fibroblasts that produce the reticulin framework of the bone marrow)
- **adipocytes** (cells which store energy in the form of fat)
- **endothelial cells**
- **bone lining cells (inactive osteoblasts^[45]), osteocytes^[41], and osteoblasts^[40].**

Westen-Bainton cells, adventitial reticular cells (ARCs), pericytes, stromal fibroblasts, and barrier cells cover two sides on the surface of bone, in particular the surface of bone to the adventitial surface of vascular sinuses and extend en bloc into the marrow [40]. Their name as well as their origin raises vivid controversy. Thus, after Krebsbach *et al.* the Westen-Bainton cells (name attributed by Westen and Baiton in 1979) are referred to by a variety of descriptive terms (reticular cells, adventitial reticular cells, and stromal fibroblasts (Figure 13) [45]. The recent evidence claimed that MSCs, named also CFU-F, are either identical to or derived from pericytes, if it taking into account the similarities in their physical relationship to the vasculature, the cellular response to growth factors, and expression of similar phenotypic markers [41], [46], [47], [48]. Moreover, Bianco P *et al.* suggested in 2001 that ARCs themselves “can be seen as *bona fide* specialized pericytes of venous sinusoids in the marrow” linking both cells together [49]. On the other hand, another controversial hypothesis has recently held that pericytes may arise directly from endothelial cells or their progenitors [50], [51].

In terms of morphology, there are similarities between BM MSCs with long projection and BM adventitial reticular cells (Figure 13) [52]. Another suggestive description, cells with “extensive, elongated, and attenuated cell processes” support the alternative use of the term “reticular” [43], [45].

Likewise, in terms of phenotype, both types of cells are similar, the MSCs sorted based on STRO-1⁺ CD106⁺ or STRO-1⁺ CD146⁺ phenotype expressed α smooth muscle actin or were positive for 3G5 antigen, which are considered to be specific for pericytes [52], [53], [54]. Other phenotypic markers shared by ARCs, BLCs, and MSCs STRO-1⁺CD106⁺CD146⁺ are: CD271 (low-affinity nerve growth factor receptor [LNGFR]), stromal cell-derived factor-1 (SDF-1) or Chemokine (C-X-C motif) ligand 12 (CXCL12), and several teams include also, few stromal / fibroblast markers: CD10, CD13, D7-FIB [52], [53]. Moreover, cytochemical stain proves their positively for alkaline phosphatase [52], [53], types I and III collagen, and osteonectin [45].

Another observation was that pericytes isolated from bovine retinal capillaries are STRO-1⁺ and exhibit the potential for differentiation into a variety of cell types including osteoblasts, adipocytes, chondrocytes, and “more mundane fibroblasts” [55], [56], [57]. Presumptive pericytes in every developing tissue also express angiopoietin-1, which signals through Tie-2 expressed by endothelial cells, and this signalization seems to be indispensable for vessel stabilization and integrity and for pericyte recruitment [41], [58].

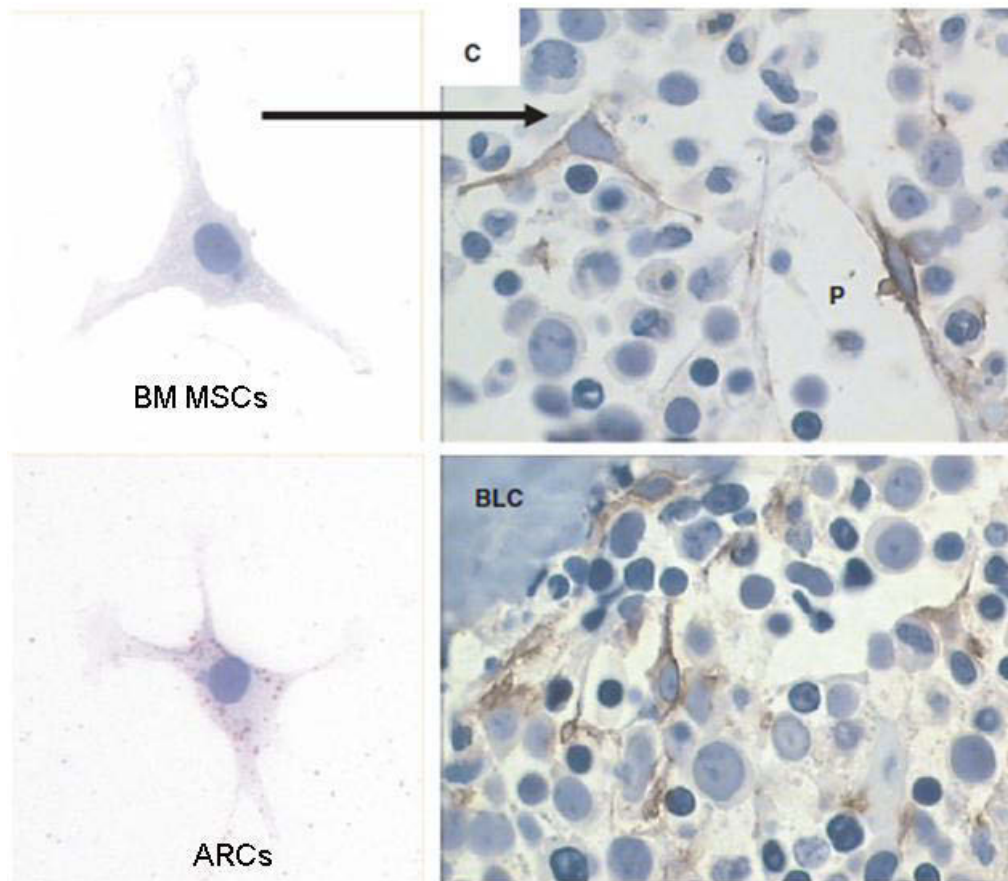


Figure 13. Morphological similarities between BM MSCs with long projections and ARCs

CD10 immunostaining of BM trephine biopsy. BM MSCs: bone marrow mesenchymal stromal cells, ARCs: adventitial reticular cells, BLCs: bone lining cells, P: pericytes. From: Jones E. and McGonagle D., Rheumatology 2008

The barrier cells are activated cells, displaying organelles associated with intense protein synthesis and secretory activity [40].

Recently, evidence has been produced that phenotype-purified human ARCs are able to generate osteoblasts [41] and adipocytes [41], [59] and to self-renew into new adventitial reticular cells and CFU-Fs *in vivo* [41].

Apparently, both in humans and mice, perisinusoidal “reticular” cells (human ARCs, and murine CXCL 12-abundant reticular (CAR) Nestin⁺ cells, which seem to be equivalent populations) play a significant role in regulating HSCs, also [41], [60].

Reticular cells send branches stretching from the bone surface to the adventitial surface of vascular sinuses (Figure 13, sinus 2) [40]. These cells synthesize reticular (argentophilic) fibres that, along with their cytoplasmic processes, extend into the haematopoietic

compartments and form a meshwork on which haematopoietic cells rest. The cell bodies, their broad processes, and their fibres constitute the reticulum of the marrow [39].

Adipocytes

In postnatal marrow, the marrow adipocytes (Figure 15) develop directly from ARCs around sinusoids (Figure 14) [41].

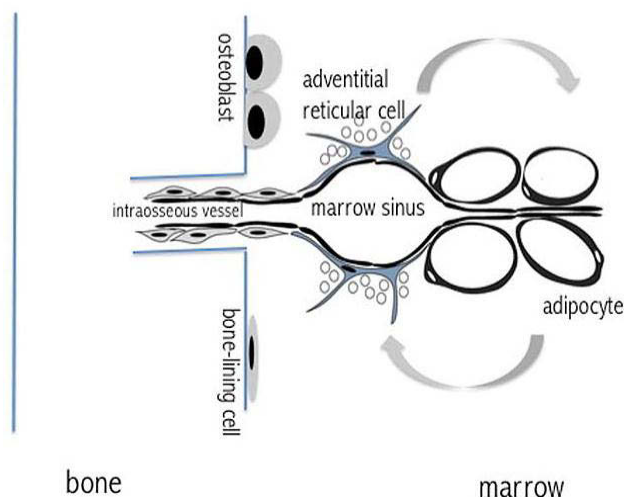


Figure 14. Model of adipocyte differentiation from ARCs.

From: Bianco P., Blood 2011

Adipocytes express leptin, osteocalcin and prolactin receptors during their differentiation, thereby promoting haematopoiesis and influencing osteogenesis [39], [61], [62], [63], [64].

Adipocyte maturation *in vitro* is inhibited by stromal-derived cytokines such as IL-1 and IL-11 [39], [65], [66].

Marrow adipocyte leptin may modulate adjacent haematopoietic progenitor growth [39], [67].

Adipocyte differentiation by marrow stromal cells is inhibited by bone morphogenetic proteins and leptin, supporting the reciprocal regulation of osteogenesis and adipogenesis in the marrow microenvironment [39], [68], [69].

Endothelial cells

Endothelial cells (Figure 15) of capillary vessels are responsible for regulating of HSCs traffic, allowing to haematopoietic mature cells to pass in circulation. Through the synthesis of growth factors, they also contribute to boosting haematopoiesis. Likewise, they enhance bone regeneration in the osseous defects; by their involvement in the formation of blood

vessels that supply oxygen and nutrients to developing bone tissue. However, it has been suggested, more recently, that endothelial cells may play a more direct role in bone development and formation, through their interactions with osteoprogenitor cells and, under certain conditions, their production of specific bone inductive factors [44], [70]. Marrow endothelial cells express von Willebrand factor antigen [39], [71], type IV collagen, and laminin [39], [72]; they also constitutively express two adhesion molecules: VCAM-1 and E-selectin [39], [73]. Other receptors that may mediate marrow cellular trafficking include fractalkine, an endothelial membrane-bound chemokine, also upregulated by cytokines [39], [74]. Marrow sinusoidal endothelium specifically expresses sialylated CD22 ligands, which are homing receptors that recirculate B lymphocytes [39], [75].

Bone cells

Osteoblasts, osteoclasts, and elongated flat cells with a spindle-shaped nucleus (flat bone-lining cells) form the marrow endosteal lining [39], [76]. Resting endosteal cells express vimentin, tenascin, alpha smooth-muscle actin, osteocalcin, CD51, and CD56 [39], [77]. Cultured human bone cells express high levels of $\alpha 1/\beta 1$, $\alpha 3/\beta 1$, and $\alpha 5/\beta 1$ integrins [39], [78]. Endosteal cells provide a homing niche for newly transplanted haematopoietic stem cells [39], [79]. Mesenchymal stromal cells positive for the STRO-1 antibody can differentiate into adipocyte, chondrocytic, and osteogenic cells [39], [80], [81], [82], [83], and similar osteogenic potential is found in STRO-1 positive vascular pericytes [39], [57]. This process of mesenchymal stromal cell to osteogenic differentiation is associated with the loss of the activated leukocyte adhesion molecule (CD166) [39], [84].

Osteoblasts

Bone-forming osteoblast progenitor cells (Figure 15), like stromal precursors, reside in the CD34 negative, STRO-1 positive marrow cell population [39], [85], [86], [87]. Bone morphogenetic protein 2, b-FGF, and TGF- β promote the growth and differentiation of these cells [39], [85], [88].

Osteoblasts expand early haematopoietic progenitor survival in long-term cultures and secrete haematopoietic growth factors such as macrophage colony stimulating factor (M-CSF), granulocyte colony stimulating factor (G-CSF), GM-CSF, IL-1, and IL-6 [39], [89], [90]. Osteoblasts also produce haematopoietic cell-cycle inhibitory factors such as TGF- β , which may contribute to their intimate role in stem cell regulation within the marrow microenvironment [39], [91].

Osteoclasts

Bone-resorbing osteoclasts (Figure 15) are derived from haematopoietic progenitors (CD34 positive, STRO-1 negative) and branches from the monocyte-macrophage lineage early during the differentiation [39], [92], [93]. KIT ligand and M-CSF act synergistically on osteoclast maturation [39], [94], and M-CSF is essential for the proliferation and maturation of osteoclast progenitors [39], [95]. Osteoprotegerin (OPG), or osteoclastogenesis inhibitory factor, is a cytokine of the tumour necrosis factor receptor superfamily, which inhibits osteoclast differentiation [39], [96]. Osteoclast maturation requires osteoprotegerin ligand (TRANCE / RANKL), an osteoclast differentiation and activation factor (ODF) elaborated by stromal cells and osteoblasts [39], [97]. Cross-linking antibodies to the adhesion receptor CD44 inhibit osteoclast formation in primary marrow cultures treated with 1 alpha 25-dihydroxyvitamin D3 [39], [98]. Similarly, blocking the expression of cadherin-6 interferes with heterotypic interactions between osteoclasts and stromal cells, impairing their ability to support osteoclast formation [39], [99].

Accessory cells (monocytes, macrophages, T cells) are progeny of haematopoietic stem cells [100]. Macrophages fulfil functional roles: haematopoietic growth factors synthesis, store iron for haemoglobin production, and carry out phagocytosis of debris [40].

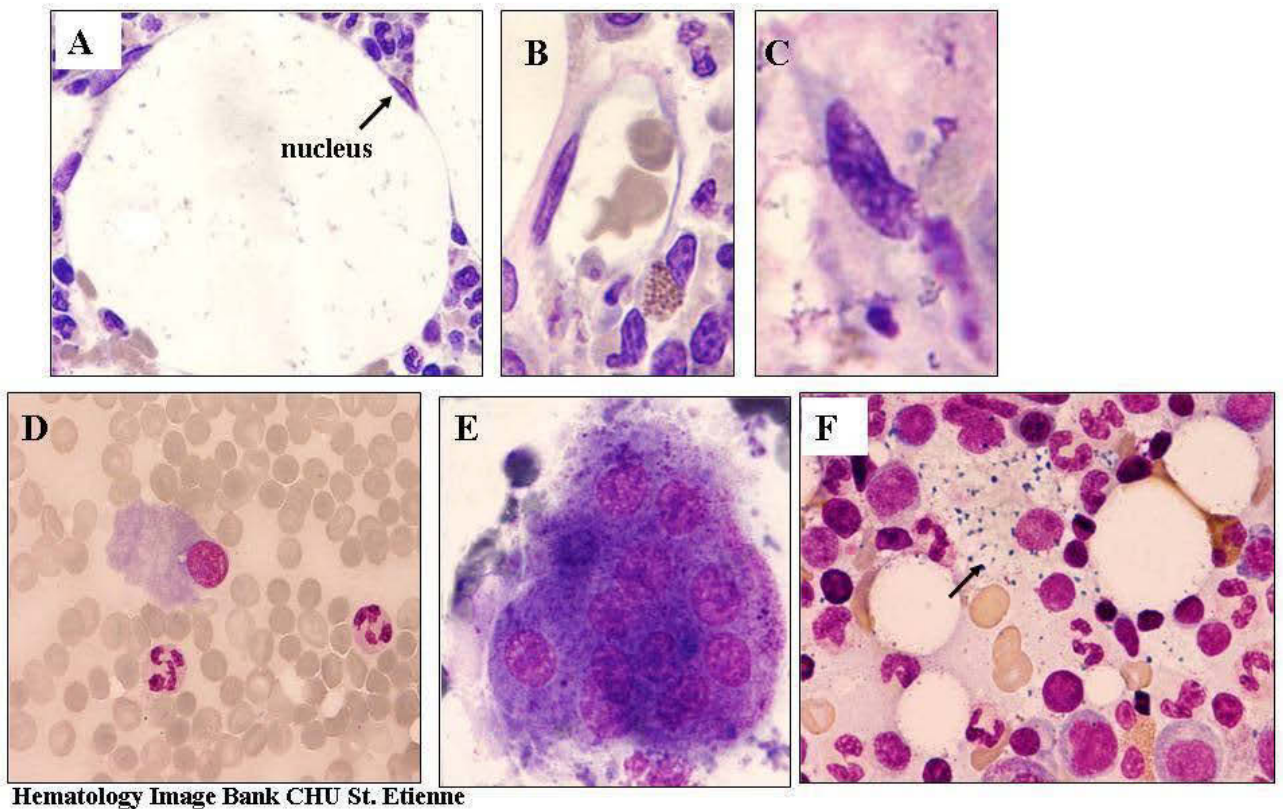


Figure 15. Bone marrow stromal cells

Wright-Giemsa Stain of bone marrow osteomedullary biopsy.

A) Adipocyte (Magnification x 400), B) Endothelial cell (Magnification x 600), C) Fibroblast (Magnification x 600), D) Osteoblasts (Magnification x 400), E) Osteoclast (Magnification x 1000), F) Macrophage (Magnification x 600)

Extracellular matrix (ECM) molecules are synthesized and secreted by microenvironmental cells and include collagens (types I, III, IV, and V), glycoproteins (fibronectin, laminin, thrombospondin, hemonectin, and tenascin), and glycosaminoglycans (hyaluronic acid and chondroitin, dermatan, and heparan sulfate). Besides providing structure to the marrow space, and a surface for cell adhesion, the microenvironment is important for haematopoietic cell homing, engraftment, migration, and the response to physiologic stress and homeostasis [100].

Recent findings prove that ECM is part of the BM microenvironmental niche, being involved in regulation of the balance between replication and differentiation of MSCs in response to appropriate signals [101].

Several mechanisms are supposed to facilitate the expansion of marrow-derived MSCs and prevent their differentiation (i.e. into osteoblasts):

- ECM modulates the activity of growth factors by controlling proteolytic activation of latent factors (i.e., transforming growth factor- β [TGF- β]);

- ECM interacts with cell surface receptors preventing the cognate ligand binding (i.e., as in the case of epidermal growth factor (EGF) receptor), or by sequestration of differentiation factors such as platelet-derived growth factor (PDGF) and bone morphogenetic proteins (BMPs), or of Wnt proteins (which are involved in MSC differentiation through LRP5 and LRP6 binding the glycosaminoglycans of the ECM);
- ECM may also bind the growth-promoting factors from the serum;
- and, ECM could enhance the function of putative accessory cells that support MSCs replication [101].

There is evidence that denatured collagen type I (DC) matrix promotes the maintenance of *in vitro* osteogenic differentiation of MSC by influencing the retention of early osteogenic functions in the late passage cells during *ex vivo* expansion [102].

The same ability to preserve MSC adipogenic potential during the late passage of MSCs *ex vivo*, expanded on the DC matrix in contrast with the MSCs expanded in culture plastic tissue was demonstrated by Mauney J. R. *et al.* in 2005 [103].

The mechanism most likely involved in influencing the ability of the DC matrix to promote retention of adipogenic differentiation potential of MSCs *in vitro* is the maintenance of certain replicative ageing-functions (i.e., cell proliferation capacity, inducibility of stress-protective proteins) [103].

I-3.3. Mesenchymal Stromal Cells

Mesenchymal stromal cells are progenitors of skeletal tissue components, such as bone, cartilage, the haematopoiesis-supporting stroma, and adipocytes. In addition, they could be experimentally induced to undergo neural or myogenic differentiation [49].

I-3.3.1. Terminology

Over the time, numerous terms were assigned to describe the adherent cells derived from many adult tissue sources displaying fibroblast-like morphology: precursors of non-haematopoietic tissue, colony forming unit-fibroblast (CFU-F), bone marrow stromal [stem] cells [BMSCs] and/or stromal precursors cells (SPCs), RS-1, RS-2, mMSCs (RS: recycling stem cells) (m: mature), multipotent adult progenitor cells (MAPCs) [104], fibrocytic cells, fibrocyte, fibrocytic colony, fibroblast, fibroblast colony, precursors for fibroblast colonies, fibroblast-like colonies, stellate colonies, fibroblastoid stromal cells, stromal cells, CD34^{-/low} haematopoietic stem cell clones with mesenchymal stem cell characteristics, circulating

skeletal stem cells, CD34⁻CD105⁺ mesenchymal cell lines, CD34-negative fibroblast-like cell lines, CD34-negative CD105-positive cell line, and mesenchymal stem cells [105], to enumerate just some of them.

Therefore, the literature surrounding the MSC is challenging and valuable information could be lost (Table 1).

Table 1 Citations in PubMed as of 17 August 2011

Search name	Citations
CFU-F (colony-forming unit fibroblastic)	457
Marrow stromal cells	10042
Mesenchymal stem cells	15073
Mesenchymal stromal cells	4107
MSCs	5608

Adapted from: Prockop D. J., Molecular Therapy 2009

A position statement of the International Society for Cytotherapy proposed to use the term “multipotent mesenchymal stromal cells” [106].

I-3.3.2. Cytomorphology and cytomorphometry

The primary low density plated cultures from BM MSCs showed heterogeneous groups of large flat cells, smaller spindle-shaped cells, and small round cells (Figure 16) [107], [108], [109], [110].

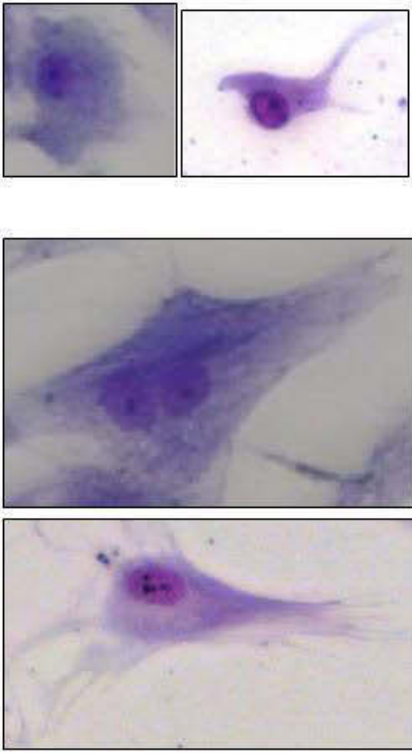
<p>Cells type „a“ rounded-shaped, multipotent, uncommitte- undifferentiated MSCs</p>		<p>cells with round-ovalar shape, mean dimensions H/W=17.6±5.9μm / 15.0±3.3μm (n=50), large euchromatic nuclei (overrated nucleous-cytoplasmic volume), 1 visible or inconspicuous nucleol, coarse chromatin,intensely basophil cytoplasm, clear or slight blurred cellular outline, sometimes with fine cytoplasmic budding, without inclusions</p>
<p>Cells type „b“ spindle-shaped, “commitment compartment” tripotent and bipotent precursor cells</p>		<p>cells with spindle shape, thin, mean dimensions H/W=135.2±49.7μm / 18.8±7.5μm (n=50), an central or eccentric round-ovalar nucleous, coarse chromatin with an visible nucleol, scanty cytoplasm, clear blurred outline, blue-violet, apparently without granulation and sometimes with fine extensions</p>
<p>Cells type „c“ large, polygonal- shaped, „mature“ cells with limited proliferative capacity</p>		<p>c.1: ovalar-polygonal cells, mean dimensions H/W= 54±12,8 μm/ 27,8±7 μm (n=50), an eccentric nucleus, reticular chromatin with 2-3 large or inconspicuous nucleoli, large, blurred cytoplasm, pale basophil, without inclusions or c.2: cells with stelar shape, mean dimensions H/W= 126±47,3μm/ 52±15,18μm (n=50), 1-2 central nucleous, reticular chromatin with 1 large nucleol or unequal multiple nucleolated, abundantly cytoplasm with 2 or 3 regions, first region, paranuclear is highly basophil with basophile inclusions, methylene blue metachromasy, second region, at periphery of cell is pale gray, with wiped outline, without inclusions. Between this two regions, paranuclear and peripheral, sometime can be a third region, purple violet with reticular structure and scattered inclusions</p>

Figure 16. MSCs morphology and morphometry

Moreover, some authors have made associations between the morphology of these cells and a possible hierarchy. Thus, spindle-shaped cells were designated as type I cells or as rapidly self-renewing cells (RS-MSCs), and those large as slowly replicating cells (SR-MSCs) arising from the type I cells when the cultures expand to confluency [111], [112], [113].

Until now, there have been limited data regarding the distribution of cell sizes in MSC populations. Using the simple criteria of size and granularity, Zohar *et al.* identified two major subpopulations of MSCs. The first, with smaller cells in the lowest 15% FSC and the lowest 15% SSC, proved to be a slowly cycling population that did not express differentiation-related markers and that displayed a high proliferative activity, multipotentiality, and capacity for self-renewal upon plating. The second population, more numerous, had large cells with the highest 15% FSC and highest 15% SSC, lacked self-renewal capacity, and had limited proliferative capacity [114]. In agreement with this, Colter *et al.* affirmed that the rapid expansion of MSCs in culture depends on the presence of a minor population of small cells [115].

A size-sieved method, using a 3- μm pore plate, also allowed the isolation of two populations. The first was a population of cells with a size greater than 3 μm . Cells in this population revealed a fibroblast-like morphology, self-renewal capacity, and multilineage potential, specific features for MSCs. The second population of cells was smaller than 3 μm , polygonal in shape and had limited renewal capacity [116]. Finally, Staszkievicz *et al.* found that the size of ear-derived MSCs ranged from 8.1 to 26.6 μm in diameter, with the majority of the population (~72%) between 12 and 20 μm [117].

I-3.3.3. Cytochemistry

The common opinion is that human CFU-F are positive for vimentin [48], [105], [118], [119], [120], type I and type III collagen [105], [121], [122], type IV collagen [105], [122], fibronectin [105], [118], [120], [122], fibrin [105], [118], acid phosphatase [105], [121], [122], α -Naphthyl-acetate esterase, α -Naphthyl-butyrate esterase [105], [121], periodic acid Schiff (PAS) [105], [122], Sudan Black [105], [122]. Likewise, part of MSCs from primary cultures express smooth muscle (sm) α -actin [105], [120].

I-3.3.4. Phenotype

To date, there is no consensus regarding a single surface antigen that could identify the MSCs. For this reason, a panel of several positive and negative markers should be employed to characterize these cells. The International Society for Cellular Therapy proposed for MSC characterization three positive markers. i.e., CD73 (ecto-5'-nucleotidase, SH3, SH4), CD105 (endoglin, SH2), and CD90, and the absence of expression for haematopoietic related markers such as CD45, CD34, CD14, and CD11b [106].

CD73 it has been demonstrated to be highly specific to characterize MSCs, and useful for the development of robust *in vitro* MSC assays [52], [82]. However, another marker, STRO-1, is worth noting, because it proved to have an enrichment capacity in CFU-Fs approximately 100-fold when compared with MSCs isolated by plastic adherence [53], [123].

Nonetheless, even though MSCs are widely thought to be CD45 negative, note that other authors have reported that CFU-Fs are CD45^{med/low} [120], [124]. Moreover, there is evidence that freshly isolated MSCs display the greatest percentage of CD45-positive cells, whereas MSCs expanded in culture over more passages almost completely lose their expression of this marker [117], [125].

Regarding the CD45 functions in non-hematopoietic cells, this molecule serves as a negative modulator of growth factor receptor tyrosine kinases, in addition to its well-established role as an activator of tyrosine kinases *src* family [126].

Endothelial-related markers have also been reported to be expressed by MSCs, although these markers excite also controversy: PECAM-1 (CD31), P-selectin (CD62P), factor VIII-related antigen, and thrombomodulin [127], [128]. In terms of HLA-molecules, MSCs express HLA-1, and do not express HLA-DR [120].

Table 2 summarize the other phenotypic markers and growth factors expressed by MSCs amplified in culture [129].

Table 2 Phenotypic characterization and expression of growth factors of human MSCs

Common name	CD designation	Detection	
Adhesion molecules*			
ALCAM	CD166	Pos	
ICAM-1	CD54	Pos	
ICAM-2	CD102	Pos	
ICAM-3	CD50	Pos	
E-selectin	CD62E	Neg	
L-selectin	CD62L	Pos	
P-selectin	CD62P	Neg	
LFA-3	CD58	Pos	
Cadherin 5	CD144	Neg	
PECAM-1	CD31	Neg	
NCAM	CD56	Pos	
HCAM	CD44	Pos	
VCAM	CD106	Pos	
Hyaluronate receptor	CD44	Pos	
Growth factors and cytokine receptors*			
IL-1R (α and β)	CD121a,b	Pos	
IL-2R	CD25	Neg	
IL-3R	CD123	Pos	
IL-4R	CD124	Pos	
IL-6R	CD126	Pos	
IL-7R	CD127	Pos	
Interferon γ R	CDw119	Pos	
TNF- α -1R	CD120a	Pos	
TNF- α -2R	CD120b	Pos	
FGFR		Pos	
PDGFR	CD140a	Pos	
Transferrin receptor	CD71	Pos	
Integrins*			
VLA- α 1	CD48a	Pos	
VLA- α 2	CD49b	Pos	
VLA- α 3	CD49c	Pos	
VLA- α 4	CD49d	Neg	Expressed in long term bone marrow cellule without induction
VLA- α 5	CD49e	Pos	IL-6
VLA- α 6	CD49f	Pos	IL-7
VLA- β chain	CD29	Pos	IL-8
β_4 integrin	CD104	Pos	IL-11
LFA-1 α chain	CD11a	Neg	IL-12
LFA-1 β chain	CD18	Neg	IL-14
Vitronectin R α chain	CD51	Neg	IL-15
Vitronectin R β chain	CD61	Pos	LIF
CR4 α chain	CD11c	Neg	M-CSF
Mac1	CD11b	Neg	Flt-3 ligand
Additional markers*			
T6	CD1a	Neg	Induced by IL-1
CD3 complex	CD3	Neg	IL-1
T4, T8	CD4, CD8	Neg	IL-1 β
Tetraspan	CD9	Pos	IL-6
LPS receptor	CD14	Neg	IL-8
LewisX	CD15	Neg	IL-11
-	CD34	Neg	IL-11
Leukocyte common antigen	CD45	Neg	G-CSF
5' terminal nucleotidase	CD73	Pos	GM-CSF
B7-1	CD80	Neg	LIF
HB-15	CD83	Neg	Not expressed
B7-2	CD86	Neg	IL-2
Thy-1	CD90	Pos	IL-3
Endoglin	CD105	Pos	IL-4
MUC18	CD146	Pos	IL-10
BST-1	CD157	Pos	IL-13

Adapted from: Deans R.J. and Moseley A. B., Experimental Hematology 2000

I-3.3.5. Schematic model depicting mesenchymal stromal cell proliferation and differentiation

The MSCs are generally thought to be resident in the perivascular compartment of many tissues, in fat, skin, muscle, and other locations [130], [131].

Their proliferation process involves two distinct cellular compartments.

In the first compartment, MSCs undergo transcriptional modification, generating precursor cells without apparent changes in phenotype and self-renewal capacity. This process especially interests the MSCs residing in adult bone marrow, which are quiescent and growth arrested in G_0/G_1 outside stimulation with growth factors. *In vitro*, upon stimulation, the multipotent, uncommitted MSCs undergo asymmetric division, giving rise to two daughter cells, one being the exact replica of the mother cell and maintaining multilineage potential, and the other daughter cell becoming a precursor cell, with a more restricted developmental programme. In this model, the precursor cell continues to divide symmetrically, generating more tripotent and bipotent precursor cells. These tripotent and bipotent precursor cells are morphologically similar to the multipotent MSCs, but differ in their gene transcription repertoire, and therefore, still reside in the stem cell compartment. The progression of MSCs to precursor cells is considered the first step in stem cell commitment. The transition or exit from the 'stem cell compartment' to the 'commitment compartment' occurs when precursor cells continue to divide symmetrically to generate unipotent progenitor cells, simultaneous with the acquisition of lineage specific properties, rendering them fully committed mature cells with distinguishable phenotypes [104].

There are eight genes whose expression is increased during all three mesenchymal lineage differentiations (multi-, bi-, and unipotent), suggesting that they represent the putative master control genes. These genes were identified as period homolog 1 (PER1), nebullette (NEBL), neuronal cell adhesion molecule (NRCAM), FK506 binding protein 5 (FKBP5), interleukin 1 type II receptor (IL1R2), zinc finger protein 145 (ZNF145), tissue inhibitor of metalloproteinase 4 (TIMP4), and serum amyloid A2. The function of these genes cover a broad range of cellular processes, including cell adhesion, protein folding, organization of actin cytoskeleton, as well as inflammatory response [104].

The lineage committed cells of MSCs can fabricate a spectrum of specialized mesenchymal tissues including bone, cartilage, muscle, marrow stroma, tendon, ligament, fat (Figure 17) and a variety of other connective tissues [131], [132].

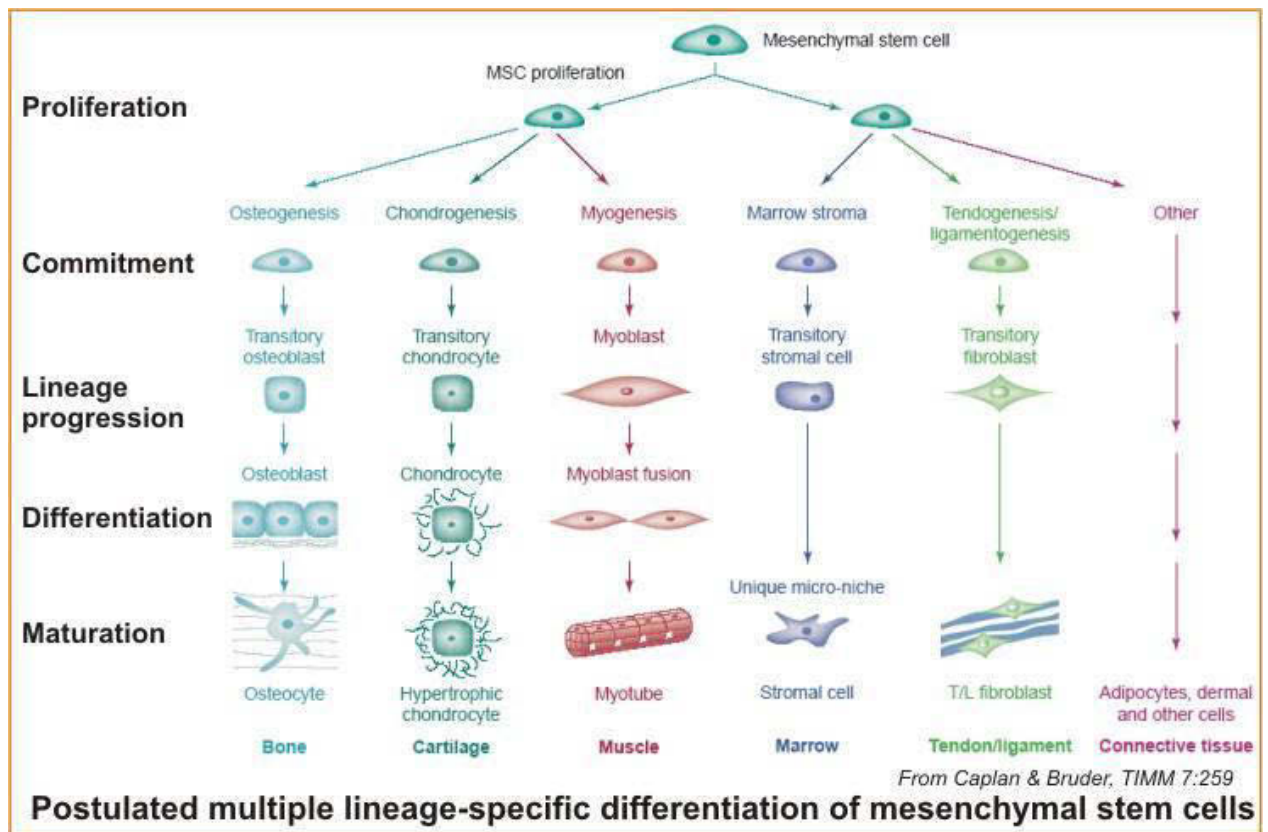


Figure 17. Schematic model of mesengenic process

The stepwise cellular transitions from the putative MSC to highly differentiated phenotypes. From: Caplan A. I. and Bruder S. P., Trends in Molecular Medicine 2001

Their commitment to a lineage can be induced by a number of stimuli (Table 3) [133].

Table 3 Inductive factors for *in vitro* mesenchymal lineage differentiation

Lineage	Inductive factors
Adipocyte	dexamethasone, indomethacin, insulin, methylisobutylxanthine, thiazolidinedione
Chondrocyte	ascorbate, bone morphogenetic protein 6, dexamethasone, transforming growth factor β
Endothelial	ascorbate, epidermal growth factor, fibroblast growth factor 2, vascular endothelial growth factor
Hematopoietic support	co-culture models
Muscle (cardiac)	5-azacytidine
Muscle (skeletal)	low serum concentration, horse serum
Muscle (smooth)	
Osteoblast	ascorbate, bone morphogenetic protein, dexamethasone, 1,25 dihydroxy vitamin D3
Tendon	mechanical stimuli

Adapted from: Gimble J. M., Transfusion Medicine and Hemotherapy 2008

I-3.3.6. Plasticity of Mesenchymal Stromal Cells

It is difficult to establish a hierarchy between MSC subpopulation, and apparently, there are differences between the proper MSCs and the plastic adherent cells that are isolated from marrow using different protocols and assigned different names. To date, the marrow-isolated adult multilineage inducible (MIAMI) cells that were isolated from marrow of vertebral bodies under low oxygen, and which keep the differentiation potential into neural cells are considered to be the nearest of embryonic stem (ES) cells [134]. It includes very small embryonic-like (VSEL) stem cells, which were isolated from murine bone marrow by positive selection using the chemokine receptor CXCR4, and the multipotent adult progenitor cells (MAPCs) isolated from human bone marrow under low oxygen and low serum [134]. These cells express genes such as Oct-4 (characteristic of ES) and Dickkopf-1 (DKK-1, an inhibitor of the canonical Wnt signalling pathway) [134]. Recently, L Basciano *et al.* showed that *in vitro* exposure of MSC to hypoxia enhanced (4-60 fold) the expression of the genes involved in extracellular matrix assembly (SMOC2), neural and muscle development (NOG, GPR56, SNTG2, LAMA), and epithelial development (DMKN). In conclusion, hypoxia maintains the cells undifferentiated and, in parallel, enhances the expression of genes involved in the development of various, mesodermal and non-mesodermal cell lineages. In this respect, hypoxia may increase both the multipotency and the trans-differentiation potential (plasticity) of MSC [135].

I-3.3.7. MSCs create their own niches *in vitro* cultures

During expansion on cultures, MSCs undergo different changes and create an *in vitro* niche. Within this niche, cells play different roles. Thus, Prockop DJ noticed in early phases of MSC cultures a population of spindle-shaped cells (type 1, or RS-MSCs) that express surface proteins with an inhibitory influence on cell adhesion [such as α_6 -integrin and podocalyxin-like protein (PODXL)]. These cells are highly motile, secrete DKK-1, and serve as nurse cells for other subpopulations; hence, they are key elements of the rapid growth phase [134]. As the colonies expand, secretion of Dkk-1 decreases and expression of PODXL and the related proteins are lost. The colonies then enter a near stationary or plateau phase, as the colonies become more tightly packed and develop distinct inner and outer regions [134], [136]. The inner regions are populated with the more commitment precursors, but this stage is readily reversible, in that replating either the inner or outer regions generates single cell-derived colonies with the same characteristics as the initial colonies [134], [136]. At each replating of

a colony at clonal density, the daughter colonies are heterogeneous in both size and their potential to differentiate as is represented in Figure 18 [134], [137], [138]. The reversibility of the cultures, however, markedly decreases if the colonies are allowed to expand to confluency, in that there is a dramatic decrease in clonogenicity (from 90% CFUs-F to <20%), and also stands out a decrease in the potential for multilineage differentiation, and increased expression of epitopes such as STRO-1 and GD-2 [134], [139].

However, even in confluent cultures resulting after several passages, a fraction of the cells remain clonogenic, suggesting that there is persistence of one or more *in vitro* niches containing different subpopulations [134].

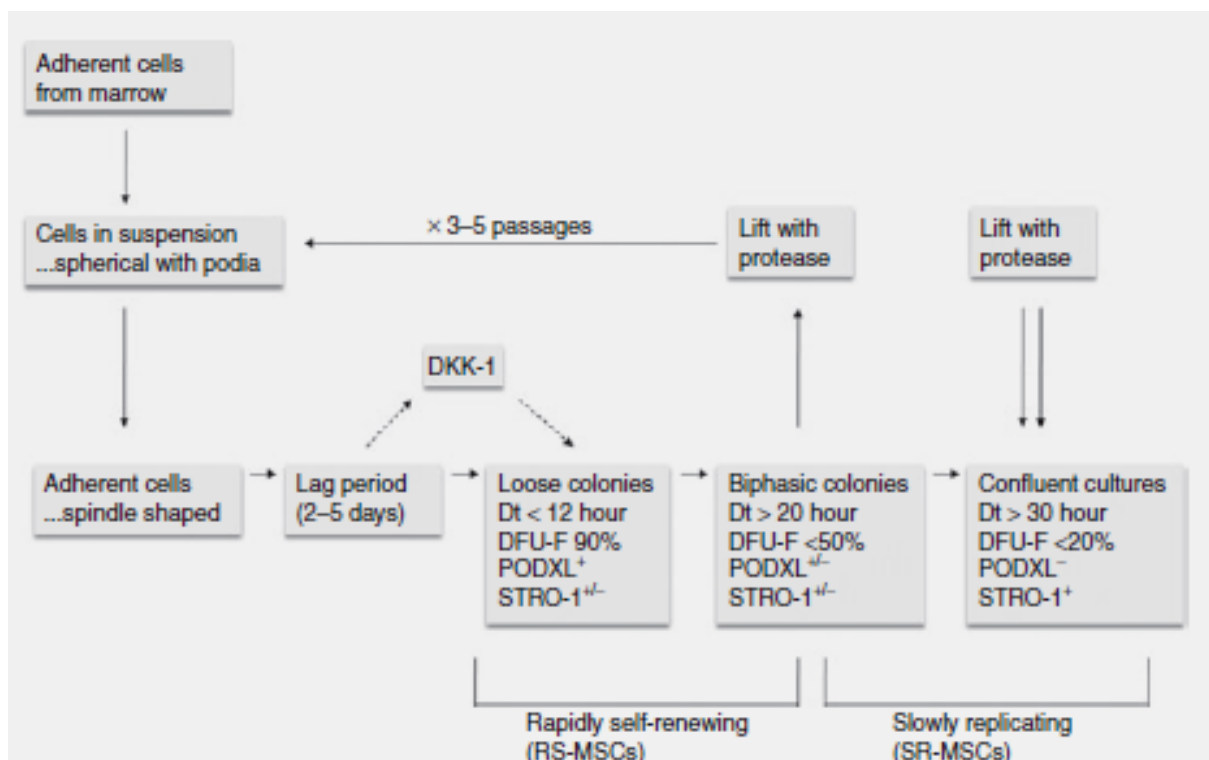


Figure 18. Schematic model depicting the changing properties of human MSCs expanded in culture. From: Prockop DJ, *Molecular Therapy* 2009

In suspension, MSCs are spherical and become spindle-shaped after adherence to culture surfaces. The cells then undergo a lag period followed by a rapid growth with doubling time (DT) of <12 hours that is driven by expression of the Wnt inhibitor Dkk-1. During the rapid growth period, the small rapidly self-renewing MSCs (RS-MSCs) express a characteristic set of surface epitopes, including podocalyxin-like protein (PODXL). They are weakly positive to STRO-1 and are highly clonogenic. As single cell-derived colonies expand, they develop

distinct inner and outer regions that define *in vitro* niches. The colonies reach a near stationary phase with DT of over 20 hours. The cells begin to lose expression of PODXL, express higher levels of STRO-1, and decrease in clonogenicity. If cells are lifted before confluency and replated at low density, the sequence is resumed through four to seven passages.

I-3.3.8. Isolation and *in vitro* expansion of Mesenchymal Stromal Cells

To date, assaying the two principal properties of MSCs, the clonal self-renewal and the multilineage differentiation potential is extremely challenging due to the low frequencies of clonogenic progenitors found in most tissues (e.g., mesenchymal clonogenic frequency in human BM is 1:10⁴ to 1:10⁶ depending on age [130]). Thus, several strategies have been employed to enhance and maintain the multilineage potential of MSCs, such as culturing cells with specific growth factors, enriching cells prior to initial plating, and / or culturing cells in a non-contact suspension culture configuration [104]. The initial proliferation of BM MSCs require the presence of minimum four growth factors, platelet-derived growth factor, basic fibroblast growth factor, transforming growth factor- β , and epidermal growth factor [105], [139]. Among these, fibroblast growth factor (FGF) play a crucial role in the self-renewal, maintenance, and proliferation of a variety of stem cells, HSCs, MSCs, neural stem cells, and ES cells [107], [140], [141], [142], [143], [144], [145], [146], and preferentially selects for the survival a particular subset of MSCs with a higher self-renewal potential [104]. Enrichment of a more homogeneous MSC starting population, particularly those that have a multilineage differentiation potential (*i.e.*, quadra- vs. bipotent cells) could also prolong MSCs life span during *in vitro* expansion [104].

Numerous attempts have been made to develop more specific procedures for the selection of different MSC subpopulations. The most common isolation methods use the MSCs' "specific", surface epitopes or adhesion molecules.

Of the first category, the broad investigated markers were STRO-1, and CD73.

Although **stromal precursor antigen-1 (STRO-1)** is widely regarded as a marker of early mesenchymal stromal precursor cells, it is also expressed on the surface of other human bone marrow (BM) cells that include glycophorin-A⁺ nucleated red cells and a small subset of CD19⁺ B-cells; however, it is not expressed on HSCs [123]. This has raised many questions about its use as a specific marker in MSC sorting protocols [52], [147]. Plasma membrane-bound ecto-5'-5'nucleotidase (CD73) has been proposed as the most useful molecule for developing robust *in vitro* MSC assays [147]. However, Simmons *et al.* reported that the

STRO-1⁺/glycophorin A⁻ population has a substantial clonogenic capacity (approximately 100-fold, enriched in colony-forming unit-fibroblast [CFU-F]). These cells are capable of generating adherent cell layers containing multiple cell types, including adipocytes, smooth muscle cells, and fibroblastic elements; furthermore, this population displays a greater ability to maintain the normal development of the human myeloid lineage than the stromal cells that are commonly isolated from unmanipulated BMs [123]. More recently, Gronthos *et al.* provided evidence that osteogenic precursors are present in the STRO-1⁺ fraction of human BM cells [148]. Psaltis *et al.* also found a strong correlation between the amount of STRO-1 with mRNA expression of transcription factors related to cellular proliferation and differentiation, which have been associated with an immature, stem-like phenotype [149].

CD73 expression has also been observed in different cells, and its physiological role is to metabolize adenosine 5'-monophosphate (AMP) to adenosine [150]. CD73 acts as a signal-transducing molecule in the human immune system (specifically, it acts as a co-stimulatory molecule in T cell activation), and it has been shown to be involved in controlling lymphocyte-endothelial cells interactions [151]. It has been hypothesized that CD73 expression in both tumour and host cells protects the tumour from incoming anti-tumour T cells and suppresses T cell functions through the CD39 (ecto-ATPase)-CD73 axis [19]. Much less is known about CD73 role in MSC biology, but its impact on cell-matrix interactions in chicken fibroblasts has been described [152].

The gold standard assay utilized to identify MSCs is the colony forming unit-fibroblast (CFU-F) assay that, at minimum, identifies adherent, spindle-shaped cells that proliferate to form colonies [153].

In this respect, in the following lines, we present the protocol provided by StemCell Technologies.

Processing of Cells and the CFU-F Assay

1. When working with a fresh bone marrow (BM) sample, the cells need to be processed to remove the red blood cells or enrich desired cells prior to culture. Choose one of the following methods:

- Ammonium chloride lysis (to remove the red blood cells)
- Isolation of the mononuclear cells by Ficoll-Paque™ density gradient separation
- Enrichment of mesenchymal stem cells using the RosetteSep® Human Mesenchymal Stem Cell Enrichment Kit

2. After processing, wash the cells by adding 10 mL of PBS with 2% FBS to the cell pellet.

Centrifuge the cells at 300 x g (~1200 rpm) for 10 minutes at 20°C. Remove the supernatant and resuspend the cells in 1 - 2 mL of Complete MesenCult® Medium (Human).

3. If working with BM cells processed with ammonium chloride or Ficoll-Paque™, perform a nucleated cell count (using 3% Acetic Acid with Methylene Blue) and dilute the cells to a stock cell concentration of 2×10^6 cells/mL in Complete MesenCult® Medium (Human).

If working with enriched mesenchymal cells isolated using the RosetteSep® Enrichment Kit for Human Mesenchymal Stem Cells, perform a cell count and dilute cells to a stock cell concentration of 5×10^5 cells/mL in Complete MesenCult® Medium (Human).

4. Plate three different cell densities by adding 1.0 mL, 0.5 mL, and 0.25 mL of the cells at stock concentration to separate 100 mm tissue culture-treated dishes (or T-25 cm² tissue culture flasks) prefilled with Complete MesenCult® Medium (Human) to a total volume of 10 mL. For ficolled or lysed BM cells, this will yield final cell count of 2×10^6 cells, 1×10^6 cells and 0.5×10^6 cells in 10 mL of medium. For RosetteSep®-enriched cells this will yield final cell count of 5×10^5 cells, 2.5×10^5 cells and 1.25×10^5 cells in 10 mL of medium.

Plating three concentrations will ensure that the resulting numbers of colonies can be scored, as there are differences in the proliferative potential of CFU-F from various bone marrow samples.

5. Place the 100 mm dishes (or T-25 cm² tissue culture flasks) into a 37°C humidified incubator with 5% CO₂ in air and >95% humidity for 14 days.

Maximum colony size and numbers are typically observed at 14 days [154].

Suggested Procedure for Staining and Enumeration of CFU-F-Derived Colonies

Staining

1. Remove the medium from cultures of CFU-F grown in 100 mm tissue culture dishes or T-25 cm² tissue culture flasks and discard into the bio-hazardous waste. The adherent colonies will remain attached to the plate.
2. Wash the culture dishes or flasks twice using PBS to remove any remaining medium. Discard the PBS from the two washes into the bio-hazardous waste.
3. Add 5 mL of methanol to each culture dish or flask for 5 minutes at room temperature.
 - a) *Addition of methanol fixes the cells to the tissue culture dishes or flasks.*
4. Remove the methanol and discard into the bio-hazardous waste. Let the culture dishes or flasks air dry at room temperature.
5. Add 5 mL of Giemsa Staining Solution to each culture dish or flask and leave for 5 minutes.

6. Remove the Giemsa Staining Solution and rinse the culture dishes or flasks with distilled water to remove non-bound stain. Rinse until water remains clear.
7. Discard the distilled water into the bio-hazardous waste and allow the tissue culture dishes or flasks to dry at room temperature.

Enumeration

CFU-F colonies from human cells are typically between 1 - 8 mm in diameter and may be scored macroscopically.

Photographs of representative CFU-F-derived colonies are shown in Section 3.3. Ensure that there is a linear relationship between the cell numbers plated and the resulting colony numbers, by confirming that there are twice as many colonies when 2×10^6 cells are plated as compared to 1.0×10^6 cells. Likewise, there should be twice as many colonies when 1.0×10^6 cells are plated as compared to 0.5×10^6 cells. Ideally there should be 10 - 40 colonies per 100 mm dish or

T-25 cm² flask. Linearity may not be observed outside this range, as the cells would have been under or overplated.

Each bone marrow sample is unique for that donor and the number of CFU-F may depend on a number of factors including age, presence of disease, and previous treatments given to the patient [154].

I-3.3.9. Functional assays for Mesenchymal Stromal Cells

In order to test the growth abilities of isolated MSCs, two properties are tracked: the clonogenic and the proliferative potential.

Clonogenic potential → *Clonogenic assay* or colony formation assay is an *in vitro* cell survival assay based on the ability of a single cell to grow into a colony. The colony is defined to consist of at least 50 cells. → *CFU-F assay* and *Plating efficiency of different subsets* evaluation.

PE is the ratio of the number of colonies to the number of cells seeded:

$$PE = \frac{\text{no. of colonies formed}}{\text{no. of cells seeded}} \times 100\%$$

Proliferative potential → *Proliferation assay*

Doubling time (time for one mitosis / division) → t/n , t = time for the MSCs plated at 1000 cells / 25 cm² to reach 80% of confluency, n = number of population doublings (means number of mitosis necessary to reach at 80% of confluency). The **number of population doubling** is calculated using formula $n = \log(x/y) / \log 2$, x = number of cells plated initial, y = number of cells at 80% of confluency.

Multilineage differentiation potential of MSCs is usually evaluated by the MSCs capacity to differentiate into three main lineages: osteogenic, adipogenic, and chondrogenic (Figure 19).

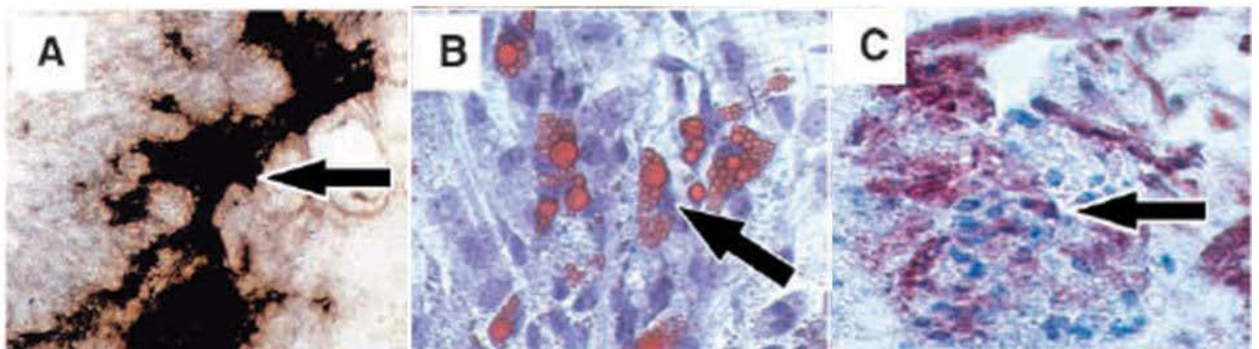


Figure 19. Multilineage differentiation potential of MSCs

A) von Kossa stain of mineralized deposits in MSCs cultures indicate osteogenic differentiation (Magnification x 200); B) Oil red-O staining indicate the presence of lipids in adipocyte cells within two weeks of adipogenic induction (Magnification x 200); C) Aggregate of collagen in cultures indicate chondrogenic differentiation (Magnification x 200). From: Gronthos et al., Journal of Cell Science 2003

I-3.4. Mechanisms of action of stromal cells on hematopoiesis

The haematopoietic niche comprises complex interactions between multiple cells and molecules.

A key player of these interactions is the osteoblast. This was proved by Nilsson S. K. *et al.*, using labelled HSCs that had been transplanted *in vivo*, and were re-found near the endosteum, where osteoblasts are also located [155]. In addition, the osteoblasts ablation results in a rapid and strong reduction in BM cellularity and a ten-fold reduction in the number of HSCs present in the BM [44].

Lodgement at the endosteal niche is driven by a calcium gradient and an array of osteoblast-mediated adhesive interactions [44]. The osteoblasts promotes HSCs migration to and lodgement at the endosteal HSC niche through adhesive molecules which it produces such as

osteopontin, N-cadherin, transmembrane c-KIT ligand stem cell factor (tm-SCF), and the polysaccharide hyaluronic acid involved in HSCs keeping at the endosteum [44].

Moreover, they signalize and regulate the survival / quiescence / proliferation of HSCs through expression of some receptors. Thus, through parathyroid-related peptide receptor (PTH1R) and activation of the protein kinase A (PKA) pathway, increase the Jagged 1 (JAG1) expression, which signals through Notch receptors on adjacent HSCs promoting their self-renewal [156]. Conversely, bone morphogenetic protein (BMP) binds to BMP receptors A and B expressed by osteoblasts, and promotes quiescence of HSCs. Likewise, osteoblasts synthesize Dkk1 (an inhibitor of Wnt signalling), and angiopoietin 1 (ANG-1), which binds to receptor tyrosine kinase TIE2 expressed on HSCs promoting HSC maintenance in the bone marrow [44], [156]. Moreover, the osteoblasts express the vascular cell adhesion molecule 1 (VCAM-1) which contributes to HSCs immobilization, protect from apoptosis and promote quiescence (Figure 20) [156].

Recently, an “endothelial HSC niche” has been described [44]. Thus, some HSCs that express CD150 are found in direct contact with the many endothelial sinuses that irrigate the BM. It is not clear, however, whether these HSCs that locate to endothelial sinuses represent cells in transit (as HSCs permanently leak into the circulation and home back to the BM) or whether they represent a separate HSC pool that is regulated differently. What is clear, however, is that these HSCs that lodge in specific endothelial niches must utilize a separate array of adhesive interactions from the HSCs. Indeed, unlike osteoblasts, BM endothelial cells that compose this endothelial niche express neither osteopontin, nor N-cadherin. Instead, they express high levels of platelet endothelial cell adhesion molecule-1 (PECAM-1/CD31), VCAM-1/CD106, P-selectin, and E-selectin whose ligands are all expressed at the surface of HSCs. Similar to the adhesion molecules expressed in the endosteal niches, P- and E-selectin-mediated adhesion regulates HSCs survival, proliferation, and differentiation. Thus, the two anatomically distinct HSC niches, endosteal and endothelial, must regulate HSC turnover differently [44].

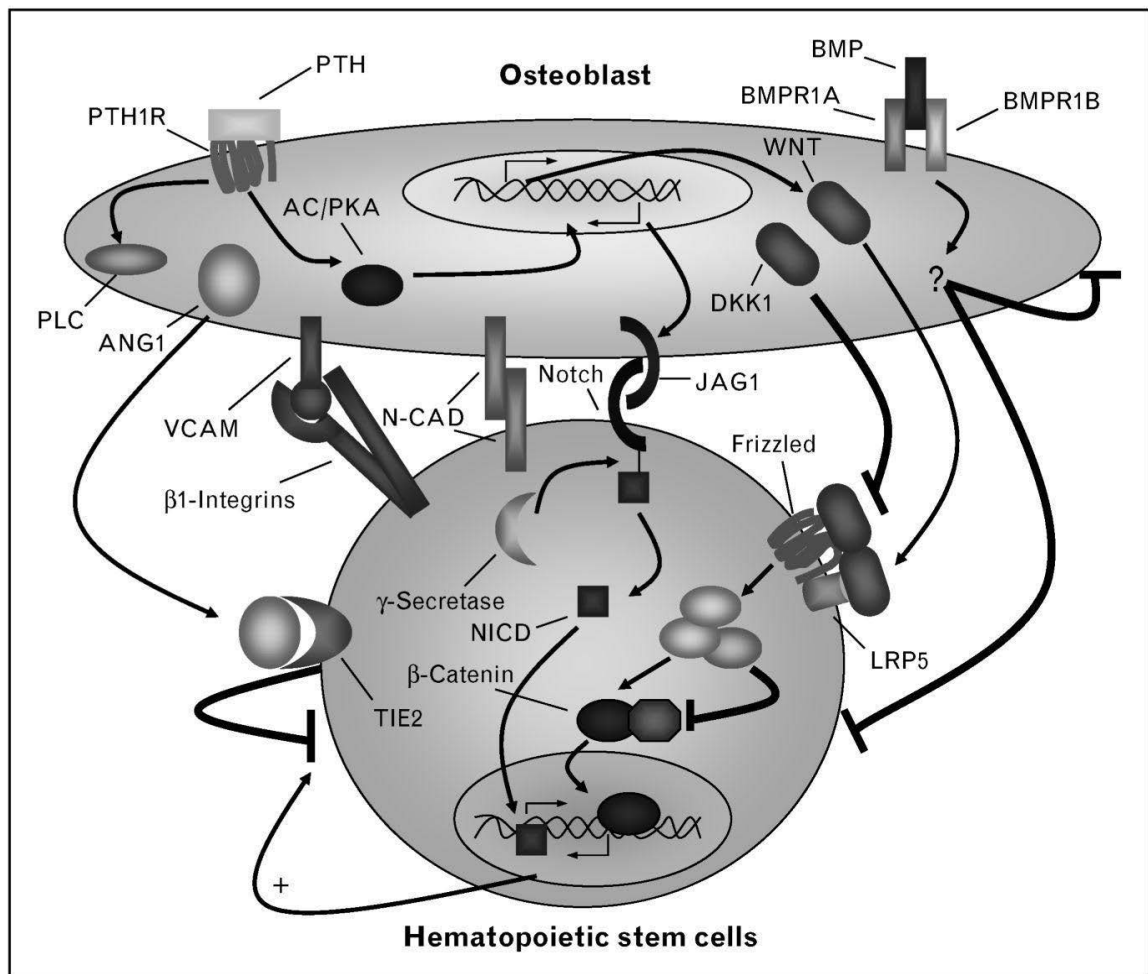


Figure 20. Molecular interactions between HSCs and osteoblasts at the endosteal HSC niche. From Benjamin J. F. et al., *Curr Opin Support Palliat Care* 2008

Another observation is that the adipocytes have a predominantly suppressive influence on haematopoiesis within the bone marrow microenvironment [157]. BM adipocytes are less haematopoiesis-supportive *in vitro* than their undifferentiated stromal or pre-adipocytic counterparts are. This is partly due to reduced production of growth factors such as GM-CSF and G-CSF [157], [158], [159]. Moreover, adipose tissue secretes neuropillin-1, lipocalin 2, adiponectin, and TNF alpha, each of which can impair haematopoietic proliferation [157]. Of note, TNF alpha and adiponectin inhibit progenitor activity despite the positive influence on the most primitive HSCs, suggesting that adipocytes prevent haematopoietic progenitor expansion while preserving the haematopoietic stem cell pool [157], [160], [161].

I-4. Conclusion

Recent data implicate cytokines, growth factors, adhesion molecules and signalling receptors as key elements in detecting and translating the extrinsic cues provided by the haematopoietic microenvironmental niches. Thus, these microenvironmental factors supply a specific set of molecules that determine or regulate the haematopoietic stem cell fate (Figure 21).

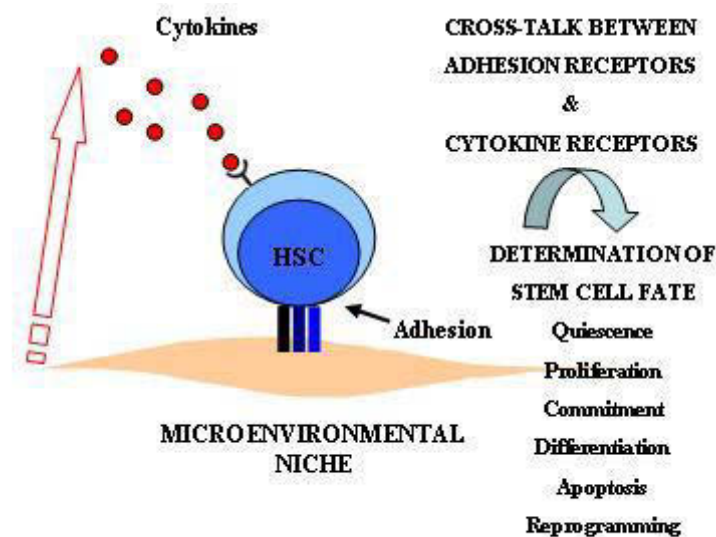


Figure 21. The hematopoietic stem cell microenvironment

Interactions between HSCs and components of their microenvironmental niche regulate stem cell fate. Adapted from: Watt S., Br. J. of Haematology 2001

Understanding these mechanisms involved in the control of the normal development of haematopoiesis, it is essential to identify those whereby bone marrow (BM) microenvironment contribute to the intramedullary abortion of haematopoietic precursors by apoptosis, and for selection of neoplastic haematopoietic clone(s), resistant to apoptosis and able to express factors promoting its (their) own growth, proliferation and migration.

Chapter II- The Myelodysplastic Syndromes

II-1. The Myelodysplastic Syndromes: Introduction

The myelodysplastic syndromes (MDS) represent a heterogeneous group of myeloid neoplasms characterized by abnormal differentiation and maturation of myeloid cells, bone marrow failure, manifested by peripheral blood cytopenias and hypercellular bone marrow, although in one quarter of the cases the bone marrow could be hypocellular, and a genetic instability with enhanced risk to transform to acute myeloid leukaemia (AML) [162], [163].

The incidence of MDS disease is estimated of 4 / 100,000 per year, but rises to 30 / 100,000 for people over 70 years [164]. In children, the annual incidence is 1-2 / million [165]. The median age decreased dramatically in recent years being 51 years in a recently published study, and the distribution of MDS subtypes demonstrated a markedly low incidence of MDS with deletion 5q (0.9%) [166]. In terms of gender, distribution is slowly greater in males [164].

Evolution to AML is about 20% and median survival is around 28 months [167].

II-2. Clonal hematopoiesis in Myelodysplastic Syndromes

To date, the dilemma of clonality seems far from being resolved. A clonal nature of the myeloid lineage is largely accepted, but the involvement of a lymphocytic lineage remains debatable [170]. The MDS clonality seems to be the result from a pre-malignant or malignant transformation, unlike the benign nature of haematopoiesis clonality from aplastic anaemia, and from paroxysmal nocturnal haemoglobinuria, where it is assumed that is due to contraction of the stem cell pool [171].

Tiu R. *et al.*, have summarized the theories, which can be put forward to explain the initial steps in the evolution of clonal stem cell diseases such as MDS. The defective stem cells may exist in a quiescent form and the abnormal stem cells carrying the genetic defect are more likely to be recruited for proliferation and to initiate the clonal evolution in the context of an overall depletion of the stem cell pool (Figure 22) [171].

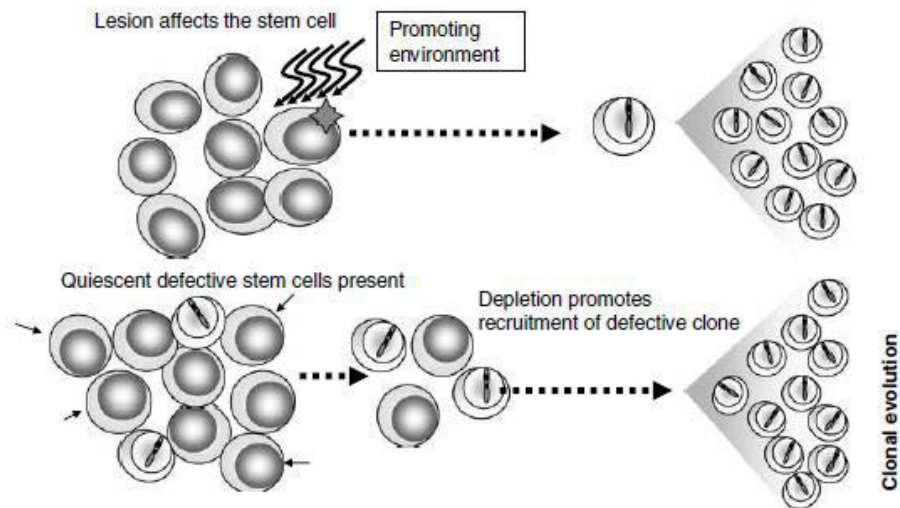


Figure 22. Mechanism leading to clonal expansion in bone marrow failure

Three possible hypotheses to explain evolution of clonal disease are illustrated. A stem cell may gain a lesion that, in the appropriate environment, leads to clonal expansion due to positive selection. Alternatively, under conditions of stem cell depletion, defective stem cells are more likely to be recruited initiating clonal evolution. From: Tiu R. et al., Leukemia 2007

In MDS, the acquisition of a genetic defect by an individual stem cell lead to the clonal expansion which may be the primary event leading to the gradual displacement of normal haematopoiesis. If chromosomal defects arise after stem cell recruitment, the early progenitors rather than true stem cells are subject to chromosomal damage and act as a source of clonal expansion (Figure 23) [171].

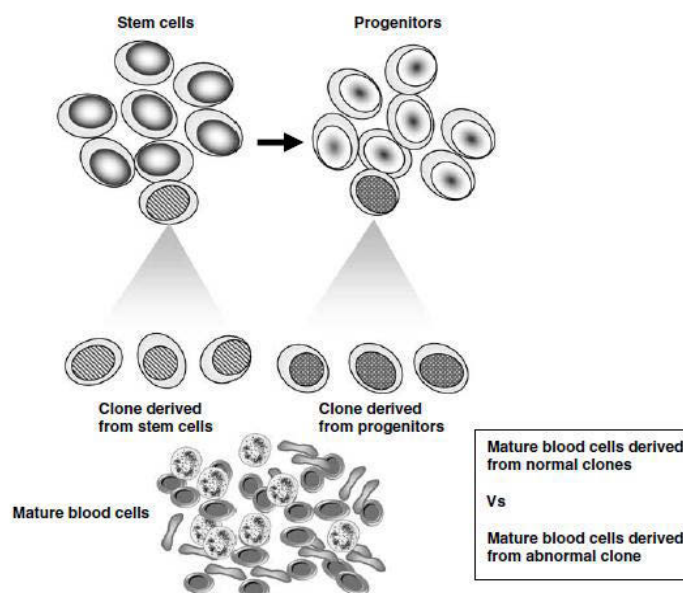


Figure 23. The nature of haematopoietic clonality in MDS.

From: Tiu R. et al., Leukemia 2007

If the clonal defect arises in a stem cell, all three lineages derived from that stem cell carry the lesion. Most of the lesions do not involve the lymph-haematopoietic stem cells, thus the lymphocytes are usually polyclonal. In some cases, the progenitor cells rather than stem cells are the initial source of clonal evolution. Both stem cell and progenitor-derived clones can variably contribute to the formation of mature progeny production.

However, this hypothesis (mechanical displacement of normal haematopoiesis) cannot explain the mechanism of cytopenia installed early in the disease.

Of note is, while telomeric erosion may accompany the persistence of a singular clone, by itself, telomere shortening is not a limiting factor for the long-term function of the defective stem cell. Likewise, activation of telomerase activity may be a part of this process, preventing simply depletion of the malignant stem cell [171].

In MDS, clonal evolution has a malignant character and is associated with the stepwise acquisition of a more aggressive phenotype, likely due to secondary defects acquired in the process of gradual clonal and subclonal selection. Additional defects may provide a growth advantage; facilitate immune escape and apoptosis resistance [171].

An increased prevalence of MDS in the elderly population is consistent with the accumulation of abnormal stem cells or deletion / depletion of normal stem cells. The best evidence for the pre-existence of many defective stem or progenitor cells could be provided if cytogenetic analysis is individually performed on purified precursors at the time when haematopoiesis is still polyclonal [171].

Another question that arises is which level of haematopoietic ontogenesis is initially affected by the clonal chromosomal defects. In MDS, the answer depends on the type of lesion taken into consideration. Thus, the cytogenetic abnormalities of chromosomes 5, 7, and 20 have been shown to be present in early multipotent CD34⁺ CD38⁻ Thy1⁺ cells [170]. In contrast, trisomy 8 was found only in myeloid lineage-restricted progenitors [170], [171]. In MDS with deletion 20q abnormality apparently the common precursor for myeloid and B-lymphocytes is affected [171].

However, in MDS the aberrant clone is capable to produce mature progeny. Thus, the differentiated progeny may correspond to a mixture of both clonal and normal cells, and the ability to produce differentiated progeny may depend on the type of the genetic lesion that in certain circumstances may result in a total maturation block. Of note is that lack of a clonal marker in all or some of the mature cells may not exclude clonality. Instead, a pathogenic chromosomal abnormality may just be a secondary lesion affecting only a subclonal population [171].

Another possibility is that the primary lesion is acquired at the level of the haematopoietic stem cells, while additional, secondary defects occur in progenitor cells [171].

II-3. Aetiology and pathophysiology of Myelodysplastic Syndromes

II-3.1 Aetiology of MDS

Traditionally, MDS is considered as either primary (idiopathic) or secondary after exposure to benzene [172], [173], occupational chemicals, particularly petroleum products, diesel derivatives, exhausts, organic solvents, fertilizers, nitro-organic explosives, [172], [174], semi-metals (arsenic and thallium), cereal dusts [175], [176], [177], prior treatment with radiation [172], [178], or chemotherapy agents [172], [179], to mention only the best documented secondary causes.

Additional data implicates exposure to tobacco [172], [180], excessive alcohol [172], [181], viral infections [172], [182], or autoimmune disorders [172], [183] as potential associations with MDS.

In light of several epidemiologic studies, there are evidences about a complex genetic predisposition in MDS, involving the DNA polymorphisms in genes that mediate DNA repair and those, which metabolize environmental carcinogens [175], [184].

Thus, the polymorphisms for two genes: for NAD(P)H: Quinone Oxidoreductase (NQO1), which plays a critical role in detoxifying benzene metabolites [175], [185], [186], and for glutathione S-transferases (GST) are strongly associated with an increased incidence of haematological malignancies [175], [187], [188], [189].

II-3.1 Pathophysiology of MDS

Recent research has revealed a further dimension to this pathophysiology, with extrinsic immunological and microenvironmental factors compounding the intrinsic stem cell defect and contributing to the pancytopenia and possibly to leukemic progression.

Table 4 summarizes the pathophysiology of MDS in relation to environmental factors exposures.

Marrow Microenvironment

To date, the role of microenvironment in MDS pathogenesis is controversial, being largely considered a disease of HSC. However, in recent years there is increasing evidence about the cellular microenvironment involvement in the pathogenic process, both by the secretory component and especially by direct interaction with HSC. Thus, in a previous study, Boudard *et al.* have reported growth defects of stromal cells isolated from MDS patients, resulting in low confluency, associated in some cases with caspase-3 activation and increases of angiogenesis [190]. The present work was focused on cell adhesion-mediated MDS pathogenesis.

Apoptosis, Dysplasia

Despite increased proliferation of the BM cells, there is an increased rate of programmed cell death. Indeed, some of the dysplastic appearance may be explained by apoptotic changes [175], [191], [192].

Certain types of behaviour related to apoptosis within the MDS disorders can be distinguished:

- in refractory anaemia (RA) / refractory anaemia with ringed sideroblasts (RARS), apoptosis always exceeded proliferation, whereas in refractory anaemia with excess of blasts (RAEB), this ratio equalized on account to increased proliferation;
- progression to RAEB in transformation (RAEB-t) / MDS-related acute myeloid leukaemia (AML), or MDS/AML was associated with a significant reduction in apoptosis, and proliferation;

These observations are supported by the fact that in RA / RARS compared with normal settings, the ratio between pro-apoptotic (Bax/Bad) versus anti-apoptotic (Bcl-2/Bcl-X) proteins is increased, whereas the disease progression was associated with a significant decrease of this ratio, due primarily to **Bcl-2 high expression** [193], [194].

Likewise, Kurotaki H and colleagues noticed that the suppression of apoptosis is the result of enhances bcl-2 expression besides the p53 accumulation in haematopoietic precursors selected from MDS-related acute myeloid leukaemia [195].

Moreover, an **increased expression of CD95 (Fas) and CD95L (Fas-L)** was noticed in CD34⁺ cells selected from the newly diagnosed MDS patients [196], [197], [198].

The increased apoptosis observed in MDS was correlated also with **increased levels of caspase-3**, which are significantly higher in RA and RARS than in chronic myelomonocytic leukaemia (CMML), RAEB and RAEB-t [199], [200].

Cytokines

Two possible mechanisms could be responsible for the increased rate of apoptosis encountered in the early stages of MDS, i.e., the apoptosis induced by soluble factors, cytokines synthesized by marrow mononuclear cells and mesenchymal stromal cells, and those related by direct cellular contact [175], [197], [201], [202], [203], [204]. In MDS, many studies link **over-synthesis of TNF- α** by BM MNCs to cell death [175], [202], [205], [206]. Furthermore, this cytokine was proved to have an inhibitory effect to both normal and MDS haematopoietic colony growth, indicating that residual normal haematopoiesis can also be blocked in MDS [175], [202], [203].

IFN- γ , IL-1, and TGF- β [175], [201], [207] as well as undefined factors produced by stromal cells have also been implicated in causing apoptosis [175], [208], but their role in producing marrow failure has not been well established. The identification of TNF- α as a key cytokine in cell death regulation and the increased susceptibility of MDS cells to TNF- α were the basis of several clinical trials of TNF- α inhibitors, which support their use to improve cytopenia [175], [201].

Moreover, the significantly higher levels of the caspase-3 were detected in the BM MNCs selected from MDS patients, which correlate with TNF- α level of cultures supernatant and with increased apoptotic index of haematopoietic precursors [209].

These observations were sustained also by Arimura K, in 2004, who noticed that matrix metalloproteinase inhibitors (MMPi) could inhibit the apoptosis priming in MDS BM cells via the inhibition of TNF- α and probably by soluble FasL secretion [210].

Angiogenesis

Data showing a significant **increase of BM microvascular density (MVD)** in MDS compared with normal controls have been reported. Surprisingly, it has been shown that MVD significantly decreases upon transformation to acute leukaemia and that MVD is significantly lower in *de novo* AML than in MDS [211].

Moreover, the bone marrow microvascular density correlates with significant **increases of serum levels of pro-angiogenic cytokines**, such as basic fibroblast growth factor (b-FGF),

hepatocyte growth factor (HGF) and tumour necrosis factor-alpha (TNF- α) [208], vascular endothelial growth factor (VEGF) [213], angiogenin, angiopoietin-1, platelet-derived growth factor, EGF(epidermal growth factor), and TGF-alpha and beta (transforming growth factor-alpha and transforming growth factor-beta) in MDS patients compared with normal settings [214]. Most of these angiogenic factors appear to be secreted by the neoplastic haematopoietic cells and appear to promote the growth and proliferation of the leukemic cells in an autocrine fashion. More importantly, angiogenic factors play a significant role in the clinical behaviour and outcome of both AML and MDS [214].

VEGF seems to be the best prognostic factor for evaluating the microvascular density, because high levels of this cellular protein were proved to correlate with short survival in MDS patients [215]. Likewise, endothelial cells release increased amounts of VEGF-C, another VEGF family member, in response to leukaemia-derived pro-angiogenic and pro-inflammatory cytokines such as b-FGF and IL-1, respectively. In turn, interaction of VEGF-C with its receptor VEGFR-3 (FLT-4) promotes the survival and proliferation of a subset of blast cells, and protects them from chemotherapy-induced apoptosis [216].

Immune Dysfunction in MDS

Hamblin *et al.* have raised the possible association between MDS with an autoimmune process, noting the emergence of autoantibody production, and monoclonal lymphocyte proliferation in some patients with MDS [175], [217]. The occasional finding of T cell clonality in MDS has been interpreted as evidence of T cell involvement in the stem cell disorder [175], [218]. MDS also shares some of the features of acquired aplastic anaemia (AA), a disease with well-known autoimmune aetiology [175], [219]. Both in AA and MDS, plasma TNF- α and IFN- γ levels are high and T cell-mediated myelosuppression held [175], [220]. The inhibitory effects of T lymphocytes on autologous granulocyte [175], [221], [222] or erythroid colony growth [175], [223] were also reported. These observations strongly suggest that, as in AA, an autoimmune T cell-mediated myelosuppression contributes to the cytopenia of MDS and that might be considered an immunosuppressive treatment in MDS which could restore the marrow functionality.

A Model of Disease Progression in MDS

A hypothetical model of MDS disease progression was proposed a decade ago [170], [175]. Transformation of normal stem cells induces danger signals or antigenic changes, hence an

autoimmune T cell response directed against the marrow cells. Both MDS clones and normal marrow cells, at various stages of differentiation, are directly inhibited by CD8⁺ T lymphocytes causing varying degrees of stem cell failure. The persisting autoimmune attack results in chronic overproduction of pro-apoptotic cytokines, especially TNF- α . This synthesis affects committed or mature cells and may contribute to a dysplastic morphology and increased apoptosis in the marrow. Despite the increased cell proliferation in MDS, the marrow fails to export sufficient cells into the blood because intramedullary apoptosis mechanism prevails over proliferation [175].

Bone marrow microenvironment as contributor to drug resistance

The soluble factors produced by bone marrow cells mediate the tumour cells homing, survival and proliferation, and the integrin-mediated adhesion sequesters the tumour cells to the microenvironmental niche [224]. All these processes are involved in the environment-mediated drug resistance. We summarize in the following some mechanisms responsible for the acquired resistance.

The BM stromal cells are regarded the main source of chemokine. They constitutively express the stromal cell-derived factor-1 (SDF-1 or CXCL12), implicated in tumour cells homing through the CXCR4 / SDF-1 axis, and in tumour cells survival and adhesion through CXCR7 binding. Moreover, the CXCR4 binding promotes enhances of VLA-4-mediated adhesion to the extracellular matrix components such fibronectin in solid tumours [224].

There are evidences that inhibitors of this pathway block tumour homing and engraftment, and reverse the cell adhesion-mediated drug resistance of tumours.

Other evidence is that integrin expression pattern is altered in tumour cells. They are involved in pathogenic process in two ways, i.e., by increasing the proliferation, migration and survival of cancerous cells, and by adhesion-mediated quiescence, which may contribute to the failure of standard cytotoxics in eradication of the tumour cells adhered to bone marrow stromal cells or to the extracellular matrix.

The principal actor of this group is β_1 integrin whose increased expression in invasive breast cancers or in small cell lung cancer negatively correlated with patient survival [224], [225], [226]. Likewise, the β_1 integrin adhesions regulate the stability and trafficking of mediators and inhibitors of apoptosis through a decrease of Bim stability or by interactions with Bcl-2 proteins.

Others integrins are noticed to be involved in carcinogenesis, including α_3 , α_4 , α_v , and β_7 [224].

II-4. Cytogenetic and Molecular abnormalities

II-4.2 Cytogenetic Abnormalities

A typical feature of MDS is the presence of invariant chromosomal abnormalities, which, with some exceptions (e.g., chronic myelomonocytic leukaemia [CMML]), atypical chronic myeloid leukaemia (aCML) are mostly unbalanced [171]. The clonal chromosomal defects affect certain chromosomes more frequently (Table 5). The resulting loss of heterozygosity (LOH) or duplications are related to malignant transformation [171].

Table 5. Invariant balanced and unbalanced chromosomal abnormalities detected by metaphase karyotyping and FISH

Type of lesion	% of cases	Chromosome lesions	Entity
Balanced	Rare	Inv3 t(3;5) t(3;3) t(5;12) t(5;17) t(5;12) t(5;21) t(11q23;v)	Primary MDS, MDS/MPD (CMML) Primary MDS Primary MDS CMML CMML CMML CMML Therapy related MDS
Unbalanced	~6-25 2-8 5-21 5 8-24 ~1-12	Del 5 / del 5q Del Y Trisomy-8 Del 17p Complex karyotype Del 7 / del 7q	Primary MDS CMML
Normal	40-60	Normal cytogenetics	Primary MDS CMML

CMML: chronic myelomonocytic leukaemia; MDS: Myelodysplastic syndrome; MPD: myeloproliferative syndrome. Adapted from: Tiu R. et al., Leukemia 2007

The **metaphase cytogenetics (MC)** is largely employed to identify the cytogenetic aberrations, which have an important role for the MDS diagnostic, prognostic, and therapeutic decision. While karyotypic abnormalities are the gold standard of MDS diagnosis, however, approximately 50% of cases do not show the chromosomal defects in routinely applied tests [171].

An alternative solution for the poor proliferation of dysplastic cells, which could be responsible for the low sensitivity of this method, is represented by **interphase fluorescent *in situ* hybridization (FISH)**, as it does not require cell division, and consequently, cell cultures, being more sensitive than traditional metaphase cytogenetics, allow detection of

smaller sized clones [171], [227], [228]. However, the latter benefit is still controversial [229].

Several FISH strategies could increase the method sensibility, such as combined control and target probes to detect genomic deletions or amplifications, dual fusion probes to identify the specific translocations, and break-apart probes to evaluate gene rearrangements [229]. However, the FISH is more reliable for the detection of duplications rather than deletions of chromosome fragments [171]. The major drawback of FISH is the limited number of probes directed towards the suspected targets [171]. The current FISH panels for MDS include probes for detections of -5/del(5q), -7/del(7q), del(20q) and trisomy 8 [229].

In order to improve the sensitivity of cytogenetic analysis, new karyotyping technologies have been developed including **single nucleotide polymorphism array-based karyotyping (SNP-A)** and **oligonucleotide array-based comparative genomic hybridization array (CGH-A)**. The major advantages of such technologies are the precise genomic scanning and the fact that they do not require cell division [171]. SNP-A karyotyping is useful in detecting loss of heterozygosity (LOH), even in cases without loss of ploidy, such as uniparental disomy (UPD), in evaluating abnormal clone dimensions relative to the total cell population present in the sample, and facilitating identification of cryptic lesions in bone marrow failure cases with normal or abnormal cytogenetics [171], [229]. Moreover, the SNP arrays may allow the identification of the invariant lesions associated with specific clinical phenotypes [171].

Comparative genomic hybridization (CGH) allows detecting changes of chromosome copy number by hybridization techniques between normal and tumour cells [172].

The parallel use of a combination of the three cytogenetic technologies – i.e., MC, FISH, and SNP-A – improved the detection rates of genetic abnormalities encountered in patients with MDS (e.g. for del(5q), -7/del(7q), trisomy 8, and del(20q) the detection rate being increased to 35% (MC+FISH), 38% (MC+SNP-A), 38% (FISH+SNP-A) and 39% when all three methods were applied [229].

II-4.1 Molecular Abnormalities

Chromosomal aberrations and genetic mutations play a pivotal role in the pathogenesis of MDS and MDS / AML. According to a proposed multistep pathogenesis of leukemia, after the initial damage of the progenitor cell, several additional alterations may affect these cells, providing them with a growth advantage (reviewed in Blau O et al [230]). The most frequent mutations along with their biological and clinical significance encountered in these pathologies are summarized in Table 6 [175], [231], [232], [233], [234], [235], and [236].

Table 6. Recurrent gene mutations in MDS and MDS/AML settings

Genetic mechanism	Gene	CRS	Cells affected by mutation	Biologic and clinical significance	Outcomes at diagnosis
Haploinsufficiency	<i>RPS14</i>	5q33	CD34 ⁺ cells	Abnormal erythroid differentiation and apoptosis ^[233]	Unknown ^[233]
	<i>miR-145</i> and <i>miR-146</i>	5q33 CDR	NA	Thrombocytosis ^[233]	Unknown ^[233]
	<i>Egr1</i>	5q31	NA	Enhances stem-cell self-renewal ^[233]	Unknown ^[233]
	<i>HSPA9</i>	5q31.2	CD34 ⁺ cells	Delayed erythroid maturation and increased apoptosis ^[233]	Unknown ^[233]
Mutations in regulators of DNA methylation	<i>DNMT3A</i>	2p	HSC/ Unfractionated BM samples	Contribute to clonal dominance ^[233]	Decreased survival ^[233]
	<i>TET2</i>	4q	NA	Impaired 5hmC production* ^[233]	Unknown ^[233]
	<i>IDH1/IDH2</i>	2q/15q	NA	Synthesis of 2-hydroxyglutarate which impares histone demethylase activity; Inhibit 5hmC production by TET2 ^[233]	Decreased survival ^[233]
Mutations affecting histone function	<i>EZH2</i> **	7q36.1	NA	Transcriptional repression ^[233]	Relatively poor survival ^[233]
	<i>UTX</i> ***	Xp11.23	NA	NA	Unknown ^[233]
	<i>ASXL1</i>	20q	NA	Regulation of histone function ^[233]	Poor prognosis ^[236]
Secondary MDS and MDS/AML or Therapy-related MDS	<i>TP53</i>	17p	NA	Mutations in the tumour suppressor ^[234]	Decreased survival ^[233]
	<i>RUNX1</i>	21q	NA	Impairment of HSC differentiation ^[234]	Decreased survival ^[233]
	<i>N/KRAS</i>	1p/12p	NA	Mutations in the signal transducer RAS ^[234]	Unknow ^[233]
	<i>FLT3-ITD</i>	13q	CD34 ⁺ cells	Impairment of HSC differentiation ^[234]	Decreased survival ^[233]
	<i>NPMc</i>	5q	NA	Impairment of normal cellular homeostasis ^[234]	Unknow ^[233]
MDS/MPN Overlap Syndromes	<i>CBL</i>	11q	NA	Marker of myelomonocytic clonal dominance without impact on clinical outcome ^[236]	Unknow ^[233]
	<i>JAK2</i>	9p	NA	Myeloid neoplasm associated with ringed sideroblasts and/or thrombocytosis ^[235]	Unknow ^[233]

* 5'-hydroxymethylcytosine (5hmC); DNA methyltransferase converts unmethylated cytosine to 5mC. 5mC is converted to 5hmC by the TET proteins in the presence of αKG generated by the IDH enzymes; ** *EZH2* (enhancer of zeste homolog 2), a polycomb group protein that methylates histones H3 (at K27) and H1 (at K26); *** *UTX*, an X-linked polycomb gene that encodes an H3K27 demethylase; NA indicates not available

Adapted from: Graubert T. & Walter M.J., *Hematology Am. Soc. Hematol. Educ. Program.* 2011

A new mutation of *SF3B1* gene was noticed in MDS cases, especially in the cases with presence of ring sideroblasts (RS) [236], [237]. This mutation was associated with better overall and leukemia-free survival [237]. *SF3B1* is located on chromosome 2q33.1 and encodes for a protein SF3B1, which associates with SF3A and 12S RNA to form the U2 small nuclear ribonucleoprotein particles, and that is believed to play a role in pre-mRNA splicing and associated transcription [237]. The occurrence of a somatic mutation of SF3B1 causes mitochondrial iron overload, ineffective erythropoiesis, and anemia, typical myelodysplastic features of RARS. The subsequent occurrence of a somatic mutation of JAK2 or MPL involves the acquisition of myeloproliferative features, including thrombocytosis (Figure 24) [235].

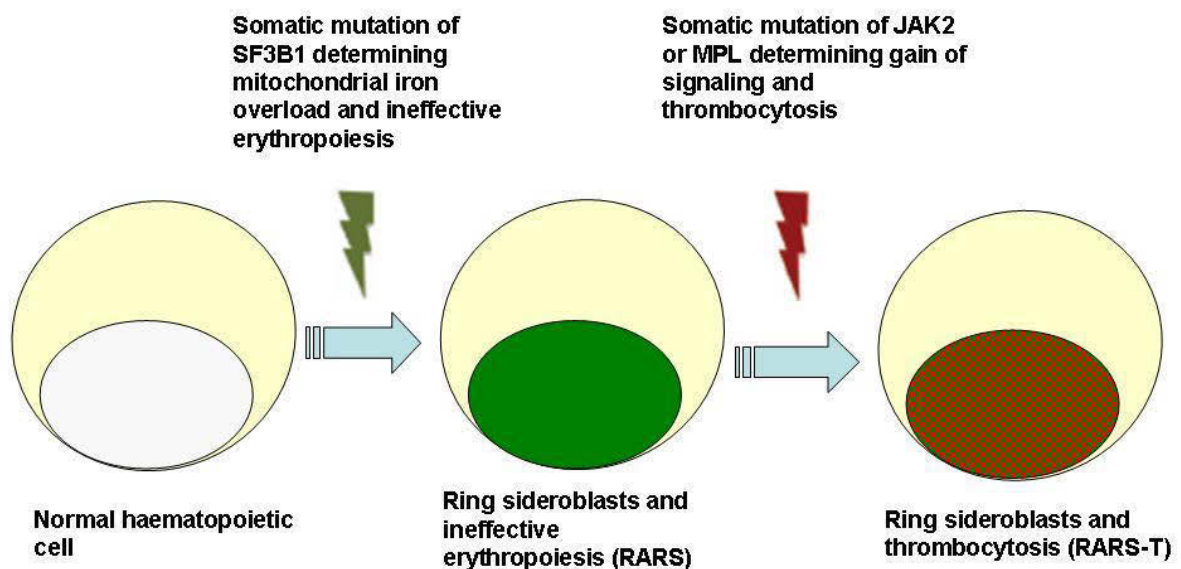


Figure 24. Schematic representation of the multiple-step molecular pathogenesis of RARS-T

(supporting the fact that the true MDS/MPN is a combination of SF3B1 and JAK2 or MPL mutations). Adapted from: Cazzola M. et al, Blood 2011.

The disease progression was associated with progressive methylation and transcriptional inactivation of the cell cycle regulatory genes (e.g. $p15^{\text{INK4b}}$) [171], [238], [239].

Recent evidences sustain the presence of the **cytogenetic aberration in MSCs** selected from MDS patients, but to a lesser extent than in the haematopoietic compartment (16% in MSC vs 37% in HCs), and more surprising these genetic abnormalities were distinct compared with those detected in leukemic blast [230]. The MSC chromosomal aberration were detected more often in MDS younger patients (median, 59 years) with poor prognostic. The median

follow-up time among patients with and without chromosomal aberrations in MSC was 19 and 33 months, respectively [230]. Chromosomes 1 and 7 were more frequently involved in MSC structural aberrations, and the most frequent aberrations were partial deletions and numerical aberrations in MDS cases. The structural aberrations (such as translocations and inversions) are the privilege of AML cases [230]. Surprisingly, it is noted that the MSCs of AML patients with FLT3 and / or NPM1 mutations were devoid of these mutations [230]. A great disadvantage of this test is the fact that the abnormal MSC clones were detected in a small number of analyzed metaphases (2-5 cells); "the large clones" involving 6-23 aberrant metaphases [230].

A potential explanation for this disadvantage is the selection of an "unstable" MSC clone which may facilitate the expansion of malignant cells [230].

II-5. Classification

The MDS classifications were conceived to perform a prognostic stratification of these heterogeneous entities. The initial FAB (French-American-British) system developed in the mid-1970s proposed the MDS subgroups definition using the cellular morphology. The FAB system focused on three criteria: percentages of blasts in BM, PB, and of BM sideroblasts. Bennett *et al.*, refined the system, in 1982, by introducing two supplementary parameters, i.e., the actual monocyte counts in PB and the presence of Auer rods in blasts [172].

To improve prognostic utility, the World Health Organization (WHO) published in 2001 a new standard classification system, which taken in consideration the cytogenetics findings [240]. Thereafter WHO classification has undergone a major revision in 2008, and the most relevant changes are:

- grouping in the "Refractory cytopenia with unilineage dysplasia (RCUD)" category of all cases which exhibit unilineage myeloid dysplasia;
- removing the "RCMD-RS = refractory dysplasia with multilineage dysplasia and ringed sideroblasts" entity;
- substituting "CMML = Chronic myelomonocytic leukaemia" with Myelodysplastic / myeloproliferative neoplasm (MDS / MPN);
- employing the percentages of circulating blasts to discriminate RAEB-1 of MDS unclassified (MDS-U);
- introducing the entity "Therapy-related secondary myeloid neoplasms" to regroup the AML and MDS chemotherapy related cases;

- adding a provisional entity, refractory cytopenia of childhood (RCC), which include children with cytopenia(s) with less than 2% blasts in the peripheral blood and less than 5% in the bone marrow and evidence of dysplasia in two or more lineages (Table 7) [241], [242].

Table 7. Peripheral blood and bone marrow findings in MDS (The 2008 revision of WHO classification)

Entity	Blood findings	BM findings
Refractory cytopenia with unilineage dysplasia (RCUD): (-RA refractory anaemia; -RN refractory neutropenia; -RT refractory thrombocytopenia)	Unicytopenia or bicytopenia ^a No or rare blasts (< 1%) ^b	Unilineage dysplasia: ≥ 10% of the cells in one myeloid lineage, < 5% blasts, < 15% of erythroid precursors are ring sideroblasts
Refractory anaemia with ring sideroblasts (RARS)	Anaemia No blasts	≥15% of erythroid precursors are ring sideroblasts, Erythroid dysplasia only, < 5% blasts
Refractory anaemia with multilineage dysplasia (RCMD)	Cytopenia(s) No or rare blasts (< 1%) ^b No Auer rods < 1 x 10 ⁹ /L monocytes	Dysplasia in ≥ 10% of the cells in ≥ 2 myeloid lineages (neutrophil and/or erythroid precursors and/or megakaryocytes), < 5% blasts in marrow, No Auer rods, ± 15% ring sideroblasts
Refractory anaemia with excess blasts-1 (RAEB-1)	Cytopenia(s) < 5% blasts ^b No Auer rods < 1 x 10 ⁹ /L monocytes	Unilineage or multilineage dysplasia 5-9% blasts No Auer rods
Refractory anaemia with excess blasts-2 (RAEB-2)	Cytopenia(s) 5-19% blasts Auer rods ± < 1 x 10 ⁹ /L monocytes	Unilineage or multilineage dysplasia 10-19% blasts Auer rods ±
Myelodysplastic syndrome-unclassified (MDS-U)	Cytopenia(s) < 1% blasts	Unequivocal dysplasia in < 10% of cells in one or more myeloid lineages when accompanied by a cytogenetic abnormality considered as presumptive evidence for a diagnosis of MDS (listed in Table 6)
MDS associated with isolated del(5q)	Anaemia Unusually normal or increased platelet count No or rare blasts (< 1%)	Normal to increased megakaryocytes with hypolobulated nuclei < 5% blasts Isolated del(5q) cytogenetic abnormality No Auer rods

^aBicytopenia may occasionally be observed. Cases with pancytopenia should be classified as MDS-U. ^bThe cases with marrow myeloblast percentage <5%, but a mean of 2% to 4% myeloblasts in the blood, should be included in RAEB-1. Cases of RCUD and RCMD with 1% myeloblasts in the blood should be classified as MDS-U. ^cCases with Auer rods and <5% myeloblasts in the blood and less than 10% in the marrow should be classified as RAEB-2. Although the finding of 5% to 19% blasts in the blood is, in itself, diagnostic of RAEB-2, cases of RAEB-2 may have <5% blasts in the blood if they present Auer rods or 10% to 19% blasts in the marrow or both. Similarly, cases of RAEB-2 may have <10% blasts in the marrow, but may be diagnosed using the other two findings: Auer rods and / or 5-19% blasts in the blood. Adapted from Vardiman J. W. et al., *Blood* 2009

II-6. Prognostic

Throughout the years, a decisive observation, such as a high number of BM blasts correlating with more rapid haematological deterioration and with severe clinical behaviour, continues to be applied even today in the prognostic staging system [243].

Greenberg *et al.*, in 1997, established a prognostic score using the multivariate analysis of clinical and biological features resulted by evaluation of 816 patients. In order to calculate a prognostic risk score, the IPSS system uses three clinical factors: percentage of marrow blasts, karyotype, and number of cytopenias (Table 8).

Table 8. IPSS Prognostic Score System

Prognostic variable	Score value				
	Low		Intermediate		High
	0	0.5	Int-1	Int-2	
BM blasts (%)	<5	5-10	-	11-20	21-30
Cytogenetics*	Good	Intermediate	Poor	-	-
Cytopenias**	0/1	2/3	-	-	-

*good prognosis: normal, 5q-, 20q-, -Y; poor prognosis: complex aberrations, -7,7q-; intermediate prognosis: all others, **haemoglobin <10g/dl, trombocytes <100x10⁹/l, absolute neutrophil count <1.5x10⁹/l. Adapted from: Haferlach T. and Kern W., Springer Berlin Heidelberg 2006

Based on this score, the median survival times were 5.7, 3.5, 1.2, 0.4 years for the IPSS risk groups “Good”, “Intermediate-1”, “Intermediate-2”, and “High”, respectively [175].

Chapter III- Focal adhesion proteins

III-1. Introduction

Focal adhesions (FAs), named also focal contacts, comprise dynamic groups of structural and regulatory proteins that link transmembrane receptors, such as integrins, to cell cytoskeleton and mediate signals involved in cell attachment, migration, differentiation, proliferation, and gene expression [244], [245].

This family consists of over 50 molecules that can be divided into three groups according to their cellular location and their role within this family (Table 9) [244], [246].

Table 9. Focal adhesion components

Location		Focal adhesion proteins
Extracellular		Collagen, fibronectin, heparan sulfate, laminin, proteoglycan, vitronectin
Transmembrane		Integrins 18 α and 8 β (24 combinations in humans), LAR-PTP receptor, layilin, syndecan-4
Cytoplasmic	Structural	Actin, α -actinin, EAST, ezrin, filamin, fimbrin, kindling, lasp-1, LIM nebulin, MENA, meosin, nexilin, paladin, parvin, profilin, ponsin, radixin, talin, tensin, tenuin, VASP, vinculin, vinexin
	Enzymatic	Protein tyrosine kinase: Abl, Csk, FAK , Pyk2, Src Protein serine/threonine kinase: ILK, PAK, PKC, Protein phosphatase: SHP-2, PTP-1B, ILKAP Modulators of small GTPase: ASAP1, DLC-1, Graf, PKL, PSGAP, RC-GAP72 Others: calpain II, PI3-K, PLC γ
	Adapters	p130Cas , caveolin-1, Crk, CRP, cten, DOCK180, DRAL, FRNK, Grb 7, Hic-5, LIP.1, LPP, Mig-2, migfilin, paxillin , PINCH, syndesmos, syntenin, Trip 6, zyxin

Adapted from: SuHaoLo, Development Biology 2006

Focal adhesions, unlike other structures involved in cell adhesion (gap junctions, tight junctions, desmosome, and hemidesmosome), are not detected as prominent structure under usual electron microscopy [245]. However, immunoelectron microscopy revealed that focal adhesions are dynamic structures which form at the anchorage site of cells to extracellular matrix (ECM), along with adhesion complexes, fibrillar adhesions, and podosomes (Figure 25) [244], [246].

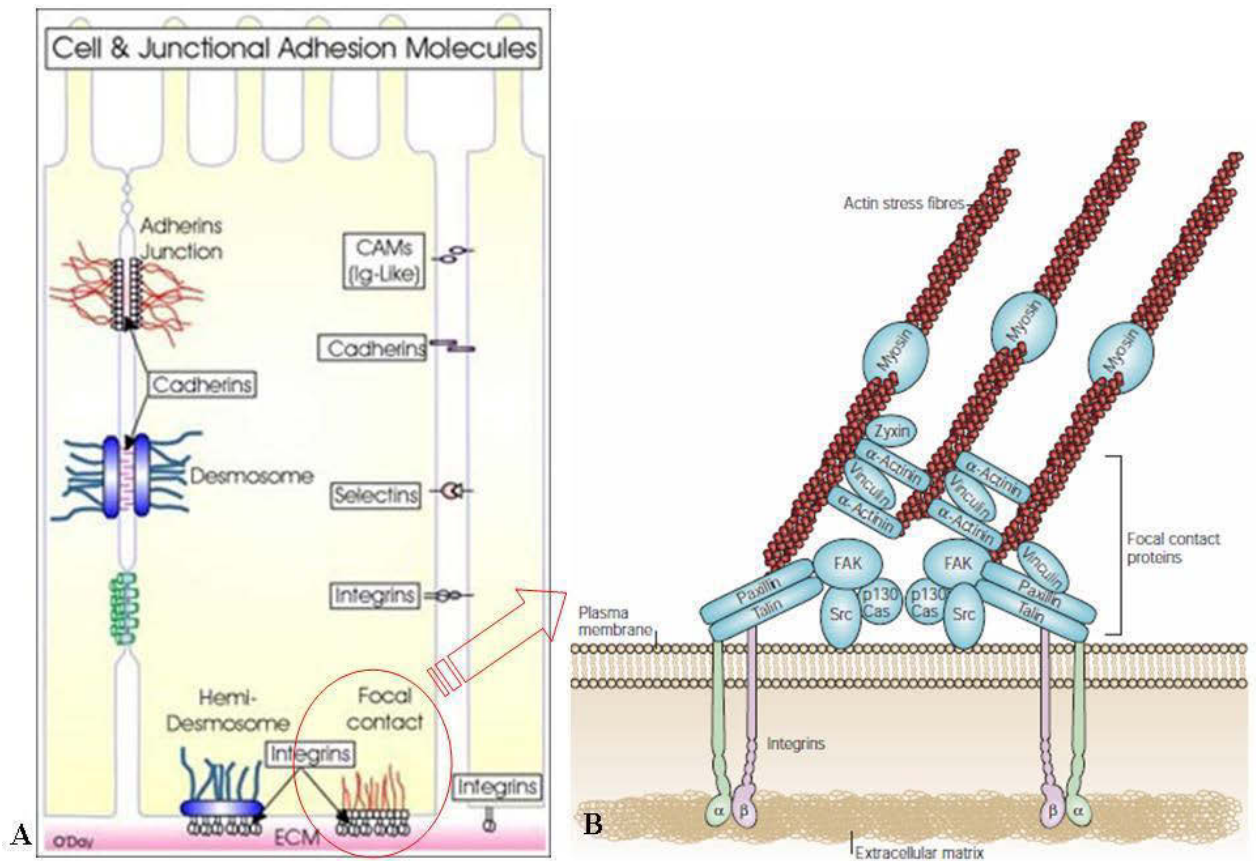


Figure 25. Cell adhesion model

(A) Overview of cell-to-cell and cell-to-extracellular matrix (ECM) adhesions.

Figure adapted from <http://www.erin.utoronto.ca>

(B) Molecular architecture of focal adhesions formed at the anchorage site of cell to ECM.

From Mitra S. K., *Nature reviews: Molecular Cell Biology* 2005

III-2. The components of focal adhesions

III-2.1 Adhesion receptors

Two main types of receptors mediate the interactions between cells and various components of the ECM: the integrins and syndecans.

In the following, we present in detail the integrins best characterized in the literature.

Integrins are heterodimeric transmembrane receptors consisting of noncovalently linked α and β subunits [246], [247], which belong to cell adhesion molecules (CAM's) family [248]. A combination between these subunits (which generate 24 different integrins) confers the ligand specificity [246], [249].

Integrins play important roles in cell adhesive interactions during normal physiological processes, e.g., embryonic development and wound repair, and during the progression of

diseases such as cancer [250]. Integrin ligands are not passive adhesive molecules; they are active participants in the cell adhesive process that leads to signal transduction. The focal adhesion kinase is phosphorylated in response to cell adhesions involving β_1 , β_2 , β_3 intracellular domains of integrins, and thereafter, it initiates signal transduction pathways. Migration, the assembly of an F-actin cytoskeleton at focal contacts, cytoplasmic changes of calcium ion concentration, modulation of proliferation and gene expression [250] are among the processes that belong to intracellular responses, involving integrins, such as $\alpha_5 \beta_1$ integrin largely expressed by cells.

Equally, these adhesions play a particular role in the growth and differentiation of haematopoietic stem cells. Integrins of the beta 1 family, mostly $\alpha_4 \beta_1$ integrin, very late activation antigen-4 (VLA-4), and $\alpha_5 \beta_1$ integrin (VLA-5) are best characterized and have been identified on committed progenitor cells as well as on more primitive stem cells. The emerging importance of the synergy between integrins and cytokine signalling pathways in the regulation of haematopoietic differentiation constitute a new paradigm in cell biology [251].

III-2.2 Focal Adhesion Kinase (FAK) Protein

FAK is a ubiquitously expressed protein-tyrosine kinase of 125-kDa, which consists of three domains: FERM (protein 4.1, ezrin, radixin and moesin homology) domain, a catalytic, kinase domain, and a focal adhesion targeting (FAT) domain. The FERM domain mediates interactions of FAK with different growth receptors like epidermal growth factor receptor (EGF receptor), platelet-derived growth factor receptor (PDGF), the tyrosine kinase ETK, and ezrin, the molecule connecting the actin cytoskeleton to the plasma membrane. The FAT domain recruits other proteins of focal contacts, such as integrins, paxillin, and talin, to kinase association in promoting motility and survival signals. This domain links also FAK to guanine nucleotide-exchange factors (GEFs) and induces the Rho activation. The last domain, towards carboxy-terminal region, FAT, contains three proline-rich regions designed to bind the proteins containing SH3 domains (Src-homology-3), such as p130Cas, the GTPase regulator associated with FAK (GRAF) and the Arf-GTPase-activating protein ASAP1. Likewise, FAK can be phosphorylated on several tyrosine residues, such as Tyr 397, 407, 576, 577, 861, and 925, and this leads to subsequent binding of Src, phospholipase C γ (PLC γ), suppressor of cytokine signalling (SOCS), growth-factor-receptor bound protein 7 (GRB7), the Shc adaptor protein, p120 RasGAP and the p85 subunit of phosphatidylinositol 3-kinase (PI3K). The phosphorylation at Tyr 925 creates site for GRB2 binding. An inhibitor of FAK catalytic

activity is FIP 200 (FAK-family interacting protein of 200 kDa), which binds the catalytic region.

In conclusion, situated at the intersection of many signalling pathways, FAK is a critical tyrosine kinase involved in a variety of processes vital for cellular physiology (Figure 26) [245], [252].

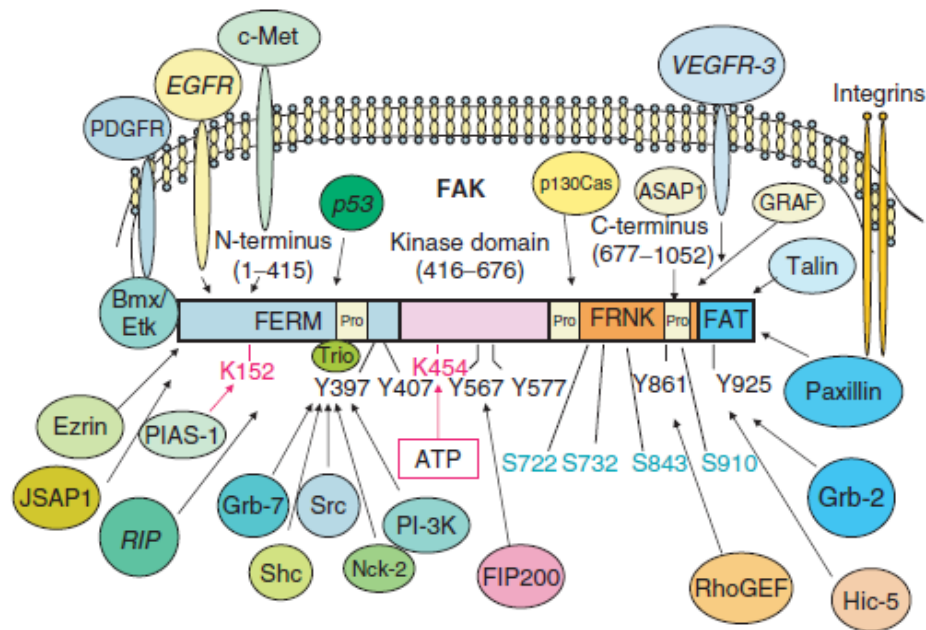


Figure 26. Schematic diagrams of FAK structure.

From Golubovskaya V.M. and Cance W.G., International Review of Cytology 2007

III-2.3 FAK-protein binding partners

FAK phosphorylation at Tyr397 site promotes Src binding, and thereafter their conformational activation, which finally leads to a dual-activated FAK-Src signalling complex. This complex is involved in phosphorylation of other proteins including two scaffolding molecules, paxillin and p130 Crk-associated substrate (CAS). Paxillin and p130CAS recruit other molecules to adhesions and regulate the organization of the actin cytoskeleton favouring the cell spreading and migration [245], [253]. Likewise, this cytoskeletal changes leads to subsequent activation of RAS-MAPK (mitogen-activated protein kinase) signalling proteins involved in cell survival [252].

Subcellular-localization studies revealed that p130CAS localize in different cellular compartments and its phosphorylation status influences cellular adhesion and cell-cycle progression [254].

Thus, nonphosphorylated p130CAS localize mainly to the cytosol, whereas the phosphorylated p130CAS is found in membranous, nuclear, and insoluble cytoskeletal fractions. Recent studies have proved that p130CAS proteins are involved in the loss of cell attachment observed in cell-cycle progression, as well as in cell morphological modelling [254]. Thus, p130CAS (-/-) fibroblasts are flat, round-shaped, and display specific characters of altered actin organization [254].

Paxillin is other protein, which shuttles between the cytoplasm and nucleus, fulfilling different functions in relation to its localization. Thus, the paxillin nuclear localization is regulated by FAK phosphorylation of the LIM domains which stimulate DNA synthesis and cell proliferation through suppression of H19 (a tumour-suppressor gene) and promoting Igf2 (gene insulin-like growth factor 2) transcription [255].

III-3. FAK functionality in cells

III-3.1 Motility

Experiments using FAK (-/-) cells show its implication not only in formation of focal adhesions, but also in their turnover that is essential for cell spreading and movement [256]. Specifically, the SH2 domain of Src, targeting Src to focal adhesions, and Tyr397 activity, as well as PI3K has been shown to be critical for FAK-mediated cell motility [252], [257], which can be blocked by the tumour suppressor gene PTEN through FAK dephosphorylation [252], [258].

III-3.2 Invasion and metastasis

FAK has been proved to regulate the invasive activity of both normal and Src-transformed fibroblasts through reconstruction of 3D-matrix adhesions [259]. While promoting the assembly of Src-CAS-CRK-DOCK180 complex in v-Src-transformed fibroblasts, the FAK results in RAC1 and JNK activation and subsequent increase of MMP2 and MMP9 expression promoting the MMP-mediated matrix degradation [259], [260], [261].

III-3.3 Survival

FAK plays a crucial role in survival signalling and has been linked to anoikis (detachment-induced apoptosis) [252], [262]. There is evidence supporting the antiapoptotic role of FAK by way of two mechanisms:

- a) induction of inhibitor-of-apoptosis proteins (IAPs) through AKT and NF- κ B survival pathways [252], [263];
- b) preventing apoptosis by keeping the caspase-3 inactive [264], or by p53 FAK regulation [265].

III-3.4 Proliferation

FAK could contribute directly on cell proliferation by three ways:

- a) by activation the RAS-ERK-MAPK (mitogen-activated protein kinase) pathway through FAK-Src signalling complex [252], [259]. FAK as well as Src are dependent on the chaperone HSP90 for their conformational stability and proper functions [266], [267], [268]. In addition, HSP90 can induce itself FAK phosphorylation and its activation in a RhoA-ROCK-dependent manner, i.e. in response to VEGF stimulation [269];
- b) by AKT signalization through PI-3K activation [252], [270];
- c) and, finally, by blocking paxillin nuclear export and stimulation of DNA synthesis and cell proliferation [255].

III-3.5 Angiogenesis

Takahashi *et al.* showed that VEGF induces FAK phosphorylation, which is accompanied by FAK translocation from perinuclear sites to the focal adhesions, and promotes its association with adaptor proteins Shc, Grb-2, and c-Src [252], [271]. This association has been shown to be important for promoting angiogenesis through FAK-Grb-MAPK signalling pathway [252], [272], [273].

III-4. FAK in tumorigenesis

III-4.1 FAK levels affect carcinogenesis

The cellular FAK expression is ubiquitous, Weiner *et al.*, in 1993, proved that low levels of FAK mRNA exist in normal tissues, while the primary and metastatic tumours significantly overexpressed FAK [252], [274]. FAK expression increases in a stepwise fashion in cell lines derived from various stages of the mouse skin carcinogenesis model [259], [275]. Recent evidence based on the use of an Inducible Cre-LOX model, which deletes FAK expression specifically in epidermal cells and in the hair follicles, has revealed that FAK contributed to both tumour formation, and the acquisition of malignancy [264].

III-4.2 FAK phosphorylation in cancer

FAK phosphorylation at different sites can be an imprint of tumour transformation of tissues and could explain some aspects of cancer behaviour [259]. Thus, the phosphorylation of FAK at Tyr397 site has been noticed in invasive tumours, but not in normal epithelium for instance [259], [276]. Likewise, other studies have shown increases of phospho-FAK-Tyr397 in different tumour types, such as carcinomas (cervical [277] and squamous cell carcinoma of larynx [278], as well as in haematological cancers [279], [280]. Moreover, FAK-Tyr397 phosphorylation is followed by the phosphorylation of other catalytic domains, such as Tyr576, Tyr577, Tyr407, Tyr861, Tyr925, which allow the full enzymatic activity of FAK or recruiting other signalling pathways [259].

FAK-Tyr925 phosphorylation was reported in colon cancers and was associated with E-cadherin deregulation during Src-induced epithelial-mesenchymal transition [259], [281]. In addition, FAK-Tyr861 phosphorylation is the imprint of VEGF stimulation and could be involved in tumour vascularisation [259], [269], and [282]. These differences of FAK phosphorylation favour the activation of different signalling pathways downstream (Figure 27). Phosphorylation at Tyr397 and Tyr925 causes the increased complex formation between FAK and its SH2-proteins, such as SRC, SHC, p85 (a phosphatidylinositol 3-kinase regulatory subunit), phospholipase C γ (PLC γ), growth factor receptor bound protein 7 (GRB7), GRB2, p120RHOGAP, which leads to mediate the signalling pathways involved in growth and survival [259]. The Src-specific FAK-Tyr925 phosphorylation is proposed to link FAK to the Ras-MAPK pathway, which is associated with adhesion changes responsible for epithelial-mesenchymal transition [283].

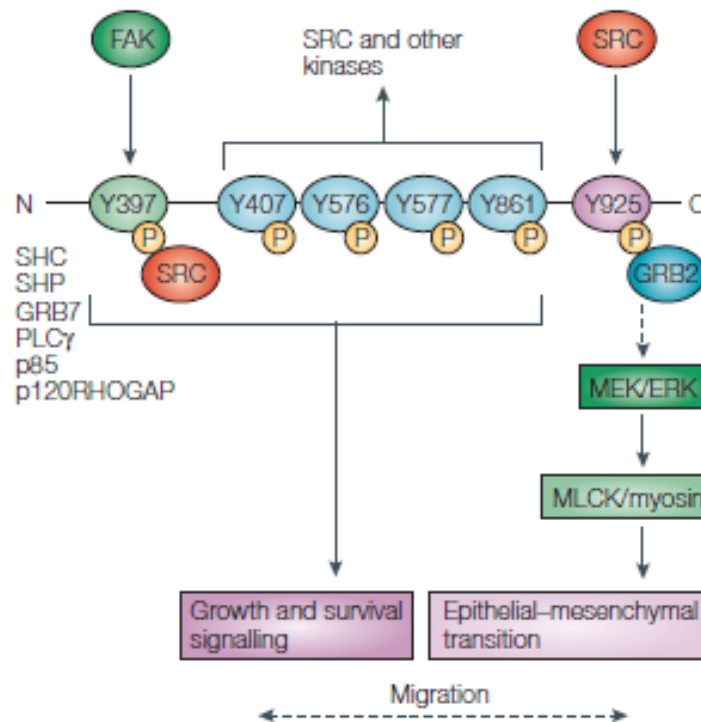


Figure 27. FAK phosphorylation regulates downstream signalling pathways.

From McLean G.W., Nature reviews: Cancer 2005

III-4.3 Model of the possible contributions of FAK in cancer development

FAK might contribute to cancerogenesis through four pathways:

- FAK contribution to growth through the RAS–MAPK (mitogen-activated protein kinase) pathway [252], [259];
- FAK-mediated induction of the invasive pathway involving signalling to RAC1 and JUN N-terminal kinase (JNK) and matrix metalloproteinases (MMPs) [259], [260], [261];
- by preventing apoptosis downstream of integrin or growth-factor-receptor signalling, via two mechanisms: keeping caspase-3 in inactive form [264], or by p53 FAK regulation [265];
- by protecting cells from anoikis, probably by FAK ability to sequester receptor-interacting protein (RIP) from the death-receptor machinery [259] (Figure 28).

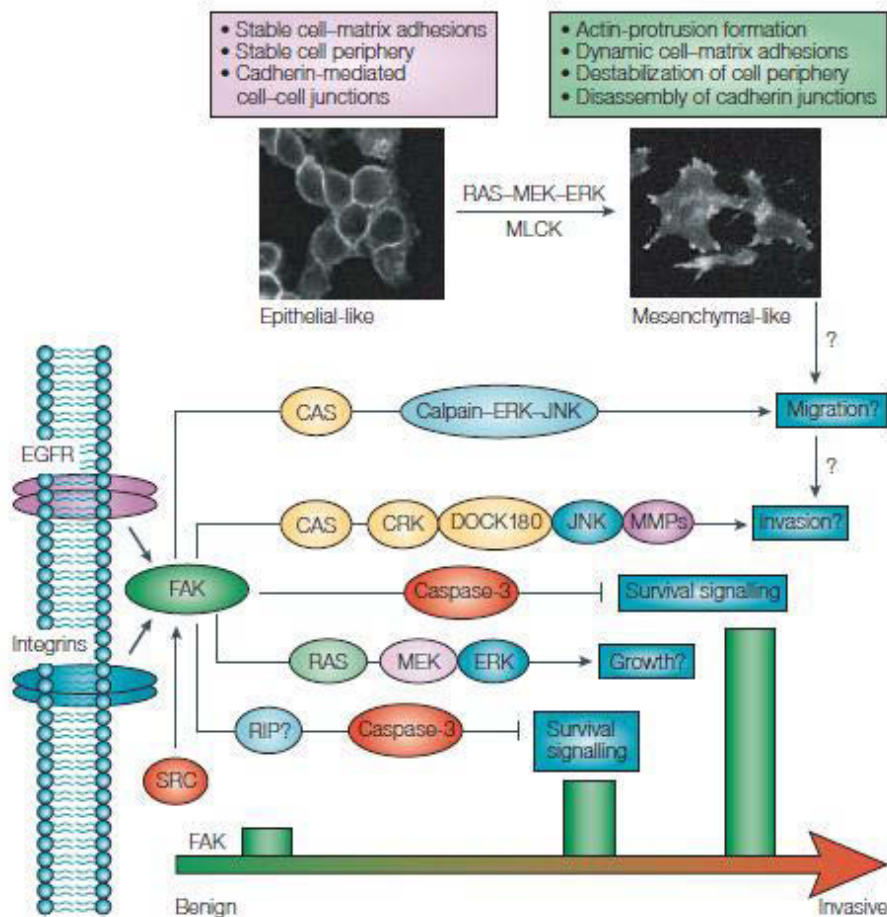


Figure 28. Model of the possible contributions of FAK in carcinogenesis.

From McLean G.W., Nature reviews: Cancer 2005

III-4.4 FAK expression in haematological malignancies

Recher *et al.*, in 2004, noticed in 42% of AML cases FAK over-expression in CD34⁺ selected cells, which correlates with an increase of migration from marrow to the circulating compartment, confers drug resistance, and negatively influences clinical outcome [279]. Moreover, in AML cells, FAK is phosphorylated constitutively on Tyr-397 residue [284]. To date, three possible hypothesis would explain this aberrant expression: a) in AML cells, 8q22–8q24 chromosomal region (containing FAK gene) is amplified in about 20% of cases [285]; b) the FAK phosphorylation could be induced by the aberrant expression of integrins [286], by chemokine receptor signalling pathways [287], by expression of Ras oncogenes [288], or autocrine production of haematopoietic growth factors such as stem cell factor [289]; c) and, finally, FAK phosphorylation may be facilitated by diminution of regulatory phosphatases activity, such as SHP-2 or PTEN [290], [291].

In line with this study, Tavernier-Tardy and colleagues confirm FAK over-expression in CD34⁺ cells selected from AML patients (with a 65.5% median percentage of positive cells). In addition, the prognostic analysis confirms the negative impact of this marker for overall patient survival, thus ranking among the phenotypic prognostic markers [292].

III-5. FAK targeted therapy

Two companies have developed ATP-competitive inhibitors to FAK, such as TAC-544 and TAE-226 (Novartis), and PF-228 (Pfizer). TAE-226 inhibits FAK, Pyk2, and the insulin-like growth factor I (IGF-I) receptor, blocks cell proliferation in culture, prevents cell invasion through Matrigel, and increases apoptosis in xenotropic tumour models. Until now, these molecules have proven effective in glioma and ovarian mouse models [265].

Chapter IV- Heat shock proteins

IV-1. Introduction

Heat shock proteins (HSPs) are a group of proteins, which act as molecular chaperones, binding other proteins in order to ensure their proper folding in the cytosol, endoplasmic reticulum, and mitochondria [293], [294]. They are also involved in intracellular transport of client proteins, in repairing or in proteasome degradation of those partially denatured by exposure to environmental stresses [294], [295], in controlling regulatory proteins, and in refolding of misfolded proteins [294].

IV-2. Heat shock protein 90 structure and functional features related to the conformational structure

HSP90 is one of the most abundant cellular chaperone proteins, formed by three structural domains: a highly conserved ATP binding domain near its N-terminus, the middle domain which is the major site of client protein binding, and the C-terminal domain which contains the dimerization interface and a conserved motif responsible for binding TPR-containing co-chaperones (Figure 29) [294], [296], [297].

HSP90 differs from other chaperones by the fact that its client proteins are tyrosine kinases (p185^{erbB2}[Her-2/neu], FAK, Akt), serine/threonine kinases (Cdk-4 and Raf-1), transcription factors (steroid hormone receptors, mutated p53, HIF-1 α , or transcription factors responsible for regulating oncoproteins FLT3, BCR-ABL, EGFR, CRAF, BRAF, MET, VEGFR) [266], [267], [268], [294], [296], [297].

The HSP90 dimerization is necessary so that HSP90 may be active and exercise its various functions. It is mainly present as homodimer form α - α or β - β , but there are also heterodimeric forms [298].

An interesting observation is the fact that, although HSP90 is abundantly expressed in most cells, only tumour cells contain HSP90 complexes in an activated high-affinity conformations unlike the normal cells where it is in a latent uncomplexed state [297]. This stronger association of client proteins to HSP90 in tumour cells might suggest a protective mechanism involved in its saving from proteasome recycling.

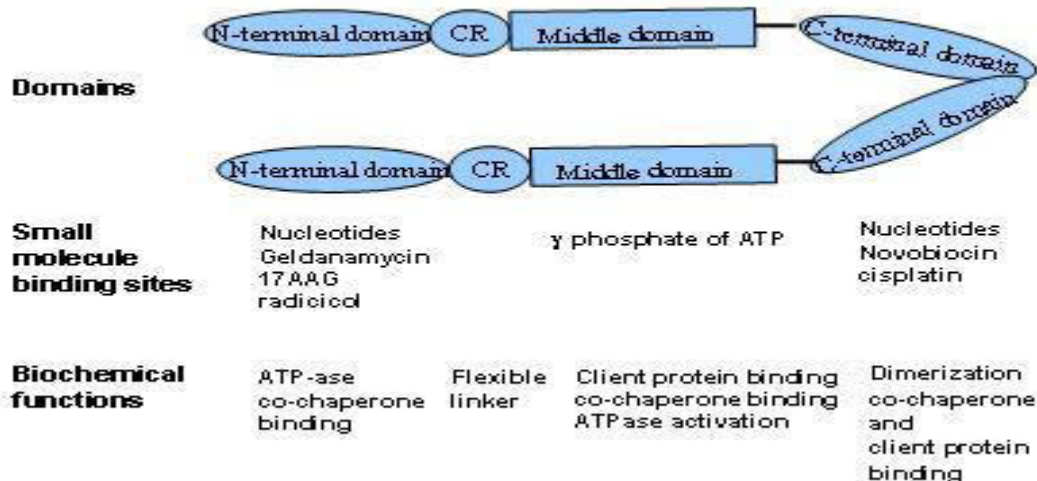


Figure 29. Structure of HSP90 dimer.

Adapted from Whitesell L. and Lindquist S.L., Nat Rev Cancer 2005

IV-3. HSP90 in tumorigenesis

The HSP90 is a potential target of anticancer therapy due to its involvement in various signalling pathways, cell proliferation, and survival, through regulation of a vast array of client proteins described above (Figure 30) [294], [299].

In the following, we review some signalling pathways involved in cancer development of which HSP90 is part:

- HSP90 controls the Akt kinase activity, involved in cancer progression by its stimulation in cell proliferation and by suppressing apoptosis;
- HSP90-BCL-ABL complexes conduce to resistance to traditional chemotherapeutic agents;
- HSP90-mutated p53 complexes conduce to disruption of normal transcriptional activity of this protein involved in cell cycle arrest and apoptosis;
- HSP90 controls the ubiquitination and proteasome degradation of HIF-1 α (a transcription factor that controls the expression of many genes, and thus, of their protein products which play a crucial role in tumour growth, angiogenesis, glucose transport and glycolysis);
- HSPs (including HSP90) controls steroid-dependent processes, by their associations in complexes, which are required to maintain the receptor in a conformation capable to binding hormone;

- HSP90 through its implication in the turnover of growth factors and other proteins, contributes to resistance to anti-growth signals, to promotion of angiogenesis, tissue invasion and metastasis [297].

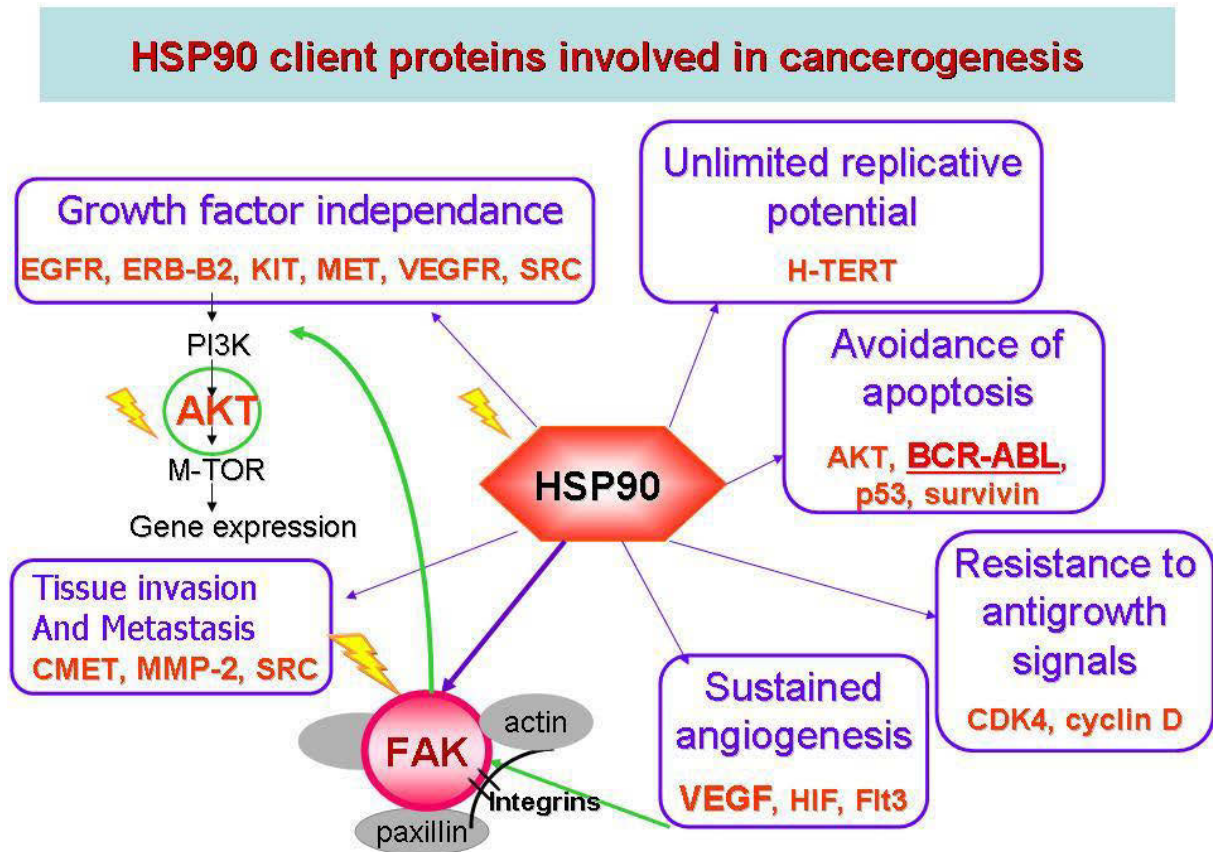


Figure 30. Model of the possible contributions of HSP90 in carcinogenesis.

From Campos L. Personal Communication AERES 2010

In AML CD34⁺ cells, the levels of HSP90 correlated with the percentages of CD34, p170, and bcl-2 positive cells, and its over-expression represents an imprint of poor-prognosis and of resistance to chemotherapy. Elevated levels of HSP90 were also found in samples exhibiting an autonomous growth in liquid culture or which form spontaneous colonies. A concomitant activation of phosphatidylinositol 3-kinase (PI3K) / Akt pathways was observed in these cases [300].

Likewise, in MDS cases with poor prognosis, Duval *et al.* reported the over-expression of HSP27, HSP60, HSP70, HSP90, and HSP110 mainly in CD34⁺ cells.

Indeed, the expression of all HSPs, except HSP70, correlates with FAB subtype, IPSS score, Bcl-2 related proteins, CD34, P glycoprotein (Pgp) expression, and with bone marrow blast

percentage. All this evidence denotes that their expression could be employed to pursue the disease progression [301].

Significantly higher levels of HSP90 (mean percentage of positive cells (38.3%), FAK (33.8%), phosphorylated FAK (31.4%), accompanied by phosphorylated Akt (26.7%) were traced in mononuclear cells (MNCs) and CD34⁺ cells from RAEB patients compared with those from RA (7.5%, 4.9%, 3.4% and 5.5%, respectively) or CMML patients (22.1, 19.8, 17.2, and 15.8%, respectively) ($p < 10^{-5}$) [280].

The addition of 17-(Allylamino)-17-demethoxygeldanamycin (17-AAG [5mM]), for 24 hours in liquid culture of BM MNCs selected from MDS patients, conduces to the downregulation of HSP90, pFAK and pAKT expression in this cells during the first 12 hours, followed by increased apoptosis at 24 hours [280].

This would indicate that HSP90 over-expression found in refractory anaemia with excess blasts (RAEB) is an unfavourable prognostic factor because it indicates resistance to apoptosis of both normal cells and the blasts.

IV-4. HSP90 as a drug target

The antiproliferative activity of HSP90 inhibitors (radicicol and geldanamycin) is thought to occur due to Src inhibition, ERB-B2 degradation, modulation of oestrogen and progesterone receptors, signalling inhibition of AKT, PI3K, or FLT3 pathways, modulation of angiogenesis, by preferential degradation of mutant BRAF (a client protein of HSP90 which is mutated in most myeloma cases or in colon cancers), or mutant EGFR (such as in lung cancer), by abrogation of ZAP-70 activity and by inhibition of P-glycoprotein function [299].

EXPERIMENTAL PART

I. Overview to Experimental Part

To date, the myelodysplastic syndromes are regarded as clonal disorders of haematopoiesis. Nonetheless, in recent years the role of stroma in etiopathogenesis of these diseases ought to be considered.

Data regarding this topic have been scarce and contradictory so far largely due to the complexity of the network of cells and molecules constituting marrow microenvironment. On the other hand, the scarcity of the data is due to the huge impact of isolation methods on the composition of MSC preparations that cause tremendous differences in the results of different groups. The most common isolation methods are based on the ability of MSCs to adhere to plastic or on the use of MSCs surface epitopes, such as specific markers or adhesion molecules.

Despite controversies [302], previous work has shown that adherent layers of BM stromal cells from patients with myelodysplasia achieved confluency at a significantly slower rate than those of normal donors [168], [190], [303]. Boudard *et al.* also showed that the stromal layer defects in MDS are associated in some cases with caspase-3 activation and increased angiogenesis [190]. Moreover, there is evidence that these abnormalities affect the functionality of haematopoietic compartment. Thus, in 2001, Tauro *et al.* showed that the stromal defects in MDS are of heterogeneous origin: altered matrix molecules and changes in superoxide cellular levels, which may contribute to abnormal survival and development of haematopoietic cells [304]. Thereafter, Tauro's team showed that this abnormal function of stromal cells in patients with MDS may contribute to increased apoptosis of haematopoietic cells within the marrow microenvironment and this effect appears to be due to the close HSC-to-stromal cells contacts, rather than the release of soluble factors [304]. The haematopoietic deficiencies have been also related to the abnormal expression of soluble factors, such as IL-1 β [190], [303], TNF α , and VEGF [190]. Long-term bone marrow cultures on myelodysplastic stroma revealed two broad patterns of haematopoietic progenitor cells (HPC) growth: a first group of cases included the patients whose cultures showed an abnormally low production of HPCs rapidly declining, i.e. within four weeks, to levels outside the normal range. The second group is the one where HPCs proliferation maintained within the normal range for at least seven weeks, albeit at the lower range limit [302]. In Coutinho *et al.* study, there was a predominance of RA and RSA cases, over other MDS (FAB classified) subtypes, of which the HPC cultures present comparatively normal growth [302].

Regarding the surface antigenic profile of MDS stromal cells vs. normal controls, there are not many references, although most of these antigens are adhesion molecules, having an important role in mediating MSCs-HPCs contacts.

Thus, Lopez-Villar *et al.* noticed a diminution of endoglin (CD105) and integrin β 4 chain (CD104) expression on MDS-MSCs [164]. Moreover, the same study indicates that the microenvironmental changes are accompanied by genomic aberrations of MSCs selected from MDS patients [168], [305].

Likewise, the BM microenvironment place ought to be considered as a contributor to drug resistance.

In this respect, the MDS-derived AML is known to be challenging from the therapeutic viewpoint due to the selection of tumour cell clones that express a multi-resistance phenotype and poor response to chemotherapy. The tumour microenvironment might influence drug response and the emergence of drug resistance in both haematological malignancies and solid tumours that metastasize to the bone marrow [224], [306]. Identification of microenvironmental targets, which enable the development of drugs that can be used in association with traditional agents to diminish the environment-mediated drug resistance, may be the response in these cases [224].

The present work aims to clarify some aspects related to adhesion deficiencies of MSCs in MDS settings, as well as their impact on its proliferation rate and on haematopoietic compartment.

II. Materials and Methods

II-1. Patients and healthy donors

Signed institutional review board–approved written informed consent was obtained from all patients and control subjects.

BM aspirates from twelve normal, thirty-five MDS, and three AML-MDS marrow samples were included in the study group.

According to 2008 World Health Organization (WHO) classification, the MDS patient's assignment to different groups was: Refractory cytopenia with unilineage dysplasia [RCUD] in thirteen cases, Refractory cytopenia with multilineage dysplasia [RCMD] in nine cases, Refractory anaemia with excess blasts-1 [RAEB-1] in nine cases, and Refractory anaemia with excess blasts-2 [RAEB-2] in four cases.

Nine of MDS patients with a mean age of 76 years (range, 56-85) and 4 control subjects with a mean age of 59 years (range, 39-69 years) were selected for focal adhesion protein's characterization.

Samples were obtained in the absence of any treatment.

Patient diagnosis was performed by cytological evaluation of BM smears after May-Grünwald-Giemsa staining and cytogenetic analysis.

Patients' clinical and biological characteristics are describes in Table 10.

Table 10 Clinical and laboratory characteristics of MDS patients and control subjects studied

Patient	Age	WHO 2008*	% blasts in PB	% blasts in BM	Hb [†] g/dL	Leucocytes x10(9)/L	Platelets x10(9)/L	PB Mo ^{††} x10(9)/L	BM cellularity	Dys- myelopoiesis	Dys- erythropoiesis	Dys- megakariopoiesis	RS [‡]	Cytogenetics	Transfusion Dependence [§]	BFU-E [‡] CFU-GM [‡]	
MDS patients																	
MDS1	73	RCUD-RA [#]	0	3.5	10.5	6.62	222	0.34	++	-	-	-	-	46XX	-	248	296
MDS2	85	RARS**	0	1	12.7	9.6	298	0.97	+++	-	++	-	(+) \geq 15%	◆	-	8	13
MDS3	72	RCUD-RT [#]	0	1	12.2	5.81	84	0.41	++	++	-	-	-	◆	-	200	184
MDS4	85	RCMD ^{†††}	0	3	10.1	3.37	100	0.44	+++	+++	++	++	(+) $<$ 15%	46.XY.del(20)(q11q13)[8]	-	160	180
MDS5	64	RCUD-RA [#]	0	2.5	9.8	3.7	308	0.26	++	++	-	-	-	46.XY	+	12	11
MDS6	78	RAEB-1 ^{‡‡}	1	11	11	3.21	324	0.21	+++	+++	+++	-	(+) $<$ 15%	46.XX.del(5)(q22q34) del(20)(q11q13)[19]	-	0	88
MDS7	84	RAEB-1 ^{‡‡}	3.5	7	9.5	3.98	445	0.15	+++	+++	-	-	-	46XX	+	28	72
MDS8	56	RAEB-2 ^{‡‡}	5	16.5	12.7	2.51	201	0.5	++	+++	-	++	-	46XX	-	19	29
MDS9	46	AML inv(3)(q21q26) ^{§§}	22	34	9.8	43.34	254	0.7	+++	++	+++	+++	-	46.XY.inv(3)(q21q26)[20]	-	174	92
Control BM																	
NBM1	39		0	0	14.7	7.65	275	0.32	++	-	-	-	-	ND	N/A	220	256
NBM2	69		0	0	13.5	6.97	175	0.28	++	-	-	-	-	ND	N/A	ND	ND
NBM3	59		0	1.5	11.7	4.69	389	0.59	+++	-	-	-	-	ND	N/A	240	248
NBM4	44		0	0	15.2	8.89	375	0.335	++	-	-	-	-	ND	N/A	268	376

*WHO indicates the World Health Organization classification of myeloid neoplasms and acute leukaemia; [†] Hb = haemoglobin; ^{††} PB Mo = peripheral blood monocyte count; [‡] RS = ringed sideroblasts; [§] Transfusion dependence: + = transfusion-dependent, and - = not transfusion dependent; [¶] Human colony-forming unit: BFU = burst-forming unit-erythroid; CFU-GM = colony-forming unit-granulocyte, macrophage; [#] RCUD- = Refractory cytopoenia with multilineage dysplasia; -RA = Refractory anaemia; -RT = Refractory thrombocytopenia; ^{†††} RCMD = Refractory cytopoenia with multilineage dysplasia; ^{**} RARS = Refractory anaemia with ringed sideroblasts; ^{‡‡} RAEB = Refractory anaemia with excess blasts; ^{§§} AML inv(3)(q21q26) = Acute myeloid leukaemia with inv(3)(q21q26.2); [◆] too few metaphases; ND=not done; N/A=not applicable

II-2. Cell Cultures

II-2.1. Culture-Expanded Mesenchymal Cells

- 1) Heparinised BM specimens are ficollated with Lymphoprep™ (AXIS-SHIELD PoC AS, Oslo, Norway) by centrifugation at 1500r/min, 30 min, 20°C, acceleration-deceleration 2;
- 2) Cells were washed 2 times: first time with RPMI 1640 medium (Eurobio, Les Ulis, France) and second time in Phosphate Buffered Saline (PBS) (Sigma-Aldrich) by centrifugation at 1500r/min, 10 min;
- 3) Number of cells were counted in Türk camera;
- 4) 2 - 2.5 millions of cells were added by T25 culture flask (25 cm²) in 10 ml MesenCult® Complete Medium (StemCell Technologies, Vancouver, BC, Canada);
- 5) Cells were incubated for 3 days at 37°C in an atmosphere of 95% air and 5% CO₂; After 1-2 days of cultures, cells which did not adhere or which are detached progressively are removed by changing medium: ½ new medium and ½ supernatant from 1st culture (BM stromal cells are isolated from haematopoietic cells due to their capacity to adhere to plastic surfaces);
- 6) Thereafter, the medium was changed twice weekly and replaced with half-new medium and half supernatant removed by culture until confluency is reached (80% confluency was obtained in 30-35 days).
- 7) After 80% confluency is reached, cells are harvested. Culture medium was removed and cells were washed once with RPMI 1640 without FCS. MesenCult® Dissociation Kit (StemCell Technologies) (2-3ml / 25cm² flask, warmed in advance) was used to detached cells from culture flasks: cells are incubate in MesenCult®-ACF Enzymatic Dissociation Solution (StemCell Technologies, Catalog #05427) at 37°C until they were detached (2-3 minutes usually; under microscopic control). The flasks were gently tapped to detaching the remaining cells.
- 8) 3 mL MesenCult®-ACF Enzyme Inhibition Solution (StemCell Technologies) was added in each flask to inhibit reaction. Cells were collected into a 25 mL conical tube and wash with 5 ml MesenCult Complete Medium (StemCell Technologies) supplemented with 20% Fetal calf serum (FCS, GIBCO® Invitrogen).
- 9) The viability and number of cells were quantified using trypan blue exclusion test.

II-2.2. Lab-Tek Cultures

After sorting, cells were collected in MesenCult[®]/ FCS (1:1) medium. Cells (1×10^3 per well) were plated on Lab-Tek[®]II Chamber Slides (Nalge Nunc International Corp.) in 0.5 ml MesenCult[®] medium and allowed to reach 70-80% confluence over 2 weeks.

II-2.3. Human Haematopoietic Colony-Forming Cell Assays

The detection and counting of erythroid burst-forming units (BFU-E) and colony-forming units-granulocyte-macrophage (CFU-GM) was performed in MethoCult[®] H4434 methylcellulose-based medium (StemCell Technologies). For this purpose, mononuclear cells containing the haematopoietic progenitors were separated from BM aspirates using density gradient centrifugation (1.077 g/cm^3) on Lymphoprep[™] (FreseniusKabi). After centrifugation, 1.25×10^4 BM mononuclear cells were resuspended in 1.2 ml MethoCult[®] (StemCell Technologies) and cultured at 37 °C and 5% CO₂ in 35-mm culture dishes (StemCell Technologies) for 14 days. Each sample was processed in duplicate. The colonies were then counted and classified based on morphological features by light microscopy.

II-3. Morphologic and morphometric analysis

II-3.1. Stroma Layers Stain

1. The medium was removed from cultures.
2. The adherent colonies which remain attached to the plate were washed twice using PBS.
3. 5 mL of Methanol (Merck Chemicals Catalog # 106035, Frankfurt, Darmstadt, Germany) were added by flask for 5 minutes at room temperature (methanol fixes the cells to the tissue culture dishes or flasks).
4. The methanol is discarded and the culture flasks are dried in air, at room temperature.
5. 5 mL of Giemsa Staining Solution (EMD Chemicals Catalog #R03055, USA) are added in each culture flask and leave for 5 minutes.
6. Finally, the Giemsa Staining Solution is removed and the culture flasks are rinsed with distilled water to remove non-bound stain.
7. The tissue culture flasks are allowed to dry at room temperature.

II-3.2. Evaluation of stroma layer composition

The stroma layer composition at 80% confluency was evaluated under an inverted microscope [Inverted (TissueFAXSi®) System, TissueGnostics GmbH (Vienna, Austria)] with a magnification x 40.

II-3.3. Morphometrical evaluation of stromal cells from primary cultures

Images were acquired in TIFF format using a PixelLINK PL-A622C/622000227 camera [Aegis Electronic Grup, Inc.], with an x 20 air objective. The field of view's (FOV) with dimensions of 650 x 489 µm, at a resolution of 1600x1200 pixels, were acquired from each flask. These images were then imported into MapInfoProfessional® 6.5 (Pitney Bowes Business Insight [formerly MapInfo Corp], USA), in order to perform measurements. Cells and nuclei were measured and values were translated from pixels in µm according to ratio: $x [1 \text{ pixel} / 1 \text{ µm in MapInfo}] = 0.406 \text{ µm microscopically (x value)}$. The calibration of measurements and the equivalence ratio has been established using the square (1 mm) of Burker-Türk camera.

II-4. Flow cytometry

II-4.1. Cell Preparation

The MSCs amplified during 30 to 35 days were harvested using the MesenCult® Dissociation Kit (StemCell Technologies), collected in glass tubes containing 5 ml MesenCult® (StemCell Technologies) with 20% FCS and filtered through a 70 µm cell strainer.

The cell number was determined using trypan blue solution (0.4% PBS).

II-4.2. Antibody staining

Cells processed above were pelleted and resuspended in 50 µl washing buffer and stained, on ice for 30 minutes.

Sources and isotypes of antibodies used are detailed in Table 11.

Cell viability was evaluated by staining with 1 µl of Propidium iodide (PI, Sigma, Poole, UK), 1 mg/ml, prior to FACS acquisition.

Data were acquired using a FACS Canto I cytometer and analyzed using DIVA software (Becton Dickinson).

Table 11 Antibody clones, isotype and source

Name	Source	Clone	Conjugate	Isotype
MSCs specific markers				
anti-STRO-1	Santa Cruz Biotechnology	sc- 47733	FITC	Mouse IgM
anti-CD73	BD Pharmingen™	AD2	PE	Mouse IgG1
Endothelium-related markers				
anti-CD31	BD Pharmingen™	M89D3	Alexa Fluor® 488	Mouse IgG2a
anti-CD106	BD Pharmingen™	51-10C9	FITC	Mouse IgG1
Hematopoietic-related markers				
anti-CD45	BD Pharmingen™	2D1	PerCP	Mouse IgG1
anti-CD16	BD Pharmingen™	B73.1	PE-Cy™7	Mouse IgG1
Adhesion markers				
anti-CD29	BD Pharmingen™	MAR4	PE-Cy™5	Mouse IgG1
anti-CD54	BD Pharmingen™	HA58	APC	Mouse IgG1
anti-CD44	BD Pharmingen™	515	PE	Mouse IgG1
anti-CD49e	BD Pharmingen™	IIA1	PE	Mouse IgG1
anti-CD144	BD Pharmingen™	55-7H1	PE	Mouse IgG1

II-5. Cell Selection

II-5.1. EasySep Immunomagnetic Selection Procedure

We performed immunomagnetic positive sorting using STRO-1 and CD73 marker expression in order to discriminate potential distinct cell subpopulations.

The fraction of STRO-1⁺ cells was immunodepleted for CD73 by exploiting the differences in epitope density and the avidity of STRO-1 mAb, the STRO-1⁺CD73⁻ cells bearing a higher number of epitope sites (Figure 31).

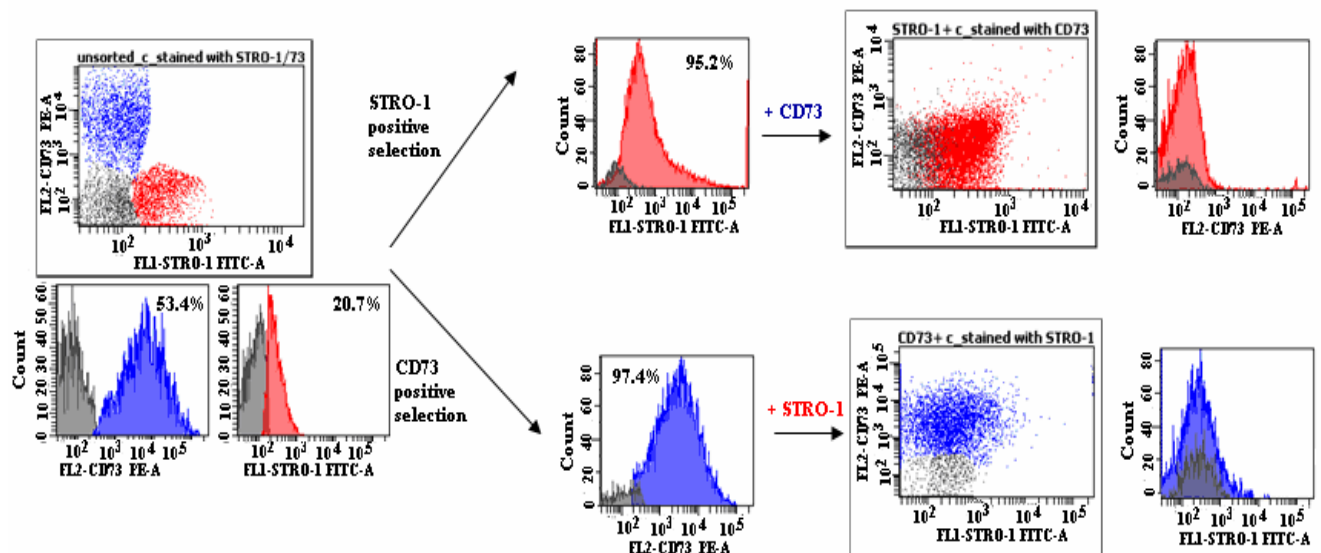


Figure 31. Experimental strategy of STRO-1 / CD73 Immunomagnetic Selection

Thus, MSCs, detached as previously described, were stained with mouse Anti-Human CD32 (Fcγ RII) blocker, then with FITC-conjugated mouse Anti-Human STRO-1, 3.0 μg/ml for 10⁷ cells for 1 hour on ice. Labelled cells were processed by adding EasySep[®] FITC Selection Cocktail 100 μg/ml of cells and EasySep[®] Magnetic Nanoparticles and by using the EasySep[®] magnet (StemCell Technologies). Following the isolation of the STRO-1 positive fraction, the remaining cells were stained with PE-conjugated mouse Anti-Human CD73 mAb (BD Pharmingen), 3.0 μg/ml for 10⁷ cells, kept for 1 hour on ice, then passed through all the remaining steps (previously described) using EasySep[®] PE Selection Kit to select the CD73-positive population (StemCell Technologies). All steps were monitored for purity and viability using flow cytometry.

The initial viabilities of the harvested cell fractions, as evaluated by trypan blue exclusion, were 79.6 ± 10.6% for normal stromal cells, 77.6 ± 7.26% for RC stromal cells, and 67.4 ± 10.2% for RAEB stromal cells.

After selection, the STRO-1⁺ and CD73⁺ fractions were enriched to >95% (96.34±2.26 for STRO-1⁺ and 97.74±0.95 for CD73⁺ cells); percentages were evaluated by cytometry from the singlets gate after excluding dead PI⁺ cells.

Four rounds of selection were performed for each population sorted.

II-6. Immunofluorescence

II-6.1. Cytospin Preparation

Cells remaining after flow-cytometry acquisition were spin down and resuspend at 5000 cells/ μ l in 4% PBS buffered paraformaldehyde solution containing 10 μ g/ml DAPI.

10 μ l of this suspension are placed on a glass slide and covered with a coverslip.

Double-stained preparations were visualized under a DM Microscope (Leica, Heidelberg, Germany) at 40 x, and respectively 100 x magnification, using a double band pass-interference filter (Omega Optical Inc, Brattleboro, VT).

II-6.2. Culture Slides Preparation

The cells were washed thoroughly to remove residual media and were fixed in paraformaldehyde 4% w/v (Merck Chemicals Catalog, Frankfurt, Darmstadt, Germany) for 10 minutes at room temperature (RT).

II-6.3. Antibody Staining of Slides

Non-specific background staining was blocked with antibody (Ab) buffer containing PBS (1x) / FCS (1% w/v) / BSA (bovine serum albumin, Sigma-Aldrich, St Louis, MO, USA, 0.1% w/v) for 1 h. Cells were then permeabilized with 0.1% Triton X-100 (Sigma-Aldrich) in PBS for 20 min before Ab application. Primary antibodies were diluted in Ab buffer before application as follows: FITC-conjugated mouse anti-human STRO-1 mAb (final dilution 1:50), and PE-conjugated mouse anti-human CD73 mAb (1:25), FITC-conjugated mouse anti-human Paxillin monoclonal Ab (mAb) (final dilution 1:50, clone 349/Paxillin, BD Bioscience), PE-conjugated mouse anti-human CD73 mAb (1:25, clone AD2, BD Pharmingen™), unconjugated rabbit anti-phospho-specific FAK [pY³⁹⁷] polyclonal Ab, (1:100, Invitrogen Corporation); mouse anti-human p130CAS mAb (1:40, clone 35B.1A4, Santa Cruz Biotechnology, Inc.), PE-conjugated mouse anti-human HSP90 α/β mAb (1:40, clone F-8, Santa Cruz Biotechnology, Inc.), FITC-conjugated mouse anti-human IgG2a,k mAb (1:50, clone G155-178, BD Pharmingen™), PE-conjugated mouse anti-human IgG1,k mAb (1:40, clone MOPC-21, BD Pharmingen™), rabbit anti-human IgG polyclonal Ab (1:100, DakoCytomation). Secondary antibodies (Invitrogen Corporation) were used at following dilutions: FITC-conjugated goat anti-mouse IgG (H+L) 1:50, PE-conjugated goat anti-mouse IgG (H+L) 1:25, Alexa Fluor 633-conjugated goat anti-rabbit IgG (H+L) 1:100 in Ab buffer. Incubation was performed overnight for primary antibodies and for 2 h for secondary antibodies at 4°C, in a moist chamber. Fixation was stopped by washing the cells 3 times with in PBS, pH 7.2.

Before acquisition, nuclear staining with 4' 6-Diamidino-2-phenylindole (DAPI, 1 µg/ml) was performed for 30 minutes at 4 °C.

Slides were mounted in Faramount Aqueous Mounting Medium (Dako Denmark).

II-6.4. Relative Fluorescence Measurements

Triple-stained preparations were visualised under an Axio Observer Z1 microscope (Carl Zeiss, Inc.) at 100X magnification. Signals were recorded simultaneously by three photomultiplier tubes (PMT 1–3). The images (TIFF format) were captured with a PixelINK PL-A622C/622000227 camera (Aegis Electronic Group, Inc.) by taking multiple exposures through bandpass optical filter sets appropriate for FITC, Texas Red, Alexa Fluor 633 and DAPI using a 100X Plan Apochromat objective.

Analysis and quantification of immunofluorescence staining was performed using ImageJ software (<http://rsb.info.nih.gov/ij/>).

Five representative fields were analysed per filter and per slide.

Data recorded for an average of 25 cells per group were exported to Excel (Microsoft) for further analysis.

II-6.5. Protein Clustering Analysis

The Origin 7.0 (Microcal Software) charts were used to display the percentage of co-localisation between the analysed proteins in each of 10 spindle-shaped cells and 10 large cells per group. The scatter plots and the colour co-localisation maps were generated by ImageJ software.

The degree of co-localisation was evaluated using the various co-localisation coefficients, and proteins belonging to the same complex were identified using the Intensity Correlation Quotient (ICQ) and intensity correlation plots (ICA) as previously described [307], [308], [309].

Depending on the value of the coefficient ICQ it can be distinguished 3 patterns of staining: **random** staining $ICQ \sim 0$ ($-0,1 < ICQ < 0,1$), **segregated** staining $0 > ICQ \geq -0,5$, the segregated pattern is assigned to those proteins with the asynchrony or complementary staining (the proteins belonging to different complexes or structures), and **dependent** staining $0 < ICQ \leq +0,5$. The dependent staining is assigned to the proteins how are the parts of the same complex and their staining intensities should vary in synchrony [307], [309].

II-6.6. Cell cycle and Apoptosis evaluation using DAPI Nuclear Counterstain

Total amount of DNA in cells was obtained by multiplying the number of intensity pixels corresponding to the signal light output of DAPI staining with nuclei area. A histogram

stretching was applied then (all pixel values from the ROIs were divided by a constant value) in order to obtain a compact set of values from highly dispersed initial values.

Apoptosis was evaluated by assessing the number of cells containing nuclear changes indicative for this process (cells with irregular edges around the nucleus, chromatin condensation and nuclear fragmentation).

II-6.7. Confocal microscopy

Confocal microscopy was carried out in MSCs cultured on Lab-Tek slides processed as described previously for common fluorescence. Images were acquired using confocal spectral TCS-SP2 microscope (Leica, Heidelberg, Germany).

II-7. Functional Assays

To assess the growth characteristics of the two major MSCs subpopulations, STRO-1⁺CD73⁻ and STRO-1⁻CD73⁺, proliferation and clonogenicity tests were performed.

II-7.1. Proliferation Tests

To do so, 1×10^3 viable MSCs (quantified using the trypan blue exclusion test) were plated in 25 cm² flasks, and the number of cells was counted on days 1, 7, and 14. We then calculated the proliferation index (the difference between the number of harvested cells and the initial plated number) and the doubling time (the duration of one mitosis) estimated by the ratio of the time necessary for 1×10^3 MSCs to reach 80% confluency and the number of population doublings. The number of population doublings was obtained using the following formula: $n = \log(x/y) / \log 2$, where “x” is the number of initial seeded MSCs and “y” is the cell harvest number [310], [311].

II-7.2. Clonogenicity Tests

The clonogenic potential of MSCs was established with plating efficiency (PE) or CFU efficiency assays. After 14 days of culture, the medium was removed and the colonies were fixed in methanol and treated with Giemsa stain. The colony numbers were then scored. A colony was defined as consisting of at least 50 cells. PE was the ratio of the number of colonies formed to the number of cells seeded x 100% [312].

II-8. Data standardization and statistical interpretation

In the present thesis, we used two types of statistical analysis: descriptive and comparative. Statistical analysis consisted in determining the arithmetic mean, standard deviation (SD),

standard error (ES), and variation coefficients (%). Student's *t*-test (p) was employed to compare the parameters among the groups and was calculated using SPSS software (SPSS 13.0 Chicago, <http://www.spss.com>) and Microsoft Excel 2003.

Differences between the groups were considered to be significant when $p \leq 0.05$.

EXPERIMENTAL RESULTS

III.1. Intrinsic growth deficiencies of mesenchymal stromal cells in myelodysplastic syndromes

-Stem Cells and Development-

-In press-

Stromal microenvironment is a target of the oncogenesis process as instrument in the control of hypoxia, acidosis and interstitial homeostasis balance, indisputable links of tumor progression. The first article exploited the fundamental information regarding the intercellular dialogue (MSC-MSC and HPC-MSC) in order to define their physiological role in bone marrow microenvironment equilibrium. His reactivity was observed during progression in the MDS risk groups, each of these entities surprising us by behaviors harmonized to haematopoietic partner requirements.

Briefly the experimental schedule for this article was:

- 1) MSCs isolated from plastic-adherent BM MNCs were amplified until 30-35 days in cultures.
- 2) Morphometric-morphologic analyses were conducted on stromal cells isolated from MDS vs. normal primary cultures.
- 3) Thereafter, stromal cells were detached, and two steps of positive selection were performed in order to discriminate the STRO-1⁺ from CD73⁺ MSCs.
- 4) Purity and viability were monitored using flow cytometry and immunofluorescence assays.
- 5) Cell yield and growth characteristics were evaluated for each fraction and for MSCs selected from MDS compared to normal controls.
- 6) Statistic analysis were employed to determine correlations between MSC phenotypic abnormalities with MSC growth, and, with haematopoietic compartment dysfunctions (Figure 32).

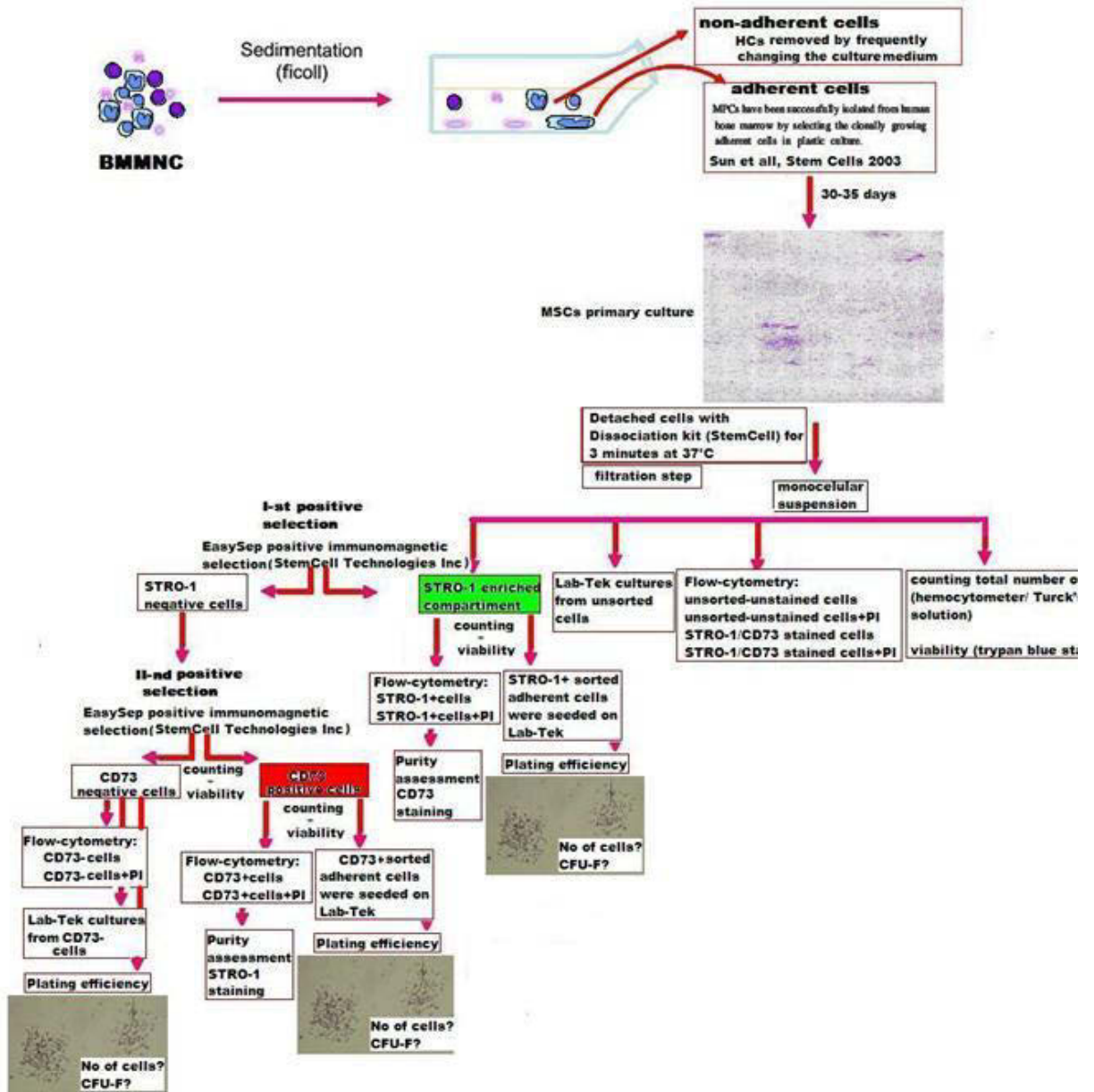


Figure 32. Experimental strategy of MSCs selection and functional assays

III.1-1. Relevance of morphological and morphometric evaluation of BM stromal cells from MDS settings vs. normal counterpart

Three culture systems were used to isolate and examine *in vitro* characteristics of stromal cells in MDS settings compared to normal controls.

In principle, the RPMI-1640 supplemented with 10% FCS, as well as MesenCult® media allowed the development of a fibroblastic stromal layer without haematopoietic cells [154], [313]. MyeloCult® HT5100 medium allows the development of a stromal layer with haematopoietic progenitors [314].

Cell confluency was scored from 0 to 3, corresponding to a stromal layer covering from < 25% (score 0), 25-50% (score 1), 50-70% (score 2), and > 75% of the area of the culture flask (score 3), respectively.

After four weeks, confluency of adherent layers was observed in all normal cultures, in all systems.

In **Refractory cytopenia**, 50% of cases (11/22) show deficiencies to reach confluency, particularly in RPMI-1640 medium, but also in MyeloCult® HT5100:

- confluency 0 in two cases,
- confluency 1 in six cases, and
- confluency 2 in three cases (Figure 33).

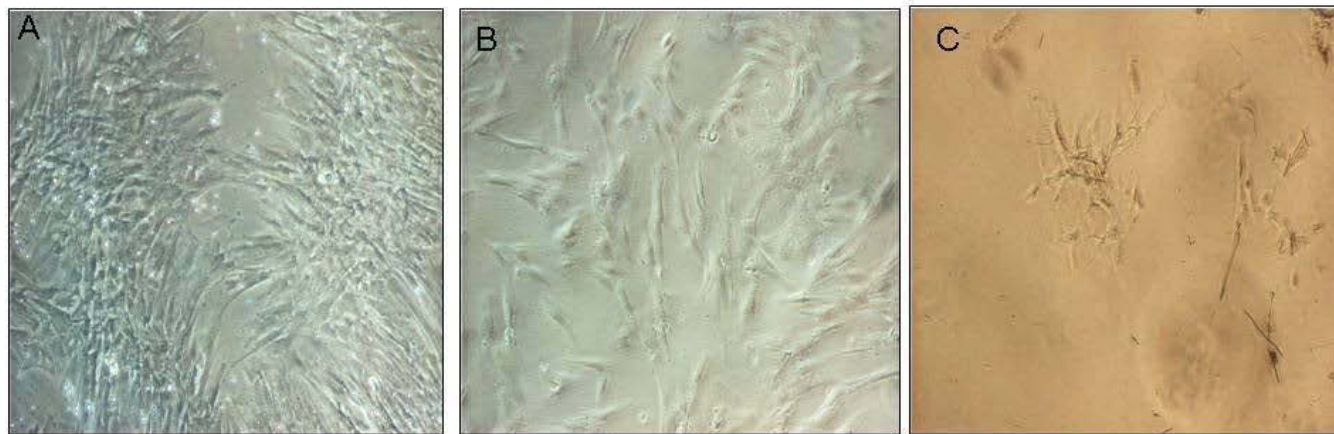


Figure 33. Representative examples for stromal cells cultures at week 4 in RPMI-1640

A) Normal cells (score confluency 3); B) 50% confluency in RA case (confluency 2); C) no confluence in a RCMD case (score 0) (Magnification 20 x)

Likewise, in **AML** cases, low confluency (score 0 and 1) was noticed in two cases (2/3), and in **RAEB** group these abnormalities were more rare and not as important (in 2/13 cases, confluency score 2)

Of note is the fact that in MDS layers exhibited spontaneous lysis in 35 (12-48) days of cultures, in RPMI-1640 especially.

In RAEB MSC cultures are noticed also:

- the colonies architecture disorganization, with clusters of aberrant proliferation, and,
- giant “amorphous” deposits in cultures.

Although, prior us, some authors has described these deposits in other haematological malignancies, or in BM metastasis, as fine meshwork of reticular fibres or reticulin / type III collagen, elastin [315], or tenascin [316], their relevance remains obscure. However, the presence of tenascin is regarded as an imprint of pathological states of the bone marrow [316].

The morphometrical evaluation of MSC primary cultures has revealed the different distribution of the three morphotypes of MSC (small, rounded-shaped; thin spindle-shaped; and large, flat cells) in MDS layers compared with normal settings; with the preponderance of the small-rounded morphotype, on the detriment of large, flat cells, which is considered the onset of terminal differentiation.

III.1-2. BM stromal cells phenotype (MDS vs. Normal controls)

The phenotypic evaluation of MSC layer composition highlights increased percentages of STRO-1⁺ cells in 20 to 30 days of culture that co-expressed CD106 and CD31 in the RAEB and RC groups. Moreover, this issue persisted in the MDS groups until 60 days, when cell autolysis occurred.

Likewise, under the MDS condition, the CD73⁺ subsets of MSCs, presents a significant reduction of all studied adhesion markers: VLA₅ or $\alpha_5\beta_1$ integrin (CD49e, CD29), ICAM-1 (intercellular adhesion molecule 1) or CD54, and of extracellular matrix protein (CD44), but the statistical significance was reach only for the CD44, and CD49e.

III.1-3. Growth particularities of BM MSCs selected from MDS vs. normal

The MSC production in STRO-1⁺ and CD73⁺ cell cultures from MDS marrows was deficient. The average proliferation index for MSCs selected from RC marrows after 2 weeks of culture was 17 times lower for STRO-1 fractions and 2.23 times lower for CD73⁺, compared with the average MSC output in normal controls. A 6.5-fold drop in STRO-1⁺ fractions and a 2.4-fold decrease in CD73⁺ cells were also recorded in the RAEB group.

In addition, the clonogenic ability of the fractions selected from MDS settings was strongly diminished and the differences were more obvious for the STRO-1⁺ CD73⁻ cells.

Thus, the MSCs selected from the RC group showed a clonogenic capacity that was 3.5 times lower for STRO-1⁺CD73⁻, and approximately 2 times lower for STRO-1⁻CD73⁺ compared with normal counterparts. The same decline was noticed for RAEB selected cells compared with normal cells (approximately 4 times lower for STRO-1⁺CD73⁻ fractions and 1.65 times lower for STRO-1⁻CD73⁺ cells, respectively).

In conclusion, the relative proliferation of MDS cultures is the result of a division process that is continuous, but occurs at a low rate and without the ability to generate the normal functional progenitors required to form colonies.

Moreover, a positive relationship was observed between the reduced intensity of CD44 expression in STRO-1⁺CD73⁺ cells in the RC and RAEB groups and the CFU efficiency obtained for CD73⁺ subsets of cells. In addition, the increased level of CD49e expression noticed in STRO-1⁺CD73⁺ and STRO-1⁻CD73⁺ cells was inversely correlated with the DTs calculated for STRO-1⁺ and CD73⁺ fractions sorted from the same RAEB cases samples.

This evidence supports the theory that MSC expansion is an adhesion-dependent process and that CD44 and CD49e molecules are involved in this process.

Likewise, a linear correlation between decreasing CD49e MFIR in MSCs (approximately 2-fold) and a 2-fold decline in the number of CFU-GM and BFU-E colonies was also noticed in the haematopoietic compartment of RAEB group.

These observations confirm the haematopoietic growth-supportive role of the MSC layers and show that this role is α 5-integrin-dependent, suggesting that MSCs derived from MDS are functionally incompetent in supporting normal HPC proliferation and differentiation.

Statistical analysis showed that the myeloid expansion is the most affected aspect.

Intrinsic Growth Deficiencies of Mesenchymal Stromal Cells in Myelodysplastic Syndromes

Carmen Mariana Aanei,^{1,2,*} Pascale Flandrin,^{1,3} Florin Zugun Eloae,² Eugen Carasevici,²
Denis Guyotat,^{3,4} Eric Wattel,⁵ and Lydia Campos^{1,3}

Myelodysplastic syndromes (MDSs) are clonal disorders of hematopoietic stem cells (HSCs) characterized by ineffective hematopoiesis. MDSs are responsible for 1 or several peripheral cytopenias. The evidence accumulated in recent years demonstrates that in addition to HSC defects, a particular role is also played by stromal microenvironment dysfunctions, which mediate the direct contact with hematopoietic precursor cells (HPCs). These interactions help regulate different adhesion-related processes, such as progenitor cell proliferation, apoptosis, clonogenic growth, and maintenance in *in vitro* cultures. As previously reported, these interactions are responsible for altering the microenvironment in MDS. Herein, we present a novel selection protocol for obtaining a standards-compliant mesenchymal stromal cell (MSC) preparation. This method allowed us to comparatively analyze 2 subpopulations of bone marrow MSCs (BM-MSCs) in terms of their adhesion profiles and growth abilities: BM-MSCs selected from MDS settings and their normal counterparts. Functional assays revealed that the MSCs from MDS are intrinsically pathological, thus showing a continuous decline of proliferation and a reduced clonogenic capacity during 14 days of culture and in the absence of signals from hematopoietic cells. The MSC growth defects were significantly correlated with decreases in CD44 adhesion molecules and CD49e ($\alpha 5$ -integrin).

Introduction

MYELODYSPLASTIC SYNDROME (MDS) disorders result from the gradual expansion of abnormal hematopoietic stem cells (HSCs) associated with the variable suppression of normal hematopoiesis [1]. There is evidence that hematopoietic precursor cells (HPCs) that are isolated from patients with MDS display defective growth *in vitro* [1,2]. Although numerous studies have addressed the quantitative and qualitative imbalances in cytokine and chemokine levels within the MDS microenvironment [3–6], there is also convincing evidence that alterations of the direct interaction between HPCs and stroma contribute to abnormal HPC growth and maturation [7–10]. Recent evidence has implicated adhesion protein CD44 in the homing and adhesion of HPCs to mesenchymal stromal cells (MSCs) by the CD44v7 isoform and by the CD44v10 ligand (CD44v10L) that they express [8,11]. In addition, Gottschling et al. showed that β_1 -integrins play an essential role in regulating self-renewing HPC divisions within the stromal environment and in maintaining stemness within the first 72 h of homing [10].

In light of these findings, we were interested in evaluating the putative growth deficiencies of MSCs from diseased individuals compared with normal individuals, and we wanted to explore their adhesion profile to identify correlations between these molecules and the MSCs internal capacities for proliferation and functional maturation.

Therefore, we used an immunomagnetic method to select different subpopulations of MSCs and use their phenotypic and functional evaluations.

Numerous attempts have been made to develop more specific procedures for isolation and characterization as well as to establish the hierarchy of different MSC subpopulations. The most common isolation methods are based on MSCs' ability to adhere to plastic or on the use of MSCs' surface epitopes, such as specific markers or adhesion molecules.

Although stromal precursor antigen-1 (STRO-1) is widely regarded as a marker of early mesenchymal stromal precursor cells, it is also expressed on the surface of other human bone marrow (BM) cells that include glycoprotein-A⁺ nucleated red cells and a small subset of CD19⁺ B-cells;

¹Laboratoire d'Hématologie, Hôpital Nord, CHU de Saint-Etienne, Saint-Etienne Cedex, France.

²Department of Immunology, Faculty of Medicine, Gr. T. Popa University of Medicine and Pharmacy, Iasi, Romania.

³Laboratoire de Biologie Moléculaire de la Cellule, UMR 5239 CNRS, Université de Saint-Étienne, Saint-Étienne, France.

⁴Service Hématologie Clinique, Institut de Cancérologie de la Loire, Saint-Priest-en-Jarez, France.

⁵Oncovirologie et Biothérapies, Centre Léon Bérard, UMR 5239 CNRS, Université de Lyon, Lyon, France.

*Current affiliation: Etablissement Français du Sang Bourgogne-Franche Comté site de Nevers, Nevers, France.

however, it is not expressed in HSCs [12]. This has raised many questions about its use as a specific marker in MSC sorting protocols [13,14]. Plasma membrane-bound ecto-5'-5'-nucleotidase (CD73) has been proposed as the most useful molecule for developing robust *in vitro* MSC assays [14]. However, Simmons et al. reported that the STRO-1⁺/glycophorin A⁻ population has a substantial clonogenic capacity (~100-fold, enriched in colony-forming unit-fibroblast [CFU-F]), which is capable of generating adherent cell layers containing multiple cell types, including adipocytes, smooth muscle cells, and fibroblastic elements; further, this population displays a greater ability to maintain the normal development of the human myeloid lineage than the stromal cells that are commonly isolated from unmanipulated BMs [12]. More recently, Gronthos et al. provided evidence that osteogenic precursors are present in the STRO-1⁺ fraction of human BM cells [15]. Psaltis et al. also found a strong correlation between the amount of STRO-1 with mRNA expression of transcription factors related to cellular proliferation and differentiation, which have been associated with an immature, stem-like phenotype [16]. CD73 expression has also been observed in different cells, and its physiological role is to metabolize adenosine 5'-monophosphate to adenosine [17]. CD73 acts as a signal transducing molecule in the human immune system (specifically, it acts as a costimulatory molecule in T cell activation), and it has been shown to be involved in controlling lymphocyte-endothelial cells interactions [18]. It has been hypothesized that CD73 expression in both tumor and host cells protects the tumor from incoming antitumor T cells and suppresses T cell functions through the CD39 (ecto-ATPase)-CD73 axis [19]. Much less is known about CD73 role in MSC biology, but its impact on cell-matrix interactions in chicken fibroblasts has been described [20]. Despite all efforts, there is no common opinion about the expression of these markers on different MSC preparations; reviewing the literature, it is not possible to establish a MSC hierarchy based on STRO-1 and CD73 expression. In this study, we used double selection based on the expression of these markers to isolate MSC subsets from the culture system.

To the best of our knowledge, this is the first study that evaluates the growth patterns of STRO-1⁺ and CD73⁺ MSC fractions derived from patients with MDS compared with normal cells and performs correlations between their adhesion profiles and their growth dysfunctions.

Materials and Methods

Patients

BM aspirates were collected from 8 healthy donors (median age, 63 years) and 20 untreated patients (median age, 73 years), 10 of whom had refractory cytopenia (RC; refractory cytopenia with unilineage dysplasia, and refractory cytopenia with multilineage dysplasia) and 10 of whom had refractory anemia with excess blasts [RAEB; refractory anemia with excess blasts-1 (RAEB-1), and refractory anemia with excess blasts-2 (RAEB-2)]. The patients' assignment to different groups was made according to the 2008 World Health Organization (WHO) classification [21].

Signed, institutional review board-approved, written, informed consent was obtained from all patients and healthy donors.

Amplification of BM-MSCs in cultures

BM mononuclear cells were separated from heparinized BM specimens using density gradient centrifugation. The cells (2×10^6) were seeded in 25-cm² culture flasks and expanded to 70%–80% confluence for 4–5 weeks at 37°C with 5% CO₂ in MesenCult[®] complete medium (StemCell Technologies). The MSCs were allowed to adhere overnight, and nonadherent cells were washed out by changing the medium. Thereafter, the medium was changed twice weekly and replaced with half new medium and half supernatant removed by culture. The MSC layer composition at 80% confluence was evaluated under an inverted microscope after Giemsa staining.

Immunofluorescent evaluation of the normal BM-MSC subpopulations

The cells were thoroughly washed to remove residual media and were fixed in paraformaldehyde 4% w/v for 10 min at room temperature. Fixation was stopped by washing the cells thrice in phosphate-buffered saline (pH 7.2).

Nonspecific background staining was blocked with an antibody (Ab) buffer containing PBS (1×)/fetal calf serum (FCS) (1% w/v)/bovine serum albumin (Sigma-Aldrich; 0.1% w/v) for 1 h. The cells were then permeabilized with 0.1% Triton X-100 (Sigma-Aldrich) in PBS for 20 min before Ab application. Before application, the antibodies were diluted in an Ab buffer of fluorescein isothiocyanate (FITC)-conjugated mouse Anti-Human STRO-1 monoclonal Ab (mAb) (final dilution 1:50, clone sc-47733, Santa Cruz Biotechnology, Inc.) and phycoerythrin (PE)-conjugated mouse Anti-Human CD73 mAb (1:25, clone AD2; BD Pharmingen[™]). Before acquisition, nuclear staining with 4',6-diamidino-2-phenylindole (DAPI; 1 µg/mL) was performed for 30 min at 4°C. Slides were mounted in Faramount Aqueous Mounting Medium (Dako Denmark). Double-stained preparations were visualized under an Axio Observer Z1 microscope (Carl Zeiss, Inc.) at 100× magnification with a 0.55 numerical aperture lens. Signals were recorded simultaneously with 3 photomultiplier tubes (PMT 1–3). The images (TIFF format) were captured with a PixeLINK PL-A622C/622000227 camera (Aegis Electronic Group, Inc.) by taking multiple exposures through bandpass optical filter sets appropriate for FITC, Texas Red, and DAPI and using a 100× Plan Apochromat objective.

Immunophenotyping of BM-MSCs with flow cytometry

The MSCs were cultured for 30–35 days. They were then harvested using the MesenCult[®] Dissociation Kit (StemCell Technologies), collected in glass tubes containing 5 mL MesenCult[®] with 20% FCS (GIBCO[®] Invitrogen), and filtered through a 70-µm cell strainer (Falcon, Becton Dickinson). The cell number and viability were evaluated using trypan blue solution (0.4% PBS). The cells were then suspended in 50 µL of washing buffer (PBS containing 1% FCS, and 0.05% EDTA) and stained on ice for 30 min with the following markers: MSC-specific markers (STRO-1, CD73, previously described), endothelium-related markers (Alexa Fluor[®] 488-conjugated mouse Anti-Human CD31 mAb, clone M89D3, BD Pharmingen; FITC-conjugated mouse Anti-Human CD106 mAb, clone

51-10C9, and BD Pharmingen), adhesion markers (PE-CyTM5-conjugated mouse Anti-Human CD29 mAb, clone MAR4, BD Pharmingen; allophycocyanin (APC)-conjugated mouse Anti-Human CD54 mAb, clone HA58, BD Pharmingen; PE-conjugated mouse Anti-Human CD44 mAb, clone 515, BD Pharmingen; and PE-conjugated mouse Anti-Human CD49e mAb, clone IIA1, BD Pharmingen), and markers associated with hematopoietic lineages (PerCP-conjugated mouse Anti-Human CD45 mAb, clone 2D1, BD Pharmingen; PE-CyTM7-conjugated mouse Anti-Human CD16 mAb, clone B73.1, BD Pharmingen). Cell viability was evaluated by staining with 1 μ L of propidium iodide (PI, 1 mg/mL; Sigma) before FACS acquisition. Data were acquired using an FACS Canto I cytometer and analyzed using DIVA software (Becton Dickinson).

The analysis strategy involved gating for singlet, followed by the exclusion of dead PI⁺ cells and final gating using specific marker expression. The level of expression of different markers was normalized using the corresponding median fluorescence intensity ratio (MFIR) for statistical analysis. The adhesion markers were tested at 20 days of culture for 5 different experiments per subpopulation and per study group.

In this study, we determined negative expression for a marker when the MFIR was <2, low- or medium-positive expression when the MFIR was between 2 and 10, and intensely positive expression when the MFIR was >10.

EasySep immunomagnetic selection of STRO-1⁺ and CD73⁺ BM-MSCs

To confirm that differences in STRO-1 and CD73 marker expression is the imprint of distinct cell subpopulations, we performed immunomagnetic positive sorting using these markers. The fraction of STRO-1⁺ cells was immunodepleted for CD73 by exploiting the differences in epitope density and the avidity of STRO-1 mAb, the STRO-1⁺CD73⁻ cells bearing a higher number of epitope sites (Fig. 3A).

Thus, MSCs, detached as previously described, were stained with Anti-Human CD32 (Fc γ RII) blocker from an EasySep[®] PE Selection Kit (StemCell Technologies), then with FITC-conjugated mouse Anti-Human STRO-1, 3.0 μ g/mL for 10⁷ cells for 1 h on ice. Labeled cells were processed by adding EasySep PE Selection Cocktail 100 μ g/mL of cells and EasySep Magnetic Nanoparticles and by using the EasySep magnet from the EasySep PE Selection Kit (StemCell Technologies). After the isolation of the STRO-1 positive fraction, the remaining cells were stained with PE-conjugated mouse Anti-Human CD73 mAb (BD Pharmingen), 3.0 μ g/mL for 10⁷ cells, kept for 1 h on ice, then passed through all the remaining steps (previously described) to select the CD73-positive population. All steps were monitored for purity and viability using flow cytometry.

The STRO-1⁺ and CD73⁺ fractions were enriched to >95% (96.34 \pm 2.26 for STRO-1⁺ and 97.74 \pm 0.95 for CD73⁺ cells), and percentages were evaluated from the singlet gate after excluding dead PI⁺ cells. Four rounds of selection were performed for each population sorted.

Cell yield and growth characteristics

To assess the growth characteristics of the 2 major MSCs subpopulations, STRO-1⁺CD73⁻ and STRO-1⁻CD73⁺, pro-

liferation and clonogenicity tests were performed. To do so, 1 \times 10³ viable MSCs (quantified using the trypan blue exclusion test) were plated in 25-cm² flasks, and the number of cells was counted on days 1, 7, and 14. We then calculated the proliferation index (the difference between the number of harvested cells and the initial plated number) and the doubling time (the duration of 1 mitosis) estimated by the ratio of the time necessary for 1 \times 10³ MSCs to reach 80% confluence and the number of population doublings. The number of population doublings was obtained using the following formula: $n = \log(x/y)/\log 2$, where "x" is the number of initial seeded MSCs and "y" is the cell harvest number [22,23].

The clonogenic potential of MSCs was established with plating efficiency (PE) or CFU efficiency assays. After 14 days of culture, the medium was removed, and the colonies were fixed in methanol and treated with Giemsa stain. The colony numbers were then scored. A colony was defined as consisting of at least 50 cells. PE was the ratio of the number of colonies formed to the number of cells seeded \times 100% [24].

Statistical analysis

Results are expressed as the mean \pm standard deviation. The significance level ($P \leq 0.05$) was determined using paired student's *t*-tests. The SPSS software package (Version 13.0; SPSS, Inc.; www.spss.com) was used for the statistical analysis.

Results

The experiments were configured to isolate and characterize different subsets of MSCs on the basis of STRO-1/CD73 expression, identify the fractions that highlight phenotypic and functional differences in MDS compared with normal cells.

Morphological and morphometric characterization of BM-MSCs from primary cultures in normal and MDS settings

Our study began with the evaluation of MSCs from primary cultures generated from MDS and normal BM aspirates to identify possible structural differences between them.

In line with previous reports, 3 major subpopulations (Fig. 1A) were distinguished in both normal and pathological settings after 30–35 days of culture. The subpopulations were round in shape, with the appearance of undifferentiated cells; thin, spindle-shaped cells; and large, flat cells.

The cellular dimensions and the proportion of different morphological subtypes identified in primary layers of MDS and normal BM cultures are presented in Table 1. The different distribution of the 3 subpopulations of cells in MDS stand out compared with normal settings. However, the slight decrease in the number of large, flat cells in MDS settings, which is considered the onset of terminal differentiation, in addition to the size differences within this population among the different study groups are worth noting. These characteristics could indicate maturation defects.

Three immunophenotypical subpopulations were discriminated from primary BM-MSCs cultures in normal and MDS settings using flow cytometry

In the next step, we decided to further evaluate MSCs amplified in culture for 30–35 days using cytometry and

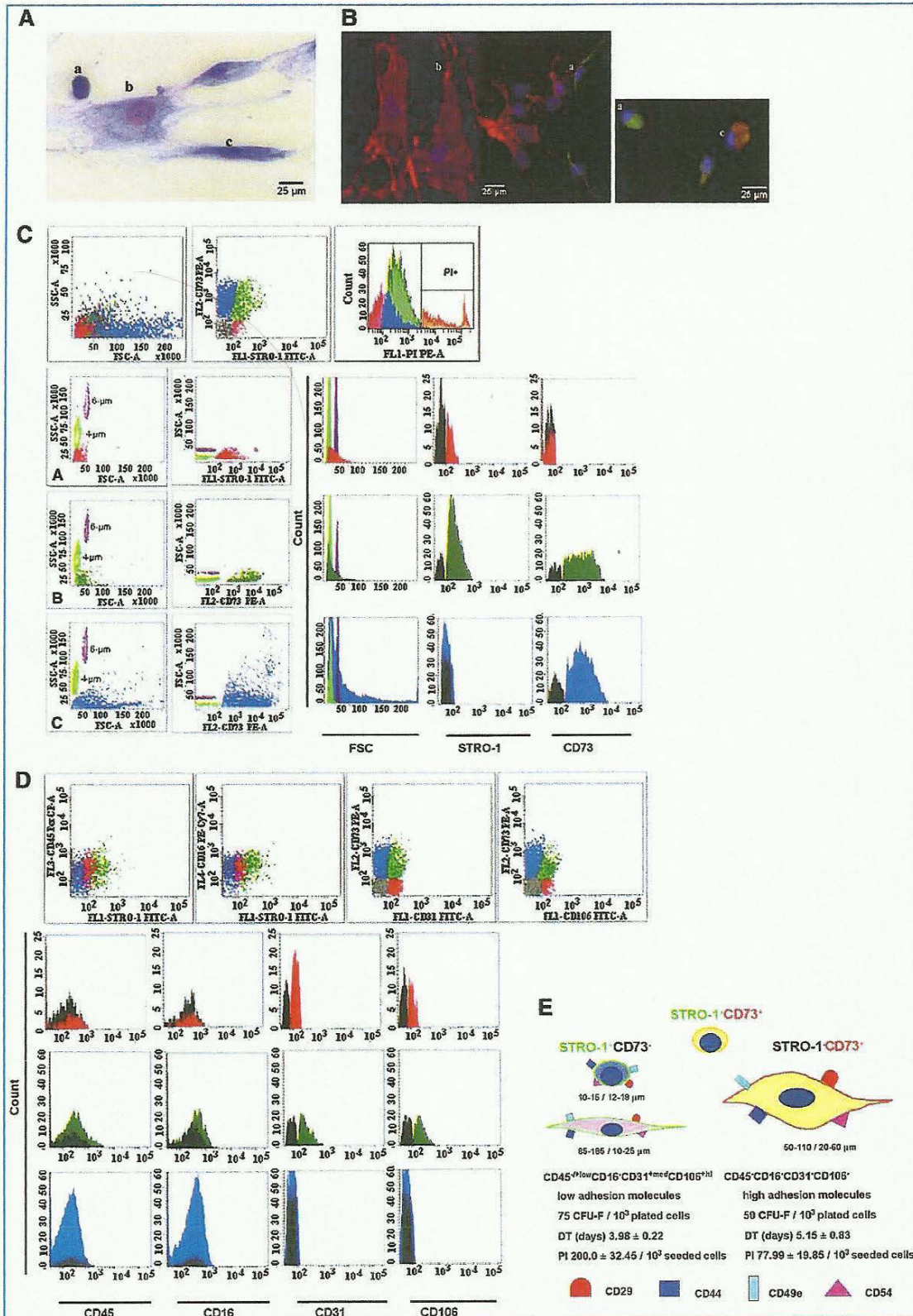


TABLE 1. MEAN DIMENSION AND PROPORTION AMONG 3 BONE MARROW STROMAL SUBPOPULATIONS AFTER 30–35 DAYS OF CULTURE IN NORMAL AND MYELODYSPLASTIC SYNDROME SETTINGS

Stroma	Stromal cell subpopulation ^a	Percentages ^b	DimensionsH/W (μm) ^c
NBM	Round-shaped	4.3% \pm 1.0% ^d	17.6 \pm 5.9 / 15.0 \pm 3.3 ^d
	Spindle-shaped	21.7% \pm 7.5% ^d	135.2 \pm 49.7 / 18.8 \pm 7.5 ^d
	Large and flat	73.9% \pm 8.2%^d	83.8 \pm 27.5 / 38.4 \pm 18.0^d
RC	Round-shaped	8.5% \pm 1.2% ^d	15.4 \pm 5.6 / 12.0 \pm 4.0 ^d
	Spindle-shaped	36.6% \pm 2.3% ^d	111.3 \pm 15.7 / 7.6 \pm 2.8 ^d
	Large and flat	54.8% \pm 1.0%^d	39.2 \pm 38.7 / 20.4 \pm 10.7^d
RAEB	Round-shaped	16.7% \pm 5.4% ^d	16.1 \pm 2.1 / 13.4 \pm 2.6 ^d
	Spindle-shaped	24.8% \pm 11.6% ^e	164.7 \pm 96.5 / 25.4 \pm 11.4 ^e
	Large and flat	58.4% \pm 13.2%^e	109.1 \pm 50.1 / 56.5 \pm 27.9^e

^aAssignment of subtypes was based on morphological characteristics.

^bValues represent mean percentages from 3 separate experiments ($n=3$) \pm SD from each group of cases.

^cThe mean dimensions were evaluated on $n_{\text{round-shaped}}=15$, $n_{\text{spindle-shaped}}=50$, and $n_{\text{large flat}}=100$ cells from each of the studied groups.

The statistical significance is ^d $P<0.05$; ^e $P=0.05$.

NBM, bone marrow-derived stroma from healthy volunteers; RC, stroma derived from refractory cytopenia patients; RAEB, stroma derived from refractory anemia with excess of blasts patients; SD, standard deviation.

The bold values highlight the main differences, in terms of distribution and size, between the three morphological types of stromal cells, in pathological settings compared to normal counterparts.

compare the results with the data obtained from the morphology-morphometry.

In line with the requirements established by the Mesenchymal and Tissue Stem Cell Committee of the International Society for Cellular Therapy [25], our panel of mAbs included specific phenotypical markers in addition to the hematopoietic-related markers CD45 and CD16.

The initial viabilities of the harvested cell fractions, as evaluated by trypan blue exclusion, were 79.6% \pm 10.6% for normal stromal cells, 77.6% \pm 7.26% for RC stromal cells, and 67.4% \pm 10.2% for RAEB stromal cells.

Distinctive features of MSCs (ie, their size and the expression of the specific markers STRO-1 and CD73) allowed us to identify 3 immunophenotypical subpopulations in primary cultures.

In terms of size, cells reading less than 50 on the FSC scale (approximately the size of 4- μm beads) were considered FSC^{low}, those that were \sim 50 on the FSC scale (the size of 4- to 6- μm beads) were designated FSC^{med}, and those with an FSC greater than 50 (larger 6- μm beads) were designated FSC^{hi} (Fig. 1C). The STRO-1⁺ CD73⁻ population is predominantly FSC^{low} and matched with the smallest population identified in the morphometric analysis. The STRO-1 and CD73 double-positive cells were predominantly FSC^{med}, but the STRO-1⁻ CD73⁺ displayed variable FSC values (Fig. 1C). This observation shows that no clear delimitation of cell subsets can be made based on size; supplementary staining

with specific markers is required for this purpose. The phenotypic expression of the STRO-1 and CD73 markers associated with cell morphology was then confirmed using fluorescent microscopy (Fig. 1B). The proportions of the 3 cell types at different culture times in normal versus MDS MSC layers, using flow cytometry, are presented in Table 2.

Immunophenotype analysis of the expression of hematopoietic- and endothelium-related markers revealed that in both normal and MDS cells groups, the STRO-1⁺ subpopulations STRO-1⁺ CD73⁻ and STRO-1⁺ CD73⁺ are CD45^{low} (MFIR=2.55 \pm 0.78, $n=20$, $P<0.001$), CD16⁻, CD31^{med} (MFIR=8.06 \pm 2.87, $n=20$, $P<0.001$), and CD106^{hi} (MFIR=12.53 \pm 5.32, $n=20$, $P<0.001$). The STRO-1⁻ CD73⁺ subpopulation was negative for all these markers (Fig. 1D). The phenotypic evaluation of MSC layer composition highlights increased percentages of STRO-1⁺ cells in 20–30 days of culture that coexpressed CD106 and CD31 in the RAEB and RC groups (Table 2). Moreover, this issue persisted in the MDS groups until 60 days, when cell autolysis occurred.

Comparative analysis of adhesion profiles of BM-MSCs derived from MDS and normal controls

We then studied the adhesion profiles of in vitro amplified MSCs using a combination of mAbs raised against surface adhesion markers, VLA₅ or α -5 β 1 integrin (CD49e, CD29), intercellular adhesion molecule 1 or CD54, and the

FIG. 1. Characterization of normal BM-MSCs amplified for 30–35 days in primary cultures. Morphological appearance (Giemsa stain; magnification, $\times 40$): a, small, round, undifferentiated cells; b, large, flat cells; and c, spindle-shaped cells (A) and immunofluorescence labeling (B). Human MSCs were double stained for STRO-1 (green) and CD73 (red). Cell nuclei are 4',6-diamidino-2-phenylindole-stained (blue). Flow cytometry evaluation according to size and expression of STRO-1 and CD73: FSC^{low} STRO-1⁺ CD73⁻ (red), FSC^{med} STRO-1⁺ CD73⁺ (green), and FSC^{var} STRO-1⁻ CD73⁺ (blue) (C). Two types of reference beads with 4- μm and 6- μm sizes were run parallel to the cells for FSC standardization. Hematopoietic and endothelium-related marker expression (D). Representative histograms were presented for each subtype of cells, as discriminated by STRO-1 and CD73 expression. Marker expression was compared with autofluorescence in unstained cells (gray). Summary of morphology, immunophenotype, and growth characteristics of the STRO-1⁺ CD73⁻ and STRO-1⁻ CD73⁺ cells (E). PI and DT were evaluated at the time of harvesting (80% confluence; 14 days of culture) for 10^3 seeded cells. BM, bone marrow; DT, doubling time; MSC, mesenchymal stromal cells; PI, proliferation index; STRO-1, stromal precursor antigen-1.

TABLE 2. BONE MARROW-MESENCHYMAL STROMAL CELL SUBPOPULATIONS IN NORMAL AND MYELODYSPLASTIC SYNDROME ENVIRONMENTS EVALUATED USING FLOW CYTOMETRY OVER THE COURSE OF 60 DAYS OF CULTURE

BM-MSC primary culture	BM-MSC subpopulation	Day 10	Day 20	Day 30	Day 40	Day 60
NBM	STRO-1 ⁺ CD73 ⁻					
	%	5.0±2.5	22.0±9.2	12.9±6.9	16.4±6.7	21.9±3.2
	Cell count	1.0±0.5	4.4±1.8	2.6±1.4	3.3±1.3	4.4±0.6
	STRO-1 ⁺ CD73 ⁺					
	%	17.0±9.9	25.8±6.4	21.7±3.3	24.2±5.9	0.7±0.2
	Cell count	3.4±2.0	5.2±1.3	4.3±0.7	4.8±1.2	0.1±0.01
RC	STRO-1 ⁻ CD73 ⁺					
	%	78.0±11.6	52.2±9.1	65.4±9	59.4±11.3	77.4±3.4
	Cell count	15.6±2.3	10.4±1.8	13.1±1.8	11.9±2.3	15.5±0.7
	STRO-1 ⁺ CD73 ⁻					
	%	7.3±1.5	13.8±5	19.5±5.5	10.7±2.8	15.3±4.1
	Cell count	1.5±0.3	2.7±1.0	3.9±1.1	2.1±0.6	3.1±0.8
RAEB	STRO-1 ⁺ CD73 ⁺					
	%	20.9±2.6	20.4±9.8	27.6±5.0	43.0±10.2	39.5±5.1
	Cell count	4.2±0.5	4.1±2.0	5.5±1.0	8.6±2.0	7.9±1.0
	STRO-1 ⁻ CD73 ⁺					
	%	71.8±7.1	65.8±12.7	52.9±6.6	46.3±7.9	45.2±6.9
	Cell count	14.3±1.4	13.2±2.5	10.6±1.3	9.3±1.6	9.0±1.4
RAEB	STRO-1 ⁺ CD73 ⁻					
	%	6.1±3.3	64.7±9.0	45.4±9.0	15.0±4.1	6.6±1.4
	Cell count	1.2±0.7	12.9±1.8	9.1±1.8	3.0±0.8	1.3±0.3
	STRO-1 ⁺ CD73 ⁺					
	%	18.1±1.5	6.8±3.2	14.0±5.8	18.0±4.1	24.2±7.1
	Cell count	3.6±0.3	1.4±0.6	2.8±1.2	3.6±0.8	4.8±1.4
RAEB	STRO-1 ⁻ CD73 ⁺					
	%	75.8±5.7	28.5±7.4	40.6±9.5	67.0±7.0	69.2±13.6
	cell count	15.2±1.1	5.7±1.5	8.1±1.9	13.4±1.4	13.9±2.7

The values are the mean percentage and actual cell count±SD from 8 separate experiments.

Cell count=mean of actual cell count×10³.

The significance level is *P*<0.05.

MSC, mesenchymal stromal cell; STRO-1, stromal precursor antigen-1.

The bold values highlight the main differences, in terms of distribution of the three BM-MSCs subpopulations discriminated by STRO-1 and CD73 expression, in MDS settings vs. normal controls.

TABLE 3. SUMMARY OF THE ADHESION PROFILE FOR IN VITRO EXPANDED MESENCHYMAL STROMAL CELLS FROM PATIENTS WITH NORMAL AND MYELODYSPLASTIC SYNDROME

		CD29		CD54		CD44		CD49e	
		% of CD29 ⁺ cells	MFIR	% of CD54 ⁺ cells	MFIR	% of CD44 ⁺ cells	MFIR	% of CD49e ⁺ cells	MFIR
NBM	STRO-1 ⁺ CD73 ⁻	29.4±11.0	45.6±13.4	27.2±9.0	18.3±4.1	34.6±12.6	3.6±1.9	38.0±15.7	4.3±2.6
	STRO-1 ⁺ CD73 ⁺	34.3±46.7	134.8±46.7	30.3±32.8	46.2±17.7	32.0±16.6	55.2±21.7	28.6±4.0	31.3±3.7
	STRO-1 ⁻ CD73 ⁺	66.3±14.8	102.4±25.9	64.8±12.7	30.8±12.4	72.4±16.9	69.6±22.9	70.9±11.0	31.2±16.9
RC	STRO-1 ⁺ CD73 ⁻	9.9±3.5	44.2±20.2	7.9±3.6	12.1±3.5	18.6±8.8	4.8±2.7	14.0±5.2	6.0±1.6
	STRO-1 ⁺ CD73 ⁺	12.6±5.2	54.6±18.1	10.9±4.9	21.7±5.3	8.9±1.9	9.2±3.9	13.9±8.8	19.6±5.9
	STRO-1 ⁻ CD73 ⁺	82.7±7.6	28.6±9.0	79.8±9.8	12.4±5.6	81.5±17.6	6.4±2.6	69.7±7.3	15.8±4.7
RAEB	STRO-1 ⁺ CD73 ⁻	59.2±7.7	18.2±4.1	56.2±4.5	22.1±5.2	73.7±15.6	2.5±0.8	71.2±13.7	3.8±1.3
	STRO-1 ⁺ CD73 ⁺	6.6±2.4	43.2±14.6	7.1±2.9	28.7±10.2	5.6±3.2	12.5±1.7	4.9±0.3	15.4±2.5
	STRO-1 ⁻ CD73 ⁺	40.3±10.3	54.5±18.9	37.6±11.1	23.0±5.0	20.7±3.0	19.1±5.5	36.6±12.6	9.6±5.3

Values represent the median MFIR of adhesion markers±SD from 5 different experiments, evaluated for each subpopulation and group of cases after 20 days of culture.

The statistical significance level was *P*<0.001.

MFIR, median fluorescence intensity ratio.

The bold values reflect the main differences, in terms of intensity of expression, for the adhesion markers evaluated on BM-MSCs from MDS settings compared to normal counterparts.

extracellular matrix protein CD44. We noticed a homogeneous expression of adhesion markers, regardless of the subpopulation analyzed or the case group (Table 3).

In the CD73⁺ subsets of cells, which did or did not co-express STRO-1, we noticed a significant reduction in CD54 and CD29 expression (~2- and 3.5-fold in dysplastic cells versus normal cells) when compared with the same subpopulations of cells, but these modifications did not reach statistical significance.

Significant differences were noticed for CD44 and CD49e markers. The CD44 drop was substantial in the STRO-1⁻CD73⁺ (11-fold) and STRO-1⁺CD73⁺ (6-fold) subpopulations from the RC group and lower in the same groups of cells from the RAEB group (3.5-fold and 4-fold, respectively). Statistical significance was achieved for the differences in CD44 expression in STRO-1⁺CD73⁺ subpopulations ($P=0.001$ for STRO-1⁺CD73⁺_{RC} and $P<0.001$ for STRO-1⁺CD73⁺_{RAEB}) compared with normal counterparts. A downward trend for CD49e was also noticed in MDS MSCs in both subpopulations of CD73⁺, registering 2-fold reductions (Fig. 2). Statistical significance was reached for both subpopulations of cells (STRO-1⁺CD73⁺ and STRO-1⁻CD73⁺) regarding CD49e expression in RAEB-

derived cells compared with normal counterparts ($P=0.002$ for STRO-1⁺CD73⁺_{RAEB} and $P<0.001$ for STRO-1⁻CD73⁺_{RAEB}).

Functional properties of the STRO-1⁺CD73⁻ and STRO-1⁻CD73⁺ MSC subclasses selected from MDS and healthy volunteers

The next steps of the study addressed subpopulations that were determined according to their specific expression of STRO-1 and CD73 markers (Fig. 3A). This selection was performed to allow the functional characterization of different cell fractions and to reduce the errors that result from comparing the different biological systems, regardless of whether the structural differences between the MDS and normal MSC primary layers are taken into account.

In the normal settings, the proliferation tests for STRO-1⁺CD73⁻ and STRO-1⁻CD73⁺ fractions revealed a plateau phase in the first 7 days of culture and logarithmic growth in the next 7 days. The STRO-1⁺CD73⁻ fractions proliferated more efficiently than the STRO-1⁻CD73⁺ fraction. The average proliferation index for STRO-1⁺CD73⁻ cells was 200.0 ± 32.45 versus 77.99 ± 19.85 for STRO-1⁻CD73⁺ cells at the harvesting

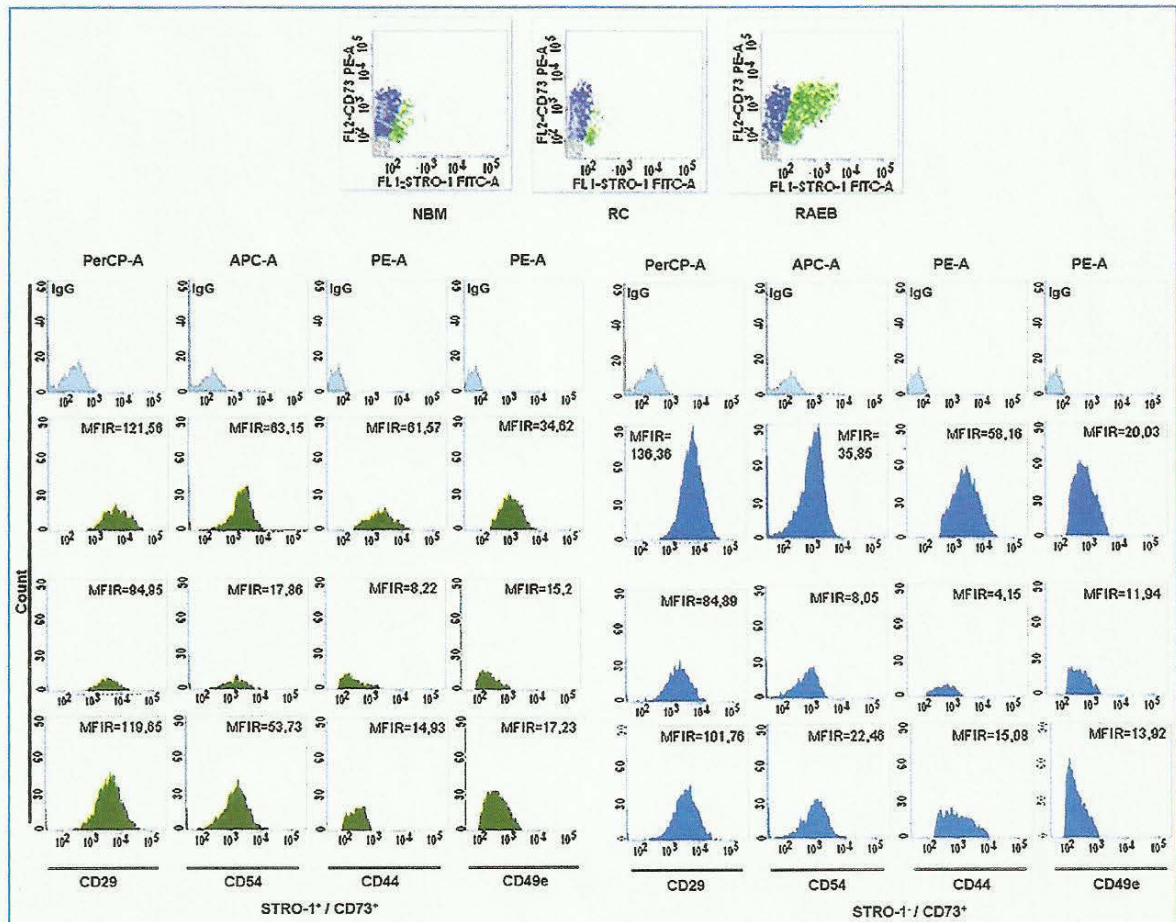


FIG. 2. Pattern of adhesion marker expression on BM-MSCs isolated from patients with MDS compared with that of healthy volunteers. Representative examples of adhesion marker expression on STRO-1⁺CD73⁺ cells (green) and STRO-1⁻CD73⁺ cells (blue) compared with isotype-matched controls (gray). MDS, myelodysplastic syndrome.

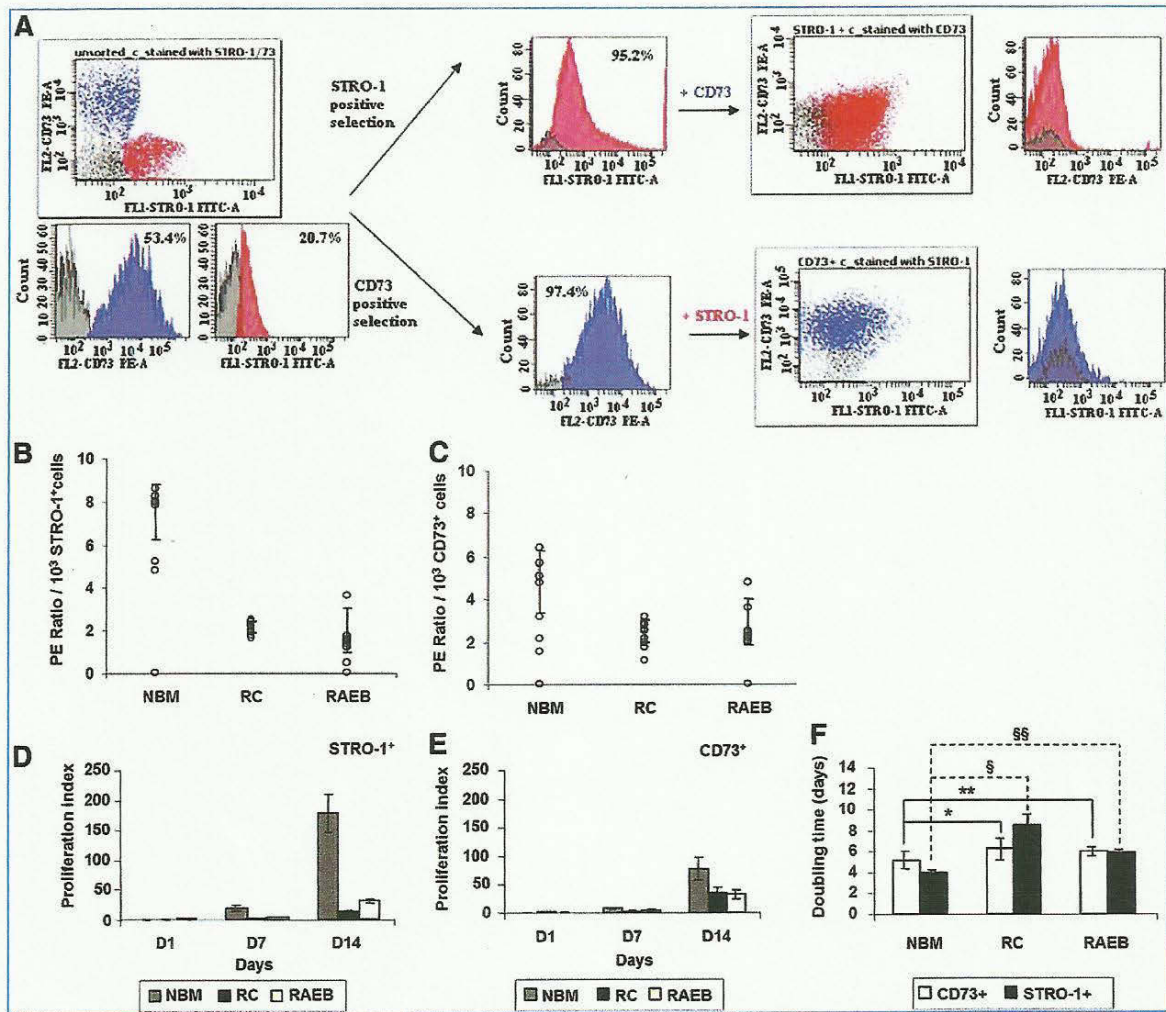


FIG. 3. Experimental strategy of STRO-1/CD73 Immunomagnetic Selection (A). Growth kinetics of STRO-1⁺CD73⁻ and STRO-1⁻CD73⁺ MSC sorted cells from normal and MDS BM (B-F). Plating efficiency of STRO-1⁺ MSCs (B) and CD73⁺ MSCs (C). Proliferation index (D, E; NBM=left column, RC=middle column, and RAEB=right column) and cell-doubling time (F) of STRO-1⁺ and CD73⁺ cell fractions from patients with MDS compared with normal cells. All values reflect the mean \pm SD. The results obtained for different groups of cases and for the 2 fractions investigated were significantly different ($P < 0.05$). Comparisons between fractions sorted from patients with MDS versus normal counterparts for 8 experimental groups ($^{*}DT_{RC\ STRO-1^{+}}$ vs. $DT_{NBM\ STRO-1^{+}}$; $^{**}DT_{RAEB\ STRO-1^{+}}$ vs. $DT_{NBM\ STRO-1^{+}}$; $^{*}DT_{RC\ CD73^{+}}$ vs. $DT_{NBM\ CD73^{+}}$; $^{**}DT_{RAEB\ CD73^{+}}$ vs. $DT_{NBM\ CD73^{+}}$) are presented: $^{*}P = 0.034$; $^{**}P = 0.242$; $^{*}P = 0.008$; $^{**}P = 0.002$, respectively. Similar viabilities (CV < 5%) were observed for the STRO-1⁻ and CD73⁻ selected fractions from the 3 groups (for STRO-1⁺ fractions: NBM STRO-1⁺ viability = 96.4 ± 2.0 , RC STRO-1⁺ viability = 95.5 ± 3.4 , and RAEB STRO-1⁺ viability = 95.3 ± 3.6 ; and for CD73⁺ fractions: NBM CD73⁺ viability = 97.1 ± 1.7 , RC CD73⁺ viability = 95.3 ± 3.2 , RAEB CD73⁺ viability = 96.2 ± 3.0). The values represent the mean percentages \pm SD of viable cells as evaluated by trypan blue exclusion. RAEB, refractory anemia with excess blasts; RC, refractory cytopenia; SD, standard deviation. Color images available online at www.liebertonline.com/scd

time (Fig. 3D, E), and the plating efficiency of STRO-1⁺CD73⁻ cells was $7.5\% \pm 1.28\%$, compared with $4.83\% \pm 1.48\%$ in the STRO-1⁻CD73⁺ fraction, for 10^3 seeded cells (Fig. 3B, C).

MSC production in STRO-1⁺ and CD73⁺ cell cultures from MDS marrows was deficient (Fig. 3D-F).

The average proliferation indexes of the STRO-1⁺ fractions from RC and RAEB patients were 17 times and 6.5 times lower than that of the normal controls, respectively (Fig. 3D-F). Moreover, for CD73⁺ fractions, a 2.5-fold drop

was recorded in patients with RC and RAEB compared with normal MSC output (Fig. 3D-F).

In addition, the clonogenic ability of the fractions selected from MDS settings was strongly diminished, and the differences were more obvious for the STRO-1⁺ CD73⁻ cells (Table 4).

Thus, the MSCs selected from the RC group showed a clonogenic capacity that was 3.5 times lower for STRO-1⁺CD73⁻, and ~ 2 times lower for STRO-1⁻CD73⁺

TABLE 4. RELATIVE COLONY-FORMING UNIT-FIBROBLAST NUMBERS OBTAINED FOR STRO-1⁺ AND CD73⁺ FRACTIONS SELECTED FROM MYELODYSPLASTIC SYNDROME COMPARED WITH NORMAL SETTINGS

		STRO-1 ⁺ CD73 ⁻ MSCs	CD73 ⁺ STRO-1 ⁻ MSCs
NBM (n=8)	% viable cells ^a	96.4±2.0	97.1±1.7
	% purity ^b	98.5±1.2	99.2±0.7
	CFU-F No./10 ³ plated cells	74.6±3.4	49.5±10.2
RC (n=8)	% viable cells ^a	95.5±3.4	95.3±3.2
	% purity ^b	98.0±0.9	98.9±0.6
	CFU-F No./10 ³ plated cells	22.2±3.8	23.9±11.6
RAEB (n=8)	% viable cells ^a	95.3±3.6	96.2±3.0
	% purity ^b	98.2±1.3	98.7±1.0
	CFU-F No./10 ³ plated cells	19.3±5.9	29.7±9.4

The results are expressed as the mean ± SD from the indicated number of independent experiments.

The significance level is $P < 0.05$.

^aThe percentage of viable cells was evaluated by trypan blue exclusion assay.

^bThe purity of selected fractions was evaluated by flow cytometry, and the values presented are the mean percentage of CD73⁺ STRO-1⁻ PI⁻/STRO-1⁺ CD73⁻ PI⁻ cells with singlet gating.

CFU-F, colony-forming unit-fibroblast; PI, propidium iodide.

compared with normal counterparts. The same decline was noticed for RAEB selected cells compared with normal cells (~4 times lower for STRO-1⁺CD73⁻ fractions and 1.65 times lower for STRO-1⁻CD73⁺ cells) (Fig. 3B, C).

In conclusion, the relative proliferation of MDS cultures is the result of a division process that is continuous, but occurs at a low rate and without the ability to generate the normal functional progenitors required to form colonies.

Decreased adhesion marker expression negatively correlates with MSC growth in MDS

To evaluate the adhesion abnormalities' significance to the functional integrity of the MSC layers in MDS, the statistical correlations of their functional parameters were determined.

A first observation resulting from this analysis was that despite a decrease in CD54 and CD29 expression in dysplastic MSCs, the comparative statistical analysis did not produce significant correlations.

However, significant correlations were obtained for the other 2 markers, CD44 and CD49e.

As indicated in Fig. 4A, a positive relationship was observed between the reduced intensity of CD44 expression in STRO-1⁺CD73⁺ cells in the RC and RAEB groups and the CFU efficiency obtained for CD73⁺ subsets of cells.

Moreover, the increased level of CD49e expression noticed in STRO-1⁺CD73⁺ and STRO-1⁻CD73⁺ cells was inversely correlated with the doubling times calculated for STRO-1⁺ and CD73⁺ fractions sorted from the same samples from RAEB cases (Fig. 4B).

This evidence supports the theory that MSC expansion is an adhesion-dependent process and that CD44 and CD49e molecules are involved in this process.

Discussion

MSCs are found in many locations, but their main reservoirs are the BM and periosteum [26]. Despite numerous attempts to characterize and understand the biology of these cells, the data remain scarce and controversial. As in previous reports [6,27], we found that isolation methods have a huge impact on the composition of MSC preparations and cause tremendous differences in different groups' results.

Further, the phenotypic pitfalls are related to the cells' detachment from the culture [28,29]. In this study, we noticed a reduction in the percentages of positive cells and a decrease in MFIR for the following markers: CD29, CD49e, CD44, CD31, and CD106 by trypsinization (data not shown).

The current study has extended the characterization of MSCs prepared with immunoselection using 2 specific markers, STRO-1 and CD73, by documenting their morphology-morphometry, phenotype, and growth kinetics. Immunomagnetic selection allowed us to isolate 2 major subpopulations. The first subpopulation, STRO-1⁺CD73⁻ cells, is less abundant in normal BM controls and displays a round or spindle shape, and, in terms of size, the cells in this population range from 5 to 26 μm . Phenotypically, they express low levels of CD45, adhesion molecules, and the endothelial-related markers CD31(PECAM-1) and CD106 (VCAM-1). In terms of growth abilities, these cells show a higher proliferation index, and they have clonogenic potential 1.5 times greater than their STRO-1⁻CD73⁺ counterparts. By contrast, the STRO-1⁻CD73⁺ fraction includes mostly larger (50 to 110 μm , on average) and more granular cells that are negative for endothelial- and hematopoietic-related markers, but they express increased levels of the adhesion markers CD44, CD54, CD29, and CD49e, which correlates with their lower rate of proliferation ($77.99 \pm 19.85/10^3$ CD73⁺ seeded cells vs. $200.0 \pm 32.45/10^3$ STRO-1⁺ seeded cells) (Fig. 1B). This difference in the expression of adhesion markers may reflect the different roles of these cells within their own in vitro niche. Prockop DJ noticed in MSC cultures a population of cells that express surface proteins with an inhibitory influence on cell adhesion [such as α_6 -integrin and podocalyxin-like protein (PODXL)]. These cells are highly motile, secrete DKK-1 (an inhibitor of the canonical Wnt signaling pathway), and serve as nurse cells for other subpopulations; thus, they are key elements of the rapid growth phase [30]. Technically, the 2 fractions could be exploited differently, STRO-1⁺ cells being more robust for carrying out in vitro MSC growth assays, whereas CD73⁺ cells have proved their utility in the evaluation of adhesion profiles. Moreover, Simmons and Torok-Storb have claimed that a STRO-1⁺ stroma layer represents a good

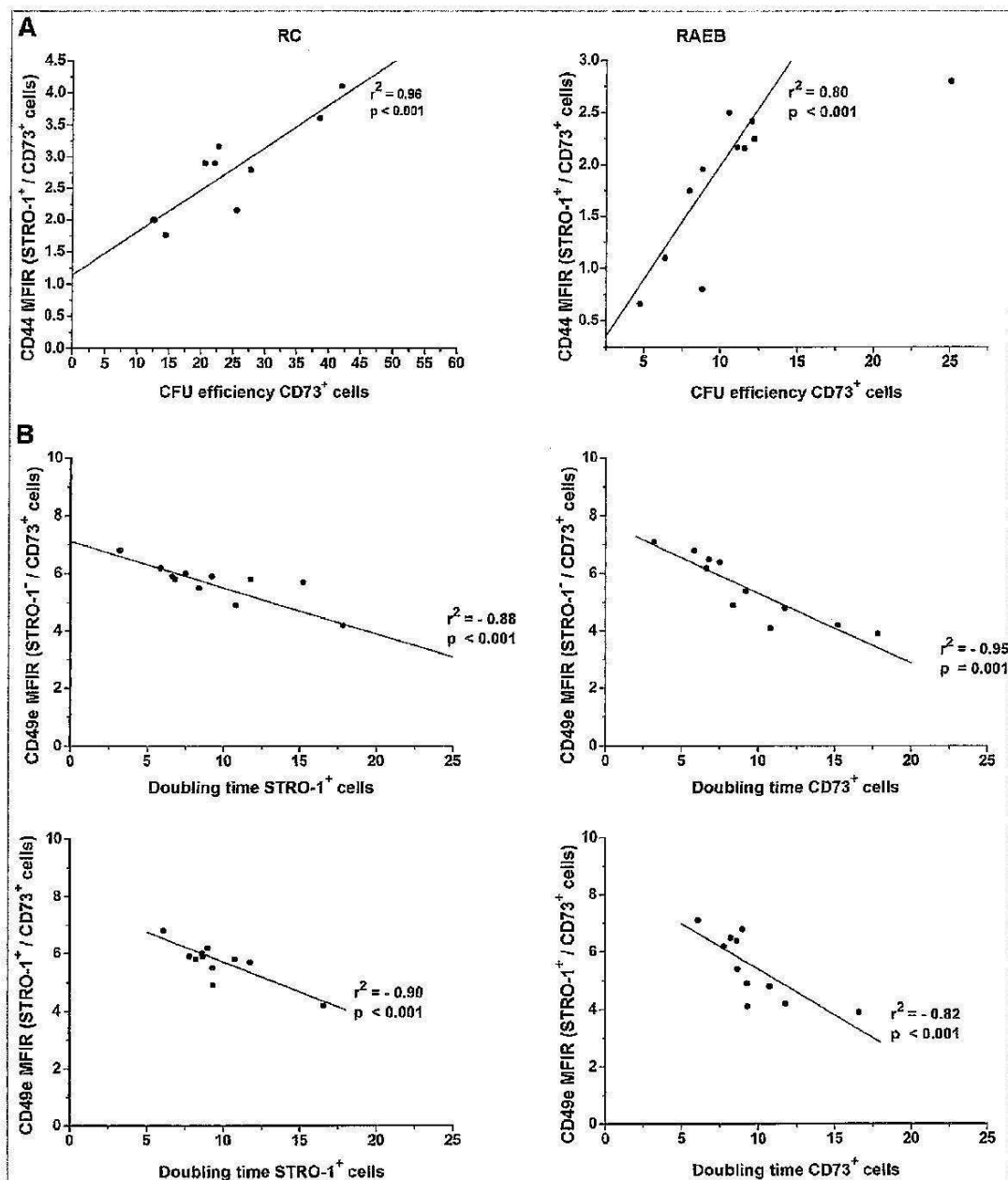


FIG. 4. CD44 and CD49e significance for MSC growth in MDS settings. The plating efficiency of CD73⁺ cells selected from MDS settings versus the intensity of CD44 expression reflect that their clonogenic potential is directly correlated with CD44 expression. The CFU efficiency of CD73⁺ cells was calculated for 1×10^3 seeded MSCs (A). CD49e expression in pathological MSCs and its impact on the proliferative potential of STRO-1⁺ and CD73⁺ cells (B). CFU, colony-forming unit.

alternative for an *in vivo* stroma for performing assays to evaluate HPC-MSc contacts. The STRO-1 molecule does not by itself affect the proliferative abilities of HPCs, and it has low affinity for complement. Thus, the STRO-1 layer appears to only provide signals when induced by the engagement of other adhesion molecules [12].

The CD106 expression was previously reported in umbilical cord blood and BM-derived MSCs [27,31], seems to be the imprint of a particular location (the nearby outer surfaces

of blood vessels), and may share an identity with the vascular pericytes [32,33]. This hypothesis is supported by the coexpression of α smooth muscle actin or 3G5 antigen, which is recognized as a specific marker for pericytes [34]. Further evidence is the fact that a minor subpopulation of STRO-1^{hi} VCAM-1⁺ cells isolated from freshly BM, described as lacking the Ki-67 antigen, appears to be a noncycling population *in vivo*, exhibits telomerase activity, and shows an undifferentiated phenotype and substantial proliferation in

vitro [34]. Their unlimited potential for division and proliferation is also supported by observations that the small number of STRO-1⁺ cells seen in cultures at later points were able to produce adherent cell layers with the same cellular composition and phenotype as those generated by STRO-1⁺ cells freshly isolated from BM [12].

Under the MDS condition, we noticed a higher number of STRO-1⁺ cells that coexpressed CD106 and CD31 between 20 and 30 days of culture and which persisted until 60 days.

Two hypotheses can be evoked from the expression of these markers in relation to MDS physiopathology: the first is related to CD106 upregulation induced by TNF α stimulation [31], and the second is related to CD106 function as a major ligand for selective CD29-mediated HPC-to-MSc adhesions, and, thus, its influence on the HPC mitotic rate and division kinetics [10].

Higher TNF α levels are common in MDS [34], and the MSCs themselves could be responsible for its synthesis in the absence of HPC stimulation. The role of this cytokine in the MDS microenvironment is probably related to its capacity to induce internal proliferative signals in MSCs, as previously noted by Kohase et al. [35].

The increased expression of CD31⁺ could be an imprint of the neoformation of blood vessels in MDS settings, as we showed in a previous study [36].

Further, the functional tests revealed MSC growth abnormalities in the absence of any contact with or stimulation by soluble molecules from HPCs and proved the pathological nature of stromal precursors in MDS settings (Fig. 3). To summarize the biological characteristics of MSCs selected from patients with MDS, 2 different patterns were observed in relation to the type of MDS. For the RC group, similarly reduced clonogenic capacity was observed for both selected fractions, STRO-1⁺ and CD73⁺, and a dramatic decrease in proliferation was largely attributable to the STRO-1⁺ cells. This issue could be explained by an extension of their doubling time to 3-fold that of normal cells (and even 1.3-fold that of RAEB cells) despite their persistence during 60 days of culturing. Similarly, the CD73⁺ fraction was unable to proliferate and produce colonies, and this reduced CFU-F number directly correlates with the loss of CD44 on their surface (Fig. 4A). By contrast, in RAEB, the proliferation rate is moderately improved due to the reduced doubling time of STRO-1 cells. However, at the end point, this was not accompanied by complete functional maturity as reflected in the CFU-F number. Overall, the doubling time of MSCs was found to inversely correlate with their CD49e expression (Fig. 4B).

In conclusion, in MDS settings, an increased number of STRO-1⁺ precursors persist with the capacity for continuous division. Since they do so at a low rate and lack the ability to complete asymmetric divisions and produce mature functional progenitors, this phenomenon might reflect the expansion of an abnormal MSC clone over time with concomitant suppression of residual normal stem cells.

Further cytogenetic studies and transcriptome decryption of MDS MSCs are required to evaluate the molecular substrate of these deficiencies.

Acknowledgments

The authors acknowledge the expertise of J. F. Mayol (CRSSA Emile Pardé, 38702 La Tronche, France) in the MSC

functional assays and of C. Lambert (Immunology Laboratory, University Hospital St. Etienne, 42055, Saint-Etienne, France) in cell sorting. Funding was provided by "Ligue Départementale contre le Cancer de la Loire," "Association Les Amis de Rémi" (France).

Author Disclosure Statement

No competing financial interests exist.

References

- Coutinho LH, CG Geary, J Chang, C Harrison and NG Testa. (1990). Functional studies of bone marrow haemopoietic and stromal cells in the myelodysplastic syndrome (MDS). *Br J Haematol* 75:16–25.
- Tennant GB, V Walsh, LN Truran, P Edwards, KI Mills and AK Burnett. (2000). Abnormalities of adherent layers grown from bone marrow of patients with myelodysplasia. *Br J Haematol* 111:853–862.
- Flores-Figueroa E, G Gutierrez-Espindola, JJ Montesinos, RM Arana-Trejo and H Mayani. (2002). In vitro characterization of hematopoietic microenvironment cells from patients with myelodysplastic syndrome. *Leuk Res* 26:687–688.
- Wetzler M, R Kurzrock, Z Estrov, E Estey and M Talpaz. (1995). Cytokine expression in adherent layers from patients with myelodysplastic syndrome and acute myelogenous leukemia. *Leuk Res* 19:23–34.
- Zhang YZ and DA WM. (2006). Expression of SDF-1 gene in bone marrow mesenchymal stem cells of patients with myelodysplastic syndrome. *Zhongguo Shi Yan Xue Ye Xue Za Zhi* 14:281–284.
- Wagner W, C Roderburg, F Wein, A Diehlmann, M Frankhauser, R Schubert, V Eckstein and AD Ho. (2007). Molecular and secretory profiles of human mesenchymal stromal cells and their abilities to maintain primitive hematopoietic progenitors. *Stem Cells* 25:2638–2647.
- Tauro S, MD Hepburn, Peddie CM, DT Bowen and MJ Pippard. (2002). Functional disturbance of marrow stromal microenvironment in the Myelodysplastic syndromes. *Leukemia* 16:785–790.
- Wagner W, F Wein, C Roderburg, R Saffrich, A Diehlmann, V Eckstein and AD Ho. (2008). Adhesion of human hematopoietic progenitor cells to mesenchymal stromal cells involves CD44. *Cells Tissues Organs* 188:160–169.
- Wagner W, F Wein, C Roderburg, R Saffrich, A Faber, U Krause, M Schubert, V Benes, V Eckstein, H Maul and AD Ho. (2007). Adhesion of hematopoietic progenitor cells to human mesenchymal stem cells as a model for cell-cell interaction. *Exp Hematol* 35:314–325.
- Gottschling S, R Saffrich, A Seckinger, U Krause, K Horsch, K Miesala K and AD Ho. (2007). Human mesenchymal stromal cells regulate initial self-renewing divisions of hematopoietic progenitor cells by a beta1-integrin-dependent mechanism. *Stem Cells* 25:798–806.
- Wagner W, R Saffrich, U Wirkner, V Eckstein, J Blake, A Ansoerge, C Schwager, F Wein, K Miesala, W Ansoerge and AD Ho. (2005). Hematopoietic progenitor cells and cellular microenvironment: behavioral and molecular changes upon interaction. *Stem Cells* 23:1180–1191.
- Simmons PJ and B Torok-Storb. (1991). Identification of stromal cell precursors in human bone marrow by a novel monoclonal antibody, STRO-1. *Blood* 78:55–62.
- Jones E and D McGonagle. (2008). Human bone marrow mesenchymal stem cells in vivo. *Rheumatology* 47:126–131.

14. Boiret N, C Rapatel, S Boisgard, S Charrier, A Tchirkov, C Bresson, L Camilieri, J Berger, L Guillouard, et al. (2003). CD43⁺CDw90(Thy-1)⁺ subset colocalized with mesenchymal progenitors in human bone marrow hematopoietic units is enriched in colony-forming unit megakaryocytes and long-term culture-initiating cells. *Exp Hematol* 31:1275–1283.
15. Gronthos S, E Graves, S Ohta and PJ Simmons. (1994). The STRO-1⁺ fraction of adult human bone marrow contains the osteogenic precursors. *Blood* 84:4164–4173.
16. Psaltis PJ, S Paton, F See, A Arthur, S Martin, S Itescu, SG Worthley, S Gronthos and AC Zannettino. (2010). Enrichment for STRO-1 expression enhances the cardiovascular paracrine activity of human bone marrow-derived mesenchymal cell populations. *J Cell Physiol* 223:530–540.
17. Colgan SP, HK Elitzschig HK, T Eckle T and LF Thompson. (2006). Physiological roles for ecto-5'-nucleotidase (CD73). *Purinergic Signal* 2:351–360.
18. Airas L, J Niemelä, M Salmi, T Puurunen, DJ Smith and S Jalkanen. (1997). Differential regulation and function of CD73, a glycosyl-phosphatidylinositol-linked 70-kD adhesion molecule, on lymphocytes and endothelial cells. *J Cell Biol* 136:421–431.
19. Wang L, J Fan, LF Thompson, Y Zhang, T Shin, TJ Curiel and B Zhang. (2011). CD73 has distinct roles in non-hematopoietic and hematopoietic cells to promote tumor growth in mice. *J Clin Invest* 121:2371–2382.
20. Stochaj U and HG Mannherz. (1992). Chicken gizzard 5'-nucleotidase functions as a binding protein for the laminin/nidogen complex. *Eur J Cell Biol* 59:364–372.
21. Vardiman J, J Thiele, D Arber, R Brunning, M Borowitz, A Porwit, NL Harris, M Le Beau, E Hellström-Lindberg, A Tefferi and C Bloomfield. (2009). The 2008 revision of the World Health Organization (WHO) classification of myeloid neoplasms and acute leukemia: rationale and important changes. *Blood* 114:937–951.
22. Chevallier N, F Anagnostou, S Zilber, G Bodivít, S Maurin, A Barrault, P Bierling, P Hernigou, P Layrolle and H Rouard. (2010). Osteoblastic differentiation of human mesenchymal stem cells with platelet lysate. *Biomaterials* 31:270–278.
23. Cristofalo VJ, RG Allen, RJ Pignolo, BG Martin and JC Beck. (1998). Relationship between donor age and the replicative lifespan of human cells in culture: a reevaluation. *Proc Natl Acad Sci U S A* 95:10614–10619.
24. Nicolaas Franken APN, HM Rodermond, J Stap, J Haveman and C van Bree. (2006). Clonogenic assay of cells in vitro. *Nat Protoc* 1:2315–2319.
25. Dominici M, K Le Blanc, I Mueller, I Slaper-Cortenbach, F Marini, D Krause, R Deans, A Keating, DJ Prockop and E Horwitz. (2006). Minimal criteria for defining multipotent mesenchymal stromal cells. The International Society for Cellular Therapy position statement. *Cytotherapy* 8:315–317.
26. Caplan AI. (2005). Review: Mesenchymal stem cells: cell-based reconstructive therapy in orthopedics. *Tissue Eng* 11:1198–1211.
27. Kern S, H Eichler, J Stoeve, H Klüter and K Bieback. (2006). Comparative analysis of mesenchymal stem cells from bone marrow, umbilical cord blood, or adipose tissue. *Stem Cells* 24:1294–1301.
28. Lee RH, MJ Seo, AA Pulin, CA Gregory, J Ylostalo and DJ Prockop. (2009). The CD34-like protein PODXL and $\alpha 6$ -integrin (CD49f) identify early progenitor MSCs with increased clonogenicity and migration to infarcted heart in mice. *Blood* 113:816–826.
29. Potapova AI, PR Brink, IS Cohen and SV Doronin. (2008). Culturing of human mesenchymal stem cells as three-dimensional aggregates induces functional expression of CXCR4 That Regulates Adhesion to Endothelial Cells. *J Biol Chem* 283:13100–13107.
30. Prockop DJ. (2009). Repair of tissues by adult stem/progenitor cells (MSCs): controversies, myths, and changing paradigms. *Am Soc Gene Ther* 17:939–946.
31. Halfon S, N Abramov, B Grinblat and I Girin. (2011). Markers distinguishing mesenchymal stem cells from fibroblasts are downregulated with passaging. *Stem Cells Dev* 20:53–66.
32. Short B, N Brouard, T Occhiodoro-Scott, A Ramakrishnan and PJ Simmons. (2003). Mesenchymal stem cells. *Arch Med Res* 35:565–571.
33. Bianco P, M Riminucci, S Gronthos and PG Robey. (2001). Bone marrow stromal cells: Nature, biology, and potential applications. *Stem Cells* 19:180–192.
34. Gronthos S, AC Zannettino, SJ Hay, S Shi, SE Graves, A Kortessidis and PJ Simmons. (2003). Molecular and cellular characterisation of highly purified stromal stem cells derived from human bone marrow. *J Cell Sci* 116:1827–1835.
35. Kohase M, D Henriksen-Destefano, LT May, J Vilček and PB Seghal. (1986). Induction of β_2 -interferon by tumor necrosis factor: a homeostatic mechanism in the control of cell proliferation. *Cell* 45:659–666.
36. Boudard D, A Viallet, S Piselli, D Guyotat and L Campos. (2003). In vitro study of stromal cell defects in myelodysplastic syndromes. *Haematologica* 88:827–829.

Address correspondence to:

Dr. Carmen Mariana Aanei
 Etablissement Français du Sang Bourgogne-Franche
 Comté site de Nevers
 1 Bd de l'Hôpital
 Nevers 58000
 France

E-mail: caanei@yahoo.com

Received for publication July 18, 2011

Accepted after revision September 13, 2011

Prepublished on Liebert Instant Online XXXX XX, XXXX

III.2. Focal adhesion protein abnormalities in myelodysplastic mesenchymal stromal cells

-Experimental Cell Research-

-Vol. 317 (2011) 2616 – 2629-

Direct cell-cell contact between haematopoietic progenitor cells (HPCs) and their cellular microenvironment is essential to maintain ‘stemness’.

In cancer biology, focal adhesion (FA) proteins are involved in survival signal transduction in a wide variety of human tumours. Thus, was noticed the role of FAK Tyr³⁹⁷ phosphorylation in promoting cell survival, cell proliferation and cell invasion by FAK–Src signalling pathway, and the recruitment of FAK and paxillin to β 1 integrin to promote cancer cell migration via mitogen activated protein kinase activation [265], [317], [318].

In this study, we assessed the expression levels and cellular localisation of focal adhesion (FA) proteins in normal and dysplastic stroma, in order to determine whether their expression correlated with the progression to malignancy.

In this order, CD73-positive mesenchymal stromal cells (MSCs) were immunostained for paxillin, pFAK [Y³⁹⁷], HSP90 α/β and p130CAS, and analysed for reactivity, intensity and cellular localization. Immunofluorescence microscopy allowed us to identify qualitative and quantitative differences, and subcellular localisation analysis revealed that in pathological MSCs, paxillin, pFAK [Y³⁹⁷], and HSP90 α/β formed nuclear molecular complexes.

Through these experiments, we found a significant relationship between the levels of expression of FA proteins, their nuclear co-localisation, and the proliferative potential of MSCs.

In addition, the increased levels of pFAK [Y³⁹⁷] in MSCs isolated from MDS patients were inversely correlated with the clonogenicity of haematopoietic progenitor cells (HPCs).

Together, our findings suggest that assessment of the subcellular FA protein co-localisation in MSCs selected from MDS patients in combination with HPC clonality studies are potential tools that could be employed to identify MDS patients with disease progression and to guide therapy.

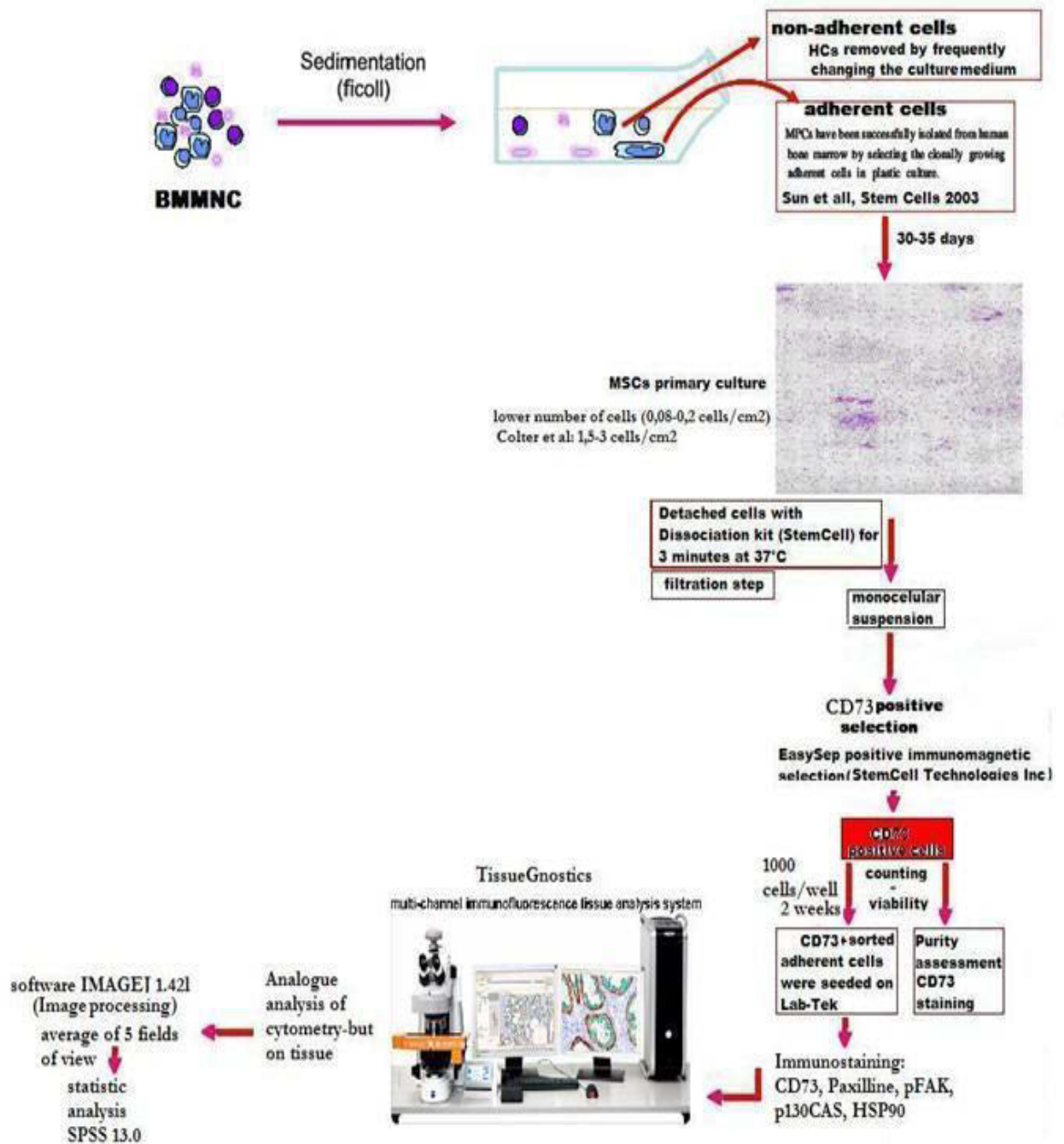


Figure 34. Experimental strategy of focal adhesion proteins evaluation on CD73⁺ MSCs Lab-Tek cultures

III.2-1. Focal adhesion proteins evaluation in MSCs selected from MDS settings vs. normal bone marrows

Multicolour fluorescent microscopy has proven to be a successful technique for FA protein analysis. It allowed us to assess the intracellular localization of proteins, and to understand the spatial relationship between these proteins via colocalization analysis.

A first remark was the bright nuclear expression of pFAK [Y³⁹⁷] in pathological MSCs, but not in focal adhesion contacts as we had expected. Over 80% of RAEB MSCs showed nuclear expression of pFAK [Y³⁹⁷].

For HSP90αβ expression, an increased level, directly correlated with pFAK [Y³⁹⁷] up-regulation was found in MSCs cells from RAEB group (2.62-fold in S-MSCs and 3.82-fold in L-MSCs). HSP90αβ immunostaining of CD73⁺ MSCs cultures show that this chaperone is abundantly expressed in the cytoplasm, but a nuclear immunoreactivity was also noticed. About 30% of normal MSCs also showed an HSP90αβ nuclear expression.

Difference from normal for RAEB MSCs consists in an overall greater expression of cytoplasmic staining and increased percentages of nuclear HSP90αβ positive cells (around 80%).

Similar percentages of paxillin positive cells were counted for all three groups.

Cellular distribution of this protein display two patterns of reactivity, diffuse cytosolic and nuclear, with remarkable differences between groups. Thus, 97-98% of RAEB MSCs shows a nuclear pattern of expression for paxillin and a paranuclear staining was revealed by large cells as well. In normal cells, the same cytoplasmic and nuclear disposition was distinguished, but 70% from paxillin positive cells have nuclear expression. In RC group, only 14-15% of paxillin positive cells have also a nuclear reactivity.

Despite the low intensities and diffuse cytoplasmic staining for p130CAS observed in all groups, a slight increase of the number of p130CAS positives cells was found in RC and RAEB groups as compared to the normal group (92%, and 96%, respectively, vs. 73%).

The co-localisation analysis of HSP90αβ with paxillin provides compelling evidence that staining for paxillin varies in synchrony with that for HSP90αβ, consistent with the formation of a complex within restricted, small areas of nuclear regions of 80-90% from RAEB S-MSCs and in 20-30% of normal S cells. Likewise, pFAK [Y³⁹⁷] strongly colocalize at paxillin and HSP90αβ in RAEB cells, while their normal counterparts display a weaker co-localization of pFAK [Y³⁹⁷] to paxillin in approximatively 40 % of studied cells, and no co-localization pFAK [Y³⁹⁷]-HSP90αβ. For RC S-MSCs we noticed very low percents of co-localization

between these three proteins (from 0.08% to 0.18%) associated to an exclusive staining pattern.

Moreover, unlike normal L-MSCs, the large cells from RAEB group had preserved an increased level of expression for pFAK [Y³⁹⁷] and a high co-localization of this protein to paxillin and HSP90αβ. The coefficients calculated for their co-localization in RAEB L-MSCs support the fact that the staining intensities vary in synchrony; consequently, these proteins are parts of the same complex (an average of 8% of co-localization was obtained for paxillin-HSP90αβ, 14% for paxillin-pFAK [Y³⁹⁷], and 9% for pFAK [Y³⁹⁷]-HSP90αβ pairs).

The significance of the particular expression of these proteins, as well as their nuclear colocalisation are the subjects of the following chapters.

III.2-2. Role of Paxillin-pFAK [Y³⁹⁷]-HSP90 signalling pathway in MSCs proliferation

Recent evidences have shown that FA proteins, mainly FAK are involved in cell growth signalling pathways [265].

Herein, we bring compelling evidences that strong paxillin nuclear immunoreactivity, and its highly co-localization to pFAK [Y³⁹⁷] and HSP90αβ in RAEB MSCs, with formation of functional active complexes with nuclear disposition, was correlated with a proliferative advantage in S-MSCs ($p < 0.01$, $r = 0.79$, Spearman test) and less significant in L-MSCs ($p < 0.05$, $r = 0.64$) (Figure 35).

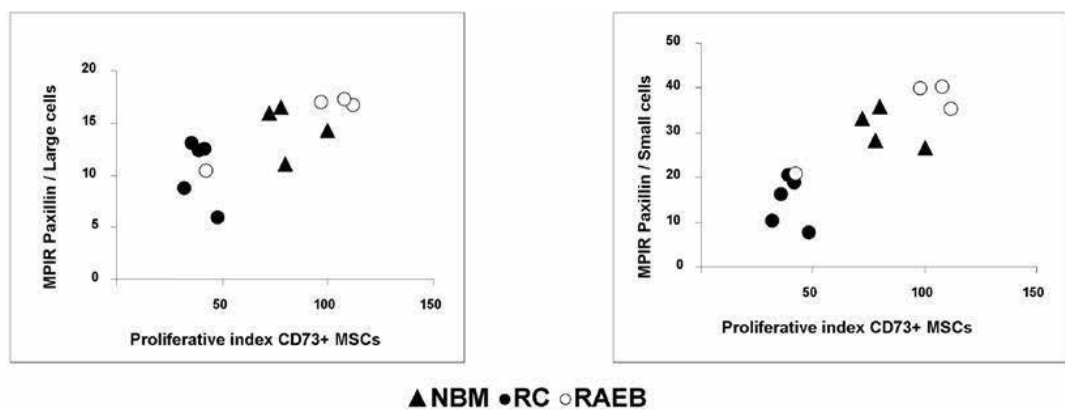


Figure 35. Correlations between paxillin expression and the proliferation rates of CD73⁺ selected MSCs

III.2-3. The impact of increased expression of pFAK [Y³⁹⁷] in MSC on MSC-HPC relationship

We have also noticed that increased levels of expression for pFAK [Y³⁹⁷] in MSCs, correlated with a decreased proliferation capacity of HPCs in same patients, i.e., 4-fold lower number of BFU-E and CFU-GM as compared to the normal counterpart, were detected in RAEB group and 1.5-fold in RC group, respectively. This dysfunction detected in the haematopoietic compartment was related rather to the level of pFAK [Y³⁹⁷] expression in MSCs compartment than to the percentage of positive cells for this marker (Figure 36).

This was revealed by the fact that comparable percentages of positive cells in RAEB and RC MSCs cultures (97% vs. 93%) did not have the same impact on the clonogenic ability of haematopoietic precursors. This lies in the differences of pFAK [Y³⁹⁷] intensity of expression between the two groups, which reversely correlated to colony-forming cells (CFC) capacities in haematopoietic compartment ($p < 0.001$, $r = -0.60$ for RAEB group, and $p = 0.001$, $r = -0.31$ for RC group, Spearman test).

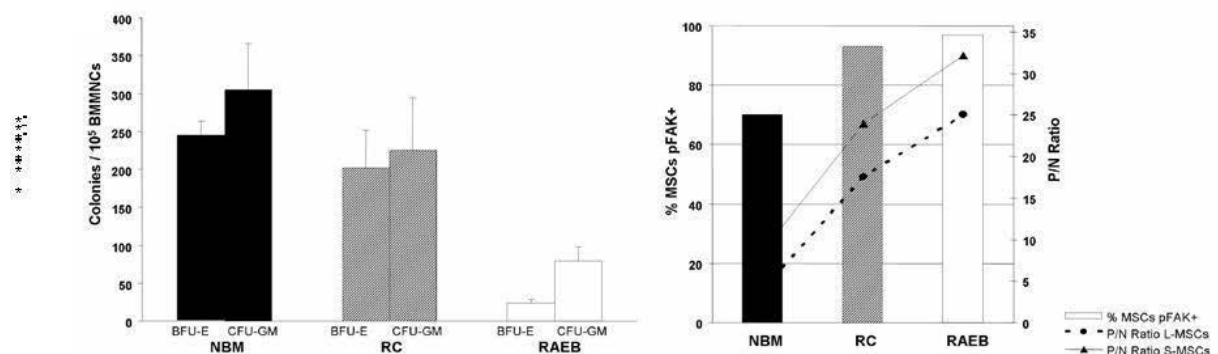
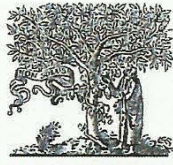


Figure 36. pFAK [Y³⁷⁹] expression in MSC vs. the clonogenic potential of HPCs selected from same cases

Left chart shows the mean number of BFU-E and CFU-GM from each group. The right chart shows the percentage of pFAK positive MSCs cells (columns, values should be compared with left scale), and the relative intensity of expression for pFAK in L-MSCs cells (dashed line) and in S-MSCs (continuous line) in the three studied groups (lines and diamond symbols, values should be compared with right scale).

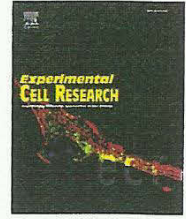
In conclusion, our results allowed us to propose a physiopathological model where a hyperexpression of phosphorylated FAK [Y³⁹⁷] in MSCs contribute to its growth dysfunction via paxillin-pFAK [Y³⁹⁷]-HSP90 signaling pathway. Moreover, these abnormalities of FA proteins train the alteration of the dialogue between MSC and haematopoietic cells, fact that support the previously stated hypothesis that MDS is a disease of “bad seeds in bad soil”.



ELSEVIER

Available online at www.sciencedirect.com

SciVerse ScienceDirect

www.elsevier.com/locate/yexcr

Research Article

Focal adhesion protein abnormalities in myelodysplastic mesenchymal stromal cells

Carmen Mariana Aanei^{a,b,*}, Florin Zugun Eloae^b, Pascale Flandrin-Gresta^{a,d},
Emmanuelle Tavernier^{c,d}, Eugen Carasevici^b, Denis Guyotat^{c,d}, Lydia Campos^{a,d}

^aLaboratoire Hématologie, CHU de Saint-Etienne, 42055, Saint-Etienne, France

^bDepartment of Immunology, Gr. T. Popa University of Medicine and Pharmacy, 700115, Iasi, Romania

^cService Hématologie Clinique, Institut de Cancérologie de la Loire, 42270, Saint-Priest-en-Jarez, France

^dCNRS UMR 5239, Université de Lyon, 42023, Saint-Etienne, France

ARTICLE INFORMATION

Article Chronology:

Received 17 April 2011

Revised version received 7 August 2011

Accepted 9 August 2011

Available online 16 August 2011

Keywords:

FAK

Paxillin

HSP90 α/β

Cell proliferation

HPC–MSC contact

Immunofluorescence analysis

ABSTRACT

Direct cell–cell contact between haematopoietic progenitor cells (HPCs) and their cellular microenvironment is essential to maintain ‘stemness’. In cancer biology, focal adhesion (FA) proteins are involved in survival signal transduction in a wide variety of human tumours. To define the role of FA proteins in the haematopoietic microenvironment of myelodysplastic syndromes (MDS), CD73-positive mesenchymal stromal cells (MSCs) were immunostained for paxillin, pFAK [Y³⁹⁷], and HSP90 α/β and p130CAS, and analysed for reactivity, intensity and cellular localisation. Immunofluorescence microscopy allowed us to identify qualitative and quantitative differences, and subcellular localisation analysis revealed that in pathological MSCs, paxillin, pFAK [Y³⁹⁷], and HSP90 α/β formed nuclear molecular complexes. Increased expression of paxillin, pFAK [Y³⁹⁷], and HSP90 α/β and enhanced nuclear co-localisation of these proteins correlated with a consistent proliferative advantage in MSCs from patients with refractory anaemia with excess blasts (RAEB) and negatively impacted clonogenicity of HPCs. These results suggest that signalling *via* FA proteins could be implicated in HPC–MSC interactions. Further, because FAK is an HSP90 α/β client protein, these results suggest the utility of HSP90 α/β inhibition as a target for adjuvant therapy for myelodysplasia.

© 2011 Elsevier Inc. All rights reserved.

Introduction

Myelodysplastic syndromes (MDS) are clonal disorders of haematopoietic stem cells (HSCs) characterised by ineffective haematopoiesis that manifest clinically as anaemia, neutropenia, and/or thrombocytopenia and increase the risk of transformation to acute myeloid leukaemia. In MDS, the bone marrow (BM) microenvironment is responsible for the intramedullary apoptosis

of HPCs, and this abnormal function appears to be dependent on close cellular contact rather than on the release of soluble factors [1]. The BM microenvironment is also responsible for the selection of neoplastic haematopoietic clone(s) that are resistant to apoptosis and express factors promoting proliferation and migration [2]. Mesenchymal stromal cells (MSCs) are key components of the haematopoietic microenvironment, and several studies have demonstrated morphological and functional changes in these cells in

* Corresponding author at: Laboratoire Hématologie, CHU de Saint-Etienne, 42055, Saint-Etienne, France. Fax: +33 38 66 18 201.

E-mail address: caanei@yahoo.com (C.M. Aanei).

MDS patients. A recent study reported morphological abnormalities of BM MSC primary cultures from MDS patients [3] including the presence of large flat cells with unipolar cytoplasm or short round cytoplasmic spikes. In addition, genomic abnormalities were also observed in MSCs from MDS patients [3–5]. From a functional point of view, Boudard et al. showed that the growth dysfunction of myelodysplastic stromal layers correlates with caspase-3 activation [6]. Over the past few years, exciting discoveries have been made in the field of MSC pathogenesis. The spontaneous transformation of MSCs is hypothesised to be a consequence of c-myc up-regulation, p16 down-regulation, and increased telomerase activity [7,8]. In terms of the potential roles of MSCs in carcinogenesis, previous studies have demonstrated that MSCs promote tumour cell invasion via the activation of matrix metalloproteinases and neoangiogenesis [8,9], modulate tumour cell cycle [9–12], and suppress the immune system of tumour-bearing hosts [8,9,12]. In this study, we assessed the expression levels and cellular localisation of focal adhesion (FA) proteins in normal and dysplastic stroma in order to determine whether their expression correlated with the progression to malignancy. Our results highlighted the differential expression of these proteins in *in vitro* cultures from MDS MSCs when compared to control MSCs from healthy donors, but the functional differences were related to the subcellular location of these proteins rather than to their overall expression levels. Through these experiments, we found a significant relationship between the levels of expression of FA proteins, their nuclear co-localisation, and the proliferative potential of MSCs. These processes are likely controlled by the RAS-MAPK (mitogen-activated protein kinase) [13,14] and AKT-mTOR activation signalling pathways [13,15] or by altered transcription of genes implicated in DNA synthesis and cell proliferation [16,17]. In addition, the increased levels of pFAK [Y³⁹⁷] in MSCs isolated from MDS patients were inversely correlated with the clonogenicity of haematopoietic progenitor cells (HPCs). Together, our findings suggest that assessment of the subcellular FA protein co-localisation in MSCs selected from MDS patients in combination with HPC clonality studies is a potential tool that could be employed to identify MDS patients with disease progression and to guide therapy.

Materials and methods

Patients and controls

BM aspirates were collected from 9 MDS patients with a mean age of 76 years (range, 56–85) and 4 control subjects with a mean age of 59 years (range, 39–69 years). Samples were obtained in the absence of any treatment. Patient diagnosis was performed by cytological evaluation of BM smears after May-Grünwald-Giemsa staining [18] and cytogenetic analysis. Patients were assigned to different groups according to the 2008 World Health Organization (WHO) classification system [19].

Patient characteristics are described in Table 1. Signed institutional review board-approved written informed consent was obtained from all patients and control subjects.

Human haematopoietic colony-forming cell assays

The detection and counting of erythroid burst-forming units (BFU-E) and colony-forming units-granulocyte-macrophage (CFU-GM) was

performed in MethoCult® H4434 methylcellulose-based medium (StemCell Technologies). For this purpose, mononuclear cells containing the haematopoietic progenitors were separated from BM aspirates using density gradient centrifugation (1.077 g/cm³) on Lymphoprep™ (FreseniusKabi). After centrifugation, 1.25×10^4 BM mononuclear cells were resuspended in 1.2 mL MethoCult® and cultured at 37 °C and 5% CO₂ in 35-mm culture dishes (StemCell Technologies) for 14 days. Each sample was processed in duplicate. The colonies were then counted and classified based on morphological features by light microscopy.

MSC amplification in primary cultures

The small amounts of aspirates imposed a pre-enrichment step of stromal cells in primary cultures.

Mononuclear cells containing the MSCs were separated from heparinised BM specimens by density gradient centrifugation as described above, then plated at a density of 8×10^4 cells/cm² and expanded to confluence for 4–5 weeks at 37 °C and 5% CO₂ in 2.5-cm² culture flasks containing 8 mL MesenCult® medium (StemCell Technologies). MSCs were allowed to adhere overnight, and non-adherent cells were washed out by changing the medium. Thereafter, medium was changed twice weekly by replacing 50% of the culture medium with fresh medium.

Evaluation of MSC layers from primary cultures

This step was performed to detect morphological abnormalities. The staining of MSC cultures was performed according to the manufacturer's instructions (StemCell Technologies) [20].

Selection of CD73⁺ highly clonogenic MSCs

When 80% confluence was achieved in primary cultures, MSCs were detached with the MesenCult® Dissociation Kit (StemCell Technologies). Cells were collected in glass tubes containing 5 mL MesenCult® with 20% Foetal Calf Serum (FCS, GIBCO® Invitrogen) and filtered through a 70-µm cell strainer (Falcon, Becton Dickinson). The cell number and viability were evaluated using Trypan Blue solution (0.4% in PBS) (StemCell Technologies). The cells were then pelleted by gentle centrifugation at 1200 rpm for 10 min, blocked with anti-human CD32 (Fcγ RII) Blocker from the EasySep® PE Selection Kit (StemCell Technologies), and stained with PE-conjugated mouse anti-human CD73 monoclonal antibody (BD Pharmingen™) at a concentration of 3.0 µg/mL per 10⁷ cells for 1 h on ice. Cells were washed with MesenCult®/FCS (1:1), and the isotype-matched controls and CD73-stained cells were analysed using a FACSCantol flow cytometer (Becton Dickinson) to determine the initial purity. For sorting, the CD73-stained cells were processed by adding the EasySep® PE Selection Cocktail (100 µg/mL) and EasySep® Magnetic Nanoparticles and then using the EasySep® magnet from the EasySep® PE Selection Kit (StemCell Technologies). Finally, 1×10^5 cells were analysed by flow cytometry to detect purity after sorting. Cell viability was evaluated by staining with 1 µL of propidium iodide (PI, 1 mg/mL, Sigma) prior to FACS acquisition. Data were analysed using the DIVA software (Becton Dickinson).

Flow cytometric analysis of CD73⁺ cell fractions demonstrated high purity (90–99% CD73⁺ PI⁻ cells within the singlet gate, as depicted in a representative example in Fig. 1C).

Table 1 - Clinical and laboratory characteristics of MDS patients and control subjects studied.

Patient	Age	WHO 2008 ^a	% blasts in PB	% blasts in BM	Hb ^b g/dL	Leuco cytes × 10 ⁹ /L	Platelets × 10 ⁹ /L	PB Mo ^c × 10 ⁹ /L	BM cellularity ^d	Dys-myelo poiesis ^e	Dys-erythro poiesis ^e	Dys-megakario poiesis ^e	RS ^f	Cytogenetics	Transfusion dependence ^g	BFU-E ^h	CFU-GM ⁱ
MDS patients																	
MDS1	73	RCUD-RA	0	3.5	10.5	6.62	222	0.34	++	-	-	-	-	46XX	-	248	296
MDS2	85	RARS	0	1	12.7	9.6	298	0.97	+++	-	++	-	-	46XX	-	8	13
MDS3	72	RCUD-RT	0	1	12.2	5.81	84	0.41	++	+	-	-	-	46XX	-	200	184
MDS4	85	RCMD	0	3	10.1	3.37	100	0.44	+++	++	++	++	(+)	46.XY,del(20)(q11q13)[8]	-	160	180
MDS5	64	RCUD-RA	0	2.5	9.8	3.7	308	0.26	++	-	-	-	-	46.XY	+	12	11
MDS6	78	RAEB-1 ^j	1	11	11	3.21	324	0.21	+++	+++	+++	-	(+)	46.XX,del 5)(q22q34)	-	0	88
MDS7	84	RAEB-1 ^j	3.5	7	9.5	3.98	445	0.15	+++	+++	-	-	-	del(20)(q11q13)[19]	+	28	72
MDS8	56	RAEB-2 ^j	5	16.5	12.7	2.51	201	0.5	++	+++	-	-	-	46XX	-	19	29
MDS9	46	AML inv(3)(q21q26) ^m	22	34	9.8	43.34	254	0.7	+++	++	+++	+++	-	46.XY,inv(3)(q21q26)[20]	-	174	92
Control																	
BM																	
NBM1	39		0	0	14.7	7.65	275	0.32	++	-	-	-	-	ND	N/A	220	256
NBM2	69		0	0	13.5	6.97	175	0.28	++	-	-	-	-	ND	N/A	ND	ND
NBM3	59		0	1.5	11.7	4.69	389	0.59	+++	-	-	-	-	ND	N/A	240	248
NBM4	44		0	0	15.2	8.89	375	0.335	++	-	-	-	-	ND	N/A	268	376

◆ Too few metaphases; ND = not done; N/A = not applicable.
^a WHO indicates the World Health Organization classification of myeloid neoplasms and acute leukaemia (Ref. [13]).

^b Hb = haemoglobin.
^c PB Mo = peripheral blood monocyte count.
^d Bone marrow cellularity: ++ = normocellularity, and +++ = hypercellularity.
^e Degree of dysplasia: ++ = moderate, and +++ = severe.
^f RS = ringed sideroblasts.
^g Transfusion dependence: + = transfusion-dependent, and - = not transfusion dependent.
^h Human colony-forming unit: BFU = burst-forming unit-erythroid; CFU-GM = colony-forming unit-granulocyte, macrophage.
ⁱ RCUD- = refractory cytopenia with multilineage dysplasia; -RA = refractory anaemia; -RT = refractory thrombocytopenia.
^j RARS = refractory anaemia with ringed sideroblasts.
^k RCMD = refractory cytopenia with multilineage dysplasia.
^l RAEB = refractory anaemia with excess blasts.
^m AML inv(3)(q21q26) = acute myeloid leukaemia with inv(3)(q21q26.2).

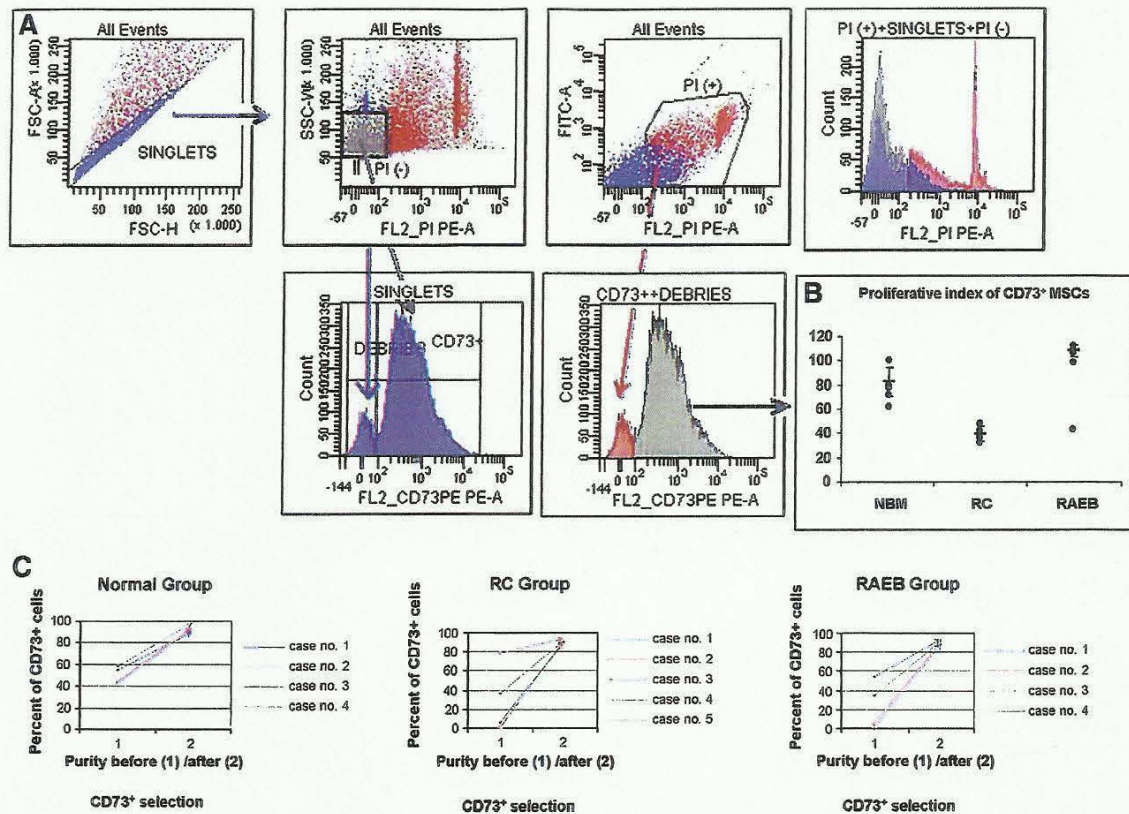


Fig. 1 – Experimental strategy for CD73 immunomagnetic selection. The analysis strategy using gating of singlet cells followed by subsequent exclusion of dead (PI⁺, red dots) cells and final gating for CD73⁺ cells (A). Proliferation index of CD73⁺ cell fractions from MDS patients compared with those from control subjects. The values reflect the mean \pm SD. The results obtained for different groups were significantly different ($p < 0.05$) (B). During EasySep[®] positive selection, a consistent increase in CD73⁺ cell percentages was observed, as illustrated by the fold increase in CD73⁺ cells. High recovery was achieved in the RC and RAEB MSC samples with low cellularity (initial, 51% \pm 6.87, final, 98% \pm 0.30 in the enriched fraction for control cells; initial, 32 \pm 24.19, final, 95% \pm 0.39 for the RC group; and initial, 44 \pm 13.5, final, 92% \pm 0.77 for the RAEB group) (C).

MSC growth characteristics

Proliferation tests were performed on CD73-selected MSCs from MDS patients and healthy control donors. To this end, 1×10^3 viable MSCs (quantified using the Trypan Blue exclusion test) were plated in 25-cm² flasks, and the number of cells was counted on days 1 and 14. We then calculated the proliferation index (the difference between the number of harvested cells and the initial plated number).

Lab-Tek cultures

After sorting, cells were collected in MesenCult[®]/FCS (1:1) medium. Cells (1×10^3 per well) were plated on Lab-Tek[®]II Chamber Slides (Nalge Nunc International Corp.) in 0.5 mL MesenCult[®] medium and allowed to reach 70–80% confluence over 2 weeks.

Immunostaining

Cells were washed thoroughly to remove residual media and fixed in 4% w/v paraformaldehyde for 10 min at room temperature (RT).

Fixation was stopped by washing cells 3 times with PBS, pH 7.2 (BD Bioscience).

Non-specific background staining was blocked with antibody (Ab) buffer containing PBS (1 \times), FCS (1% w/v) and BSA (bovine serum albumin, Sigma-Aldrich, 1% w/v) for 1 h. Cells were then permeabilised with 0.1% Triton X-100 (Sigma-Aldrich) in PBS for 20 min before Ab application. Primary antibodies were diluted in Ab buffer before application of the following antibodies: FITC-conjugated mouse anti-human paxillin monoclonal Ab (mAb) (final dilution 1:50, clone 349/Paxillin, BD Bioscience), PE-conjugated mouse anti-human CD73 mAb (1:25, clone AD2, BD Pharmingen[™]), unconjugated rabbit anti-phospho-specific FAK [pY³⁹⁷] polyclonal Ab, (1:100, Invitrogen Corporation), mouse anti-human p130CAS mAb (1:40, clone 35B.1A4, Santa Cruz Biotechnology, Inc.), PE-conjugated mouse anti-human HSP90 α/β mAb (1:40, clone F-8, Santa Cruz Biotechnology, Inc.), FITC-conjugated mouse anti-human IgG2a,k mAb (1:50, clone G155-178, BD Pharmingen[™]), PE-conjugated mouse anti-human IgG1,k mAb (1:40, clone MOPC-21, BD Pharmingen[™]), and rabbit anti-human IgG polyclonal Ab (1:100, DakoCytomation). Secondary antibodies (Invitrogen Corporation) were as follows:

FITC-conjugated goat anti-mouse IgG (H+L) 1:50, PE-conjugated goat anti-mouse IgG (H+L) 1:25, and Alexa Fluor 633-conjugated goat anti-rabbit IgG (H+L) 1:100 in Ab buffer. Samples were incubated overnight with primary antibodies and for 2 h with secondary antibodies at 4 °C in a moist chamber. Before acquisition, nuclear staining with 4', 6-Diamidino-2-phenylindole (DAPI, 1 µg/mL) was performed for 30 min at 4 °C. Slides were mounted in Faramount Aqueous Mounting Medium (Dako Denmark).

Relative fluorescence measurements and protein clustering analysis

Triple-stained preparations were visualised under an Axio Observer Z1 microscope (Carl Zeiss, Inc.) at 100× magnification. Signals were recorded simultaneously by three photomultiplier tubes (PMT 1–3). The images (TIFF format) were captured with a PixeLINK PL-A622C/622000227 camera (Aegis Electronic Group, Inc.) by taking multiple exposures through bandpass optical filter sets appropriate for FITC, Texas Red, Alexa Fluor 633 and DAPI using a 100× Plan Apochromat objective.

Analysis and quantification of immunofluorescence staining were performed using ImageJ software (<http://rsb.info.nih.gov/ij/>). Five representative fields were analysed per filter and per slide. Data recorded for an average of 25 cells per group were exported to Excel (Microsoft) for further analysis.

Protein clustering analysis was performed using the “dye overlay” method previously described by Li et al. [21]. The Origin 7.0 (Microcal Software) charts were used to display the percentage of co-localisation between the analysed proteins in each of 10 spindle-shaped cells and 10 large cells per group. The scatter plots and the colour co-localisation maps were generated by ImageJ software. The degree of co-localisation was evaluated using the various co-localisation coefficients, and proteins belonging to the same complex were identified using the Intensity Correlation Quotient (ICQ) and intensity correlation plots (ICA) as previously described [21–23]. We distinguished three patterns of staining: random staining (assigned to those proteins with $ICQ \sim 0$ ($0.1 < ICQ < +0.1$)), segregated or non-overlapping staining (assigned to those proteins with no co-localisation or complementary staining with $-0.1 > ICQ \geq -0.5$), and dependent or co-localised staining (assigned to those proteins with $+0.1 < ICQ \leq +0.5$) [21,23].

Statistical analysis

Results are expressed as the mean \pm standard deviation (SD). The parameters were compared among the groups by using SPSS software (SPSS 13.0 Chicago, <http://www.spss.com>) to perform the Student's *t*-test (*p*). Differences between the groups were considered to be significant when $p \leq 0.05$.

Results

Morphological assessment of MSC layers in primary cultures

Stromal layers represent a key regulator of the haematopoietic microenvironment. Therefore, our study began with the evaluation of stromal composition and function to clarify whether MDS could be a disease of the stroma. We first observed that MSC layer

morphology was different in normal donors than in MDS patients (Figs. 2A, B, C). Disorganisation of colony architecture was observed in samples from patients displaying refractory anaemia with excess blasts (RAEB); furthermore, these samples displayed increased synthesis of matrix components and giant “amorphous” deposits in cultures (Fig. 2B). These findings were accompanied by dysplastic changes in MSCs similar to those described in the haematopoietic lineage. The most frequently encountered morphology was the megaloblastoid form (thin, flat and round-shaped MSCs), which is likely caused by altered actin organisation (Fig. 2D). Despite their “mature” appearance, these cells retained the ability to proliferate and form colonies (Fig. 2C). Other noteworthy changes were cells with “flame” paranuclear regions, cytoplasmic amorphous substance deposits (Figs. 2E, F), giant nuclei, nuclear irregularities (Fig. 2G), and large, branched cytoplasmic budding (Fig. 2H).

Functional evaluation of CD73⁺ MSCs selected from MDS cultures

These morphological changes were accompanied by functional abnormalities in MDS stromal layers. Comparison of the proliferation capacities of the MSCs selected from MDS patients to those from control subjects demonstrated deficient MSC production in CD73⁺ MSC cultures derived from BM from patients with refractory cytopoemia (RC) (Fig. 1B). The average proliferation index for MSCs selected from RC BM after 2 weeks of culture was 50% of that in control samples (40 ± 6.4 vs. 83 ± 12.1 , $p < 0.05$). In contrast, proliferation was increased approximately 1.5-fold in CD73⁺ cells from the RAEB group when compared to control cells (Fig. 1B). These observations provide evidence for growth and survival abnormalities in MSCs from MDS patients when cultured under the same conditions as control cells.

FA proteins in CD73⁺ cells from MDS cultures and control cultures

Recent evidence has shown that FA proteins, specifically FAK, are involved in cell growth signalling pathways. As such, we assessed two principal FA proteins, paxillin and pFAK [Y³⁹⁷], as well as two regulators of their activity, HSP90 α/β and p130CAS, for expression, intensity and cellular localisation in MDS and control cells.

Table 2 displays the percentages of MSCs positive for the four proteins of interest and the relative intensity of expression of these proteins in pathological cells and control cells. Representative images showing protein expression and relative protein intensities are depicted in Fig. 3.

No significant differences were found in the relative fluorescence intensity of the markers between S cells and L cells in the same group, but significant differences in the expression of pFAK [Y³⁹⁷], paxillin, and HSP90 α/β were observed between the groups, RAEB and RC vs. control group.

The large cells in the RAEB and RC groups displayed 6-fold and 4-fold increases in pFAK [Y³⁹⁷] expression, respectively, as compared to the control cells. Further, S-MSCs showed an increase in pFAK [Y³⁹⁷] expression of almost 4-fold and 3-fold in the RAEB and RC groups, respectively, when compared to the control samples. Subcellular localisation analysis for this protein provided surprising data. We observed bright nuclear expression of pFAK [Y³⁹⁷] in pathological MSCs but not in FA contacts, as we had expected. Over 80% of RAEB MSCs showed nuclear expression of pFAK [Y³⁹⁷].

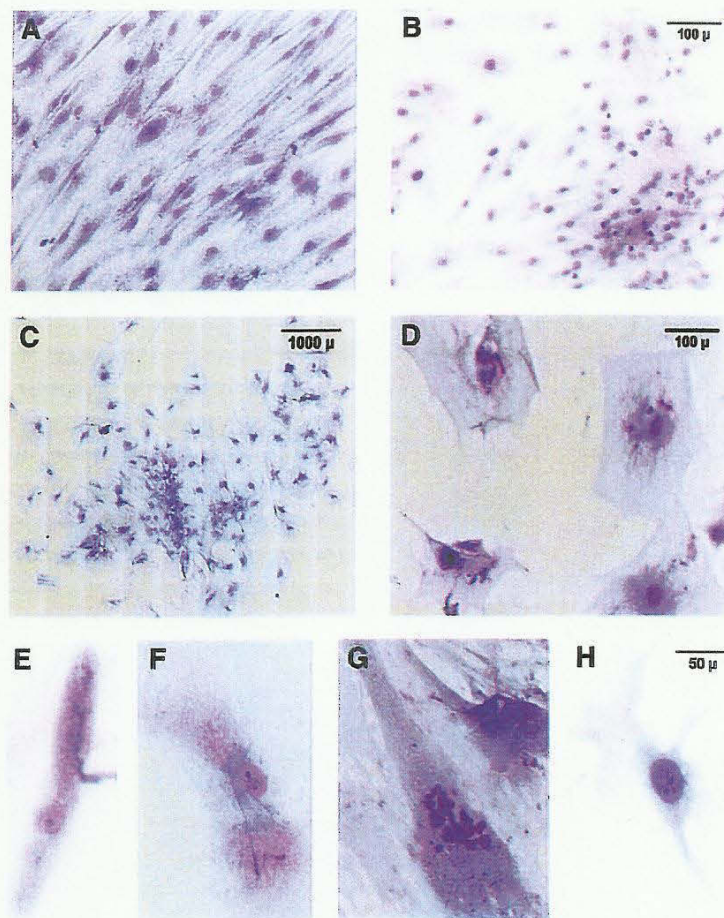


Fig. 2 – Representative fields of view of 35-day primary cultures. MSCs isolated by plastic adherence from BM aspirates (Giemsa staining). A representative example of the disorganisation of AREB-t MSC culture architecture (B) as compared to the normal counterpart (A). L-MSC colony (C), detail of atypical large cells, (thin, flat, with rounded appearance; issues that can arise from altered actin organisation) (D). E, F, G, and H depict dysplastic changes of MSCs.

Increased expression of HSP90 α/β , which directly correlated with pFAK [pY³⁹⁷] up-regulation, was found in MSCs from the RAEB group (2.62-fold in S-MSCs and 3.82-fold in L-MSCs). HSP90 α/β immunostaining of CD73⁺ MSC cultures showed that this chaperone was abundantly expressed in the cytoplasm, but

nuclear immunoreactivity was also observed. Approximately 30% of normal MSCs also showed HSP90 α/β nuclear expression. Overall, RAEB MSCs displayed enhanced cytoplasmic staining and an increased frequency of nuclear HSP90 α/β staining (around 80%) when compared to control cells.

Table 2 – Immunofluorescence analysis of FA proteins in MDS vs. control CD73⁺ MSCs.

Marker	NBM			RC			RAEB		
	%+ MSCs	P/N ratio		%+ MSCs	P/N ratio		%+ MSCs	P/N ratio	
		L	S		L	S		L	S
pFAK [pY ³⁹⁷]	70 ± 4.96	3.85 ± 1.19	8.25 ± 1.67	93 ± 3.97	17.04 ± 2.39	23.3 ± 4.09	97 ± 1.82	24.35 ± 4.16	31.62 ± 3.38
paxillin	96 ± 3.78	14.44 ± 2.43	16.99 ± 4.26	92 ± 2.79	12.66 ± 5.19	14.69 ± 5.48	98 ± 1.73	19.02 ± 3.28	20.49 ± 3.54
p130CAS	73 ± 7.58	4.71 ± 1.93	7.30 ± 1.41	92 ± 2.12	10.32 ± 1.18	11.29 ± 4.99	96 ± 2.98	8.98 ± 0.93	10.29 ± 1.54
HSP90 α/β	89 ± 4.35	7.37 ± 1.11	7.16 ± 2.92	94 ± 2.77	6.15 ± 1.21	9.42 ± 1.82	93 ± 3.86	28.15 ± 1.08	18.82 ± 0.67

Percentages of positive cells represent mean values ($n_{\text{NBM}}=4$, $n_{\text{RAEB}}=4$, $n_{\text{RC}}=5$) ± SD. An average of 300 cells was evaluated per case. Relative fluorescence intensity or P/N ratio (ratio between mean pixel intensity (MPI) of positive cells and that of isotype controls) was evaluated for 25 cells per group and marker. P/N ratio values are expressed as mean ± SD.

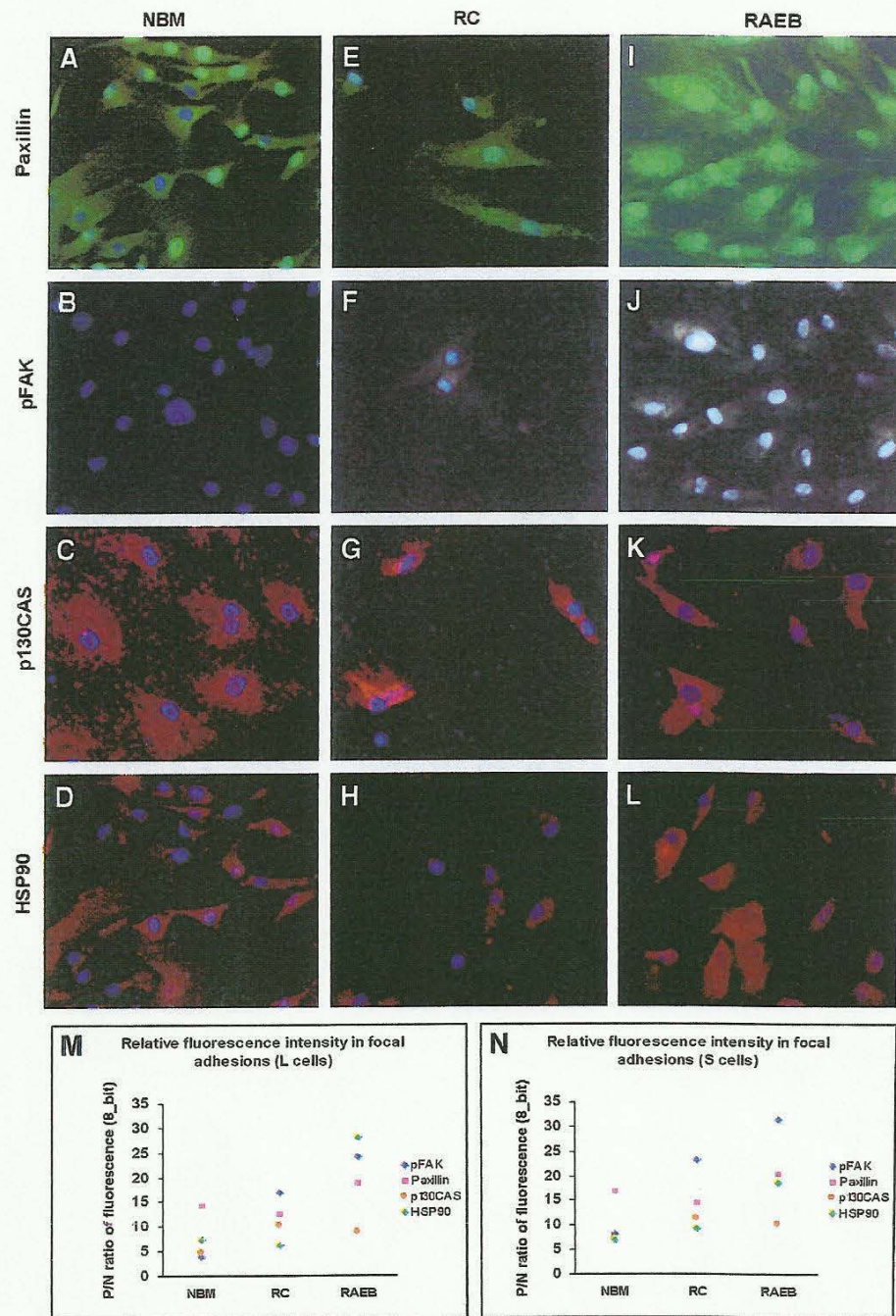


Fig. 3 – Representative IF images of 2-week cultures of CD73-selected MSCs from control, RC, and RAEB groups on Lab-Tek slides. Human MSCs were triple-stained with FITC-conjugated mouse anti-human Paxillin mAb, either PE-conjugated mouse anti-human HSP90 α/β mAb or unconjugated mouse anti-human p130 Cas followed by R-PE-conjugated goat anti-mouse IgG (H + L) mAb and unconjugated rabbit anti-FAK [pY³⁹⁷] followed by Alexa Fluor 633-conjugated goat anti-rabbit IgG (H + L). Nuclei were stained with DAPI (blue). (A–L) Relative fluorescence intensity for pFAK [Y³⁹⁷], Paxillin, p130CAS, and HSP90 α/β ; diamond symbols represent mean values of 25 cells/sample, $n_{\text{normal group}} = 4$, $n_{\text{RAEB}} = 4$, $n_{\text{RC}} = 5$.

Similar percentages of paxillin-positive cells were found in all three groups. This protein displayed either diffuse cytosolic or nuclear cellular distribution, and remarkable differences were observed

between the groups. Indeed, 97–98% of RAEB MSCs showed a nuclear expression pattern for paxillin, and paranuclear staining was observed in large cells. In control cells, the same cytoplasmic and

nuclear expression patterns were observed, but 70% of paxillin-positive cells displayed nuclear paxillin staining. In the RC group, only 14–15% of paxillin-positive cells displayed nuclear reactivity.

Despite the low intensities and diffuse cytoplasmic staining of p130CAS observed in all groups, a slight increase in the number of p130CAS-positive cells was observed in the RC and RAEB groups when compared to the control group (92%, and 96%, respectively, vs. 73%).

Co-localisation analysis of FA proteins in MDS CD73⁺ MSCs

Due to limitations of the analysis programme, protein co-localisation was studied by comparing the localisation of pairs of two proteins in each type of cells and by comparing protein localisation in each disease group to that in the control group.

HSP90 α / β forms complexes with paxillin in RAEB S-MSCs and in some normal S-MSCs

Our findings were consistent with HSP90 α / β -paxillin association in 20–30% of control S-MSCs (Fig. 4B.1) and in 80–90% of RAEB MSCs (Fig. 4C.1). We found that an average of 3% from cellular area of control cells (range, 1–4%) and 4% of RAEB cells (range, 1–7%) showed co-localisation of HSP90 α / β and paxillin, and this co-localisation mainly occurred in the nucleus (Fig. 4D). The Manders coefficients, which represent the co-localisation yield, were consistent with high co-localisation in both control cells and RAEB cells ($M_{\text{Pax}/\text{HSP90}} = 0.975 \pm 0.002$, $M_{\text{HSP90}/\text{Pax}} = 0.964 \pm 0.006$, and $R_r = 0.958 \pm 0.005$ for normal S-MSCs and $M_{\text{Pax}/\text{HSP90}} = 0.973 \pm 0.002$, $M_{\text{HSP90}/\text{Pax}} = 0.978 \pm 0.001$, $R_r = 0.967 \pm 0.001$, for RAEB S-MSCs). In addition, the ICA plots used to assess the covariance of the fluorescent signals for these proteins were strongly skewed toward positive values in both RAEB MSCs and control MSCs in which co-localisation was observed, further supporting a highly co-localised, dependent staining pattern. Furthermore, the calculated ICQ values for RAEB S-MSCs were consistently positive and highly significant ($+0.14 \pm 0.09$; $p < 0.001$; $N = 33$) (Fig. 4C.1). Only a fraction of control MSCs showed a dependent staining pattern, with an ICQ of $+0.27 \pm 0.03$ ($p < 0.001$; $N = 12$), which correlates well with the image depicted in the paxillin-HSP90 α / β intensity plot (Fig. 4B.1).

A low co-localisation index was detected in 2 of 5 S-MSC samples collected from RC patients (0.08% and 0.18%, respectively), and this finding was accompanied by a low Manders value and ICQ coefficient, and segregated, non-overlapping staining patterns.

This analysis provides compelling evidence that paxillin expression varies in synchrony with that of HSP90 α / β , consistent with the formation of a complex within restricted, small nuclear regions in RAEB S-MSCs and in 20–30% of control S-MSCs.

pFAK [Y³⁹⁷] strongly co-localises with paxillin and HSP90 α / β in RAEB cells but not in RC S-MSCs

Co-localisation analysis for pFAK [Y³⁹⁷] and paxillin in RAEB S-MSCs revealed a high degree of overlap of the two proteins in the nucleus. The percentage of co-localisation per studied cell varied from 1 to 7%, with an average of 4% per cell, and the Manders coefficients were very close to 1 ($M_{\text{Pax}/\text{pFAK}} = 0.993 \pm 0.009$ and $M_{\text{pFAK}/\text{Pax}} = 0.911 \pm 0.008$, $R_r = 0.994 \pm 0.003$). In addition, a complete co-localisation of these proteins was indicated both by positively skewed ICA plots (Fig. 4C.2) and by positive ICQ values ($+0.16 \pm 0.04$; $p < 0.001$; $N = 35$).

In contrast, in the control S-MSCs, areas in which paxillin and HSP90 α / β were co-localised exhibited weak fluorescence intensity

for pFAK [Y³⁹⁷], demonstrating a low percentages of co-localisation ($0.07 \pm 0.02\%$) or in the majority of cases, no co-localisation (non-clustered pFAK [Y³⁹⁷]). Fig. 4B.2 presents a representative example of a random staining pattern for paxillin and pFAK [Y³⁹⁷] in control S-MSCs. Positive ICQ values were obtained in only 16 of 40 studied cells, with an average ICQ value that was very close to 0 ($+0.05 \pm 0.02$, $0.1 > p > 0.05$; $N = 16$). A non-overlapping staining pattern was observed for the RC S-MSCs; therefore, these two proteins did not co-localise in cells from this group. In 4 of the 50 assessed cells, very little co-localisation ($0.04 \pm 0.01\%$) was observed, with an average ICQ value of -0.27 ± 0.08 ($p = 0.05$; $N = 46$) (data not shown).

Double staining of pFAK [Y³⁹⁷] and HSP90 α / β in RAEB S-MSCs revealed similar patterns of distribution for those two proteins (Fig. 4C.3), with 1–9% co-localisation (average 6%), which was mainly nuclear, with Manders coefficients of $M_{\text{pFAK}/\text{HSP90}} = 0.877 \pm 0.006$ and $M_{\text{pHSP90}/\text{pFAK}} = 0.996 \pm 0.001$ ($R_r = 0.959 \pm 0.014$). The scatter plot revealed a similar staining pattern. The calculated ICQ values were consistently positive and highly significant ($+0.16 \pm 0.04$, $p > 0.001$) (Fig. 4C.3). A segregated, non-overlapping staining pattern was observed for pFAK [Y³⁹⁷] and HSP90 α / β expression in normal S-MSCs, as the pixel intensities were distributed along the axes of the scatter plot (Fig. 4B.3). Positive ICQ values were obtained in 9 of the 40 analysed cells ($+0.07 \pm 0.02$, $0.1 > p > 0.05$; $N = 9$), whereas for all other cells, ICQ values were negative, corresponding to the segregated pattern (-0.28 ± 0.08 , $p < 0.001$; $N = 31$) (Fig. 4B.3).

In RC S-MSCs, the results were consistent with a random pattern of expression for pFAK [Y³⁹⁷] and HSP90 α / β , as ICQ values were close to 0 and highly significant (-0.07 ± 0.02 , $p = 0.009$; $N = 40$) (data not shown).

In conclusion, we observed a strong co-localisation of the three proteins in RAEB S-MSCs, whereas only 40% of the control cells displayed low co-localisation of pFAK [Y³⁹⁷] and paxillin, and no co-localisation of pFAK [Y³⁹⁷] and HSP90 α / β was observed.

RAEB L-MSCs retain features of S cells including the high degree of co-localisation of pFAK [Y³⁹⁷], paxillin, and HSP90 α / β in the nuclear and paranuclear regions

Unlike normal L-MSCs, the large cells from the RAEB group expressed an increased level of pFAK [Y³⁹⁷] (Table 2) and a high degree of co-localisation of pFAK [Y³⁹⁷] with paxillin and HSP90 α / β (Fig. 5). Analysis of the degree of co-localisation of these proteins in RAEB L-MSCs demonstrated that the staining intensities of the three proteins varied in synchrony, suggesting that these proteins were parts of the same complex (an average of 8% co-localisation was observed for paxillin-HSP90 α / β , 14% colocalisation was observed for paxillin-pFAK [Y³⁹⁷], and 9% colocalisation was observed for pFAK [Y³⁹⁷]-HSP90 α / β pairs (Fig. 5)). Co-localisation maps illustrate a paranuclear and nuclear staining pattern for these proteins. In all co-localisation analyses, the scatter plots revealed highly co-localised staining patterns (Fig. 5) and positive ICQ values ($+0.28 \pm 0.06$, $p < 0.01$, $N = 32$ for paxillin-HSP90 α / β ; $+0.33 \pm 0.04$, $p < 0.01$, $N = 36$ for paxillin-pFAK [Y³⁹⁷]; and $+0.25 \pm 0.05$, $p < 0.05$, $N = 36$ for pFAK [Y³⁹⁷]-HSP90 α / β). The Manders and Pearson's coefficients, which were close to 1 for all three pairs of proteins, confirmed significant co-localisation ($M_{\text{Pax}/\text{HSP90}} = 0.966 \pm 0.019$, $M_{\text{HSP90}/\text{Pax}} = 0.993 \pm 0.002$, $R_r = 0.920 \pm 0.017$; $M_{\text{Pax}/\text{pFAK}} = 0.996 \pm 0.002$, $M_{\text{pFAK}/\text{Pax}} = 0.926 \pm 0.011$, $R_r = 0.948 \pm 0.002$; $M_{\text{pFAK}/\text{HSP90}} = 0.901 \pm 0.010$, $M_{\text{HSP90}/\text{pFAK}} = 0.999 \pm 0.001$, $R_r = 0.928 \pm 0.026$).

Co-localisation of these proteins was not found in controls or RC L-MSCs (data not shown).

A. IgG Negative Controls



B. Normal MSCs



B.1. Paxillin / HSP90



B.2. Paxillin / pFAK



B.3. pFAK / HSP90



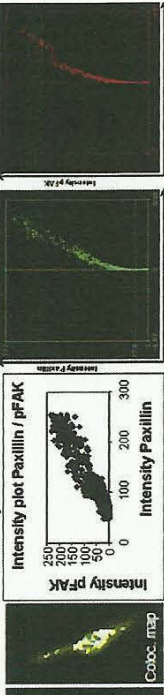
C. RAEB MSCs



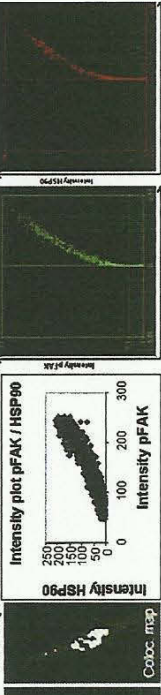
C.1. Paxillin / HSP90



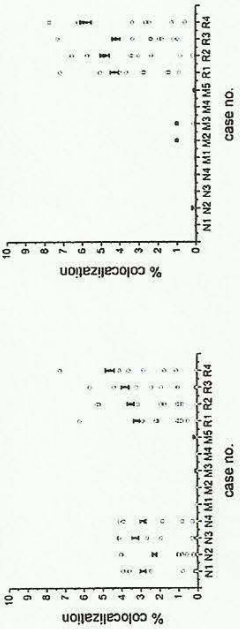
C.2. Paxillin / pFAK



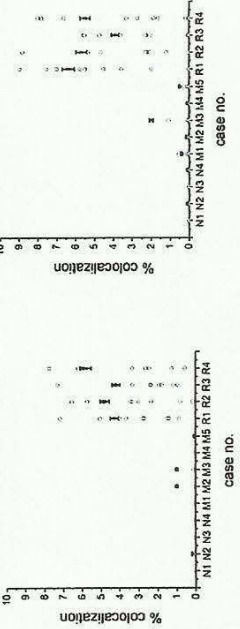
C.3. pFAK / HSP90



D. S cells Paxillin/HSP90 colocalization



S cells Paxillin/pFAK colocalization



S cells pFAK/HSP90 colocalization



Paxillin nuclear expression and its co-localisation with pFAK [Y³⁹⁷] and HSP90α/β in CD73⁺ MSCs and correlation with proliferative potential

Strong nuclear paxillin immunoreactivity and high degrees of co-localisation of paxillin with pFAK [Y³⁹⁷] and HSP90α/β in RAEB S-MSCs that displayed functional nuclear active complexes were correlated with a proliferative advantage ($p < 0.01$, $r = 0.79$, Spearman test). Similar results were observed in L-MSCs, but the statistical significance of these results was lower ($p < 0.05$, $r = 0.64$) (Fig. 6A).

FA protein dysfunction in CD73⁺ MSCs from MDS patients is inversely correlated with down-regulation of clonogenic potential in haematopoietic precursors

Increased levels of expression of pFAK [Y³⁹⁷] in MSCs correlated with decreased proliferation capacity of haematopoietic progenitors, as HPCs from the RAEB group formed 4-fold and those from RC group 1.5-fold fewer BFU-E and CFU-GM than control HPCs. The Spearman's test showed a negative correlation between the intensity of expression of pFAK [Y³⁹⁷] in MSCs cultures and BFU-E, CFU-GM numbers that arise from HPCs selected from MDS patients ($p < 0.001$, $r = -0.60$ for the RAEB group, and $p = 0.001$, $r = -0.31$ for the RC group). The different abilities of RAEB and RC MSCs to affect haematopoietic clonogenicity can instead be explained by differences in pFAK [Y³⁹⁷] expression intensity between the two groups than the percentage of pFAK [Y³⁹⁷]-positive cells (Fig. 6B).

Discussion

There are still unresolved questions about the role of the haematopoietic microenvironment in MDS pathogenesis. Decoding FAK signalling pathways and understanding whether adhesion-mediated processes contribute to the transduction of intrinsic proliferative signals and affect HPC–MSC interactions are goals relevant to the development of targeted therapeutics. The implications of overexpression of FAK and HSP90α/β in HSCs on leukaemogenesis, cell motility, cell cycle progression, and survival advantages have been reported previously [24,25]. To our knowledge, this is the first study focused on the biological characterisation of the functional roles of FA proteins in MSCs selected from MDS patients and healthy control subjects.

In accordance with quality criteria required by the International Society for Cellular Therapy (ISCT) standards [26], a two-stage selection process was performed to obtain a highly clonogenic MSC population from BM aspirates. The first stage involved the pre-enrichment of MSCs from BM aspirates, using the standard method of plastic adherence. The second stage involved the purification of CD73⁺ cells by immunoselection. Similar to CD105 and CD90, previous studies [27,28] have demonstrated that

CD73 (also known as ecto-5'-nucleotidase) is a highly specific marker for MSCs that is useful for the development of robust *in vitro* MSC assays. The EasySep® method simplifies the selection of CD73⁺ viable cell fractions to prevent flow cytometry-induced loss of MSC viability, which has been reported to occur in 20–25% of the large cell subpopulation and 40% of the small cell subpopulation [29]. Highly purified CD73⁺ MSCs were used for further analyses. Multicolour fluorescent microscopy has proven to be a successful technique for FA protein analysis. It allowed us to assess the intracellular localisation of proteins and to understand the spatial relationship between these proteins *via* colocalisation analysis.

Our results demonstrate that MSCs isolated from high-risk MDS patients display pathological behaviour in primary and secondary cultures. In line with previous observations [3], the RAEB MSCs showed significant morphological abnormalities. We noted two major types of changes: dysplastic changes similar to those described in the haematopoietic counterpart and features indicative of altered actin organisation. Ilić et al. have reported the latter changes in mouse FAK (–/–) fibroblasts [30]. The morphological changes in these cells are accompanied by functional changes relevant to RAEB, such as proliferative advantages, and to RC, such as proliferative defects.

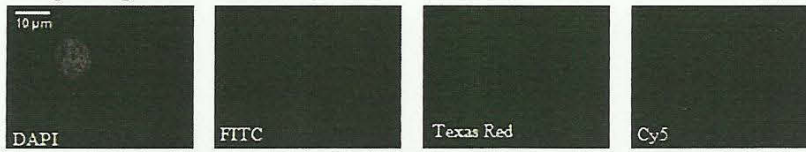
The dramatic changes in proliferation observed in RAEB MSCs are present in both S-MSCs and L-MSCs. Despite having morphological features that suggest a mature non-proliferative status, L-MSCs from RAEB cultures display a robust complex of FA proteins in the nuclear area, suggesting that these cells have proliferative behaviour similar to that of S-MSCs. Only 40% of control S-MSCs displayed nuclear co-localisation of these proteins, and no co-localisation was observed in control L-MSCs. These results suggest that the proliferation observed in control cultures can be attributed to the 40% of S-MSCs that exhibit nuclear co-localisation of FA proteins. Moreover, turnover of these complexes occurs in normal MSCs, as demonstrated by the fact that HSP90α/β does not co-localise with pFAK, allowing it to undergo proteasome-mediated recycling. In RC samples, the absence of these nuclear protein complexes in both S-MSCs and L-MSCs correlates well with the “deserted”, non-proliferative appearance of these cultures.

These physiological dysfunctions might be explained by qualitative defects in FA proteins, including differences in expression levels, nuclear localisation, and protein complex formation.

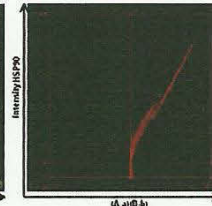
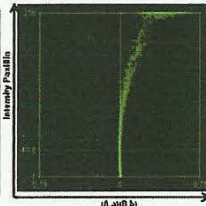
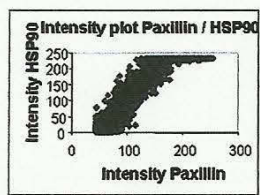
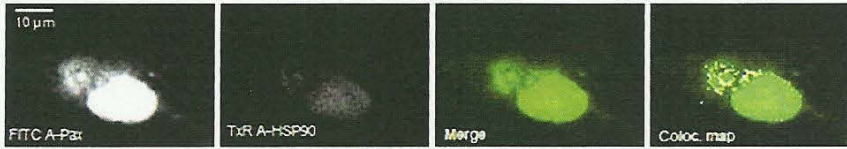
Together with previous findings, our results suggest some mechanisms by which co-localisation of pFAK [Y³⁹⁷], HSP90α/β and paxillin could contribute to an increased rate of proliferation in MSCs. For example, pharmacologic inhibition of HSP90α/β leads to decreased FAK signalling and consequently causes growth inhibition similar to that caused by FAK inhibition [31]. Recent evidence suggests that FAK contributes to cell growth by influencing both the proliferation rate and apoptosis. FAK was initially suggested to induce cell proliferation through activation of the RAS-ERK-MAPK

Fig. 4 – Complementation analysis of FA proteins and HSP90αβ in S-MSCs. Representative IF images for Paxillin-HSP90α/β (B.1), Paxillin-pFAK [Y³⁹⁷] (B.2), and HSP90α/β-pFAK [Y³⁹⁷] (B.3) double staining in control cells and in RAEB cells (C.1, C.2, C.3, left pictures from each panel). Comparative IgG negative controls are presented in A. Intensity correlation analysis. Scatter plots for HSP90α/β staining vs. Paxillin, Paxillin vs. pFAK [Y³⁹⁷], and HSP90α/β vs. pFAK [Y³⁹⁷] in control (B.1–B.3, middle plots) and RAEB (C.1–C.3, middle plots) S-MSCs. The right panels depict ICA plots of staining intensities of protein pairs against their respective (A-a) (B-b) values (B.1–B.3 for normal S-MSCs and C.1–C.3 for RAEB). Quantification of the number of co-localised points per cell; pairs of 2 proteins were analysed. Each circle corresponds to the percentage values of contact points per analysed cell. The horizontal bar represents the mean ± SD for 10 cells examined per group. N = normal MSCs, M = RC MSCs, R = RAEB MSCs (D).

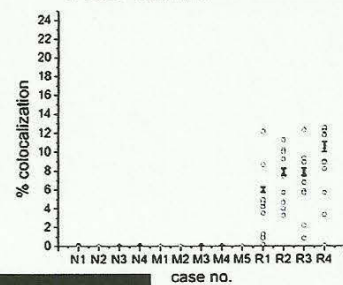
A. IgG Negative Controls



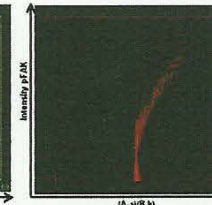
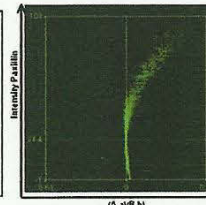
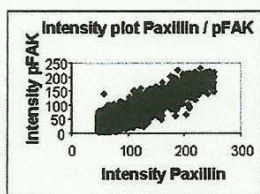
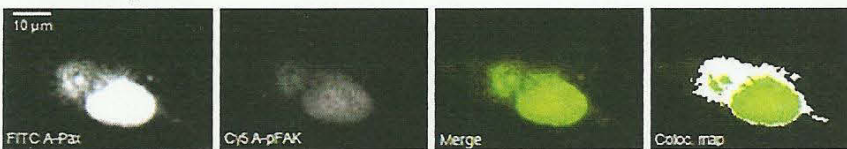
B. Paxillin-HSP90



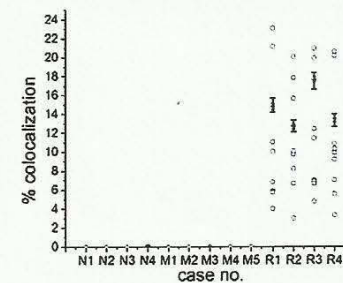
L cells Paxillin/HSP90 colocalization



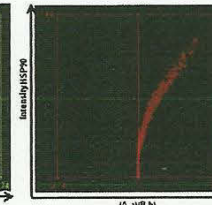
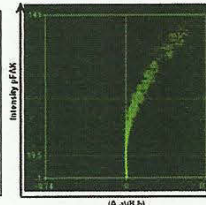
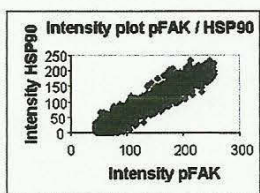
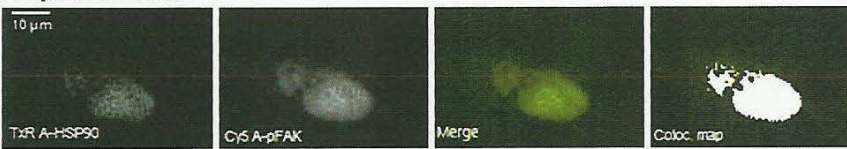
C. Paxillin-pFAK



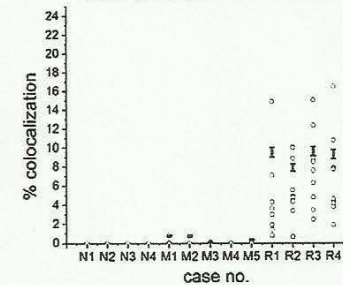
L cells Paxillin/pFAK colocalization



D. pFAK-HSP90



L cells pFAK/HSP90 colocalization



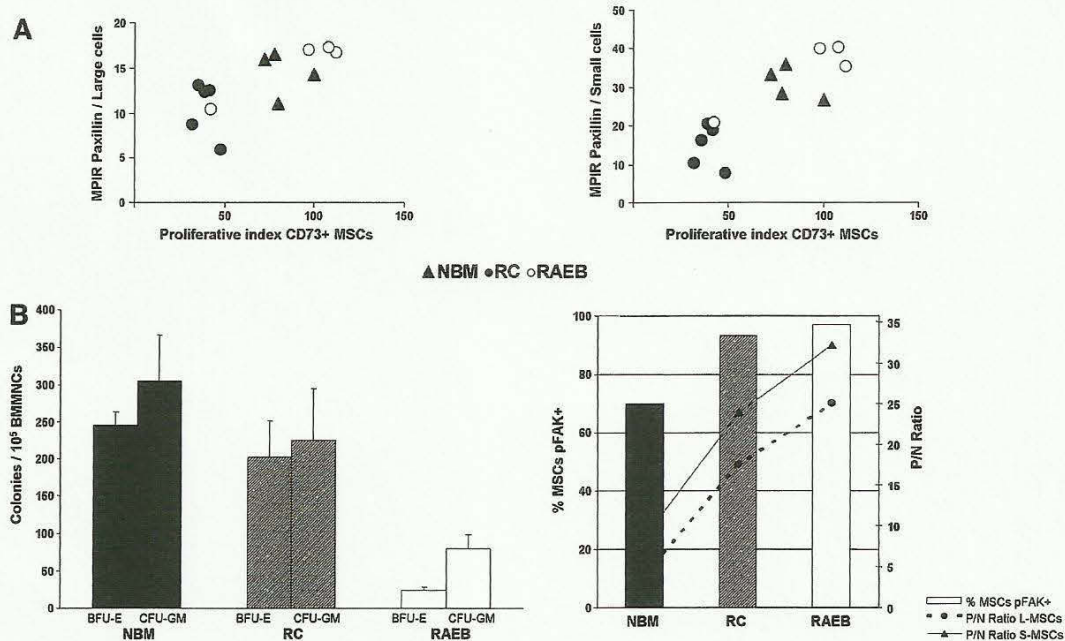


Fig. 6 – Comparative analysis of paxillin expression and proliferative capacities of CD73-selected MSCs from MDS patients and control subjects (A). pFAK expression in MSCs vs. the clonogenicity of HPCs, evaluated in the same samples. The left chart shows the mean number of BFU-E and CFU-GM in each group. The right chart shows the percentage of pFAK-positive MSCs (columns, values should be compared with the left scale), and the relative intensity of expression for pFAK in L-MSCs (dashed line) and in S-MSCs (continuous line) in the three studied groups (lines and diamond symbols, values should be compared with the right scale) (B).

(mitogen-activated protein kinase) pathway via the FAK-Src signalling complex [13,14]. Both FAK and Src are dependent on the chaperone HSP90 α/β for their conformational stability and proper function [31–33]. Furthermore, HSP90 α/β can induce FAK phosphorylation and activation in a RhoA-ROCK-dependent manner in response to VEGF stimulation [34]. In contrast, inhibition of HSP90 prevents c-Src phosphorylation and expression of downstream targets including paxillin and p130CAS [32]. A second possible mechanism by which pFAK [Y³⁹⁷] may affect survival and proliferation is through PI-3K-mediated activation of AKT signalling [13,15]. A third potential mechanism involves the binding of FAK to paxillin, which induces paxillin phosphorylation and conformational modification, blocking its nuclear export [16]. In support of this mechanism, nuclear localisation of paxillin has been shown to stimulate DNA synthesis and cell proliferation [16,35] by suppressing the transcription of the tumour suppressor gene H19 and enhancing Igf2 expression at the translational level [16]. Finally, there is evidence to suggest that FAK regulates p53 through its FERM domain. Lim et al. demonstrated that the loss of FAK in embryos led

to p53 activation and the up-regulation of the cell cycle progression inhibitor p21, and that increased expression of p53 and p21 was associated with a block in MSC proliferation in the embryo [17]. In addition, FAK may prevent apoptosis. McLean et al. further confirmed the role of FAK in inhibiting apoptosis by demonstrating that it was required to prevent caspase-3 activation [36]. Furthermore, FAK-overexpressing cells are resistant to apoptosis induced by hydrogen peroxide, etoposide and radiation, and proteomic analysis of these cells showed increased levels of stress proteins such as HSP90 α/β , ribosomal proteins and antioxidant enzymes [37].

Another hypothesis that arises from our study involves the putative role of FAK [Y³⁹⁷] in MSC–HPC interactions and the implication of this interaction on the modulation of HPC clonogenicity. A recent study showed that FAK regulates integrin expression in human fibroblasts [38]. Three adhesion proteins have been suggested to be involved in HPC–MSC contact and to play a role in the maintenance of the human HPC niche. Specifically, Gottschling et al. showed that β_1 -integrins (CD29) play an essential role in regulating self-renewing HPC division within the stromal

Fig. 5 – Paxillin, HSP90 α/β and pFAK [Y³⁹⁷] association in L-RAEB MSCs. Images show double-labelled large MSC, paxillin-FITC and HSP90 α/β -PE (panel B), paxillin-FITC and pFAK-Alexa 633 (panel C), pFAK-FITC and HSP90 α/β -PE (panel D) staining compared with isotype controls (panel A). Each panel depicts (from left to right and from top to bottom) the single-stained green/red IF images, the merged channels image, a colour co-localisation map, a 2-D co-localisation fluorogram generated from the red and green intensities within the component images, and the ICA plots for the green or red channel for each panel. The last chart in each panel depicts the paxillin-HSP90 α/β -pFAK [Y³⁹⁷] co-localisation analysis in RAEB L-cells. The horizontal bar represents the mean \pm SD for 10 cells examined per sample. N = normal MSCs, M = RC MSCs, R = RAEB MSCs.

environment and in maintaining “stemness” within the first 72 h of homing [39]. During regenerative stress, two integrin complexes ($\alpha_4\beta_1$, and $\alpha_4\beta_7$) are essential for the self-renewal of HSCs [40,41].

Further, CD49e (α_5 -integrin) was shown to be involved in the adhesion of KG1a human immature haematopoietic cells to MSCs. Wagner et al. showed reduced KG1a adhesion upon treatment with antibodies specific for CD49e [42]. In line with this observation, we found that increased levels of pFAK [Y³⁹⁷] inversely correlated with the levels of expression of α_5 -integrin in both large and small MSC cells, and we observed a statistically significant correlation between this reduction in α_5 -integrin expression and decreased clonogenicity in HPCs (manuscript in preparation). In addition, Wagner et al. implicated the expression of CD44 in the homing and adhesion of HPCs to MSCs [42]. Recently, the CD44 isoform CD44v7, which supports HPC homing, was detected on the surface of MSCs [43]; additionally, MSCs were found to express the CD44v10 ligand CD44v10L, which is involved in progenitor cell adhesion and maturation [44].

Finally, luciferase reporter assays have suggested a role for FAK in activation of NF- κ B secondary to TNF- α stimulation [45]; consequently, FAK could regulate the transcription of various proteins induced by this cytokine. Thus, the up-regulation of CD106 on the MSC surface secondary to TNF- α stimulation [46] could influence the selective CD29-mediated adhesion of HPCs to MSCs and therefore contribute to the regulation of the HPC mitotic rate and division kinetics [39].

In conclusion, increased expression of FA proteins and their strong association with HSP90 α/β in nuclear complexes are fundamental features of RAEB MSCs. These data demonstrate that MSCs selected from high-risk MDS patients are intrinsically pathological and may influence HSC behaviour through direct interactions. To clarify whether these dysfunctions are the result of transdifferentiation abnormalities or dysfunctions of common precursor cells, further studies should address the cytogenetics of RAEB MSCs. Moreover, correlations between MSC abnormalities and MDS prognosis and resistance to chemotherapy could lead to a new classification system in which MDS patients could be assigned to risk groups based on their haematopoietic microenvironment characteristics.

Acknowledgments

We are grateful to Constantin Aanei for the artwork and to Annie Viallet for the technical help. Funding was provided by “Ligue Départementale contre le Cancer de la Loire”, “Association Les Amis de Rémi” (France), and Molecular Medicine Interdisciplinary Platform (Gr. T. Popa University of Medicine and Pharmacy, Iasi, Romania).

REFERENCES

- [1] S. Tauro, M.D. Hepburn, C.M. Peddie, D.T. Bowen, M.J. Pippard, Functional disturbance of marrow stromal microenvironment in the myelodysplastic syndromes, *Leukemia* 16 (2002) 785–790.
- [2] U. Dührsen, D.K. Hossfeld, Stromal dysfunction in neoplastic bone marrow diseases, *Annals of Hematology* 73 (1996) 53–70.
- [3] M.K. Yüksel, P. Topçuoğlu, M. Kural, O. İlhan, The clonogenic potential of hematopoietic stem cells and mesenchymal stromal cells in various hematologic diseases: a pilot study, *Cytotherapy* 12 (2010) 38–44.
- [4] E. Flores-Figueroa, R.M. Arana-Trejo, G. Gutiérrez-Espíndola, Mesenchymal stem cells in myelodysplastic syndromes: phenotypic and cytogenetic characterization, *Leukemia Research* 29 (2005) 215–224.
- [5] O. Lopez-Villar, J.L. Garcia, F.M. Sanchez-Guijo, C. Robledo, E.M. Villaron, P. Hernández-Campo, N. Lopez-Holgado, M. Diez-Campelo, M.V. Barbado, J.A. Perez-Simon, J.M. Hernández-Rivas, J.F. San-Miguel, M.C. del Cañizo, Both expanded and uncultured mesenchymal stem cells from MDS patients are genomically abnormal, showing a specific genetic profile for the 5q- syndrome, *Leukemia* 23 (2009) 664–672.
- [6] D. Boudard, A. Viallet, S. Piselli, D. Guyotat, L. Campos, *In vitro* study of stromal cell defects in myelodysplastic syndromes, *Haematologica* 88 (2003) 827–829.
- [7] Y. Yang, S. Cai, L. Yang, S. Yu, J. Jiang, X. Yan, X. Zhang, L. Liu, J. Du, S. Cai, K.L. Paul Sung, Targeting eradication of malignant cells derived from human bone marrow mesenchymal stromal cells, *Experimental Cell Research* 316 (2010) 3329–3341.
- [8] G. Lazennec, C. Jorgensen, Concise review: adult multipotent stromal cells and cancer: risk or benefit? *Stem Cells* 26 (2008) 1387–1394.
- [9] R. Karnauskas, Q. Niu, S. Talapatra, D. Plas, M. Greene, J. Crispino, C. Rudin, Bcl-xL and Akt cooperate to promote leukemogenesis *in vivo*, *Oncogene* 22 (2003) 688–698.
- [10] Y.M. Zhao, J.Y. Li, J.P. Lan, X.Y. Lai, J. Sun, J. Yu, Y.Y. Zhu, F.F. Zeng, Q. Zhou, H. Huang, Cell cycle dependent telomere regulation by telomerase in human bone marrow mesenchymal stem cells, *Biochemical and Biophysical Research Communications* 369 (2008) 1114–1119.
- [11] K. Ohshima, K. Karube, K. Shimazaki, H. Kamma, J. Suzumiya, M. Hamasaki, M. Kikuchi, Imbalance between apoptosis and telomerase activity in myelodysplastic syndromes: possible role in ineffective hemopoiesis, *Leukemia & Lymphoma* 44 (2003) 1339–1346.
- [12] A. Uccelli, L. Moretta, V. Pistoia, Mesenchymal stem cells in health and disease, *Nature Reviews. Immunology* 8 (2008) 726–736.
- [13] V. Golubovskaya, W. Cance, Focal adhesion kinase signaling cancer, *International Review of Cytology* 263 (2007) 103–153.
- [14] W.G. McLean, N.O. Carragher, E. Avizienyte, J. Evans, V.G. Brunton, M.C. Frame, The role of focal-adhesion kinase in cancer — a new therapeutic opportunity, *Nature Reviews* 5 (2005) 505–515.
- [15] M.J. van Nimwegen, M. Huigsloot, A. Camier, I.B. Tijdsen, B. van de Water, Focal adhesion kinase and protein kinase B cooperate to suppress doxorubicin-induced apoptosis of breast tumor cells, *Molecular Pharmacology* 70 (2006) 1330–1339.
- [16] J.M. Dong, L.S. Lau, Y.W. Ng, L. Lim, E. Manser, Paxillin nuclear-cytoplasmic localization is regulated by phosphorylation of the LD4 motif: evidence that nuclear paxillin promotes cell proliferation, *The Biochemical Journal* 418 (2009) 173–184.
- [17] S.T. Lim, D. Mikolon, D.G. Stupack, D. Schlaepfer, FERM control of FAK function: implications for cancer therapy, *Cell Cycle* 7 (15) (2008) 2306–2314.
- [18] M. Stetler-Stevenson, D.C. Arthur, N. Jabbour, X.Y. Xie, J. Mollndrem, A.J. Barrett, D. Venzon, M.E. Rick, Diagnostic utility of flow cytometric immunophenotyping in myelodysplastic syndrome, *Blood* 98 (2001) 979–987.
- [19] J. Vardiman, J. Thiele, D. Arber, R. Brunning, M. Borowitz, A. Porwit, N.L. Harris, M. Le Beau, E. Hellström-Lindberg, A. Tefferi, C. Bloomfield, The 2008 revision of the World Health Organization (WHO) classification of myeloid neoplasms and acute leukemia: rationale and important changes, *Blood* 114 (2009) 937–951.
- [20] Enumeration, Expansion, and Differentiation of Human Mesenchymal Stem Cells Using Mesencult®, Technical Manual, StemCell Technologies Inc, 2007.
- [21] Q. Li, A. Lau, T.J. Morris, L. Guo, C.B. Fordyce, E.F. Stanley, A syntaxin 1, G α_o , and N-type calcium channel complex at a presynaptic nerve terminal: analysis by quantitative immunocolocalization, *The Journal of Neuroscience* 24 (2004) 4070–4081.

- [22] O. Ramírez, A. Ggarcía, R. Rojas, A. Couve, S. Härtel, Confined displacement algorithm determines true and random colocalization in fluorescence microscopy, *Journal of Microscopy* 239 (2009) 173–183.
- [23] S. Bolte, F. Cordelières, A guided tour into subcellular colocalization analysis in light microscopy, *Journal of Microscopy* 224 (2006) 213–232.
- [24] P. Flandrin, D. Guyotat, A. Duval, J. Cornillon, E. Tavernier, N. Nadal, L. Campos, Significance of heat-shock protein (HSP) 90 expressions in acute myeloid leukemia cells, *Cell Stress & Chaperones* 13 (2008) 357–364.
- [25] L. Campos, F. Solly, C. Aanei, P. Flandrin, D. Guyotat, HSP90 is overexpressed in high-risk myelodysplastic syndromes and associated with higher expression and activation of FAK, *Leukemia Research* 33 (May 2009) S45.
- [26] M. Dominici, K. Le Blanc, I. Mueller, I. Slaper-Cortenbach, F. Marini, D. Krause, R. Deans, A. Keating, D.J. Prockop, E. Horwitz, Minimal criteria for defining multipotent mesenchymal stromal cells. The International Society for Cellular Therapy position statement, *Cytotherapy* 8 (2006) 315–317.
- [27] E. Jones, D. McGonagle, Human bone marrow mesenchymal stem cells *in vivo*, *Rheumatology* 47 (2008) 126–131.
- [28] N. Boiret, C. Rapatel, S. Boisgard, S. Charrier, A. Tchirkov, C. Bresson, L. Camilleri, J. Berger, L. Guillaouard, J.J. Guérin, P. Pigeon, J. Chassagne, M.G. Berger, CD43⁺CDw90(Thy-1)⁺ subset colocalized with mesenchymal progenitors in human bone marrow hematopoietic units is enriched in colony-forming unit megakaryocytes and long-term culture-initiating cells, *Experimental Hematology* 31 (2005) 1275–1283.
- [29] R. Zohar, J. Sodek, C.A.G. McCulloch, Characterization of stromal progenitor cells enriched by flow cytometry, *Blood* 90 (1997) 3471–3481.
- [30] D. Ilić, Y. Furuta, S. Kanazawa, N. Takeda, K. Sobue, N. Nakatsuji, S. Nomura, J. Fujimoto, M. Okada, T. Yamamoto, Reduced cell motility and enhanced focal adhesion contact formation in cells from FAK-deficient mice, *Nature* 12 (1995) 539–544.
- [31] J. Schwock, N. Dhani, M. Ping-Jiang Cao, J. Zheng, R. Clarkson, N. Radulovich, R. Navab, L.C. Horn, D.W. Hedley, Targeting focal adhesion kinase with dominant-negative FRNK or Hsp90 inhibitor 17-DMAG suppresses tumor growth and metastasis of SiHa cervical xenografts, *Cancer Research* 69 (2009) 4750–4759.
- [32] X. Liu, Z. Yan, L. Huang, M. Guo, Z. Zhang, C. Guo, Cell surface heat shock protein 90 modulates prostate cancer cell adhesion and invasion through the integrin- β 1/focal adhesion kinase/c-Src signaling pathway, *Oncology Reports* 25 (5) (2011) 1343–1351.
- [33] H.J. Ochel, G. Gademann, Heat-shock protein 90: potential involvement in the pathogenesis of malignancy and pharmacological intervention, *Onkologie* 25 (5) (2002) 466–473.
- [34] F. LeBoeuf, F. Houle, J. Huot, 39175–39185, Regulation of vascular endothelial growth factor receptor 2-mediated phosphorylation of focal adhesion kinase by heat shock protein 90 and Src kinase activities, *The Journal of Biological Chemistry* 279 (37) (2004) 39175–39185.
- [35] M. Kasai, J. Guerrero-Santorio, R. Friedman, E.S. Leman, R.H. Getzenberg, D.B. DeFranco, The group 3 LIM domain protein paxillin potentiates androgen receptor transactivation in prostate cancer cell lines 1, *Cancer Research* 63 (2003) 4927–4935.
- [36] W.G. McLean, N.H. Komiyama, B. Serrels, H. Asano, L. Reynolds, F. Conti, K. Hodivala-Dilke, D. Metzger, P. Chambon, S.G.N. Grant, M.C. Frame, Specific deletion of focal adhesion kinase suppresses tumor formation and blocks malignant progression, *Genes & Development* 18 (2004) 2998–3003.
- [37] R. Utsubo, Y. Sonoda, R. Takahashi, S. Iijima, E. Aizu-Yokota, T. Kasahara, Proteome analysis of focal adhesion kinase (FAK)-overexpressing cells, *Biological & Pharmaceutical Bulletin* 27 (11) (2004) 1735–1741.
- [38] E.K. Michael, D.W. Dumbauld, K.L. Burns, S.K. Hanks, A.J. García, Focal adhesion kinase modulates cell adhesion strengthening *via* integrin activation, *Molecular Biology of the Cell* 20 (2009) 2508–2519.
- [39] S. Gottschling, R. Saffrich, A. Seckinger, U. Krause, K. Horsch, K. Miesala, A.D. Ho, Human mesenchymal stromal cells regulate initial self-renewing divisions of hematopoietic progenitor cells by a β 1-integrin-dependent mechanism, *Stem Cells* 25 (2007) 798–806.
- [40] G.V. Priestley, L.M. Scott, T. Ulyanova, T. Papayannopoulou, Lack of α 4 integrin expression in stem cells restricts competitive function and self-renewal activity, *Blood* 107 (7) (2006) 2959–2967.
- [41] M.L. Scott, G.V. Priestley, T. Papayannopoulou, Deletion of α 4 integrins from adult hematopoietic cells reveals roles in homeostasis, regeneration, and homing, *Molecular and Cellular Biology* 23 (2003) 9349–9360.
- [42] W. Wagner, F. Wein, C. Roderburg, R. Saffrich, A. Diehlmann, V. Eckstein, A.D. Ho, Adhesion of human hematopoietic progenitor cells to mesenchymal stromal cells involves CD44, *Cells, Tissues, Organs* 188 (2008) 160–169.
- [43] O. Christ, U. Günther, R. Haas, M. Zöller, Importance of CD44v7 isoforms for homing and seeding of hematopoietic progenitor cells, *Journal of Leukocyte Biology* 69 (2001) 343–352.
- [44] M. Rösel, S. Khaldoyanidi, V. Zawadzki, M. Zöller, Involvement of CD44 variant isoform v 10 in progenitor cell adhesion and maturation, *Experimental Hematology* 27 (1999) 698–711.
- [45] W.P. Tseng, C.M. Su, C.H. Tang, FAK activation is required for TNF- α -induced IL-6 production in myoblasts, *Journal of Cellular Physiology* 223 (2) (2010) 389–396.
- [46] S. Halfon, N. Abramov, B. Grinblat, I. Ginis, Markers distinguishing mesenchymal stem cells from fibroblasts are downregulated with passaging, *Stem Cells and Development* 20 (2011) 53–66.

III.3. Heat-Shock-Protein (HSP)-90 is overexpressed in high-risk myelodysplastic syndromes and associated with higher expression and activation of Focal Adhesion Kinase (FAK)

- Haematologica-

-Submitted-

This article proposes the assessment of three key proteins involved in cell signalling, FAK, HSP90, and Akt, in the haematopoietic component of MDS settings. Surprisingly is the fact that the percentages of blasts directly correlate with the HSP90, Akt, FAK, and pFAK expression on HPC. Moreover, the patients' survival, as well as the time to transformation into overt leukemia was significantly shorter in MDS cases with higher levels of expression for these proteins in blasts or HPC. These data raises the possibility of using these tests as prognostic tools in MDS. Thereafter we found that 17-AAG (an inhibitor of HSP90) diminishes the CD34⁺ and HPC survival in liquid culture, especially in high-risk MDS cases. Short-term exposure to 17-AAG also down regulates pAKT and pFAK levels. Overall, these data support the implication of this signalling network in MDS and AML pathogenesis and raises the possibility their exploitation as therapeutic target through HSP90 inhibition.

Heat-Shock-Protein (HSP)-90 is overexpressed in high-risk myelodysplastic syndromes and associated with higher expression and activation of Focal Adhesion Kinase (FAK)

Françoise Solly¹, Pascale Flandrin¹, Carmen Aanei², Jérôme Cornillon³, Emmanuelle Tavernier^{2,3}, Nathalie Nadal¹, Franck Morteux², Denis Guyotat^{2,3}, Eric Wattel², Lydia Campos^{1,2}

¹CHU de Saint-Etienne

²UMR5239 CNRS Université de Lyon Faculté Jean Monnet Saint-Etienne

³Institut de Cancérologie de la Loire

Correspondance : Dr F. Solly
Laboratoire d'Hématologie
CHU de Saint-Etienne
42055 Saint-Etienne CEDEX 2

ABSTRACT

Myelodysplastic syndromes (MDS) are characterized by a high risk of evolution into acute myeloid leukaemia (AML). The pathogenesis of this evolution is still unclear. Some studies indicate that aberrant activation of survival signalling pathways is involved. The 90-kDa heat shock protein (HSP90) is implicated in the conformational maturation, stabilization and degradation of different protein kinases and has therefore a key role in signal transduction. Focal Adhesion Kinase (FAK), a non-receptor tyrosine kinase, is involved in the integrin-mediated signal transduction pathway. The aim of our study was to investigate the role of HSP90 in MDS pathogenesis and evolution, and its potential role in protein signalling and FAK activation.

The expression of HSP90, phosphorylated Akt (pAkt), FAK and phosphorylated FAK (pFAK) were assessed by multicolour flow cytometry in bone marrow (BM) mononuclear cells (MNC) and gated CD34-positive (CD34+) cells from 177 MDS samples at diagnosis. The levels of all proteins studied were significantly higher in MNC from patients with refractory anaemia with excess of blasts (RAEB) than in MNC from patients with refractory anaemia (RA) or chronic myelomonocytic leukemia (CMML). The same difference was observed in CD34+ cells. High levels of HSP90, FAK, pFAK and pAKT were associated with shorter survival and increased risk of progression to acute leukaemia.

The effects of inhibition of HSP90 were evaluated in 25 RAEB samples by incubating cells with 17-AAG, an inhibitor of HSP90. A downregulation of HSP90, pFAK and pAKT was observed in MNC and CD34+ cells at 12 hours, associated with increased apoptosis as assessed by activated caspase 3 and annexin V expression.

Our data suggest the implication of HSP90 in the pathogenesis of MDS with excess of blasts and evolution to overt leukaemia, in association with FAK and Akt activation. Moreover this signalling network could be a therapeutic target through HSP90 inhibition.

INTRODUCTION

The myelodysplastic syndromes (MDS) are a heterogeneous group of diseases with regard to initial presentation and evolution (1). Patients with MDS usually present with one or several peripheral cytopenias despite a normo- or hypercellular bone marrow (BM). This apparent paradox has been linked to an excessive intramedullary apoptosis (2-4) but mechanisms underlying this phenomenon are not fully understood yet. We and others have demonstrated that apoptosis results from the activation of caspases, particularly caspase 3 (5, 6). The microenvironment is also implicated in the pathogenesis through the secretion of proapoptotic cytokines (Fas and Trail) (7, 8). Increased apoptosis is observed in all forms of MDS, but is higher in patients with better prognosis and comparatively lower in patients with an excess of blasts (5, 6).

Apoptosis is a tightly regulated phenomenon, and caspase activation is controlled by the bcl-2-family proteins. Indeed we showed that the apoptotic disorder was associated with an imbalance between proteins of the bcl-2 family, with an upregulation of anti-apoptotic proteins bcl-2 and bcl-X_L in the forms with excess of blasts (9). More recently the role of Heat Shock Proteins (HSP) in cell protection and apoptosis regulation has been demonstrated. HSP are a group of highly conserved proteins, which act as molecular chaperones in order to ensure the proper folding of synthesized proteins, or their refolding under denaturing conditions (10). They also play a role in protein degradation via the proteasome machinery. A member of the HSP family, HSP90 is abundantly expressed in the cytoplasm of most human cells. HSP90 exists in two main isoforms: HSP90 α , inducible, and HSP90 β , constitutive (11). It exerts its role by forming a multiprotein complex with high ATPase activity, in cooperation with cochaperones, including HSP70 (12). HSP90 clients are implicated in cell cycling, receptor function, signal transduction and apoptosis. High levels of HSP90 α protein or HSP90 mRNA have been reported in many types of cancer cells, such as pancreatic carcinomas, breast cancer, ovarian cancer, lung and renal cancer, gastric cancer (reviewed in ¹³). Furthermore, HSP90 exists mainly in the activated (complexed) form in cancer cells, whereas in non malignant cells only a small part of HSP90 is activated (14).

More limited data are available regarding the expression of HSP90 in haematological malignancies and particularly in acute leukemia and MDS : high expression of HSP90 protein and HSP90 α RNA has been reported by Yufu et al in leukemia cell lines and a small series of acute leukemia patients (15). We recently reported on the expression of HSP90 in a larger series of patients with acute myeloid leukaemia (AML) (16). Higher HSP90 levels, as assessed by flow cytometry, were associated with a poor prognosis and with higher

expression of activated signal transduction proteins PI3K, AKT and ERK. Other reports show that HSP90 is necessary for the maintenance of oncoproteins such as bcr-abl (17), mutated c-kit (18), and flt3 (19, 20).

HSP90 activation and functional properties necessitate the binding of ATP to a specific pocket. The benzoquinone ansamycins herbimycin A and geldanamycin are potent inhibitors of HSP90, binding tightly to the ATP pocket and preventing the formation of an active HSP90 complex (21). The less toxic geldanamycin-derivative 17-allylamino-demethoxy geldanamycin (17-AAG) presents a much higher (up to 100-fold) affinity for HSP90 complexes than for uncomplexed HSP90, which confers to this drug a highly specific anti-tumoral activity (22). 17-AAG (tespimycin) and other HSP90 inhibitors are now considered as targeted therapy for cancer (23).

In a preliminary study, we have shown that HSP27, 70 and 90 are over-expressed in advanced MDS as compared to early MDS and normal BM (24). This suggests their possible implication in MDS pathogenesis and evolution. Here we report on the clinical and biological significance of HSP90 expression in a series of 177 patients with MDS. We evaluated the expression of HSP90 and of relevant client proteins (pAKT, implicated in cell survival and autonomous growth, and pFAK, implicated in tissue invasion and metastasis) at diagnosis and in some cases after evolution to a higher grade MDS or to overt AML. The use of multicolour flow cytometry allowed us to specifically study subsets of cells (ie CD34⁺). We show that HSP90 and FAK are overexpressed in high risk cases, and that CD34⁺ cells are highly sensitive to the HSP90 inhibitor 17-AAG.

MATERIALS AND METHODS

Patients

One hundred and seventy-seven patients with MDS and chronic myelomonocytic leukemias (CMML) at diagnosis were included into this study between January 2006 and October 2010. All patients gave an informed consent. Diagnosis was carried out according to WHO recommendations (25) and confirmed by two separate observers. As we included CMML cases, the FAB classification was also used to distinguish sub-groups (26). Cytogenetics was available for 152 cases. Detailed clinical and biological characteristics are given in Table 1.

MDS and control cells

Cells were collected by bone marrow aspiration into heparin-containing vials. Mononuclear cells (MNC) were separated on a Ficoll gradient (Eurobio, Les Ulis, France), washed twice with phosphate-buffered saline (PBS), resuspended in RPMI 1640 (Eurobio) and incubated for two hours at 37°C on sterile plastic dishes. Non adherent cells were then recovered, washed twice in PBS and immediately processed for further studies.

As controls, normal marrow cells were harvested from 6 healthy bone marrow donors and processed identically.

CD34+ cells

Normal and MDS CD34+ cells were isolated by an immunomagnetic method using the direct CD34 Progenitor Cell Isolation Kit (Miltenyi Biotec). More than 90% of the isolated cells were CD34-positive (CD34+) after cytometry analysis.

Cultures

Short-term liquid cultures

Non-adherent MNC and CD34+ cells were incubated in RPMI1640 at 37°C in fully humidified atmosphere with 5% CO₂ in the presence of different concentrations of 17 AAG, or of DMSO for controls) for 24 hours. 17-AAG was purchased from Sigma-Aldrich Corp. (St. Louis, MO), diluted in dimethylsulfoxide (DMSO) and stored at –20°C before use.

After these treatments, cells were washed in PBS and viable cells were enumerated using a trypan blue exclusion test.

All experiments were performed in triplicate.

Clonogenic assays

Normal and MDS/CMML MNC were incubated in triplicate in methylcellulose and growth factor-containing culture medium (STEM α .ID, STEM α , Saint-Clément-les-Places, France). In some experiments cultures were performed in the presence of 17-AAG (or DMSO alone for control) which was added into the culture medium to obtain the appropriate final concentration. CFU-GM and BFU-E were scored after 14 days of incubation.

Antigen expression and flow cytometry

The samples were surface-stained with CD45-PE-Cy5 (clone J33, Beckman-Coulter France, Villepinte, France) and CD34-FITC (clone 8G12, BD Biosciences, San José, CA, USA) antibodies for 15 mn at room temperature. Then, the cells were washed and fixed with 3.7% paraformaldehyde for 20 mn. The staining of intracellular proteins was performed after permeabilization in 0.2% Triton X100 (15 mn at room temperature). The specific antibodies for this study were HSP90-phycoerythrin (PE)-conjugated antibody (Clone F8 SCL3-119 which recognizes both HSP90 α and β isoforms, Santa Cruz Biotechnology, Santa Cruz, CA), FAK-PE (clone H-1, Santa Cruz), pFAK-PE (clone K73-480, BD Biosciences), pAkt (S473)-AL FL647 (clone M-89-61, BD Biosciences), Akt-AL FL647 (mouse, clone 55PKBa/Akt, BD Biosciences). Cells were incubated for 1 hour at room temperature, washed and re-suspended in PBS before analysis. The isotype controls used for the phospho-proteins were matched to the primary antibodies at identical concentrations (27). Cell populations were gated according to CD45/side scatter (SSC) analysis.

Flow cytometry analysis was performed with a Becton-Dickinson FACS Canto II cytometer, using the DIVA software. At least 10000 events were analyzed. Results were expressed as mean fluorescence intensity ratios (MFIR) (ratio of stained sample/control).

Apoptosis

Annexin V staining

Untreated and drug-treated cells were incubated with Annexin-V fluorescein and propidium iodide (PI) (DakoCytomation) in HEPES buffer. After incubation for 15 min in the dark, cells were analyzed by flow cytometry. Live cells were determined by PI exclusion. Early apoptotic fraction was determined by annexin-V-positive and PI-negative stain.

Activated caspase-3 expression

Cytospins were also used to study the caspase-3 activation by Alkaline Phosphatase-Anti Alkaline Phosphatase-(APAAP) technique. We used an amplification combination of alkaline

phosphatase (AP) and avidin-biotinylated enzyme complex (ABC) technique (Vectastain Universal mouse and rabbit kit, Vector Laboratories, Burlingame, CA). Cytospins were fixed for 90 seconds with acetone at room temperature. They were rehydrated in PBS for 5 min. Non-specific binding was blocked with horse serum during 20 minutes. Then slides were incubated for 30 minutes with polyclonal rabbit anti active caspase-3 clone (Cell Signaling, Beverly, MA), washed twice in PBS for 5 minutes and incubated with biotinylated horse anti-mouse or rabbit secondary antibody for 30 minutes, rinsed again for 5 minutes in PBS, and reincubated for 30 minutes with biotinylated alkaline phosphatase complex (ABC reagent). After a new step washing in PBS slides were incubated with an appropriate enzyme substrate solution (Fast red) until optimal red granular reaction (20-30 minutes). Slides were rinsed respectively with PBS and distilled water before a counterstain nuclear step consisting of an incubation for 7 minutes with Meyer's Haematoxylin (Dako). After washing in distilled water, PBS, and distilled water again, slides were finally mounted in Fluorotech aqueous media (Valbiotech, Paris, France). Controls were performed by replacing the primary rabbit antibody by an irrelevant antibody of the same isotype. Slides were examined using X10 magnification by two observers. Cells were considered stained if any diffuse reddish cytoplasmic staining could be identified. A scale of three levels of red staining was used to assess intensity of staining : 0 for no staining, 1 for weak staining, 2 for strong staining and 3 for very strong staining. The percentage of positive cells (strong or very strong staining) was determined after counting 100 cells.

Statistical analysis

Mann-Whitney (or Kruskal-Wallis) non parametric tests were used to compare the means of two (or more) groups. Proportions were compared by Chi-square test (or Fisher's test when a group comprised less than 10 units). Correlations were performed using a Spearman rank correlation test.

Survival curves were plotted according to the Kaplan-Meir method. Survival duration of different groups was compared by the log-rank test. Multivariate analysis of survival was performed using a Cox regression model.

Statistical tests were computed by the IBM SPSS statistical software and data plots were performed using the Prim5 software.

RESULTS

Expression of HSP90, FAK, pFAK and pAKT

Expression of HSP90 was weak in MNC and in the “blast” gate (CD45^{dim}/SSC^{low}) of normal marrow cells. We also observed a low expression of FAK and pFAK. pAKT was not detected above control level in normal MNC. Results were similar in normal CD34⁺ cells for all proteins studied.

In MDS MNC cells HSP90 and other protein levels were significantly higher in high-risk cases according to FAB classification (Fig. 1). When cases were stratified according to WHO classification, the expression was higher in RAEB-I + RAEB-II (pooled together) versus other forms. The expression of HSP90 was also higher in RAEB-II vs RAEB-I ($p < 0.05$) and there was a trend for higher levels in RCMD versus RA (with or without ringed sideroblasts) ($p=0.06$). Similar results were obtained considering percent positive cells instead of MFIR (data not presented). There were also significant differences regarding cytogenetics sub-groups. HSP90, FAK, and pFAK levels were lower in good prognosis than in intermediate and poor prognosis forms (fig. 2). pFAK levels were also more elevated in poor prognosis forms than in intermediate. The same differences were observed in CD34⁺ cells, but, in addition pAKT levels were also different in good versus intermediate or poor prognosis groups. 5q- cases expressed similar levels as other good prognosis cases. Finally, although these proteins were not detected only in the “blast” gate (CD45/SSC low) of MNC cells, we observed a weak linear correlation between the percentage of blasts (as assessed by cytology or by cytometry) and the expression of HSP90, pAKT, FAK and pFAK ($r^2=0.62$ to 0.71).

These proteins were also expressed at significantly higher levels in CD34⁺ cells than in CD34-negative MNC ($p < 10^{-4}$ for all proteins). We therefore compared the level of expression in CD34⁺ cells in the different sub-types of MDS and in CMML. Again, we observed a higher expression of HSP90, pAKT, FAK and pFAK in RAEB than in RA/RAS, CMML exhibiting intermediate levels (Figure 1). This shows that the differences regarding expression in MNC cells were not only due to the higher percentage of blasts or CD34⁺ cells in high-risk cases.

Predictive value

Because of the correlation with other relevant clinical factors such as cytogenetics and percentage of blasts we studied the prognostic value of HSP90, pAKT, FAK and pKAK expression. For univariate analysis, patients were arbitrarily placed into two categories : high level (MFIR equal to or above median value) or low level (MFIR below median value).

Survival duration and time to transformation into overt leukemia were significantly shorter in patients with high expression of HSP90, pAKT, pFAK and FAK (fig 3). For all those intracellular proteins, the percent of positive cells were significantly higher in the groups of increasingly poor prognosis as defined by the IPSS (Table 2). In multivariate analysis, we studied the effects of known parameters such as age, cytogenetics (or IPSS), percentage of blasts and marker expression. Only cytogenetics (or IPSS), percentage of blasts and percent of CD34+ cells remained independent prognostic factors.

Transformation into AML

Transformation occurred in 87 cases in total, after a mean delay of 386 days. Nineteen cases could be reevaluated at the time of transformation. This included 9 cases with a diagnosis of RA and 10 RAEB. The blast percentage was 6.5% (± 5.9) at diagnosis and 42% (± 16) after transformation.

As presented in Figure 4, the levels of HSP90, FAK, pFAK and pAKT were significantly higher after transformation than at diagnosis. This was the case in MNC ($p < 10^{-4}$) and more interestingly in CD34+ cells ($p < 10^{-4}$).

Inhibition of HSP90 (Figure 5)

The effects of inhibition of HSP90 were studied by exposing MNC to 17-AAG for up to 24 hours. Thirty-nine cases of RAEB expressing high levels of HSP90 were studied. In the presence of 2 μM 17-AAG, the percentages of viable cells at 12 and 24 hours were respectively 60 and 32 of control without 17-AAG. At a concentration of 5 μM , the percentage of viable cells was 38% at 12 hours, and no viable cell could be recovered at 24 hours. 17-AAG significantly increased the percentage of apoptotic cells, as assessed by activated caspase-3 expression and annexin V binding. After 12 hours of exposure to 17-AAG 5 μM , more than 90% cells were apoptotic. In clonogenic assay, the yield of colonies was heterogeneous in the absence of 17 AAG (mean number \pm SD of CFU-GM, clusters and BFU-E : 60 \pm 80, 139 \pm 136, 19 \pm 14 respectively). At a concentration of 5 μM , 17-AAG completely inhibited the growth of all types of colonies in semi-solid medium.

The effects of 17-AAG on protein expression was studied after 12 hours of culture. The same staining technique was used as for uncultured cells. In addition, we also assessed the expression of HSP70, which has been reported to be upregulated in the presence of HSP90 inhibitors. The levels of HSP90, FAK, pFAK and pAKT were significantly in the presence of 2 and 5 μM of 17-AAG. This effect was more evident in CD34+ cells than in MNC. By contrast, expression of HSP70 was not significantly modified in both cell types.

DISCUSSION

In this paper, we show that high expression of HSP90 is associated with more advanced disease and worse clinical prognosis. As expected, this was significantly correlated with other known prognostic features such as cytogenetics and blast percentage which appear to be of importance in multivariate analysis. One interesting point is the fact that CD34+ cells from advanced cases also expressed the higher levels, when compared to CD34+ cells of good prognosis cases or normal marrows. This implies that progression to advanced disease is associated with a distinct transduction pathways profile at the CD34+ progenitor level, where an imbalance between proliferation and apoptosis has already been described (28). In line with this observation, we also show that when patients could be retested at the time of transformation into overt leukemia, the expression of HSPs and signaling molecules was significantly increased. This is also consistent with the already known overexpression of HSP90 in acute myeloid leukemia (15, 16).

We also studied the expression of the activated forms of known clients of HSP90, pAKT and pFAK. These proteins are implicated in signal transduction and their constitutive activation is a hallmark of transformation in many cancer models. Again a higher expression was observed in MNC and in CD34+ cells of MDS with poor prognosis or adverse cytogenetics. Indeed high expression of HSP, FAK and pAKT was associated with higher risk of transformation and poor survival. High levels of HSP and FAK are predictive of resistance to chemotherapy in AML as shown by our group (16) and others (29). More controversial data exist regarding the prognostic significance of pAKT activation in AML cells. While we (16) and others (30) have observed a poor prognosis, Bardet et al showed that pAKT expression as detected by flow cytometry implied a better prognosis, that was observed independently of cytogenetics, although pAKT was higher in CBF and intermediate cases (31). These discrepancies may be the consequence of different technical approaches, but mainly due to the fact that different sites of phosphorylation were assessed in these studies. Again, we show that levels in CD34+ cells were higher at time of evolution to AML than at diagnosis, irrespective of the initial classification of MDS. Taken together, these findings favor a role for these proteins in disease initial type and in the pathogeny of evolution into overt AML.

The second point raised in our study is the possibility to target in vitro HSP90. HSP90 inhibitors such as geldanamycin, 17-AAG or 17-DMAG have anti-tumoral activity by inhibiting proliferation and inducing apoptosis (32, 33). In leukemia cells 17-AAG alone or in combination with chemotherapy inhibits cell growth and induces apoptosis (34). Moreover, in specific leukemia subtypes characterized by the presence of mutations or rearrangements of genes such as *flt-3* or *bcr-abl* resulting in high expression of constitutively activated

oncoproteins, the association of HSP90 inhibitors and targeted drugs is highly effective in-vitro (35-36). Although the exact mechanism by which HSP90 inhibitors interfere with leukemia cell survival is not fully understood, we have also demonstrated that 17-AAG was able to induce apoptosis in primary AML cells, in correlation with HSP90 and activated AKT levels (16). In MDS, we show that 17-AAG readily inhibits CD34+ and MNC cells survival in liquid culture, at least in samples from high grade MDS. Short-term exposure to 17-AAG also down regulates pAKT and pFAK levels. This is consistent with the mechanism 17-AAG-induced apoptosis suggested by Nimmanapalli et al, implicating a modulation of apoptotic proteins of the bcl-2 family downstream of Akt, Raf-1 and Src down-regulation (37). We also show in our model a downregulation of FAK and pFAK after exposure to 17-AAG. FAK is a cytoplasmic protein tyrosine kinase localised to regions called focal adhesions. Many stimuli can induce activation of FAK, including integrins and growth factor. The major site of autophosphorylation, tyrosine 397, is a docking site for the SH2 domains of Src family proteins. Phosphorylated FAK binds and activates proteins forming the FAK complex, and facilitate the generation of downstream signals necessary to regulate cell functions, like motility, survival and proliferation. Dysregulation of FAK could participate in the development of cancer, and abnormal activation of FAK has been described in AML. Our data suggest that FAK, as a client of HSP90, could be indirectly targeted by HSP90 inhibition.

Epigenetic therapies are increasingly used in MDS. The HDAC inhibitors show a clinical activity in high-grade MDS. Acetylation of HSP90 by exposure to histone-deacetylase (HDAC)-6 inhibitors results in an inhibition of its chaperone function (38). The combination of an inhibitor of HDAC and 17-AAG is highly active in-vitro against cells of chronic myeloid leukemia in blast crisis and AML cells harboring a mutation of flt-3 (39). HDAC6 inhibitors, alone or in combination with another HSP90 inhibitor, may represent a potential targeted therapy of high risk MDS with possible dual mechanism of action.

REFERENCES

1. Tefferi A, Vardimian JW. Myelodysplastic syndromes. *N Engl J Med*. 2009;361(19):1872-85.
2. Yoshida Y. Apoptosis may be the mechanism responsible for the premature intramedullary cell death in the myelodysplastic syndrome. *Leukemia* 1993; 7: 144-146.
3. Bogdanovic AD, Trpinac DP, Jankovic GM, Bumbasirevic VZ, Obradovic M, Colovic MD. Incidence and role of apoptosis in myelodysplastic syndrome: morphological and ultrastructural assessment. *Leukemia* 1997; 11: 656-659.
4. Raza A, Gezer S, Mundle S, Gao XZ, Alvi S, Borok R, Rifkin S, Iftikhar A, Shetty V, Parcharidou A, Loew J, Marcus B, Khan Z, Chaney C, Showel J, Gregory S, Preisler H. Apoptosis in bone marrow biopsy samples involving stromal and hematopoietic cells in 50 patients with myelodysplastic syndromes. *Blood* 1995; 86: 268-276.
5. Boudard D, Sordet O, Vasselon C, Revol V, Berthéas MF, Freyssenet D, Viallet A, Piselli S, Guyotat D, Campos L. Expression and activity of caspases 1 and 3 in myelodysplastic syndromes. *Leukemia* 2000; 14: 2045-2051.
6. Parker JE, Mufti GJ, Rasool F, Mijovic A, Devereux S, Pagliuca A. The role of apoptosis, proliferation, and the Bcl-2-related proteins in the myelodysplastic syndromes and acute myeloid leukemia secondary to MDS. *Blood* 2000; 96:3932-8.
7. Claessens YE, Bouscary D, Dupont JM, et al. In vitro proliferation and differentiation of erythroid progenitors from patients with myelodysplastic syndromes: evidence for Fas-dependant apoptosis. *Blood* 2002 99:1594-601.
8. Campioni D, Secchiero P, Corallini F et al. Evidence for a role of TNF-related apoptosis-inducing ligand (TRAIL) in the anemia of myelodysplastic syndromes. *Am J Pathol* 2005;166:557-63.
9. Boudard D, Vasselon C, Bertheas MF, Jaubert J, Mounier C, Reynaud J, et al. Expression and prognostic significance of Bcl-2 family proteins in myelodysplastic syndromes. *Am J Hematol* 2002;70:115-25.
10. Richter K, Haslbeck M, Buchner J. The heat shock response : life on the verge of death *J Mol Cell*. 2010 40(2):253-66.
11. Young JC, Moarefi I, Hartl FU. 2001. HSP90: a specialized but essential protein-folding tool. *J Biol Cell* 154: 267-273.

12. Hernandez MP, Sullivan WP, Toft DO. 2002. The assembly and intermolecular properties of the hsp70-Hop-hsp90 molecular chaperone complex. *J Biol Chem* 277: 38294-38304.
13. Ochel HJ and Gademan G. 2002. Heat-shock protein90: potential involvement in the pathogenesis of malignancy and pharmacological intervention. *Onkologie* 25: 466-473.
14. Kamal A, Thao L, Sensintaffar J, et al. 2003. A high-affinity conformation of Hsp90 confers tumour selectivity on Hsp90 inhibitors. *Nature* 425: 407-410.
15. Yufu Y, Nishimura J, Nawata H. 1992. High constitutive expression of heat shock protein 90 alpha in human acute leukemia cells. *Leuk Res* 16: 597-605.
16. Flandrin P, Guyotat D, Duval A, Cornillon J, Tavernier E, Nadal N, Campos L. [Significance of heat-shock protein \(HSP\) 90 expression in acute myeloid leukemia cells](#). *Cell Stress Chaperones*. 2008; 13(3):357-64.
17. An WG, Schulte TW, Neckers LM. 2000. The heat shock protein 90 antagonist geldanamycin alters chaperone association with p210bcr-abl and v-src proteins before their degradation by the proteasome. *Cell Growth Differ* 11: 355-360.
18. Fumo G, Akin C, Metcalfe DD, Neckers L. 2004. 17-allylamino-17-demethoxygeldanamycin (17-AAG) is effective in down-regulating mutated, constitutively activated KIT protein in human mast cells. *Blood* 103: 1078-1084.
19. Minami Y, Kiyoi H, Yamamoto Y, Yamamoto K, Ueda R, Saito H, Naoe T. 2002. Selective apoptosis of tandemly duplicated FLT3-transformed leukemia cells by Hsp90 inhibitors. *Leukemia* 16: 1535-1540.
20. Yao Q, Nishiushi R, Li Q, Kumar AR, Hudson WA, Kersey JH. 2003. FLT3 expressing leukemias are selectively sensitive to inhibitors of the molecular chaperone heat shock protein 90 through destabilization of signal transduction-associated kinases. *Clin Cancer Res* 9: 4483-4493.
21. Grenert JP, Sullivan WP, Fadden P, et al. 1997. The amino-terminal domain of heat shock protein 90 (hsp90) that binds geldanamycin is an ATP/ADP switch domain that regulates hsp90 conformation. *J Biol Chem* 272: 23843-23850.
22. Schultze TW and Neckers LM. 1998. The benzoquinoneansamycin 17-allylamino-17-demethoxygeldanamycin binds to HSP90 and shares important biologic activity with geldanamycin. *Cancer Chemother Pharmacol* 42: 273-279.
23. Jegou G, Hazoumé A, Seigneuric R, Garrido C. Targeting heat shock proteins in cancer. *Cancer Lett* 2010 Nov 13 (Epub ahead of print).

24. Duval A, Oлару D, Flandrin-Gresta P, Nadal N, Cornillon J, Guyotat D, Campos L. Expression and prognostic significance of heat-shock proteins in myelodysplastic syndromes. *Haematologica* 2006; 91: 713-714.
25. Swerdlow SH, Campo E, Harris NL, Jaffe EL, Pileri SA, Stein H, et al. WHO classification of tumors of haematopoietic and lymphoid tissues. Lyon: IARC, 2008.
26. Bennett JM, Catovsky D, Daniel MT, Flandrin G, Galton DA, Gralnick HR, Sultan C. Proposals for the classification of the myelodysplastic syndromes. *Br J Haematol* 1982; **51**: 189-199.
27. Krutzig PO, Nolan GP. 2003. Intracellular phosphor-protein staining techniques for flow cytometry: monitoring single cell signaling events. *Cytometry part A* 55A:61-70.
28. Parker JE, Mufti GJ, Rasool F, Mijovic A, Devereux S, Pagliuca A. The role of apoptosis, proliferation, and the Bcl-2-related proteins in the myelodysplastic syndromes and acute myeloid leukemia secondary to MDS. *Blood*. 2000 96:3932-8.
29. Recher C, Ysebaert L, Beyne-Rauzy O, Mansat-De Mas V, Ruidavets JB, Cariven P, Demur C, Payrastra B, Laurent G, Racaud-Sultan C. Expression of focal adhesion kinase in acute myeloid leukemia is associated with enhanced blast migration, increased cellularity, and poor prognosis. *Cancer Res*. 2004 64:3191-7.
30. Kornblau SM, Womble M, Qiu YH, Jackson CE, Chen W, Konopleva M, Estey EH, Andreeff M. 2006. Simultaneous activation of multiple signal transduction pathways confers poor prognosis in acute myelogenous leukemia. *Blood* 108 : 2358-2365.
31. Tamburini J, Elie C, Bardet V, Chapuis N, Park S, Broët P, Cornillet-Lefebvre P, Lioure B, Ugo V, Blanchet O, Ifrah N, Witz F, Dreyfus F, Mayeux P, Lacombe C, Bouscary D. Constitutive phosphoinositide 3-kinase/Akt activation represents a favorable prognostic factor in de novo acute myelogenous leukemia patients. *Blood*. 2007 110:1025-8.
32. Goetz MP, Toft DO, Ames MM, Erlichman C. 2003. The Hsp90 chaperone complex as a novel target for cancer therapy. *Ann Oncol* 14: 1169-1176.
33. Hostein I, Robertson D, DiStefano F, Workman P, Clarke PA. 2001. Inhibition of signal transduction by the Hsp90 inhibitor 17-allylamino-17-demethoxygeldanamycin results in cytostasis and apoptosis. *Cancer Res* 61: 4003-4009.
34. Mesa RA, Loegering D, Powell HL, et al. 2005. Heat shock protein 90 inhibition sensitizes acute myelogenous leukemia cells to cytarabine. *Blood* 106: 318-327.
35. George P, Bali P, Cohen P, et al. 2004. Co-treatment with 17-allylamino-demethoxygeldanamycin (17-AAG) and FLT3 kinase inhibitor PKC412 is highly effective against human AML cells with mutant FLT3. *Cancer Res* 64: 3645-3652.

36. Radujkovic A, Schad M, Topaly J, et al. 2005. Synergistic activity of imatinib and 17-AAG in imatinib-resistant CML cells overexpressing BCR-ABL – Inhibition of P-glycoprotein function by 17-AAG. *Leukemia* 19: 1198-1206.
37. Nimmanapalli R, O'Bryan E, Kuhn D, Yamaguchi H, Wang HG, Bhalla KN. 2003. Regulation of 17-AAG-induced apoptosis: role of BCL2, Bcl-XL, and Bax downstream of 17-AAG-mediated down-regulation of Akt, Raf-1, and Src kinases. *Blood* 102: 269-275.
38. Bali P, Pranpat M, Bradner J et al. Inhibition of histone deacetylase 6 acetylates and disrupts the chaperone function of heat shock protein 90: a novel basis for antileukemia activity of histone deacetylase inhibitors. *J Biol Chem* 2005;280:26729-34.
39. George P, Bali P, Annavarapu S, et al. 2005. Combination of the histone deacetylase inhibitor LBH589 and the hsp90 inhibitor 17-AAG is highly active against human CML-BC cells and AML cells with activating mutation of FLT3. *Blood* 105: 1768-1776.

Table 1 : patient characteristics

Median age (range)	66 years (11-91)
Sex (M/F)	99/78
WHO classification (N)	
RA	20
RAS	1
RCMD	24
RCMD-RS	2
RAEB-I	38
RARB-II	55
5q-	14
CMML (N)	23
Cytogenetic prognostic groups (N=152)	
Good	91
Intermediate	32
Poor	29
IPSS (N=152)	
Low	56
Intermediate-1	44
Intermediate-2	32
High	20
Median follow-up (days)	593
Median time to transformation (days) (87 patients)	386

Table 2 : Expression of HSP90, pAKT, FAK and pFAK according to IPSS risk category

IPSS	Mean Fluorescence Intensity Ratio			
	HSP90	pAKT	FAK	pFAK
Low	54	6	16	25
Int-1	73	9	21	29
Int-2	85	13	29	47
High	86	15	34	51

Figure 1

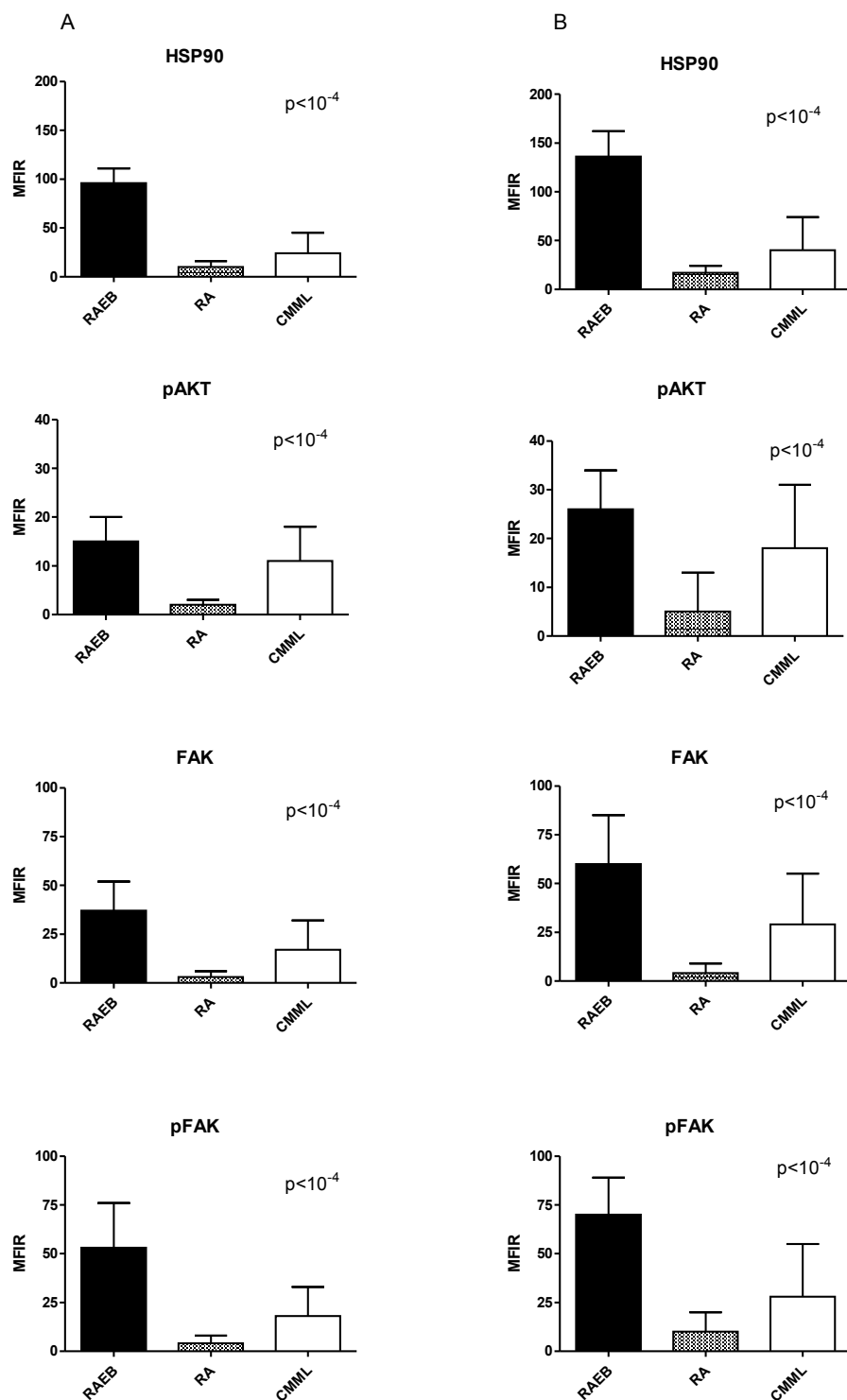


Figure 2

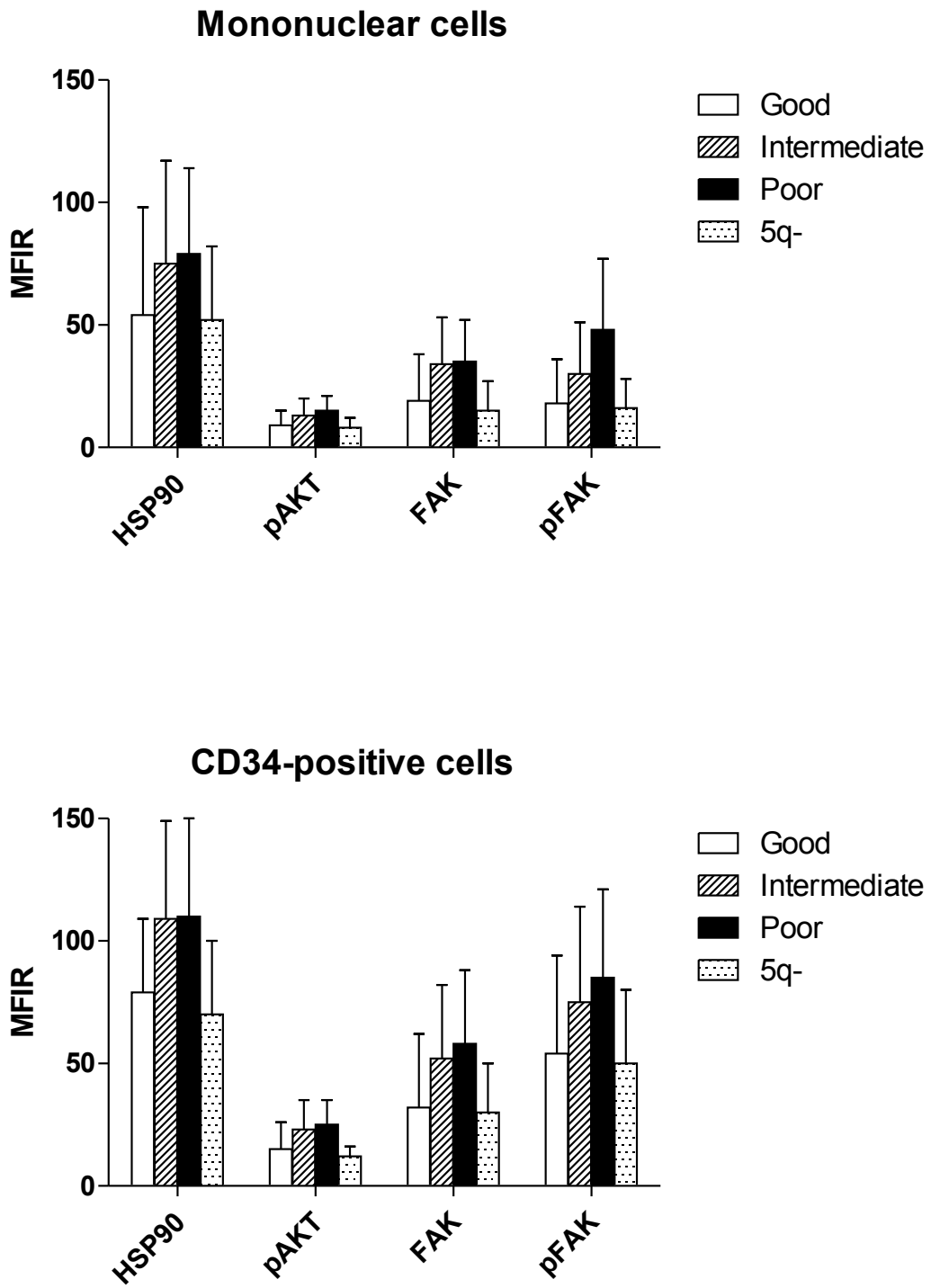


Figure 3

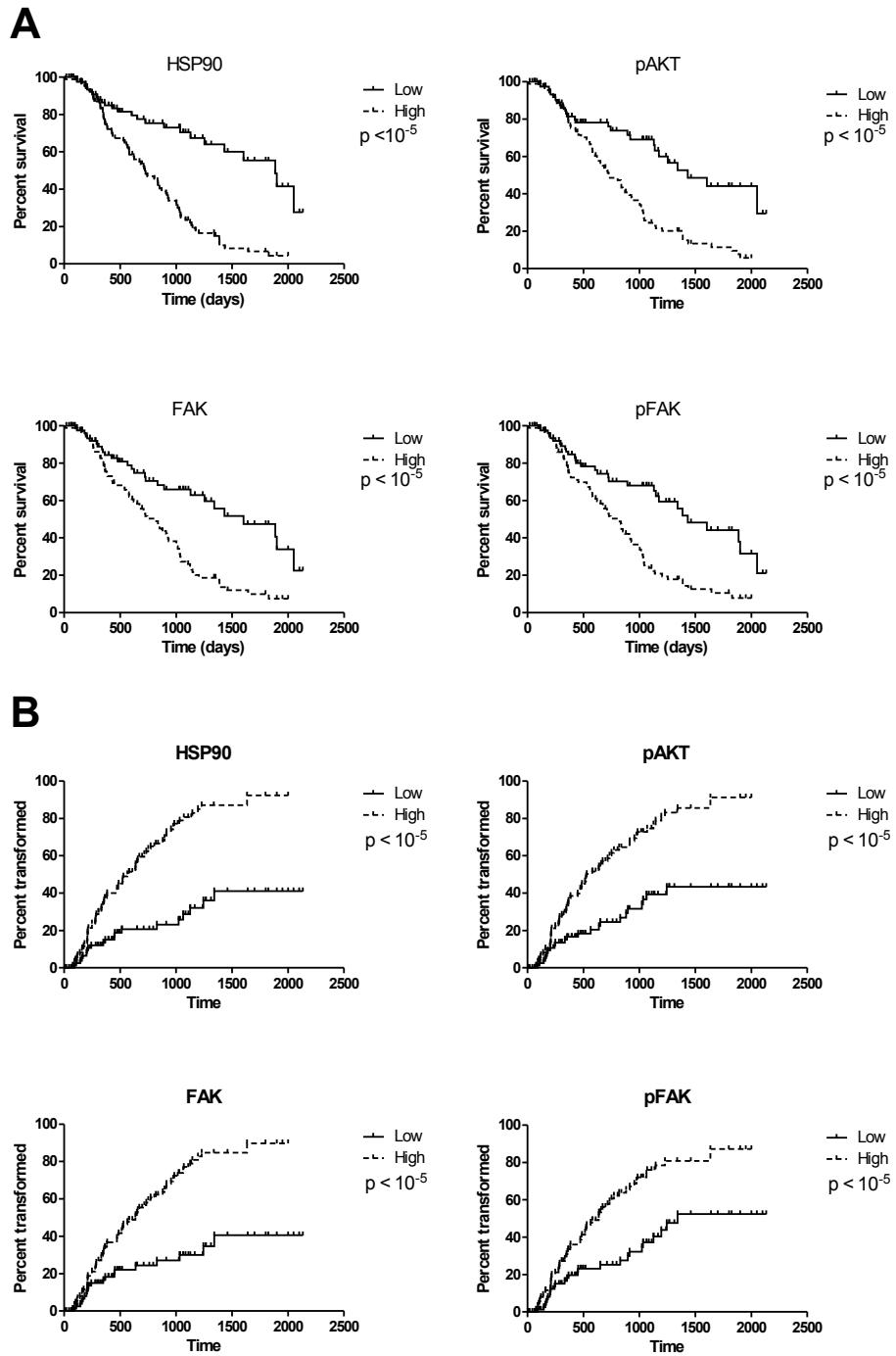


Figure 4

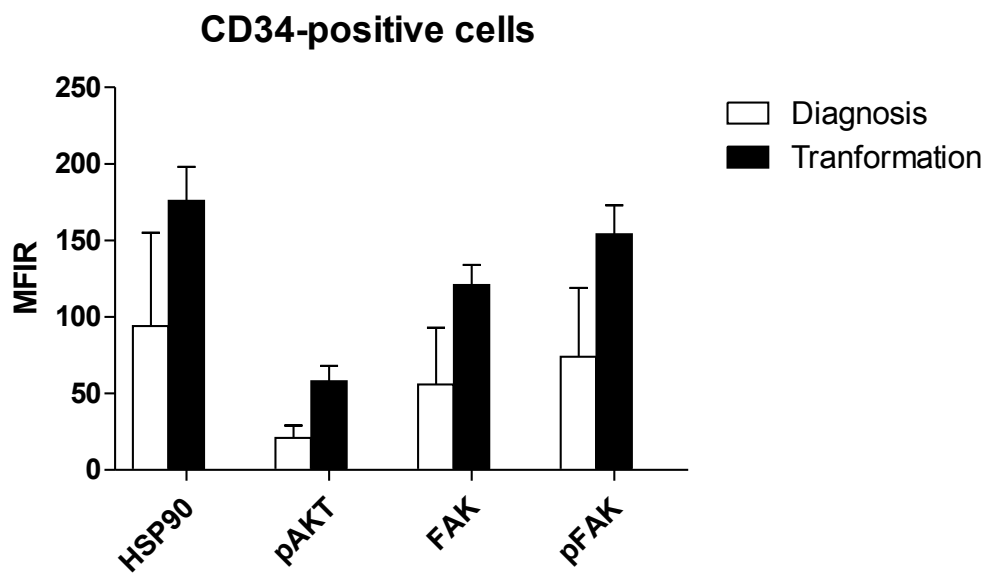
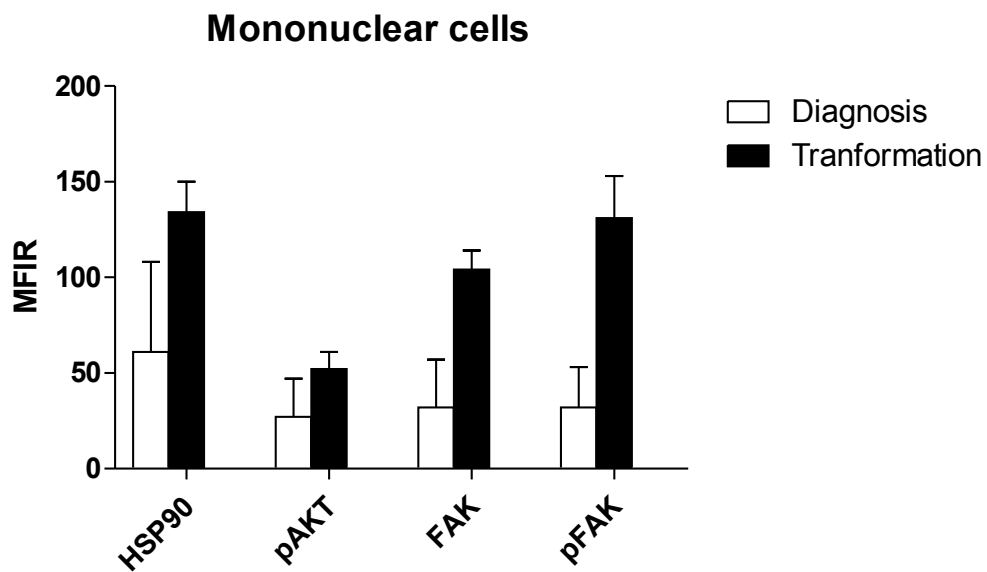
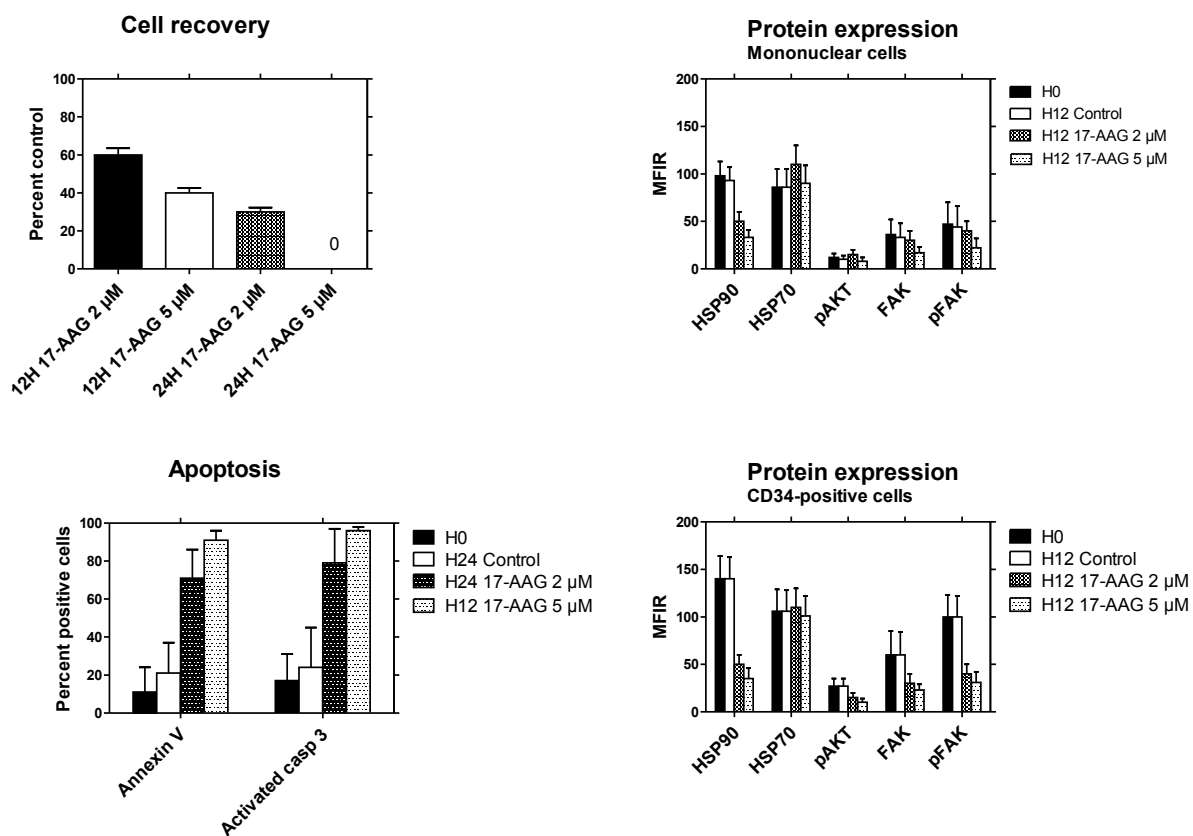


Figure 5



GENERAL DISCUSSION

The present work is dedicated to the argumentation of the morpho-molecular roles of mesenchymal stromal cells (MSCs) in myelodysplastic syndromes (MDS) pathogenesis.

Myelodysplastic syndromes represent a heterogeneous group of myeloid neoplasms in terms of severity, prognostic, progression to acute myeloid leukemia (AML) and therapeutic approach solutions.

The evidence accumulated in recent years significantly improved the understanding of the pathogenic mechanisms responsible for the selection of neoplastic hematopoietic clone(s), resistant to apoptosis and able to express factors promoting its own growth, proliferation and migration.

The understanding the mechanisms by which neoplasia manages to integrate the stromal components in tumorigenesis process represents also a major source of progress. The haematopoietic stem cells (HSC)-MSC relationship is a critical point in the haematopoietic malignancies pathogenesis, and the current technical approaches provide limited and rather slow progresses.

The complexity of our subject required the integration of the knowledge of several areas: haematologic oncology, cytology, immunology and molecular biology, that along with our strongly motivation for the subject constituted a solid foundation for developing and promoting this doctoral theme.

Preliminary hypothesis was that the MSCs, the genitors of the all stromal cells have a pathologic behaviour in MDS and are unable to generate a microenvironment suitable to haematopoietic cells development.

This project establishes the immunophenotypic profile and the growth patterns of MSCs from MDS microenvironment associated to the malignant haematopoietic clone, throughout of the MDS disease evolution to acute leukemia, highlighting the distortion aspects related to adhesion processes, such as cell proliferation, clonogenic growth and neoangiogenesis.

With our results we want to extend the current level of knowledge in the MDS field by decoding the signalling pathways involving the focal adhesion proteins with impact in neoplasia dynamics and to inventory the common or distinctive elements of the tumour-support system relationship in order to identify the discreet pathogenic models which could be employed as therapeutical targets.

1. Myelodysplasia could be also a disease of stroma?

The MDS pathophysiology remains a highly controversial topic.

To date the MDS is generally regarded as clonal disorders of haematopoiesis; the disease origin is thought to be in a genetic transformation of haematopoietic stem / progenitor cells.

However new insights reevaluates the microenvironment place from indifferent spectator to principal actor.

Thereby, there is the histopathologic evidence of the microenvironment disruption in MDS.

In line with previous data, [168], [190], [303], we noticed the confluence deficiencies and spontaneous lysis in 25-50% of MDS stromal cells amplified during 30-35 days *in vitro* cultures, especially in refractory cytopenia (RC) cases. Moreover, stand out also the different distribution of the three morphotypes of MSCs (rounded-shaped; thin, spindle-shaped; and large, flat cells) in MDS layers compared to normal settings. The slight decrease in the number of large, flat cells in refractory cytopenia with unilineage dysplasia (RCUD) settings, which is considered the onset of terminal differentiation, in addition to the size differences within this population among the different study groups are worth noting. These characteristics could indicate maturation defects.

There are some research teams which attribute the MSC failure in primary cultures from MDS on account to the aging mechanisms of (stem) cell population(s) during long-term cultures, that induce an decreasing ability to self-renew and to properly differentiation [319]. Our evidences are not consistent with this hypothesis because the normal MSC control does not reach these changes during the 30 days of cultures.

In addition, we have arguments that MSC cultures from RAEB fulfill the "dysplasia" criteria requested by histopathologic term, which has been defined as "a loss in the uniformity of the individual cells, as well as a loss in their architectural orientation" [320]. Thus, the RAEB MSC cultures were characterized by a higher rate and disordered proliferation (which no longer comply with so-called "the cohesive zone formulation" or "cell-substrate contact areas", that are formed predominantly by larger cells in the middle and are surrounded by a cuff of spindle-shape cells to the periphery) [134], [321] reflected in the microscopic image by colonies architecture disorganization with clusters of aberrant proliferation.

Moreover, it seems that these cells have an intense metabolic activity transposed into giant "amorphous" deposits in cultures.

At the cellular level, MDS stromal cells depict dysplastic changes very similar those met in haematopoietic compartment, and issues related to altered actin organization, such as thin and

flat morphologically altered cells, as Ilić et al. have already reported in mouse FAK (-/-) fibroblasts [256].

In addition, we have compelling arguments that MSC from RCUD settings show a continuous decline of proliferation and a reduced clonogenic capacity during 14 days of CFU-F cultures, in the absence of signals from hematopoietic cells, and these growth deficiencies are significantly correlated with diminution of CD44 and CD49e ($\alpha 5$ -integrin) adhesion molecules.

Besides these obvious, the last decade provides evidence about the cytogenetic abnormalities of MSCs selected from MDS patients [168], [230], and [305]. Of note is the fact that the MSC cytogenetic aberrations differs from the haematopoietic cells chromosomal abnormalities of the same subjects [230]. Moreover, the Blau et al. study revealed that only a fraction of the culture cells harbor cytogenetic alteration, that support the hypothesis of abnormal MSC clones existence, which probably are favored during malignancy advancement. In addition, Varga et al. proves a CAFC (cobblestone area-forming cells) frequencies diminution when normal hematopoietic cells were incubated on MDS stromal cells, compared to normal stromal layer-containing control cultures [322]. Furthermore, the same team noticed a marked reduction in the plasticity of mesenchymal stem cells of MDS patients compared with those of normal marrow donors, in neurogenic and adipogenic differentiation ability and hematopoiesis supporting capacity *in vitro* [322].

All these evidences are consistent with hypothesis that myelodysplastic stroma environment along with intrinsic changes in a hematopoietic stem/progenitor cell clone might equally contribute to the abnormal hematopoiesis in MDS.

2. The phenotypic characterization of the MSC niche in *in vitro* primary cultures

In order to identify the potential phenotypic abnormalities of MSC in MDS settings, our study begins with normal MSC cultures assessment.

The first description of the *in vitro* MSC niche belongs to Prockop DJ which argues the different roles fulfilled by the cellular subpopulations within this niche. He noticed in stationary MSC cultures the colonies comprising two major regions, the inner region populated by the more commitment precursors, and the outer one formed by a population of cells that express surface proteins with an inhibitory influence on cell adhesion [such as $\alpha 6$ -integrin and podocalyxin-like protein (PODXL)]. The last ones are highly motile, secrete DKK-1 (an inhibitor of the canonical Wnt signalling pathway), and serve as nurse cells for other subpopulations; thus, they are key elements of the rapid growth phase [134].

The flow-cytometric approach of MSCs harvested from *in vitro* primary cultures allows discrimination of three types of cells that match in terms of size and granularity those identified by morphological and morphometrical evaluation. Moreover, supplementary staining with two MSC specific markers, STRO-1 and CD73, complements and supports previous data, i.e., in these cultures there are three cellular phenotypes: STRO-1⁺CD73⁻, STRO-1⁺CD73⁺, and STRO-1⁻CD73⁺.

The STRO-1⁺ cells were CD45^{low}, expressed the vascular endothelial-related markers, CD106 (VCAM-1) and CD31 (PECAM-1), and had decreased levels of the adhesion markers CD44, CD54, CD29, and CD49e.

This particular expression for the two endothelial-related markers, CD106 and CD31 raised the question if they are not the imprint of a population with an anatomical distinct location in BM: pericytes which coexist with mesenchymal cells in our cultures? Or their association with the STRO-1 molecule it does not mean the fact that this is a potential MSC subpopulation, more immature in MSC developmental hierarchical tree?

The first hypothesis is sustained by Bianco P *et al.* in 2001, and Short B *et al.* in 2003 that interprets the CD106 expression, previously reported in umbilical cord blood (UCB) and BM-derived MSCs [323], [324], as the imprint of a particular location (the nearby outer surfaces of blood vessels) and may share an identity with the vascular pericytes [49], [55]. Moreover, this hypothesis is supported by the co-expression of α smooth muscle actin or 3G5 antigen on these cells, which is recognized as a specific marker for pericytes [53].

The second hypothesis is supported by Gronthos S *et al.* in 2003, which described a minor subpopulation of STRO^{hi} VCAM-1⁺ cells isolated from freshly BM, possessing CFU-F forming capacity, which appears to be a non-cycling population *in vivo*, because the Ki-67 expression lack on this minor subpopulation, exhibits telomerase activity, and shows an undifferentiated phenotype and substantial proliferation *in vitro* [53]. Moreover, these highly proliferative clones derived from single STRO-1^{hi} VCAM-1⁺ cells exhibited osteogenic, chondrogenic and adipogenic cell differentiation *in vitro* [53]. Their unlimited potential for division and proliferation is also supported by observations that the small number of STRO-1⁺ cells seen in cultures at later points were able to produce adherent cell layers with the same cellular composition and phenotype as those generated by STRO⁺ cells freshly isolated from BM [123].

Likewise, as previously reported by Simmons PJ *et al.* in 1994 and Gronthos S *et al.* in 1996 [127], [128], we found that the STRO-1⁺ cells express CD31, too, and possible phenotypic pitfalls, which may contribute to the tremendous differences between different groups is the fact that PECAM is sensitive to trypsin [308].

Thereafter, a low level of CD45 expression in STRO-1⁺ cells cannot be excluded. A possible explanation for this expression may be the fact that, in non-haematopoietic cells, CD45 functions as a negative modulator of growth factor receptor tyrosine kinases in addition to its well-established role as activator of src family tyrosine kinases [126].

Unlike the STRO-1 positive cells, the STRO-1⁻CD73⁺ were negative for all these markers and displayed increased levels of adhesion markers. This difference in the expression of adhesion markers may reflect the different roles of these cells within their own *in vitro* niche.

Technically, the two fractions could be exploited differently, STRO-1⁺ cells being more robust for carrying out *in vitro* MSC growth assays, whereas CD73⁺ cells have proven their utility in the evaluation of adhesion profiles. Moreover, PJ Simmons and B Torok-Storb have claimed that a STRO-1⁺ stroma layer represents a good alternative for an *in vivo* stroma for performing assays to evaluate HPC-MSK contacts. The STRO-1 molecule does not affect the proliferative abilities of HPCs by itself and it has low affinity for complement. Thus, the STRO-1 layer appears to only provide signals when induced by the engagement of other adhesion molecules [123].

Afterwards, the immunomagnetic selection allowed us to isolate the two major subpopulations that correspond to those previously described in terms of size and growth abilities.

The first population, STRO-1⁺ CD73⁻, was numerically lower in normal BM controls and displayed a rounded shape or long cytoplasmic extensions; in terms of size, cells in this population ranged between 5 and 26 μm . In cytometry, the STRO-1⁺ cells fell to near 50 on the FSC. These cells met the criteria for a quiescent, slowly cycling population supported by the morphological appearance of resting cells, approximately 2-fold higher clonogenic capacity upon plating and 2.3-fold higher proliferation efficiency at 14 days of culture compared with the STRO-1⁻ CD73⁺ fraction.

On the other hand, the STRO-1⁻CD73⁺ fraction included mostly larger (50 to 110 μm , on average) and more granular cells with lower proliferative and clonogenic potential.

3. What would be the phenotypic features of MDS cultures?

Under the MDS condition, we noticed a higher number of STRO-1⁺ cells that coexpressed CD106 and CD31 between 20 and 30 days of culture and which persisted until 60 days in the RC group. From the expression of these markers in relation to MDS pathophysiology, two hypotheses can be evoked: the former is related to CD106 upregulation

induced by TNF α stimulation [321]; high levels of TNF α are common in MDS [190], and MSCs themselves could be responsible for its synthesis in the absence of HPC stimulation. The role of this cytokine in the MDS microenvironment is probably related to its capacity to induce internal proliferative signals in MSC cells, as previously noted by Kohase *et al.* [308]. The latter is related to CD106 function as a major ligand for selective CD29-mediated HPC-to-MSC adhesions, and thus, its influence on the HPC mitotic rate and division kinetics [309].

The increased expression of CD31⁺ could be an imprint of the neoformation of blood vessels in MDS settings, as Boudard D *et al.* showed in a previous study [190].

In addition, in MDS settings, the CD73⁺ fractions of MSC display a significant reduction of adhesion markers, CD29, CD54, CD44, and CD49e.

4. MSC growth deficiencies in MDS are directly correlated with diminution of adhesion markers expression:

Furthermore, the functional tests revealed MSC growth abnormalities in the absence of any contact with or stimulation by soluble molecules from HPCs and proved the pathological nature of stromal precursors in MDS settings.

Thus, MSC production in STRO-1⁺ and CD73⁺ cell cultures from refractory cytopenia with unilineage dysplasia (RCUD) and refractory dysplasia with multilineage dysplasia (RCMD) marrows was deficient, and, in addition, the clonogenic ability of these fractions was strongly diminished. We conclude that the relative proliferation in MSC cultures from RCUD and RCMD is the result of a continuous division process occurring at a low rate and lacking the ability to generate the normal functional progenitors required to form colonies. By contrast, in refractory anaemia with excess of blasts (RAEB) settings, the proliferation rate is moderately improved due to the reduced doubling time of STRO-1 cells. However, this was not accompanied, at the end point, by complete functional maturity as reflected in the CFU-F number.

Likewise, the diminution of CFU-F capacity of CD73⁺ fractions in MDS settings that directly correlates with the CD44 mitigate on their surface should be pointed out. In addition, the doubling time of MSCs from MDS inversely correlate with their expression for CD49e. In conclusion, the MSC growth defects were significantly correlated with decreases in CD44 and CD49e (α 5-integrin) adhesion molecules.

5. The diminution of adhesion markers expression on MSC surface interfere with HSC clonogenicity

The preliminary results indicate the fact that the clonogenic potential of HPC is controlled by adhesion mechanisms dependent on stroma, and $\alpha 5$ -integrin is one of the molecules involved in this process. This is supported by statistical data which proved that the diminution of $\alpha 5$ -integrin expression in MSC correlate significantly with the decreased clonogenic potential of myeloid and erythroid precursors, selected from the same cases, and from both groups, RC and RAEB.

In light of these observations, then we intended to decode the focal adhesion (FA) signalling pathways and to understand whether adhesion-mediated processes contribute to transduction of intrinsic proliferative signals, as well as their impact on HPC-to-MSc interactions.

6. Molecular mechanisms whereby the FA proteins can contribute to the increased proliferation of MSCs selected from RAEB settings

The proliferation differences occur in RAEB cultures compared to normal settings can be attributed both to smaller cells (S-MSCs) as well as to large, more mature ones (L-MSCs), which present the qualitative defects of FA proteins (focal adhesion kinase [FAK], and paxillin), such as intensity differences, nuclear localization, and their association in complexes. Moreover, the MSCs from RAEB cultures highlight a strong complexation of FA proteins to HSP90 in nuclear area, which support a proliferative behaviour of these cells. This hypothesis is confirmed by the experiments in which the pharmacologic inhibition of HSP90 on cells leads to decreased FAK signalling, and consequently, displays growth-inhibitory effects similar to FAK inhibition alone [266]. In addition, this high co-localisation to HSP90 indicates the cessation of proteasome-mediated recycling of these proteins.

There are some possible molecular mechanisms whereby the pFAK [Y³⁹⁷] / HSP90 $\alpha\beta$ and paxillin co-localization could contribute to the increased rate of proliferation of MSCs (Figure 37).

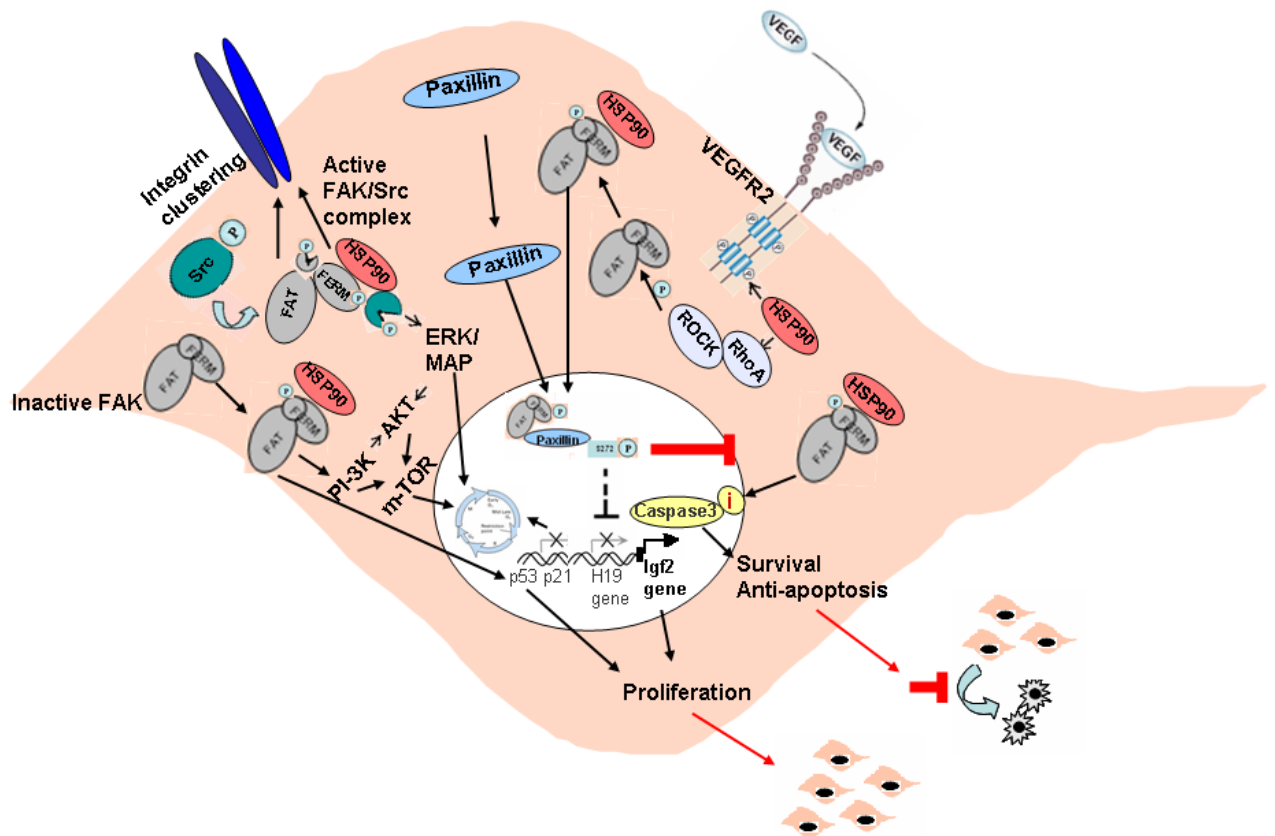


Figure 37. Model of FAK signalling pathways possibly involved in intrinsic proliferation of MSCs

Recent evidences support the FAK contribution to cell growth both by influencing the proliferation rate as well as apoptosis also.

First assumption of the FAK involvement to cell proliferation was activation the RAS-ERK-MAPK (mitogen-activated protein kinase) pathway through FAK-Src signaling complex [252], [259].

FAK, as well as Src are dependents on the chaperon HSP90 for their conformational stability and proper functions [266], [267], [268].

Also, HSP90 can induce itself FAK phosphorylation and its activation in a RhoA-ROCK-dependent manner, i.e. in response to VEGF stimulation [325].

Concomitantly, the HSP90 inhibition ceased also the c-Src phosphorylation, as well as their downstream targets paxillin and p130CAS [267].

The second possibility of FAK [Y³⁹⁷] involving in survival and proliferation is AKT signalization through PI-3K activation [252], [270].

Finally, FAK binding at paxillin induce its phosphorylation and conformational modification, blocking its nuclear export [255]. This particular nuclear localization of paxillin have proved that stimulate DNA synthesis and cell proliferation [255], [326], by suppression of H19 (a tumor-suppressor gene) transcription and promoting Igf2 expression at the translational level [255].

Likewise FAK could prevent apoptosis by two mechanisms. There are evidences about p53 FAK regulation by its FERM domain. Lim et al. proved that loss of FAK on chicken embryos lead to p53 activation and the up-regulation of p21 expression (a cell cycle progression inhibitor) accompanied by the blocking of MSCs proliferation in the embryo [327]. McLean *et al.* sustain the role of FAK in preventing apoptosis by its requirement to keep caspase-3 inactive [264]. In addition, FAK-overexpressing cells are resistant to apoptosis induced with hydrogen peroxide, etoposide and radiation, and proteome analysis of these cells showed increased levels of stress proteins such as HSP90, ribosomal proteins and antioxidant enzymes [328].

7. Molecular mechanisms whereby pFAK expression can influence the clonogenicity of haematopoietic precursors (HPC)

Another hypothesis that arises from our study is the putative role of FAK [Y³⁹⁷] expression on MSCs in HPC-to-MSc interactions and thus its implication in modulating HPC clonogenic capacities (Figure 38).

has implicated in the homing and adhesion of HPCs to MSCs [332]. And, recently, was noticed on the MSCs surface the expression for a CD44 isoform, CD44v7, which supports haematopoietic progenitor cell homing [333], and for a ligand of CD44v10 molecule expressed by HPC, CD44v10 L, which is involved in progenitor cell adhesion and maturation [334].

Finally, there are evidences also about the FAK involvement in kappa B-luciferase activation secondary to TNF- α stimulation [335], and consequently, FAK could regulate the transcription of various proteins induced by this cytokine. Thus, the CD106 upregulation on the MSCs surface, secondary to the TNF α stimulation [336] could influence the selective CD29-mediated HPC-to-MSC adhesions, and hence contribute to the HPC mitotic rate control and division kinetics [321].

PERSPECTIVES

Several studies remain to complete these results:

The differential expression of the phenotypic markers, STRO-1 and CD73, could be used for establishing of a cellular hierarchy in the MSC niche?

In order to establish a putative hierarchy of these subpopulations of MSCs (STRO-1⁺ CD73⁻ and STRO-1⁻ CD73⁺), it would be necessary the assesment of the expression patterns of genes, such as Oct-4 (characteristic of embryonic cells), and DKK-1 (an inhibitor of the canonical Wnt signaling pathway). Moreover, the expression of other surface epitopes such as the “anti-cell adhesion proteins,” e.g., α_6 -integrin and podocalyxin-like protein (PODXL), can be used for this purpose, as recently suggested by D J Prockop [134].

The distribution changes of MSC morphotypes in primary culture layers could be accompanied by the changes of differentiation potential responsible for the extinction / restriction of a mature cell type?

The differentiation capacities of the MSC subpopulations selected from MDS settings compared to normal controls could raise new questions about the pathogenesis of these diseases.

How integrates our results in the hierarchy of molecular events responsible for the common lesion of HSC and MSC?

To clarify whether these dysfunctions are the result of transdifferentiation abnormalities or dysfunction of a common precursor cells, further studies should address to the cytogenetic characterization and transcriptome decryption of MDS MSCs.

Is α_5 integrin involved in HPC division symmetry?

To confirm the role of α_5 -integrins in the regulation of HPC fate (i.e., clonogenic potential and self-renewing divisions capacity), an *in vitro* surrogate model for haematopoietic niche could be imagined using the co-cultures of MSCs fractions with CD34⁺CD133⁺ cells, in the absence

or presence of an anti- α_5 -integrin blocking antibody, as well as conducting tests to evaluate cell division symmetry and LTC-IC assays.

Which is the echo of these results in diagnostic customization in MDS?

Correlations between MSCs abnormalities (i.e., adhesion deficiencies, growth dysfunctions, abnormal expression of FA proteins) with MDS prognosis and resistance to chemotherapy could lead to a new classification of MDS cases into risk groups involving microenvironment factors.

CONCLUDING REMARKS

1. Our results reinforce the concept “bad seeds in bad soil” that underlies the neoplastic evolution in MDS settings.
2. Herein we bring arguments that MSCs isolated from MDS have a pathological behaviour in primary and secondary cultures and that they actively contribute in some neoplastic signalling pathways involving the adhesion-related processes, such as cell proliferation, apoptosis, clonogenic growth and neoangiogenesis.
3. Structural and functional analysis allowed us the identification of morpho- and immunophenotypes that could be involved in the conflict between HSC - “adhesive” microenvironment, proposing also an *in vitro* study model of the relationship between these two partners.
4. Our preliminary data justify the rising interest concerning the untapped potential of microenvironmental prognostic factors as distinctive item of MDS lesion, and sustain the further validation, in a broader context, of the diagnostic value of microenvironmental entities inventory as part of pathophysiological process evaluation in MDS.
5. The perception of the stroma-related disease mechanisms may underlie to the development of alternative therapeutic approaches.

REFERENCES

1. Amy J. Wagers and Irving L. Weissman. Plasticity of Adult Stem Cells Review. *Cell*. 2004; 116:639–648.
2. Junying Yu, Maxim A. Vodyanik, Kim Smuga-Otto, Jessica Antosiewicz-Bourget, Jennifer L. Frane, Shulan Tian, Jeff Nie, Gudrun A. Jonsdottir, Victor Ruotti, Ron Stewart, Igor I. Slukvin, and James A. Thomson. Induced Pluripotent Stem Cell Lines Derived from Human Somatic Cells. *Science*. 2007; 5858:1917-1920.
3. Hyenjong Hong, Kazutoshi Takahashi, Tomoko Ichisaka, Takashi Aoi, Osami Kanagawa, Masato Nakagawa, Keisuke Okita, and Shinya Yamanaka. Suppression of induced pluripotent stem cell generation by the p53–p21 pathway. *Nature*. 2009; 460:1132-1136.
4. Marius Wernig, Alexander Meissner, Ruth Foreman, Tobias Brambrink, Manching Ku, Konrad Hochedlinger, Bradley E. Bernstein, and Rudolf Jaenisch. *In vitro* reprogramming of fibroblasts into a pluripotent ES-cell-like state. *Nature*. 2007; 448:318-325.
5. Jos Domen, Amy Wagers, and Irving L. Weissman. Chapter 2: Bone Marrow (Hematopoietic) Stem Cells. *Stem Cell Information* [World Wide Web site], Bethesda, MD: National Institutes of Health, U.S. Department of Health and Human Services. 2011.
6. Anna Marciniak-Czochra, Thomas Stiehl, and Wolfgang Wagner. Modeling of replicative senescence in hematopoietic development. *Aging*. 2009; 8:723-733.
7. Sean J. Morrison and Irving L. Weissman. The Long-Term Repopulating Subset of Hematopoietic Stem Cells Is Deterministic and Isolatable by Phenotype. *Immunity*. 1994; 1:661-673.
8. Derrick J. Rossi, Jun Seita, Agnieszka Czechowicz, Deepta Bhattacharya, David Bryder, Irving L. Weissman. Spotlight on DNA Damage, Hematopoietic Stem Cell Quiescence Attenuates DNA Damage Response and Permits DNA Damage Accumulation During Aging. *Cell Cycle*. 2007; 19:2371-2376.
9. Engelhardt M, M Lübbert, Y Guo. CD34⁺ or CD34⁻ : which is the more primitive? *Leukemia*. 2002; 16:1603-1608.
10. Gao Z, MJ Fackler, W Leung, R Lumkul, M Ramirez, N Theobald, HL Malech, CI Civin. Human CD34⁺ cell preparations contain over 100-fold greater NOD/SCID mouse engrafting capacity than do CD34⁻ cell preparations. *Experimental Hematology*. 2001; 29:910–921.
11. Mo A Dao, Jesusa Arevalo, Jan A Nolte. Reversibility of CD34 expression on human stem cells that retain the capacity for secondary reconstitution. *Blood*. 2003; 101:112-118.

12. Ploemacher RE, NHC Brons. Separation of CFU-S from primitive cells responsible for reconstitution of the bone marrow hemopoietic stem cell compartment following irradiation: evidence for a pre-CFU-S cell. *Experimental Hematology*. 1989; 17:263–266.
13. Sean J. Morrison and Judith Kimble. Review article Asymmetric and symmetric stem-cell divisions in development and cancer. *Nature*. 2006; 441:1068-1074.
14. Nakauchi H, H Takano, H Ema, M Osawa. Further characterization of CD34^{low}/negative mouse hematopoietic stem cells. *Annals of the New York Academy of Sciences*. 1999; 872:57-66.
15. Kapil Mehta, Umar Shahid, and Fabio Malavasi. Human CD38, a cell-surface protein with multiple functions. *The FASEB Journal*. 1996; 10:1408-1417.
16. William Craig, Robert Kay, Robert L. Cutler, and Peter M. Lansdorp. Expression of Thy-1 on Human Hematopoietic Progenitor Cells. *The Journal of Experimental Medicine*, © The Rockefeller University Press. 1993; 177:1331-1342.
17. Giuliana Ferrari, Gabriella Cusella–De Angelis, Marcello Coletta, Egle Paolucci, Anna Stornaiuolo, Giulio Cossu, Fulvio Mavilio. Muscle Regeneration by Bone Marrow-Derived Myogenic Progenitors. *Science*. 1998; 279:1528-1530.
18. Olafur E. Sigurjonsson, Marie-Claude Perreault, Torstein Egeland, and Joel C. Glover. Adult human hematopoietic stem cells produce neurons efficiently in the regenerating chicken embryo spinal cord. *Proceedings of the National Academy of Sciences of the United States of America*. 2005; 14:5227–5232.
19. Christopher R.R. Bjornson, Rodney L. Rietze, Brent A. Reynolds, M. Cristina Magli, Angelo L. Vescovi. Turning Brain into Blood: A Hematopoietic Fate Adopted by Adult Neural Stem Cells *In Vivo*. *Science*. 1999; 283:534-537.
20. Trang Hoang. The origin of hematopoietic cell type diversity. *Oncogene*. 2004; 23:7188–7198.
21. Ludovica Bruno, Reinhard Hoffmann, Fraser McBlane, John Brown, Rajeev Gupta, Chirag Joshi, Stella Pearson, Thomas Seidl, Clare Heyworth, and Tariq Enver. Molecular Signatures of Self-Renewal, Differentiation, and Lineage Choice in Multipotential Hemopoietic Progenitor Cells *In Vitro*. *Molecular and Cellular Biology*. 2004; 2:741–756.
22. Sabine Herblot, Peter D. Aplan, and Trang Hoang. Gradient of E2A Activity in B-Cell Development. *Molecular and Cellular Biology*. 2002; 3:886–900.
23. Sabine Herblot, Ann-Muriel Steff, Patrice Hugo, Peter D. Aplan, and Trang Hoang. SCL and LMO1 alter thymocyte differentiation: inhibition of E2A-HEB function and pre-T α chain expression. *Nature Immunology*. 2000; 2:138-144.

24. Joshua Wechsler, Marianne Greene, Michael A. McDevitt, John Anastasi, Judith E. Karp, Michelle M. Le Beau, and John D. Crispino. Acquired mutations in GATA1 in the megakaryoblastic leukemia of Down syndrome. *Nature Genetics*. 2002; 32:148-152.
25. Thomas Pabst, Beatrice U. Mueller, Pu Zhang, Hanna S. Radomska, Sailaja Narravula, Susanne Schnittger, Gerhard Behre, Wolfgang Hiddemann, and Daniel G. Tenen. Dominant-negative mutations of CEBPA, encoding CCAAT/enhancer binding protein- α (C/EBP α), in acute myeloid, Leukemia. *Nature Genetics*. 2001; 27:263-270.
26. Rodney P. DeKoter and Harinder Singh. Regulation of B Lymphocyte and Macrophage Development by Graded Expression of PU.1. *Science*. 2000; 288:1439-1441.
27. Richard Dahl, Jonathan C. Walsh, David Lancki, Peter Laslo, Sangeeta R. Iyer, Harinder Singh, and M. Celeste Simon. Regulation of macrophage and neutrophil cell fates by the PU.1:C/EBP α ratio and granulocyte colony-stimulating factor. *Nature Immunology*. 2003; 4:1029-1036.
28. Qi-Long Ying, Jennifer Nichols, Ian Chambers, and Austin Smith. BMP Induction of Id Proteins Suppresses Differentiation and Sustains Embryonic Stem Cell Self-Renewal in Collaboration with STAT3. *Cell*. 2003; 115:281–292.
29. Hideaki Nakajima and James N. Ihle. Granulocyte colony-stimulating factor regulates myeloid differentiation through CCAAT/enhancer-binding protein. *Blood*. 2001; 4:897-905.
30. Richard Martin, Rachid Lahlil, Annette Damert, Lucile Miquerol, Andras Nagy, Gordon Keller, and Trang Hoang. SCL interacts with VEGF to suppress apoptosis at the onset of hematopoiesis. *Development and Disease*. 2004; 131:693-702.
31. Rajotte D, HB Sadowski, A Haman, K Gopalbhai, S Meloche, L Liu, G Krystal, and Trang Hoang. Contribution of both STAT and SRF/TCF to c-fos promoter activation by granulocyte-macrophage colony-stimulating factor. *Blood*. 1996; 8:2906-2916.
32. Richard L. Riley, Jennean Knowles, and Anne M. King. Levels of E2A protein expression in B cell precursors are stage-dependent and inhibited by stem cell factor (c-kit ligand). *Experimental Hematology*. 2002; 30:1412–1418.
33. Rice KL, Hormaeche I, Licht JD. Epigenetic regulation of normal and malignant hematopoiesis. *Oncogene*. 2007; 26:6697-6714.
34. Howard Cedar and Yehudit Bergman. Epigenetics of haematopoietic cell development. *Nature Reviews Immunology*. 2011; 11:478-488.
35. Charlotte Ling and Leif Groop. Epigenetics: A Molecular Link Between Environmental Factors and Type 2 Diabetes. *Diabetes*. 2009; 58:2718-2725.

36. Ivan V Gregoretti, Yun-Me Lee and Holly V Goodson. Molecular evolution of the histone deacetylase family: functional implications of phylogenetic analysis. *Journal of molecular biology*. 2004; 338:17-31.
37. Laure Coulombel. Identification of hematopoietic stem/progenitor cells: strength and drawbacks of functional assays. *Oncogene*. 2004; 23:7210–7222.
38. Human Colony-Forming Cell Assay Using MethoCult®, Technical Manual. *StemCell Technologies*. Catalog #28404, 2004.
39. Ernest Beutler, Marshall A. Lichtman, Barry S. Coller, Thomas J. Kipps Uri Seligsohn, Camille N. Abboud. Chapter 4: Structure of the marrow and the hematopoietic microenvironment. In *Williams Hematology*. 2001.
40. Gregory S. Travlos. Normal Structure, Function, and Histology of the Bone Marrow. *Toxicologic Pathology*. 2006; 34:548–565.
41. Paolo Bianco. Bone and the hematopoietic niche: a tale of two stem cells. *Blood*. 2011; 20:5281-5288.
42. Wilkins BS. Histology of normal haemopoiesis: Bone marrow histology I. *Journal of Clinical Pathology*. 1992; 45:645-649.
43. William F. Kern, MD. PDQ Hematology. *PDQ Series*. BC Decker Inc Hamilton. London, 2002.
44. Lévesque J- P, IG Winkler, SR Larsen, JEJ Rasko. Bone Marrow-Derived Progenitors. *Springer-Verlag Berlin Heidelberg*. 2007; 3-37.
45. Krebsbach PH, Serghei A. Kuznetsov, Paolo Bianco, PG Robey. Bone marrow stromal cells: characterization and clinical application. *Critical reviews in oral biology and medicine*. 1999; 2:165-181.
46. Crisan M, S Yap, L Casteilla, SW Chen, M Corselli, TS Park. A perivascular origin for mesenchymal stem cells in multiple human organs. *Cell Stem Cell*. 2008; 3:301–313.
47. Sacchetti B, A Funari, S Michienzi, S Di Cesare, S Piersanti, I Saggio, E Tagliafico, S Ferrari, PG Robey, M Riminucci, Paolo Bianco. Self-renewing osteoprogenitors in bone marrow sinusoids can organize a hematopoietic microenvironment. *Cell*. 2007; 131:324–336.
48. Lindolfo Da Silva Meirelles, Arnold I. Caplan, Nance Beyer Nardi. In Search of the *In Vivo* Identity of Mesenchymal Stem Cells. *Stem Cells*. 2008; 26:2287–2299.
49. Paolo Bianco, Mara Riminucci, Stan Gronthos, Pamela Gehron Robey. Bone marrow stromal stem cells: Nature, biology, and potential applications. *Stem Cells*. 2001; 19:180-192.
50. DeRuiter MC, RE Poelmann, JC VanMunsteren, V Mironov, RR Markwald, AC Gittenberger-de Groot. Embryonic endothelial cells transdifferentiate into mesenchymal cells

expressing smooth muscle actins *in vivo* and *in vitro*. *Circulation Research*. 1997; 80:444-451.

51. Yamashita J, H Itoh, M Hirashima, M Ogawa, S Nishikawa, T Yurugi, M Naito, K Nakao, S Nishikawa. Flk1-positive cells derived from embryonic stem cells serve as vascular progenitors. *Nature*. 2000; 408:92-96.

52. Jones E and D McGonagle. Human bone marrow mesenchymal stem cells *in vivo*. *Rheumatology*. 2008; 47:136-131.

53. Stan Gronthos, Andrew C.W. Zannettino, Shelley J. Hay, Songtao Shi, Stephen E. Graves, Angela Kortessidis, and Paul J. Simmons. Molecular and cellular characterisation of highly purified stromal stem cells derived from human bone marrow. *Journal of Cell Science*. 2003; 116:1827-1835.

54. Shi S and Stan Gronthos. Perivascular niche of postnatal mesenchymal stem cells in human bone marrow and dental pulp. *Journal of Bone and Mineral Research*. 2003; 18:696-704.

55. Brenton Short, Nathalie Brouard, Teresa Occhiodoro-Scott, Anand Ramakrishnan, Paul J. Simmons. Mesenchymal Stem Cells – Review Article. *Archives of Medical Research*. 2003; 34:565-571.

56. Schor AM, AE Canfield, AB Sutton, E Arciniegas, TD Allen. Pericyte differentiation. *Clinical Orthopaedics and Related Research*. 1995; 313:81-91.

57. Doherty MJ, BA Ashton, S Walsh, JN Beresford, ME Grant, AE Canfield. Vascular pericytes express osteogenic potential *in vitro* and *in vivo*. *Journal of Bone and Mineral Research*. 1998; 13:828-838.

58. Suri C, PF Jones, S Patan, S Bartunkova, PC Maisonpierre, S Davis, TN Sato, GD Yancopoulos. Requisite role of angiopoietin-1, a ligand for the TIE2 receptor, during embryonic angiogenesis. *Cell*. 1996; 7:1171-1180.

59. Serghei A. Kuznetsov, Mara Riminucci, Navid Ziran, Takeo W. Tsutsui, Alessandro Corsi, Laura Calvi, Henry M. Kronenberg, Ernestina Schipani, Pamela Gehron Robey, Paolo Bianco. The interplay of osteogenesis and hematopoiesis: expression of a constitutively active PTH/PTHrP receptor in osteogenic cells perturbs the establishment of hematopoiesis in bone and of skeletal stem cells in the bone marrow. *The Journal of Cell Biology*. 2004; 6:1113-1122.

60. Méndez-Ferrer S, TV Michurina, F Ferraro, AR Mazloom, BD Macarthur, SA Lira, DT Scadden, A Ma'ayan, GN Enikolopov, PS Frenette. Mesenchymal and haematopoietic stem cells form a unique bone marrow niche. *Nature*. 2010; 466:829-834.

61. Laharrague P, D Larrouy, AM Fontanilles, N Truel, A Campfield, R Tenenbaum, J Galitzky, JX Corberand, L Pénicaud, L Casteilla. High expression of leptin by human bone marrow adipocytes in primary cultures. *The FASEB Journal*. 1998; 9:747-752.
62. Benayahu D, A Shamay, S Wientroub. Osteocalcin (BGP), gene expression, and protein production by marrow stromal adipocytes. *Biochemical and Biophysical Research Communications*. 1997; 13:442-446.
63. McAveny KM, JM Gimble, L Yu-Lee. Prolactin receptor expression during adipocyte differentiation of bone marrow stroma. *Endocrinology*. 1996; 137:5723-5726.
64. Gimble JM, CE Robinson, X Wu, KA Kelly. The function of adipocytes in the bone marrow stroma: an update. *Bone*. 1996; 19:421-428.
65. Delikat S, RJ Harris, DW Galvani. IL-1 beta inhibits adipocyte formation in human long-term bone marrow culture. *Experimental Hematology*. 1993; 21:31-37.
66. Keller DC, XX Du, EF Srour, R Hoffman, and DA Williams. Interleukin-11 inhibits adipogenesis and stimulates myelopoiesis in human long-term marrow cultures. *Blood*. 1993; 82:1428-1435.
67. Tavassoli M. Fatty evolution of marrow and the role of adipose tissue in hematopoiesis. *Handbook of the Hemopoietic Microenvironment*, edited by M Tavassoli, Humana Press, Clifton, NJ, 1989; 157-187.
68. Gimble JM, C Morgan, K Kelly, X Wu, V Dandapani, C-S Wang, V Rosen. Bone morphogenetic proteins inhibit adipocyte differentiation by bone marrow stromal cells. *Journal of Cellular Biochemistry*. 1995; 58:393-402.
69. Thierry Thomas, Francesca Gori, Sundeep Khosla, Michael D. Jensen, Bartolome Burguera, and B. Lawrence Riggs. Leptin acts on human marrow stromal cells to enhance differentiation to osteoblasts and to inhibit differentiation to adipocytes. *Endocrinology*. 1999; 140:1630-1638.
70. Kaigler D, PH Krebsbach, Z Wang, ER West, K Horger, and DJ Mooney. Transplanted Endothelial Cells Enhance Orthotopic Bone Regeneration, *Journal of Dental Research*. 2006; 7:633-637.
71. Hasthorpe S, M Bogdanovski, J Rogerson, JM Radley. Characterization of endothelial cells in murine long-term marrow culture: Implication for hemopoietic regulation. *Experimental Hematology*. 1992; 20:476-481.
72. Perkins S, RA Fleischman. Stromal cell progeny of murine bone marrow fibroblast colony-forming units are clonal endothelial-like cells that express collagen IV and laminin. *Blood*. 1990; 75:620-625.

73. Schweitzer KM, AM Dräger, P van der Valk, SF Thijsen, A Zevenbergen, AP Theijsmeijer, CE van der Schoot, and MM Langenhuijsen. Constitutive expression of E-selectin and vascular cell adhesion molecule-1 on endothelial cells of hematopoietic tissues. *The American Journal of Pathology*. 1996; 148:165-175.
74. Toshio Imai, Kunio Hieshima, Christopher Haskell, Masataka Baba, Morio Nagira, Miyuki Nishimura, Mayumi Kakizaki, Shin Takagi, Hisayuki Nomiyama, Thomas J. Schall, Osamu Yoshie. Identification and molecular characterization of fractalkine receptor CX3CR1, which mediates both leukocyte migration and adhesion. *Cell*. 1997; 91:521-530.
75. Lars Nitschke, Helen Floyd, David J.P. Ferguson, and Paul R. Crocker. Identification of CD22 ligands on bone marrow sinusoidal endothelium implicated in CD22-dependent homing of recirculating B cells. *The Journal of Experimental Medicine*. 1999; 189:1513-1518.
76. Ahmed Deldar, Leon Weiss, Hugh Lewis. Bone lining cells and hematopoiesis: an electron microscopic study of canine bone marrow. *The Anatomical Record*. 1985; 213:187-201.
77. Sillaber C, S Walchshofer, I Mosberger, A Gaiger, I Simonitsch, A Chott, K Lechner, P Valent. Immunophenotypic characterization of human bone marrow endosteal cells. *Tissue Antigens*. 1999; 53:559-568.
78. Saito T, SM Albelda, CT Brighton. Identification of integrin receptors on cultured human bone cells. *Journal of Orthopaedic Research*. 1994; 12:384-394.
79. Nilsson SK, MS Dooner, CY Tiarks, HU Weier, PJ Quesenberry. Potential and distribution of transplanted hematopoietic stem cells in a nonablated mouse model. *Blood*. 1997; 89:4013-4020.
80. Park SR, RO Oreffo, JT Triffitt. Interconversion potential of cloned human marrow adipocytes *in vitro*. *Bone*. 1999; 24:549-554.
81. James E. Dennis, Anita Merriam, Amad Awadallah, Jung U. Yoo, Brian Johnstone, and Arnold I. Caplan. A quadripotential mesenchymal progenitor cell isolated from the marrow of an adult mouse. *Journal of Bone and Mineral Research*. 1999; 14:700-709.
82. Mark F. Pittenger, Alistair M. Mackay, Stephen C. Beck, Rama K. Jaiswal, Robin Douglas, Joseph D. Mosca, Mark A. Moorman, Donald W. Simonetti, Stewar Craig, Daniel R. Marshak, Multilineage Potential of Adult Human Mesenchymal Stem Cells. *Science*. 1999; 284:143-147.
83. Oyajobi BO, A Lomri, M Hott, PJ Marie. Isolation and characterization of human clonogenic osteoblast progenitors immunoselected from fetal bone marrow stroma using STRO-1 monoclonal antibody. *Journal of Bone and Mineral Research*. 1999; 14:351-361.

84. Bruder SP, NS Ricalton, RE Boynton, TJ Connolly, N Jaiswal, J Zaia, FP Barry. Mesenchymal stem cell surface antigen SB-10 corresponds to activated leukocyte cell adhesion molecule and is involved in osteogenic differentiation. *Journal of Bone and Mineral Research*. 1998; 13:655-663.
85. Long MW, JA Robinson, EA Ashcraft, KG Mann. Regulation of human bone marrow-derived osteoprogenitor cells by osteogenic growth factors. *The Journal of Clinical Investigation*. 1995; 95:881-887.
86. Stan Gronthos, AC Zannettino, SE Graves, S Ohta, SJ Hay, PJ Simmons. Differential cell surface expression of the STRO-1 and alkaline phosphatase antigens on discrete developmental stages in primary cultures of human bone cells. *Journal of Bone and Mineral Research*. 1999; 14:47-56.
87. Stewart K, S Walsh, J Screen, CM Jefferiss, J Chainey, GR Jordan, JN Beresford. Further characterization of cells expressing STRO-1 in cultures of adult human bone marrow stromal cells. *Journal of Bone and Mineral Research*. 1999; 14:1345-1356.
88. Hanada K, JE Dennis, AI Caplan. Stimulatory effects of basic fibroblast growth factor and bone morphogenetic protein-2 on osteogenic differentiation of rat bone marrow-derived mesenchymal stem cells. *Journal of Bone and Mineral Research*. 1997; 12:1606-1614.
89. Taichman RS, SG Emerson. The role of osteoblasts in the hematopoietic microenvironment. *Stem Cells*. 1998; 16:7-15.
90. Ahmed N, MA Khokher, HT Hassan. Cytokine-induced expansion of human CD34⁺ stem/progenitor and CD34⁺CD41⁺ early megakaryocytic marrow cells cultured on normal osteoblasts. *Stem Cells*. 1999; 17:92-99.
91. Gehron Robey Robey, MF Young, KC Flanders, NS Roche, P Kondaiah, AH Reddi, JD Termine, MB Sporn, AB Roberts. Osteoblasts synthesize and respond to transforming growth factor-type b (TGF-beta) *in vitro*. *Journal of biophysical and biochemical cytology*. 1987; 105:457-463.
92. Matayoshi A, C Brown, JF DiPersio, J Haug, Y Abu-Amer, H Liapis, R Kuestner, R Pacifici. Human blood-mobilized hematopoietic precursors differentiate into osteoclasts in the absence of stromal cells. *Proceedings of the National Academy of Sciences of the United States of America*. 1996; 93:10785-10790.
93. Roodman GD. Cell biology of the osteoclast. *Experimental Hematology*. 1999; 27:1229-1241.
94. Demulder A, SV Suggs, KM Zsebo, T Scarcez, GD Roodman. Effects of stem cell factor on osteoclast-like cell formation in long-term human marrow cultures. *Journal of Bone and Mineral Research*. 1992; 7:1337-1344.

95. Tanaka S, N Takahashi, N Udagawa, T Tamura, T Akatsu, ER Stanley, T Kurokawa, T Suda. Macrophage colony-stimulating factor is indispensable for both proliferation and differentiation of osteoclast progenitors. *The Journal of Clinical Investigation*. 1993; 91:257-263.
96. Shalhoub V, J Faust, WJ Boyle, CR Dunstan, M Kelley, S Kaufman, S Scully, G Van, DL Lacey. Osteoprotegrin and osteoprotegrin ligand effects on osteoclast formation from human peripheral blood mononuclear cell precursors. *Journal of Supramolecular Structure and Cellular Biochemistry*. 1999; 72:251-261.
97. Takahashi N, N Udagawa, T Suda. A new member of tumor necrosis factor ligand family, ODF/OPGL/TRANCE/RANKL, regulates osteoclast differentiation and function. *Biochemical and Biophysical Research Communications*. 1999; 256:449-455.
98. Kania JR, T Kehat-Stadler, SR Kupfer. CD44 antibodies inhibit osteoclast formation. *Journal of Bone and Mineral Research*. 1997; 12:1155-1164.
99. Mbalaviele G, R Nishimura, A Myoi, M Niewolna, SV Reddy, D Chen, J Feng, D Roodman, GR Mundy, T Yoneda. Cadherin-6 mediates the heterotypic interactions between the hemopoietic osteoclast cell lineage and stromal cells in a murine model of osteoclast differentiation. *Journal of Biophysical and Biochemical Cytology*. 1998; 141:1467-1476.
100. Ronald Hoffman et al., Chapter 13: Anatomy and Physiology of Hematopoiesis. In *Hematology: Basic Principles and Practice*, 3rd ed., Churchill Livingstone Inc., 2000.
101. Chen XD, V Dusevich, JQ Feng, SC Manolagas, RL Jilka. Extracellular matrix made by bone marrow cells facilitates expansion of marrow-derived mesenchymal progenitor cells and prevents their differentiation into osteoblasts. *Journal of bone and mineral research*. 2007; 22:1943-1956.
102. Mauney JR, C Kirker-Head, L Abrahamson, G Gronowicz, V Volloch, DL Kaplan. Matrix-mediated retention of *in vitro* osteogenic differentiation potential and *in vivo* bone-forming capacity by human adult bone marrow-derived mesenchymal stem cells during *ex vivo* expansion. *Journal of biomedical materials research*. 2006; 79:464-475.
103. Mauney JR, V Volloch, DL Kaplan. Matrix-mediated retention of adipogenic differentiation potential by human adult bone marrow-derived mesenchymal stem cells during *ex vivo* expansion. *Biomaterials*. 2005; 26:6167-6175.
104. Baksh D, L Song, RS Tuan. Adult mesenchymal stem cells: characterization, differentiation, and application in cell and gene therapy. *Journal of Cellular and Molecular Medicine*. 2004; 3:301-316.
105. Qiling He, Chao Wan, Gang Li. Concise review: Multipotent Mesenchymal Stromal Cells in Blood. *Stem Cells*. 2007; 25:69-77.

106. Dominici M, K Le Blanc, I Mueller, I Slaper-Cortenbach, F Marini, D Krause, R Deans, A Keating, DJ Prockop, and E Horwitz. Minimal criteria for defining multipotent mesenchymal stromal cells. The International Society for Cellular Therapy position statement. *Cytotherapy*. 2006; 8:315-317.
107. Seung-Cheol Choi, Su-Jin Kim, Ji-Hyun Choi, Chi-Yeon Park, Wan-Joo Shim, Do-Sun Lim. Fibroblast Growth Factor-2 and -4 Promote the Proliferation of Bone Marrow Mesenchymal Stem Cells by the Activation of the PI3K-Akt and ERK1/2 Signaling Pathways. *Stem Cells and Development*. 2008; 17:725–736.
108. Wieczorek G, C Steinhoff, R Schulz, M Scheller, M Vingron, HH Ropers, and UA Nuber. Gene expression profile of mouse bone marrow stromal cells determined by cDNA microarray analysis. *Cell and Tissue Research*. 2003; 311:227–237.
109. Kinnaird T, E Stabile, MS Burnett, M Shou, CW Lee, S Barr, S Fuchs, and SE Epstein. Local delivery of marrow derived stromal cells augments collateral perfusion through paracrine mechanisms. *Circulation*. 2004; 109:1543–1549.
110. Yoon J, WJ Shim, YM Ro, and DS Lim. Transdifferentiation of mesenchymal stem cells into cardiomyocytes by direct cell-to-cell contact with neonatal cardiomyocyte but not adult cardiomyocytes. *Annals of Hematology*. 2005; 84:715–721.
111. Ryang Hwa Lee, Min Jeong Seo, Andrey A. Pulin, Carl A. Gregory, Joni Ylostalo, and Darwin J. Prockop. The CD34-like protein PODXL and α 6-integrin (CD49f) identify early progenitor MSCs with increased clonogenicity and migration to infarcted heart in mice, *Blood*. 2008; 113:816-826.
112. Colter DC, I Sekiya, DJ Prockop. Identification of a subpopulation of rapidly self-renewing and multipotential adult stem cells in colonies of human marrow stromal cells. *Proceedings of the National Academy of Sciences of the United States of America*. 2001; 98:7841-7845.
113. Mets T, G Verdonk. *In vitro* aging of human bone marrow derived stromal cells. *Mechanisms of Ageing and Development*. 1981; 16:81-89.
114. Ron Zohar, Jaro Sodek, and Christopher AG McCulloch. Characterization of Stromal Progenitor Cells Enriched by Flow Cytometry, *Blood*. 1997; 90:3471-3481.
115. David C Colter, Reiner Class, Carla M. DiGirolamo, and Darwin J. Prockop. Rapid expansion of recycling stem cells in cultures of plastic-adherent cells from human bone marrow. *Proceedings of the National Academy of Sciences of the United States of America*. 2000; 97: 3213-3218.

116. Shih-Chieh Hung, Nien-Jung Chen, Shie-Liang Hsieh, Hung Li, Hsiao-Li Ma, and Wai-Hee Lo. Isolation and Characterization of Size-Sieved Stem Cells from Human Bone Marrow. *Stem Cells*. 2002; 20:249–258.
117. Jaroslaw Staszkievicz, Trivia P. Frazier, Brian G. Rowan, Bruce A. Bunnell, Ernest S. Chiu, Jeffrey M. Gimble and Barbara Gawronska-Kozak, Cell growth characteristics, differentiation frequency, and immunophenotype of adult ear mesenchymal stem cells. *Stem Cells and Development*. 2010; 19:83-92.
118. Kassis I, L Zangi, R Rivkin, L Levdansky, S Samuel, G Marx, R Gorodetsky. Isolation of mesenchymal stem cells from G-CSF mobilized human peripheral blood using fibrin microbeads. *Bone Marrow Transplant*. 2006; 37:967–976.
119. Ad Ho, W Wagner, W Franke. Heterogeneity of mesenchymal stromal cell preparations. *Cytotherapy*. 2008; 4:320-330.
120. Frederic Deschaseaux, Florelle Gindraux, Rafika Saadi, Laurent Obert, David Chalmers, and Patrik Herve. Direct selection of human bone marrow mesenchymal stem cells using an anti-CD49a antibody reveals their CD45^{med, low} phenotype. *British Journal of Haematology*. 2003; 122:506-517.
121. Serghei A. Kuznetsov, MH Mankani, Stan Gronthos, K Satomura, Paolo Bianco, PG Robey. Circulating skeletal stem cells. *The Journal of Cell Biology*. 2001; 5:1133-1140.
122. Fernández M, V Simon, G Herrera, C Cao, H Del Favero, JJ Minguell. Detection of stromal cells in peripheral blood progenitor cell collections from breast cancer patients. *Bone Marrow Transplant*. 1997; 20:265–271.
123. Simmons PJ and B Torok-Storb. Identification of stromal cell precursor in human bone marrow by a novel monoclonal antibody, STRO-1. *Blood*. 1991; 78:55-62.
124. Moubarak Mouiseddine, Noëlle Mathiru, Johanna Stefani, Christelle Demarquay, and Jean-Marc Bertho. Characterization and Histological Localization of Multipotent Mesenchymal Stromal Cells in the Human Postnatal Thymus. *Stem Cells and Development*. 2008; 17:1165-1174.
125. Kumamoto M, T Nishiwaki, N Matsuo, H Kimura, and K Matsushima. Minimally cultured bone marrow mesenchymal stem cells ameliorate fibrotic lung injury. *European Respiratory Journal*. 2009; 3:740-748.
126. Kulas DT, BJ Goldstein, RA Mooney. The transmembrane protein-tyrosine phosphatase LAR modulates signaling by multiple receptor tyrosine kinases. *The Journal of Biological Chemistry*. 1996; 271:748-754.

127. Simmons PJ, Stan Gronthos, A Zannettino, S Ohta, S Graves. Isolation, characterization and functional activity of human marrow stromal progenitors in hemopoiesis. *Progress in Clinical and Biological Research*. 1994; 389:271-280.
128. Stan Gronthos and PJ Simmons. The Biology and Application of Human Bone Marrow Stromal Cell Precursors. *Journal of Hematotherapy*. 1996; 5:15-23.
129. Deans RJ and AB Moseley. Mesenchymal stem cells: Biology and potential clinical uses. *Experimental Hematology*. 2000; 28:875-884.
130. Rahul Sarugaser, Lorraine Hanoun, Armand Keating, William L. Stanford, John E. Davis. Human Mesenchymal Stem Cells Sel-Renew and Differentiate According to a Deterministic Hierarchy. *PloS One*. 2009; No. 8.
131. Arnold I. Caplan and Scott P. Bruder. Mesenchymal stem cells: building blocks for molecular medicine in the 21st century. *Trends in Molecular Medicine*. 2001; 6:259-264.
132. Arnold I. Caplan. The mesengenic process. *Clinics in Plastic Surgery*. 1994; 21:429–435.
133. Jeffrey M. Gimble, Farshid Guilak, Mark E. Nuttall, Solomon Sathishkumar, Martin Vidal, Bruce A. Bunnell. *In vitro* Differentiation Potential of Mesenchymal Stem Cells. *Transfusion Medicine and Hemotherapy*. 2008; 35:228-238.
134. Darwin J. Prockop. Repair of Tissues by Adult Stem/Progenitor Cells (MSCs): Controversies, Myths, and Changing Paradigms. *Molecular Therapy*. 2009; 6:939-946.
135. Leticia Basciano, Christophe Nemos, Bernard Foliguet, Natalia de Isla, Marcelo de Carvalho, Nguyen Tran, Ali Dalloul. Long term culture of mesenchymal stem cells in hypoxia promotes a genetic program maintaining their undifferentiated and multipotent status. *BMC Cell Biology*. 2011; 12:1-12.
136. Ylostalo J, N Bazhanov, DJ Prockop. Reversible commitment to differentiation by human multipotent stromal cells in single-cell-derived colonies. *Experimental Hematology*. 2008; 36:1390–1402.
137. Digirolamo CM, D Stokes, D Colter, DG Phinney, R Class, and DJ Prockop. Propagation and senescence of human marrow stromal cells in culture: a simple colony-forming assay identifies samples with the greatest potential to propagate and differentiate. *British Journal of Haematology*. 1999; 107:275–281.
138. Serghei A. Kuznetsov, PH Krebsbach, K Satomura, J Kerr, M Riminucci, D Benayahu, PG Robey. Single-colony derived strains of human marrow stromal fibroblasts form bone after transplantation *in vivo*. *Journal of Bone and Mineral Research*. 1997; 12:1335–1347.

139. Lee RH, MJ Seo, AA Pulin, CA Gregory, J Ylostalo, and DJ Prockop. The CD34-like protein PODXL and $\alpha 6$ -integrin (CD49f) identify early progenitor MSCs with increased clonogenicity and migration to infarcted heart in mice. *Blood*. 2009; 113:816–826.
140. Craig CG, V Tropepe, CM Morshead, BA Reynolds, S Weiss, and D van der Kooy. *In vivo* growth factor expansion of endogenous subependymal neural precursor cell populations in the adult mouse brain. *The Journal of Neuroscience*. 1996; 16:2649–2658.
141. Quito FL, J Beh, O Bashayan, C Basilico, and RS Basch. Effects of fibroblast growth factor-4 (k-FGF) on long-term cultures of human bone marrow cells. *Blood*. 1996; 87:1282–1291.
142. Gritti A, P Frolichsthal-Schoeller, R Galli, EA Parati, L Cova, SF Pagano, CR Bjornson, and AL Vescovi. Epidermal and fibroblast growth factors behave as mitogenic regulators for a single multipotent stem cell-like population from the subventricular region of the adult mouse forebrain. *The Journal of Neuroscience*. 1999; 19:3287-3297.
143. Bianchi G, A Banfi, M Mastrogiacomo, R Notaro, L Luzzatto, R Cancedda, and R Quarto. *Ex vivo* enrichment of mesenchymal cell progenitors by fibroblast growth factor 2. *Experimental Cell Research*. 2003; 287:98–105.
144. Wang L, L Li, P Menendez, C Cerdan, and M Bhatia. Human embryonic stem cells maintained in the absence of mouse embryonic & broblasts or conditioned media are capable of hematopoietic development. *Blood*. 2005; 105:4598–4603.
145. Yeoh JS, R van Os, E Weersing, A Ausema, B Dontje, E Vellenga, and G de Haan. Fibroblast growth factor-1 and -2 preserve long-term repopulating ability of hematopoietic stem cells in serum-free cultures. *Stem Cells*. 2006; 24:1564–1572.
146. Yeoh JS and G de Haan. Fibroblast growth factors as regulators of stem cell self-renewal and aging. *Mechanisms of Ageing and Development*. 2007; 128:17–24.
147. Boiret N, C Rapatel, S Boisgard, S Charrier, A Tchirkov, C Bresson, L Camilleri, J Berger, L Guillouard, JJ Guérin, P Pigeon, J Chassagne, and MG Berger. CD43⁺CDw90(Thy-1)⁺ subset colocalized with mesenchymal progenitors in human bone marrow hematon units is enriched in colony-forming unit megakaryocytes and long-term culture-initiating cells. *Experimental Hematology*. 2003; 31:1275-1283.
148. Stan Gronthos, E Graves, S Ohta, and PJ Simmons. The STRO-1⁺ fraction of adult human bone marrow contains the osteogenic precursors. *Blood*. 1994; 84:4164-4173.
149. Psaltis PJ, S Paton, F See, A Arthur, S Martin, S Itescu, SG Worthley, Stan Gronthos, and AC Zannettino. Enrichment for STRO-1 expression enhances the cardiovascular paracrine activity of human bone marrow-derived mesenchymal cell populations. *Journal of Cellular Physiology*. 2010; 223:530-540.

150. Colgan SP, HK Eltzschig HK, T Eckle T, and LF Thompson. Physiological roles for ecto-5'-nucleotidase (CD73). *Purinergic Signalling*. 2006; 2:351-360.
151. Airas L, J Niemelä, M Salmi, T Puurunen, DJ Smith, and S Jalkanen. Differential Regulation and Function of CD73, a Glycosyl-Phosphatidylinositol-linked 70-kD Adhesion Molecule, on Lymphocytes and Endothelial Cells. *The Journal of Cell Biology*. 1997; 136:421-431.
152. Stochaj U and HG Mannherz. Chicken gizzard 5'-nucleotidase functions as a binding protein for the laminin/nidogen complex. *European Journal of Cell Biology*. 1992; 59:364-372.
153. Friedenstein AJ, RK Chailakhjan, KS Lalykina. The development of fibroblast colonies in monolayer cultures of guinea-pig bone marrow and spleen cells. *Cell and Tissue Kinetics*. 1970; 3:393-403.
154. Enumeration, expansion, and differentiation of human mesenchymal stem cells using Mesencult[®], *StemCell Technologies technical manual*, catalog # 28453, 2007.
155. Nilsson SK, HM Johnston, JA Coverdale. Spatial localization of transplanted hemopoietic stem cells: inferences for the localization of stem cell niches. *Blood*. 2001; 97:2293–2299.
156. Benjamin J. Frisch, Rebecca L. Porter, and Laura M. Calvi. Hematopoietic niche and bone meet. *Current Opinion in Supportive and Palliative Care*. 2008; 2:211–217.
157. Olaia Naveiras, Valentina Nardi, Pamela L. Wenzel, Frederic Fahey, and George Q. Daley. Bone marrow adipocytes as negative regulators of the hematopoietic microenvironment. *Nature*. 2009; 460:259–263.
158. Nishikawa M, K Ozawa, A Tojo, T Yoshikubo, A Okano, K Tani, K Ikebuchi, H Nakauchi, S Asano. Changes in hematopoiesis-supporting ability of C3H10T1/2 mouse embryo fibroblasts during differentiation. *Blood*. 1993; 81:1184–1192.
159. Corre J, C Barreau, B Cousin, JP Chavoïn, D Caton, G Fournial, L Penicaud, L Casteilla, P Laharrague. Human subcutaneous adipose cells support complete differentiation but not self-renewal of hematopoietic progenitors. *Journal of Cellular Physiology*. 2006; 208:282–288.
160. Zhang Y, A Harada, H Bluethmann, JB Wang, S Nakao, N Mukaida, K Matsushima. Tumor necrosis factor (TNF) is a physiologic regulator of hematopoietic progenitor cells: increase of early hematopoietic progenitor cells in TNF receptor p55-deficient mice *in vivo* and potent inhibition of progenitor cell proliferation by TNF alpha *in vitro*. *Blood*. 1995; 86:2930–2937.

161. DiMascio L, C Voermans, M Uqoezwa, A Duncan, D Lu, J Wu, U Sankar, T Reya. Identification of adiponectin as a novel hemopoietic stem cell growth factor. *The Journal of Immunology*. 2007; 178:3511–3520.
162. Maryalice Stetler-Stevenson, Diane C. Arthur, Nicholas Jabbour, Xiu Y. Xie, Jeff Molldrem, A. John Barrett, David Venzon, and Margaret E. Rick. Diagnostic utility of flow cytometric Immunophenotyping in myelodysplastic syndrome. *Blood*. 2001; 98:979-987.
163. Michael R. Loken, Arjan van de Loosdrech, Kiyoyuki Ogata, Alberto Orfao, Denise A. Wells. Flow cytometry in myelodysplastic syndromes: Report from a working conference. *Leukemia Research*. 2008; 32:5–17.
164. Germing U, C Strupp, A Kundgen, D Bowen, C Aul, R Haas, N Gattermann. No increase in age-specific incidence of Myelodysplastic Syndromes. *Haematologica*. 2004; 89:905-910.
165. Passmore SJ, JM Chessells, H Kempiski, IM Hann, PA Brownbill, CA Stiller. Paediatric myelodysplastic syndromes and juvenile myelomonocytic leukaemia in the UK: a population-based study of incidence and survival. *British Journal of Haematology*. 2003; 121:758-767.
166. Jung SW, SY Lee, DW Jekarl, M Kim, J Lim, Y Kim, K Han, YJ Kim, SG Cho, J Song. Cytogenetic characteristics and prognosis analysis in 231 myelodysplastic syndrome patients from a single institution. *Leukemia Research*. 2010; [PubMed: 21146871].
167. Morel P, M Hebbbar, JL Lai, A Duhamel, C Preudhomme, E Wattel, F Bauters, P Fenaux. Cytogenetic analysis has strong independent prognostic value in de novo myelodysplastic syndromes and can be incorporated in a new scoring system: a report on 408 cases. *Leukemia*. 1993; 79:1315-1323.
168. Lopez-Villar O, JL Garcia, FM Sanchez-Guijo, C Robledo, EM Villaron, P Hernández-Campo, N Lopez-Holgado, M Diez-Campelo, MV Barbado, JA Perez-Simon, JM Hernández-Rivas, JF San-Miguel, MC del Cañizo. Both expanded and uncultured mesenchymal stem cells from MDS patients are genomically abnormal, showing a specific genetic profile for the 5q- syndrome. *Leukemia*. 2009; 23:664-672.
169. Philip Nivatpumin and Steven D. Gore, IV. Molecular Biology of Myelodysplasia, In HJ Deeg, DT Bowen, SD Gore, T Haferlach, MM Le Beau, C. Niemeyer, Hematologic Malignancies: Myelodysplastic Syndromes, eds., Springer Berlin Heidelberg 2006.
170. Suneel D. Mundle, Lingering biologic dilemmas about the status of the progenitor cells in myelodysplasia. *Archives of Medical Research*. 2003; 34:515-519.

171. R Tiu, L Gondek, C O'Keefe, J P Maciejewski. Clonality of the stem cell compartment during evolution of myelodysplastic syndromes and other bone marrow failure syndromes. *Leukemia*. 2007; 21:1648-1657.
172. E.D. Warlick and B.D. Smith. Myelodysplastic Syndromes: Review of Pathophysiology and Current Novel Treatment Approaches. *Current Cancer Drug Targets*. 2007; 7:541-558.
173. Yin SN, RB Hayes, MS Linet, GL Li, M Dosemeci, LB Travis, CY Li, ZN Zhang, DG Li, WH Chow, S Wacholder, YZ Wang, ZL Jiang, TR Dai, WY Zhang, WJ Chao, PZ Ye, QR Kou, XC Zhang, XF Lin, JF Meng, CY Ding, JS Zho, WJ Blot. A cohort study of cancer among benzene-exposed workers in China: overall results. *American Journal of Industrial Medicine*. 1996; 29:227-235.
174. West RR, DA Stafford, A Farrow, A Jacobs. Occupational and environmental exposures and myelodysplasia: a case-control study. *Leukemia Research*. 1995; 19:127-139.
175. Eva Hellström-Lindberg and Luca Malcovati. Supportive care, growth factors, and new therapies in myelodysplastic syndromes. *Blood Reviews*. 2008; 22:75-91.
176. Nisse C, C Lorthois, V Dorp, E Eloy, J M Haguenoer, P Fenaux. Exposure to occupational and environmental factors in myelodysplastic syndromes. Preliminary results of a case-control study. *Leukemia*. 1995; 9:693-699.
177. West RR, DA Stafford, AD White, DT Bowen, RA Padura. Cytogenetic abnormalities in the myelodysplastic syndromes and occupational or environmental exposure. *Blood*. 2000; 95:2093-2097.
178. William C. Moloney. Radiogenic leukemia revisited. *Blood*. 1987; 70:905-908.
179. Pedersen-Bjergaard J, P Philip, SO Larsen, M Andersson, G Daugaard, J Ersboll, SW Hansen, K. Hou-Jensen, D Nielsen, TC Sigsgaard. Therapy-related myelodysplasia and acute myeloid leukemia. Cytogenetic characteristics of 115 consecutive cases and risk in seven cohorts of patients treated intensively for malignant diseases in the Copenhagen series. *Leukemia*. 1993; 7:1975-1986.
180. Pasqualetti P, V Festuccia, P Acitelli, A Collacciani, A Giusti, R Casale. Tobacco smoking and risk of haematological malignancies in adults: a case-control study. *British Journal of Haematology*. 1997; 97:659-662.
181. Ido M, C Nagata, N Kawakami, H Shimizu, Y Yoshida, T Nomura, H Mizoguchi. A case-control study of myelodysplastic syndromes among Japanese men and women. *Leukemia Research*. 1996; 20:727-731.
182. Suneel D. Mundle, K Allampallam, RK Aftab, B Dangerfield, J Cartlidge, D Zeitler, E Afenya, S Alvi, V Shetty, P Venugopal, A Raza. Presence of activation-related m-RNA for

EBV and CMV in the bone marrow of patients with myelodysplastic syndromes. *Cancer Letters*. 2001; 164:197-205.

183. Dalamaga M, E Petridou, FE Cook, D Trichopoulos. Risk factors for myelodysplastic syndromes: a case-control study in Greece. *Cancer Causes Control*. 2002; 13:603-608.

184. Frederica P. Perera. Environment and cancer: who are susceptible? *Science*. 1997; 278:1068-1073.

185. Rothman N, MT Smith, RB Hayes, RD Traver, B Hoener, S Campleman, GL Li, M Dosemeci, M Linet, L Zhang, L Xi, S Wacholder, W Lu, KB Meyer, N Titenko-Holland, JT Stewart, S Yin, D Ross. Benzene poisoning, a risk factor for hematological malignancy, is associated with the NQ01 ⁶⁰⁹C→T mutation and rapid fractional excretion of chlorzoxazone. *Cancer Research*. 1997; 57:2839-2842.

186. Larson RA, Y Wang, M Banerjee, J Wiemels, C Hartford, MM Le Beau, MT Smith. Prevalence of the inactivating ⁶⁰⁹C→T polymorphism in the NAD(P)H: quinine oxidoreductase (NQ01) gene in patients with primary and therapy-related myeloid leukemias. *Blood*. 1999; 94:803-807.

187. Chen H, DP Sandler, JA Taylor, DL Shore, E Liu, CD Bloomfield, DA Bell. Increased risk for myelodysplastic syndromes in individuals with glutathione transferase theta 1 (GSTT1) gene defect. *Lancet*. 1996; 347:295-297.

188. Preudhomme C, C Nisse, M Hebbar, M Vanrumbeke, A Brizard, JL Lai, P Fenaux. Glutathione S transferase theta 1 gene defects in myelodysplastic syndromes and their correlation with karyotype and exposure to potential carcinogens. *Leukemia*. 1997; 11:1580-1582.

189. Atoyebi W, R Kusec, C Fidler, TE Peto, J Boultonwood, JS Wainscoat. Glutathione S-transferase gene deletions in myelodysplasia. *Lancet*. 1997; 349:1450-1451.

190. Boudard D, A Viallet, S Piselli, D Guyotat, L Campos. *In vitro* study of stromal cell defects in myelodysplastic syndromes. *Haematologica*. 2003; 88:827-829.

191. Hatfill SJ, ED Fester, JG Steyler. Apoptotic megakaryocyte dysplasia in myelodysplastic syndrome. *Hematologic pathology*. 1993; 8:87-93.

192. Clark DM, I Lampert. Apoptosis is a common histopathological finding in myelodysplasia; The correlate of ineffective hematopoiesis. *Leukemia Lymphoma*. 1990; 2:415-418.

193. Jane E. Parker, Ghulam J. Mufti, Feyrooz Rasool, Aleksandar Mijovic, Stephen Devereux, and Antonio Pagliuca. The role of apoptosis, proliferation, and the Bcl-2-related proteins in the myelodysplastic syndromes and acute myeloid leukemia secondary to MDS. *Blood*. 2000; 96:3932-3938.

194. Boudard D, C Vasselon, MF Berthéas, J Jaubert, C Mounier, J Reynaud, A Viallet, S Chautard, D Guyotat, L Campos. Expression and prognostic significance of Bcl-2 family proteins in myelodysplastic syndromes. *American Journal of Hematology*. 2002; 70:115-125.
195. Kurotaki H, Y Tsushima, K Nagai, S Yagihashi. Apoptosis, bcl-2 expression and p53 accumulation in myelodysplastic syndrome, myelodysplastic-syndrome-derived acute myelogenous leukemia and de novo acute myelogenous leukemia, *Acta Haematologica*. 2000; 102:115-123.
196. Ribeiro E, CS Lima, K Metze, I Lorand-Metze. Flow cytometric analysis of the expression of Fas/FasL in bone marrow CD34⁺ cells in myelodysplastic syndromes: relation to disease progression. *Leukemia Lymphoma*. 2004; 45:309-313.
197. Gersuk GM, C Beckham, MR Loken, P Kiener, JE Anderson, A Farrand, AB Troutt, JA Ledbetter, HJ Deeg. A role for tumour necrosis factor-alpha, Fas and Fas-Ligand in marrow failure associated with myelodysplastic syndrome. *British Journal of Haematology*. 1998; 103:176-188.
198. Zhang Z, J Xie. Expression of Fas, FasL and Bcl-2 and apoptosis of bone marrow CD34⁺ cells in patients with myelodysplastic syndrome. *Zhongguo Shi Yan Xue Ye Xue Za Zhi*. 2003; 11:274-277.
199. Bouscary D, YL Chen, M Guesnu, F Picard, F Viguiet, C Lacombe, F Dreyfus, M Fontenay-Roupie. Activity of the caspase-3/ CPP32 enzyme is increased in "early stage" myelodysplastic syndromes with excessive apoptosis, but caspase inhibition does not enhance colony formation *in vitro*. *Experimental Hematology*. 2000; 28:784-791.
200. Boudard D, O Sordet, C Vasselon, V Revol, MF Berthéas, D Freyssenet, A Viallet, S Piselli, D Guyotat, L Campos. Expression and activity of caspases 1 and 3 in myelodysplastic syndromes. *Leukemia*. 2000; 14:2045-2051.
201. Raza A, S Mundle, V Shetty, S Alvi, H Chopra, L Span, A Parcharidou, S Dar, P Venugopal, R Borok, S Gezer, J Showel, J Loew, E Robin, S Rifkin, D Alston, B Hernandez, R Shah, H Kaizer, S Gregory. Novel insights into the biology of myelodysplastic syndromes: excessive apoptosis and the role of cytokines. *International journal of hematology*. 1996; 63:265-278.
202. Kitagawa M, I Saito, T Kuwata, S Yoshida, S Yamaguchi, M Takahashi, T Tanizawa, R Kamiyama, K Hirokawa. Overexpression of tumor necrosis factor (TNF)-alpha and interferon (IFN)-gamma by bone marrow cells from patients with myelodysplastic syndromes. *Leukemia*. 1997; 11:2049-2054.

203. Deeg HJ, C Beckham, MR Loken, E Bryant, M Lesnikova, HM Shulman, T Gooley. Negative regulators of hemopoiesis and stroma function in patients with Myelodysplastic syndrome. *Leukemia Lymphoma*. 2000; 37:405-414.
204. Verhoef GE, P De Schouwer, JL Ceuppens, J Van Damme, W Goossens, MA Boogaerts. Measurement of serum cytokines levels in patients with myelodysplastic syndromes. *Leukemia*. 1992; 2:1268-1272.
205. Peddie CM, CR Wolf, LI Mclellan, AR Collins, DT Bowen. Oxidative DNA damage in CD34⁺ myelodysplastic cells is associated with intracellular redox changes and elevated plasma tumour necrosis factor- α concentration. *British Journal of Haematology*. 1997; 99:625-631.
206. Ganser A, OG Ottmann, G Seipelt, A Lindemann, U Hess, G Geissler, A Maurer, J Frisch, G Schulz, R Mertelsmann, D Hoelzer. Effect of long-term treatment with recombinant human interleukin-3 in patients with myelodysplastic syndromes. *Leukemia*. 1993; 7:696-701.
207. Suneel D. Mundle, P Venugopal, JD Cartlidge, DV Pandav, L Broady-Robinson, S Gezer, EL Robin, SR Rifkin, M Klein, DE Alston, BM Hernandez, D Rosi, S Alvi, VT Shetty, SA Gregory, A Raza. Indication of an involvement of interleukin-1 converting enzyme-like protease in intramedullary apoptotic cell death in the bone marrow of patients with myelodysplastic syndromes. *Blood*. 1996; 88:2640-2647.
208. Aizawa S, M Hiramoto, H Hoshi, K Toyama, D Shima, H Handa. Establishment of stromal cell line from an MDS RA patient which induced an apoptotic change in hematopoietic and leukemic cells *in vitro*. *Experimental Hematology*. 2000; 28:148-155.
209. Suneel D. Mundle, S Reza, A Ali, Y Mativi, V Shetty, P Venugopal, SA Gregory, A Raza. Correlation of tumor necrosis factor alpha (TNF alpha) with high Caspase 3-like activity in myelodysplastic syndromes. *Cancer Letters*. 1999; 140:201-207.
210. Arimura K, N Arima, K Matsushita, H Ohtsubo, H Fujiwara, T Kukita, A Ozaki, T Hagiwara, H Hamada, K Yoshino, C Tei. Matrix metalloproteinase inhibitor reduces apoptosis induction of bone marrow cells in MDS-RA. *European Journal of Haematology*. 2004; 73:17-24.
211. Tamara Keith, Yuko Araki, Masaki Ohyagi, Maki Hasegawa, Kouhei Yamamoto, Morito Kurata, Yasunori Nakagawa, Kenshi Suzuki, Masanobu Kitagawa. Regulation of angiogenesis in the bone marrow of myelodysplastic syndromes transforming to overt leukaemia. *British Journal of Haematology*. 2007; 137:206-215.
212. Alexandrakis MG, FH Passam, CA Pappa, J Damilakis, G Tsirakis, E Kandidaki, AM Passam, EN Stathopoulos, DS Kyriakou. Serum evaluation of angiogenic cytokine basic fibroblast growth factor, hepatocyte growth factor and TNF- α in patients with

- myelodysplastic syndromes: correlation with bone marrow microvascular density. *International journal of immunopathology and pharmacology*. 2005; 18:287-295.
213. Alvaro Aguayo, Hagop Kantarjian, Taghi Manshour, Cristi Gidel, Elihu Estey, Deborah Thomas, Charles Koller, Zeev Estrov, Susan O'Brien, Michael Keating, Emil Freireich, and Maher Albitar. Angiogenesis in acute and chronic leukemias and myelodysplastic syndromes. *Blood*. 2000; 96:2240-2245.
214. Albitar M. Angiogenesis in acute myeloid leukemia and myelodysplastic syndrome. *Acta Haematologica*. 2001; 106:170-176.
215. Verstovsek S, S Lunin, H Kantarjian, T Manshour, S Faderl, J Cortes, F Giles, M Albitar. Clinical relevance of VEGF receptors 1 and 2 in patients with chronic myelogenous leukemia. *Leukemia Research*. 2003; 27:661-669.
216. Dias S, M Choy, K Alitalo, S Rafii. Vascular endothelial growth factor (VEGF)-C signaling through FLT-4 (VEGFR-3) mediates leukemic cell proliferation, survival, and resistance to chemotherapy. *Blood*. 2002; 99:2179-2184.
217. Hamblin TJ. Immunological abnormalities in Myelodysplastic syndromes. *Seminars in hematology*. 1996; 33:150-162.
218. Culligan DJ, P Cachia, J Whittaker, A Jacobs, RA Padua. Clonal lymphocytes are detectable in only some cases of MDS. *British Journal of Haematology*. 1992; 81:346-352.
219. Young NS, J Maciejewski. The pathophysiology of acquired aplastic anemia. *The New England journal of medicine*. 1997; 336:1365-1372.
220. Barrett AJ, Y Saunthararajah, J Molldrem. Myelodysplastic syndrome and aplastic anemia; distinct entities or diseases linked by a common pathophysiology? *Seminars in hematology*. 2000; 37:15-29.
221. Smith MA, JG Smith. The occurrence subtype and significance of hematopoietic inhibitory T cells (HIT cells) in myelodysplasia: an *in vitro* study. *Leukemia Research*. 1991; 5:597-601.
222. Molldrem JJ, YZ Jiang, MA Stetler-Stevenson, D Mavroudis, N Hensel, AJ Barrett. Haematological response of patients with myelodysplastic syndrome to antithymocyte globulin is associated with a loss of lymphocytemediated inhibition of CFU-GM and alterations in T cell receptor V beta profiles. *British Journal of Haematology*. 1998; 102:1314-1322.
223. Sugarawa T, K Endo, T Shishido, A Sato, J Kameoka, O Fukuhara, K Yoshinaga, A Miura. T-cell mediated inhibition of erythropoiesis in myelodysplastic syndromes. *American Journal of Hematology*. 1992; 41:304-305.

224. Mark B. Meads, Lori A. Hazlehurst and William S. Dalton. The Bone Marrow Microenvironment as a Tumor Sanctuary and Contributor to Drug Resistance. *Clinical Cancer Research*. 2008; 14:2519-2526.
225. Oshita F, Y Kameda, N Hamanaka, H Saito, K Yamada, K Noda, A Mitsuda. High expression of integrin $\beta 1$ and p53 is a greater poor prognostic factor than clinical stage in small-cell lung cancer. *American journal of clinical oncology*. 2004; 27:215-219.
226. Yao ES, H Zhang, YY Chen, et al. Increased h1 integrin is associated with decreased survival in invasive breast cancer. *Cancer Research*. 2007; 67:659-64.
227. Beyer V, C Castagné, D Mühlematter, V Parlier, J Gmür, U Hess, T Kovacsovics, S Meyer-Monard, A Tichelli, A Tobler, E Jacky, U Schanz, M Bargetzi, A Hagemeyer, T de Witte, G van Melle, M Jotterand. Systematic screening at diagnosis of -5/del(5)(q31), -7, or chromosome 8 aneuploidy by interphase fluorescence in situ hybridization in 110 acute myelocytic leukemia and high-risk myelodysplastic syndrome patients: concordances and discrepancies with conventional cytogenetics. *Cancer genetics and cytogenetics*. 2004; 152:29-41.
228. Romeo M, ML Chauffaille, MR Silva, DM Bahia, J Kerbauy. Comparison of cytogenetics with FISH in 40 myelodysplastic syndrome patients. *Leukemia Research*. 2002; 26:993-996.
229. Hideki Makishima, Manjot Rataul, Lukasz P Gondek, Jungwon Huh, James R Cook, Karl S Theil, Mikkael A Sekeres, Elizabeth Kuczkowski, Christine O'Keefe and Jaroslaw P Maciejewski. FISH and SNP-A karyotyping in myelodysplastic syndromes: Improving cytogenetic detection of del(5q), monosomy 7, del(7q), trisomy 8 and del(20q). *Leukemia research*. 2009; 34:447-453.
230. Olga Blau, Claudia Dorothea Baldus, Wolf-Karsten Hofmann, Gundula Thiel, Florian Nolte, Thomas Burmeister, Seval Türkmen, Ouidad Benlasfer, Elke Schumann, Annette Sindram, Mara Molquentin, Stefan Mundlos, Ulrich Keilholz, Eckhard Thiel, Igor Wolfgang Blau. Mesenchymal stromal cells of myelodysplastic syndrome and acute myeloid leukemia patients have distinct genetic abnormalities compared with leukemic blasts. *Blood*. 2011; 118:5583-5592.
231. Padua RA, BA Guinn, AI Al-Sabah, M Smith, C Taylor, T Pettersson, S Ridge, G Carter, D White, D Oscier, S Chevret, R West. RAS, FMS and p53 mutations and poor clinical outcome in myelodysplasias: a 10-year follow-up. *Leukemia*. 1998; 12:887-892.
232. Shih LY, TL Lin, PN Wang, JH Wu, P Dunn, MC Kuo, CF Huang. Internal tandem duplication of fms-like tyrosine kinase 3 is associated with poor outcome in patients with Myelodysplastic syndrome. *Cancer*. 2004; 101:989-998.

233. Timothy Graubert and Matthew J. Walter. Genetics of Myelodysplastic Syndromes: New Insights. *Hematology*. 2011;543-549.
234. Jean-Loup Huret. Atlas of Genetics and Cytogenetics in Oncology and Haematology. 2011; ISSN 1768-3262.
235. Malcovati L, Della Porta MG, Pietra D, Boveri E, Pellagatti A, Galli A, Travaglino E, Brisci A, Rumi E, Passamonti F, Invernizzi R, Cremonesi L, Boulwood J, Wainscoat JS, Hellström-Lindberg E, Cazzola M. Molecular and clinical features of refractory anemia with ringed sideroblasts associated with marked thrombocytosis. *Blood*. 2009; 114:3538-45.
236. Mario Cazzola, Luca Malcovati, and Rosangela Invernizzi. Myelodysplastic/Myeloproliferative Neoplasms. *Hematology*. 2011; 264-272.
237. Mrinal M. Patnaik, Terra L. Lasho, Janice M. Hodnefield, Ryan A. Knudson, Rhett P. Ketterling, Guillermo Garcia-Manero, David P. Steensma, Animesh Pardanani, Curtis A. Hanson and Ayalew Tefferi, SF3B1 mutations are prevalent in myelodysplastic syndromes with ring sideroblasts but do not hold independent prognostic value. *Blood*. 2011; doi: 10.1182/blood-2011-09-377994.
238. Toshiki Uchida, Tomohiro Kinoshita, Hirokazu Nagai, Yohsuke Nakahara, Hidehiko Saito, Tomomitsu Hotta, and Takashi Murate. Hypermethylation of the p15^{INK4b} gene in myelodysplastic syndromes. *Blood*. 1997; 90:1403-1409.
239. Bruno Quesnel, Gaelle Guillerm, Rodolphe Vereecque, Eric Wattel, Claude Preudhomme, Francis Bauters, Michael Vanrumbeke, and Pierre Fenaux. Methylation of the p15^{INK4b} gene in Myelodysplastic syndromes is frequent and acquired during disease progression. *Blood*. 1998; 91:2985-2990.
240. Jaffe ES, NL Harris, H Stein, JW Vardiman. Eds. World Health Organization Classification of Tumours: pathology and genetics of tumours of haematopoietic and lymphoid tissues. 2001, IARC Press, Lyon.
241. James W. Vardiman, Jürgen Thiele, Daniel A. Arber, Richard D. Brunning, Michael J. Borowitz, Anna Porwit, Nancy Lee Harris, Michelle M. Le Beau, Eva Hellström-Lindberg, Ayalew Tefferi, and Clara D. Bloomfield. The 2008 revision of the World Health Organization (WHO) classification of myeloid neoplasms and acute leukemia: rationale and important changes. *Blood*. 2009; 114:937-951.
242. Jean Feuillard, Valérie Andrieu, Franck Trimoreau. Comment diagnostiquer les syndromes myélodysplasiques? Cytologie et Cytométrie en flux. In Pierre Fenaux, Lyonel Adès, François Dreyfus, Les syndromes myélodysplasiques de l'adulte. John Libbey Eurotext. 2011.

243. Alan F, Avery A. Sanfberg, and Donald C. Doll. Myelodysplastic Syndromes. In John P. Greer, John Foerster, George M. Rodgers, Frixos Paraskevas, Bertil Glader, Daniel A. Arber, Robert T. Means. *Wintrobe's Clinical Hematology*, Lippincott Williams & Wilkins. 2003.
244. Su Hao Lo. Focal adhesions: what's new inside. *Developmental Biology*. 2006; 294:280-291.
245. Satyajit K. Mitra, Daniel A. Hanson, David D. Schlaepfer. Focal adhesion kinase: in command and control of cell motility. *Nature Reviews Molecular Cell Biology*. 2005; 6:56-68.
246. Adi Dubash , MM Menold, T Samson, R García-Mata, E Boulter, R Doughman, K Burridge. Focal Adhesions: New angles on an old structure. *International Reviews in Cell and Molecular Biology*. 2009; 277:1-65.
247. Hynes RO. Integrins: bidirectional, allosteric signaling machines. *Cell*. 2002;110; 673–687.
248. Borowska K, B Jedrych, K Czerny, S Zabielski. The role of integrins in the physiologic and pathogenic processes. *Pol Merkur Lekarski*. 2006; 21:362-366.
249. Humphries JD, A Byron, MJ Humphries. Integrin ligands at a glance. *Journal of Cell Science*. 2006; 119:3901–3903.
250. Akiyama SK. Integrins in cell adhesion and signaling. *Human Cell*. 1996; 9:181-186.
251. Coulombel L, I Auffray, MH Gaugler, M Roseblatt. Expression and function of integrins on hematopoietic progenitor cells. *Acta Haematologica*. 1997; 97:13-21.
252. Golubovskaya V and W Cance. Focal adhesion kinase signaling cancer. *International Review of Cytology*. 2007; 263:103-153.
253. Donna J Webb, K Donais, LA Whitmore, SM Thomas, CE Turner, JT Parsons, AF Horwitz. FAK-Src signalling through paxillin, ERK and MLCK regulates adhesion disassembly. *Nature Cell Biology*. 2004; 6:154-161.
254. Geraldine M. O'Neill, Sarah J. Fashena, Erica A. Golemis. Integrin signalling: a new Cas(t) of characters enters the stage. *Trends in Cell Biology*. 2000; 10:111-119.
255. Dong JM, LS Lau, YW Ng, L Lim, E Manser. Paxillin nuclear-cytoplasmic localization is regulated by phosphorylation of the LD4 motif: evidence that nuclear paxillin promotes cell proliferation. *Biochemical Journal*. 2009; 418:173–184.
256. Ilić D, Y Furuta, S Kanazawa, N Takeda, K Sobue, N Nakatsuji, S Nomura, J Fujimoto, M Okada, T Yamamoto. Reduced cell motility and enhanced focal adhesion contact formation in cells from FAK-deficient mice. *Nature*. 1995; 12:539-544.

257. Yeo MG, MA Partridge, EJ Ezratty, Q Shen, GG Gundersen, and EE Marcantonio. Src SH2 arginine 175 is required for cell motility: Specific focal adhesion kinase targeting and focal adhesion assembly function. *Molecular and Cellular Biology*. 2006; 26:4399–4409.
258. Tamura M, J Gu, K Matsumoto, S Aota, R Parsons, and KM Yamada. Inhibition of cell migration, spreading, and focal adhesions by tumor suppressor PTEN. *Science*. 1998; 280:1614–1617.
259. McLean GW, NO Carragher, E Avizienyte, J Evans, VG Brunton, and MC Frame. The role of focal-adhesion kinase in cancer. A new therapeutic opportunity. *Nature Reviews Cancer*. 2005; 5:505-515.
260. Hsia DA, SK Mitra, CR Hauck, DN Streblov, JA Nelson, D Ilic, S Huang, E Li, GR Nemerow, J Leng, KS Spencer, DA Cheresh, DD Schlaepfer. Differential regulation of cell motility and invasion by FAK. *The Journal of cell biology*. 2003; 160:753-767.
261. Hauck CR, DA Hsia, DD Schlaepfer. The focal adhesion kinase - a regulator of cell migration and invasion. *IUBMB Life*. 2002; 53:115-119.
262. Frisch SM, K Vuori, E Ruoslahti, and PY Chan-Hui. Control of adhesion-dependent cell survival by focal adhesion kinase. *Journal of Cell Biology*. 1996; 134:793–799.
263. Sonoda Y, Y Matsumoto, M Funakoshi, D Yamamoto, SK Hanks, and T Kasahara. Anti-apoptotic role of focal adhesion kinase (FAK). Induction of inhibitor-of apoptosis proteins and apoptosis suppression by the overexpression of FAK in a human leukemic cell line, HL-60. *The Journal of Biological Chemistry*. 2000; 275:16309–16315.
264. McLean WG, Noboru H Komiyama, Bryan Serrels, Hideo Asano, Louise Reynolds, Francesco Conti, Kairbaan Hodivala-Dilke, Daniel Metzger, Pierre Chambon, Seth GN Grant, Margaret C Frame. Specific deletion of focal adhesion kinase suppresses tumor formation and blocks malignant progression. *Genes & Development*. 2004:2998-3003.
265. Ssang-Taek Lim, David Mikolon, Dwayne G. Stupack, and David D. Schlaepfer. FERM Control of FAK Function: Implications for Cancer Therapy. *Cell Cycle*. 2008; 7:2306–2314.
266. Schwock J, Neesha Dhani, Mary Ping-Jiang Cao, Jinzi Zheng, Richard Clarkson, Nikolina Radulovich, Roya Navab, Lars-Christian Horn, David W Hedley. Targeting Focal Adhesion Kinase with Dominant-Negative FRNK or Hsp90 Inhibitor 17-DMAG Suppresses Tumor Growth and Metastasis of SiHa Cervical Xenografts. *Cancer Research*. 2009; 69:4750-4759.
267. Liu X, Z Yan, L Huang, M Guo, Z Zhang, C Guo. Cell surface heat shock protein 90 modulates prostate cancer cell adhesion and invasion through the integrin- β 1/focal adhesion kinase/c-Src signaling pathway. *Oncology Reports*. 2011; 25:1343-1351.

268. Ochel HJ and G Gademann. Heat-shock protein 90: potential involvement in the pathogenesis of malignancy and pharmacological intervention. *Onkologie*. 2002; 25:466-473.
269. Le Boeuf F, François Houle, Jacques Huot. Regulation of Vascular Endothelial Growth Factor Receptor 2-mediated phosphorylation of Focal Adhesion Kinase by Heat Shock Protein 90 and Src Kinase activities. *The Journal of Biological Chemistry*. 2004; 279:39175-39185.
270. MJ van Nimwegen, M Huigsloot, A Camier, I B Tijdens, B van de Water. Focal adhesion kinase and protein kinase B cooperate to suppress doxorubicin-induced apoptosis of breast tumor cells. *Molecular Pharmacology*. 2006; 70:1330-1339.
271. Takahashi N, Y Seko, E Noiri, K Tobe, T Kadowaki, H Sabe, and Y Yazaki. Vascular endothelial growth factor induces activation and subcellular translocation of focal adhesion kinase (p125FAK) in cultured rat cardiac myocytes. *Circulation Research*. 1999; 84:1194–1202.
272. Mitra SK and DD Schlaepfer. Integrin-regulated FAK-Src signaling in normal and cancer cells. *Current Opinion in Cell Biology*. 2006; 18:516–523.
273. Mitra SK, D Mikolon, JE Molina, DA Hsia, DA Hanson, A Chi, ST Lim, JA Bernard-Trifilo, D Ilic, DG Stupack, DA Cheresch, and DD Schlaepfer. Intrinsic FAK activity and Y925 phosphorylation facilitate an angiogenic switch in tumors. *Oncogene*. 2006; 25:5969–5984.
274. Weiner TM, ET Liu, RJ Craven, and WG Cance. Expression of focal adhesion kinase gene and invasive cancer. *Lancet*. 1993; 342:1024–1025.
275. Quintanilla M, K Brown, M Ramsden, and A Balmain. Carcinogen-specific mutation and amplification of Ha-ras during mouse skin carcinogenesis. *Nature*. 1986; 322:78–80.
276. Sorina Grisar-Granovsky, Zaidoun Salah, Myriam Maoz, Diana Pruss, Uziel Beller, Rachel Bar-Shavit. Differential expression of Protease activated receptor 1 (Par1) and pY397FAK in benign and malignant human ovarian tissue samples. *International Journal of Cancer*. 2005; 113:372–378.
277. Moon HS, WI Park, EA Choi, HW Chung, and CS Kim. The expression and tyrosine phosphorylation of E-cadherin/catenin adhesion complex, and focal adhesion kinase in invasive cervical carcinomas. *International Journal of Gynecological Cancer*. 2003; 13:640–646.
278. Aronsohn MS, HM Brown, G Hauptman, and LJ Kornberg. Expression of focal adhesion kinase and phosphorylated focal adhesion kinase in squamous cell carcinoma of the larynx. *Laryngoscope*. 2003; 113:1944–1948.

279. Christian Recher, Loic Ysebaert, Odile Beyne-Rauzy, Veronique Mansat-De Mas, Jean-Bernard Ruidavets, Pascal Cariven, Cecile Demur, Bernard Payrastra, Guy Laurent, and Claire Racaud-Sultan. Expression of Focal Adhesion Kinase in Acute Myeloid Leukemia Is Associated with Enhanced Blast Migration, Increased Cellularity, and Poor Prognosis. *Cancer Research*. 2004; 64:3191–3197.
280. Campos L, F Solly, C Aanei, P Flandrin, D Guyotat. HSP90 is overexpressed in high-risk myelodysplastic syndromes and associated with higher expression and activation of FAK. *Leukemia Research*. 2009; 33:S45.
281. Egle Avizienyte, Anne W. Wyke, Robert J. Jones, Gordon W. McLean, M. Andrew Westhoff, Valerie G. Brunton, and Margaret C. Frame. Src-induced de-regulation of E-cadherin in colon cancer cells requires integrin signalling. *Nature Cell Biology*. 2002; 4:632-638.
282. Brian P. Eliceiri, Xose S. Puente, John D. Hood, Dwayne G. Stupack, David D. Schlaepfer, Xiaozhu Z. Huang, Dean Sheppard, and David A. Cheresch. Src-mediated coupling of focal adhesion kinase to integrin $\alpha\beta 5$ in vascular endothelial growth factor signaling. *The Journal of Cell Biology*. 2002; 157:149-160.
283. Avizienyte E, VJ Fincham, VG Brunton, and MC Frame. Src SH3/2 domain-mediated peripheral accumulation of Src and phospho-myosin is linked to deregulation of E-cadherin and the epithelial–mesenchymal transition. *Molecular Biology of the Cell*. 2004; 15:2794–2803.
284. Schlaepfer DD, CR Hauck, DJ Sieg. Signaling through focal adhesion kinase. *Progress in Biophysics and Molecular Biology*. 1999; 71:435–478.
285. Schoch C, J Chistodoulou, W Hiddemann, and T Haferlach. A distinct pattern of gained and lost chromosomal regions emerges in acute myeloid leukemia (AML) with complex aberrant karyotype: a study on 41 patients analyzed with 24 color FISH and comparative genomic hybridization (CGH). *Blood*. 2002; 100:308a.
286. Liesveld JL, JF Dispersio, CN Abboud. Integrins and adhesive receptors in normal and leukemic CD34⁺ progenitors cells potential regulatory checkpoints for cellular traffic. *Leukemia Lymphoma*. 1994; 14:19–28.
287. Zhang XF, JF Wang, E Matczak, JA Proper, JE Gropman. Janus kinase 2 is involved in stromal cell-derived factor-1 α -induced tyrosine phosphorylation of focal adhesion proteins and migration of hematopoietic progenitor cells. *Blood*. 2001; 97:3342–3348.
288. Akagi T, K Murata, T Shishido, H Hanafusa. v-Crk activates the phosphoinositide 3-kinase/AKT pathway by utilizing focal adhesion kinase and H-Ras. *Molecular and Cellular Biology*. 2002; 22:7015–7023.

289. Takahira H, A Gotoh, A Ritchie, HE Broxmeyer. Steel factor enhances integrin mediated tyrosine phosphorylation of focal adhesion kinase (pp125FAK) and paxillin. *Blood*. 1997; 89:1574–1584.
290. Eok-Soo Oh, Haihua Gu, Tracy M. Saxton, John F. Timms, Sharon Hausdorff, Ernst U. Frevert, Barbara B. Kahn, Tony Pawson, Benjamin G. Neel, and Sheila M. Thomas¹. Regulation of Early Events in Integrin Signaling by Protein Tyrosine Phosphatase SHP-2. *Molecular and Cellular Biology*. 1999; 4:3205-3215.
291. Gautam A, ZR Li, G Bepler. RRM1-induced metastasis suppression through PTEN regulated pathways. *Oncogene*. 2003; 22:2135–2142.
292. Emmanuelle Tavernier-Tardy, Jérôme Cornillon, Lydia Campos, Pascale Flandrin, Amélie Duval, Nathalie Nadal, Denis Guyotat. Prognostic value of CXCR4 and FAK expression in acute myelogenous leukemia. *Leukemia Research*. 2009; 33:764–768.
293. Lindquist S and Craig EA. The heat-shock proteins. *Annual Reviews of Genetics*. 1998; 22:631-677.
294. Goetz MP, DO Toft, MM Ames, and C Erlichman. The Hsp90 chaperone complex as a novel target for cancer therapy. *Annals of Oncology*. 2003; 14:1169–1176.
295. Schneider C, L Sepp-Lorenzino, E Nimmesgern, O Ouerfelli, S Danishefsky, N Rosen, FU Hartl. Pharmacologic shifting of a balance between protein refolding and degradation mediated by Hsp90. *Proceedings of the National Academy of Sciences of the United States of America*. 1996; 93:14536-14541.
296. Jackson SE, C Queitsch, D Toft. HSP90: from structure to phenotype. *Nature Structural & Molecular Biology*. 2004; 11:1152-1155.
297. Kamal A, L Thao, J Sensintaffar, L Zhang, M Boehm, L Fritz, F Burrows. A high-affinity conformation of Hsp90 confers tumour selectivity on Hsp90 inhibitors. *Nature*. 2003; 425:407-410.
298. Minami Y, Y Kimura, H Kawasaki, K Suzuki, and I Yahara. The carboxy-terminal region of mammalian hsp90 is required for its dimerization and function *in vivo*. *Molecular and Cellular Biology*. 1994; 14:1459-1464.
299. Banerji U. Heat shock protein 90 as a drug target: some like it hot. *Clinical Cancer Research*. 2009; 15:9-14.
300. Flandrin P, D Guyotat, A Duval, J Cornillon, E Tavernier, N Nadal, L Campos. Significance of heat-shock protein (HSP) 90 expressions in acute myeloid leukemia cells. *Cell Stress and Chaperones*. 2008; 13:357-364.

301. Amélie Duval, Daniela Olaru, Lydia Campos, Pascale Flandrin, Nathalie Nadal, Denis Guyotat. Expression and prognostic significance of heat-shock proteins in myelodysplastic syndromes. *Haematologica*. 2006; 91:713-714.
302. Coutinho LH, CG Geary, J Chang, C Harrison, NG Testa. Functional studies of bone marrow haemopoietic and stromal cells in the myelodysplastic syndrome (MDS). *British Journal of Haematology*. 1990; 75:16-25.
303. Tennant GB, V Walsh, LN Truran, P Edwards, KI Mills, AK Burnett. Abnormalities of adherent layers grown from bone marrow of patients with myelodysplasia. *British Journal of Haematology*. 2000; 111:853-862.
304. Tauro S, MD Hepburn, DT Bowen, and MJ Pippard . Assessment of stromal function, and its potential contribution to deregulation of hematopoiesis in the myelodysplastic syndromes. *Haematologica*. 2001; 86:1038-1045.
305. Eugenia Flores-Figueroa, Rosa Maria Arana-Trejo, Guillermo Gutiérrez-Espíndola, Adrián Pérez-Cabrera, Hector Mayani. Mesenchymal stem cells in myelodysplastic syndromes: phenotypic and cytogenetic characterization. *Leukemia Research*. 2005; 29:215-224.
306. Dührsen U and DK Hossfeld. Stromal abnormalities in neoplastic bone marrow diseases. *Annals of Hematology*. 1996; 73:53-70.
307. Li Q, A Lau, TJ Morris, L Guo, CB Fordyce, EF Stanley. A Syntaxin 1, $G\alpha_o$, and N-Type Calcium Channel Complex at a Presynaptic Nerve Terminal: Analysis by Quantitative Immunocolocalization. *The Journal of Neuroscience*. 2004; 24:4070-4081.
308. Ramírez O, A Ggarcía, R Rojas, A Couve, S Härtel. Confined displacement algorithm determines true and random colocalization in fluorescence microscopy. *Journal of Microscopy*. 2009; 239:173–183.
309. Bolte S and F Cordelières. A guided tour into subcellular colocalization analysis in light microscopy. *Journal of Microscopy*. 2006; 224:213-232.
310. Chevallier N, F Anagnostou, S Zilber, G Bodivit, S Maurin, A Barrault, P Bierling, P Hernigou, P Layrolle and H Rouard. Osteoblastic differentiation of human mesenchymal stem cells with platelet lysate. *Biomaterials*. 2010; 31:270-278.
311. Cristofalo VJ, RG Allen, RJ Pignolo, BG Martin, and JC Beck. Relationship between donor age and the replicative lifespan of human cells in culture: a reevaluation. *The Proceedings of the National Academy of Sciences of the USA*. 1998; 95:10614-10619.
312. Nicolaas Franken APN, HM Rodermond, J Stap, J Haveman, and C van Bree. Clonogenic assay of cells *in vitro*. *Nature Protocols*. 2006; 1:2315-2319.

313. Agematsu K, Nakahori Y. Recipient origin of bone marrow-derived fibroblastic stromal cells during all periods following bone marrow transplantation in humans. *British Journal of Haematology*. 1991; 79:359-365.
314. Dexter TM, TD Allen, LG Lajtha. Conditions controlling the proliferation of haemopoietic stem cells *in vitro*. *Journal of Cellular Physiology*. 1977; 91:335-44.
315. William Bloom and Don W. Fawcett. A Textbook of Histology. Publisher: W. B. Saunders. 10th edition. 1975.
316. Soini Y, D Kamel, M Apaja-Sarkkinen, I Virtanen, V-P Lehto. Tenascin immunoreactivity in normal and pathological bone marrow. *Journal of Clinical Pathology*. 1993; 46:218-221.
317. Abdelkader Hamadi, Maya Bouali, Monique Dontenwill, Herrade Stoeckel, Kenneth Takeda, Philippe Ronde. Regulation of focal adhesion dynamics and disassembly by phosphorylation of FAK at tyrosine 397. *Journal of Cell Science*. 2005; 118:4415-4425.
318. David L Crowe and Arthur Ohannessian. Recruitment of focal adhesion kinase and paxillin to $\beta 1$ integrin promotes cancer cell migration via mitogen activated protein kinase activation. *BMC Cancer*. 2004; 4:1-8.
319. Valerie D. Roobrouck, Fernando Ulloa-Montoya, Catherine M. Verfaillie. Self-renewal and differentiation capacity of young and aged stem cells. *Experimental Cell Research*. 2008; 314:1937–1944.
320. Bartl R, Frisch B, Baumgart R. Morphologic classification of the myelodysplastic syndromes (MDS): combined utilization of bone marrow aspirates and trephine biopsies. *Leukemia Research*. 1992; 16:15–33.
321. Gottschling S, R Saffrich, A Seckinger, U Krause, K Horsch, K Miesala K, and AD Ho. Human mesenchymal stromal cells regulate initial self-renewing divisions of hematopoietic progenitor cells by a $\beta 1$ -integrin-dependent mechanism. *Stem Cells*. 2007; 25:798-806.
322. Varga Gergely, Kiss Judit, Várkonyi Judit, Vas Virág, Farkas Peter, Pálóczi Katalin, Uher Ferenc. Inappropriate Notch activity and limited mesenchymal stem cell plasticity in the bone marrow of patients with myelodysplastic syndromes. *Pathology Oncology Research*. 2007; 13:311-319.
323. Kumato M, Nishiwaki T, Matsuo N, Kimura H, Matsushima K, Minimal cultured bone marrow mesenchymal stem cells ameliorate fibrotic lung injury, *European Respiratory Journal*. 2009; 34:740-748.

324. Kern S, H Eichler, J Stoeve, H Klüter and K Bieback. Comparative analysis of mesenchymal stem cells from bone marrow, umbilical cord blood, or adipose tissue. *Stem Cells*. 2006; 24:1294-1301.
325. LeBoeuf F, F Houle, J Huot. Regulation of Vascular Endothelial Growth Factor Receptor 2-mediated phosphorylation of Focal Adhesion Kinase by Heat Shock Protein 90 and Src Kinase activities. *The Journal of Biological Chemistry*. 2004; 279:39175-39185.
326. Kasai M, J Guerrero-Santoro, R Friedman, ES Leman, RH Getzenberg, DB DeFranco. The Group 3 LIM Domain Protein Paxillin Potentiates Androgen Receptor Transactivation in Prostate Cancer Cell Lines 1. *Cancer Research*. 2003; 63:4927-4935.
327. Lim ST, D Mikolon, DG Stupack, D Schlaepfer. FERM Control of FAK Function: Implications for Cancer Therapy. *Cell Cycle*. 2008; 7:2306-2314.
328. Utsubo R, Y Sonoda, R Takahashi, S Iijima, E Aizu-Yokota, T Kasahara. Proteome Analysis of Focal Adhesion Kinase (FAK)-Overexpressing Cells. *Biological & Pharmaceutical Bulletin*. 2004; 27:1735-1741.
329. Michael EK, DW Dumbauld, KL Burns, SK Hanks, AJ García. Focal Adhesion Kinase Modulates Cell Adhesion Strengthening via Integrin Activation. *Molecular Biology of the Cell*. 2009; 20:2508–2519.
330. Priestley GV, LM Scott, T Ulyanova, T Papayannopoulou. Lack of $\alpha 4$ integrin expression in stem cells restricts competitive function and self-renewal activity. *Blood*. 2006; 107:2959-2967.
331. Scott ML, GV Priestley, T Papayannopoulou. Deletion of $\alpha 4$ Integrins from Adult Hematopoietic Cells Reveals Roles in Homeostasis, Regeneration, and Homing. *Molecular and Cellular Biology*. 2003; 23:9349–9360.
332. Wagner W, F Wein, C Roderburg, R Saffrich, A Diehlmann, V Eckstein, AD Ho. Adhesion of Human Hematopoietic Progenitor Cells to Mesenchymal Stromal Cells Involves CD44. *Cells Tissues Organs*. 2008; 188:160-169.
333. Christ O, U Günther, R Haas, M Zöller. Importance of CD44v7 isoforms for homing and seeding of hematopoietic progenitor cells. *Journal of Leukocyte Biology*. 2001; 69:343-352.
334. Rösel M, S Khaldoyanidi, V Zawadzki, M Zöller. Involvement of CD44 variant isoform v 10 in progenitor cell adhesion and maturation. *Experimental Hematology*. 1999; 27:698-711.
335. Tseng WP, CM Su, CH Tang. FAK activation is required for TNF-alpha-induced IL-6 production in myoblasts. *Journal of Cellular Physiology*. 2010; 223:389-396.

336. Halfon S, N Abramov, B Grinblat, and I Ginis. (2011). Markers distinguishing mesenchymal stem cells from fibroblasts are downregulated with passaging. *Stem cells and development*. 2011; 20:53-66.

ANNEXES

HSP90 is overexpressed in high-risk myelodysplastic syndromes and associated with higher expression and activation of FAK

-Leukemia Research-

- Vol. 33 (2009): S45-

This summary report is one of the first attempts proving our interest to identify new signalling pathways responsible for the survival of CD34⁺ blasts in high-risk MDS, and, which may contributes to the progression to leukemia. Among the analyzed proteins, FAK, HSP90 and Akt correlated with a poor prognosis, which raises the question whether HSP90 inhibitors (FAK and Akt being client-proteins for HSP90) could not be used as alternative therapy in MDS?

C023 HSP90 is overexpressed in high-risk myelodysplastic syndromes and associated with higher expression and activation of Fak

L. Campos^{1*}, F. Solly², C. Aanei³, P. Flandrin², D. Guyotat⁴. ¹Laboratoire Hématologie, CHU St. Etienne, France; ²Laboratoire Hématologie, France; ³Laboratoire Immunologie, Romania; ⁴Département Hématologie, ICL, France

*E-mail: lydia.campos@chu-st-etienne.fr

Myelodysplastic syndromes (MDS) are characterized by a high risk of evolution into acute myeloid leukaemia (AML). The pathogenesis of this evolution is still unclear. Some studies indicate that aberrant activation of survival signaling pathways is involved. The 90-kDa heat shock protein (HSP90) is implicated in the conformational maturation and stabilization of protein kinases and has key roles in signal transduction, protein folding, and protein degradation. HSP90 levels are increased in AML cells, and associated with resistance to chemotherapy induced apoptosis. HSP90 is involved in the formation of focal adhesions. Focal Adhesion Kinase (FAK), a non-receptor tyrosine kinase, is involved in the integrin-mediated signal transduction pathway. FAK was found over-expressed and constitutively activated in solid tumors. In AML, FAK expression is associated with enhanced blast migration and poor prognosis. FAK also exerts a potent antiapoptotic effect through adhesion to extracellular matrix and stromal cells. The aim of our study was to investigate the role of HSP90 in high-risk MDS and its potential role on focal adhesion. The expression of HSP90, pFAK, and pAkt was assessed by multicolor flow cytometry in bone marrow (BM) mononuclear cells (MNC) and CD34+ cells from 170 MDS at diagnosis: 93 refractory anemia with excess of blasts (RAEB), 54 refractory anemia (RA) and 23 chronic myelomonocytic leukemia (CMML).

The levels of HSP90 (mean percentage of positive cells 38.3), FAK (33.8%), phosphorylated FAK (31.4%), and phosphorylated Akt (26.7%) were significantly higher in MNC from RAEB patients than in those from RA (7.5%, 4.9%, 3.4% and 5.5% respectively) or CMML patients (22.1, 19.8, 17.2 and 15.8% respectively) ($p < 10^{-5}$).

The same difference was observed in CD34+ cells. Mean percent of positive cells in RAEB were 62.3% for HSP90, 68.2% for pFAK, 51.2% for pAkt versus 4.98, 4.6 and 4.62 respectively in RA, and 21%, 21.9 and 17.7% respectively in CMML, showing that the increased levels observed in MNC of RAEB was not only due to increased percentage of blasts. The effects of inhibition of HSP90 were evaluated in 25 RAEB samples by incubating cells with 17-AAG (5 μ M) for 24 hours in liquid culture. A down-regulation of HSP90, pFAK and pAKT was observed in CD34+ cells at 12 hours, followed by increased apoptosis at 24h as assessed by activated caspase 3 and annexin V expression.

Our results suggest that FAK, HSP90 and Akt activation are associated with cell survival and may contribute to the progression to leukemia. Moreover this signaling network could be a therapeutic target through HSP90 inhibition by 17-AAG.

C024 Association of NQO1 C609T polymorphism with chromosomes 5 and/or 7 abnormalities in patients with MDS/AML

C. Stavropoulou, S. Zachaki, K. Manola, G. Voutsinas, H. Orphanidou, V. Georgakakos, C. Sambani*. *NCSR Demokritos, Athens, Greece*

*E-mail: csambani@ipta.demokritos.gr

Introduction: Models for development of sporadic myelodysplastic syndromes (MDS) and acute myeloid leukemia (AML) suggest the role of cumulative genetic and toxic chemical factors in genetically predisposed individuals. The widely expressed detoxification enzyme NAD(P)H:quinone oxidoreductase 1 (NQO1) is involved in the cellular response to oxidative damage and irradiation protecting cells against mutagenicity from free radicals and toxic oxygen metabolites. NQO1 is subject to a genetic polymorphism (C609T) leading to a change in its amino acid sequence (Pro187Ser). Homozygotes for the mutant allele (T/T) completely lack NQO1 activity and heterozygotes (C/T) have low enzyme activity compared with wild type individuals (C/C). Therefore, the inactivating NQO1 polymorphism may predispose individuals to a greater risk of myeloid malignancies and/or promote specific types of chromosome changes.

Purpose: To investigate the potential role of NQO1 C609T inborn polymorphism in MDS pathogenesis, we studied the NQO1 genotypes on a large group of Greek MDS patients and controls. We focused on the frequency of NQO1 polymorphism in MDS/AML patients with abnormalities of chromosomes 5 and/or 7, since these represent recurrent aberrations that follow genotoxic exposures.

Methods: The incidence of NQO1 C609T polymorphism was examined in 261 MDS patients and 270 matched healthy controls using a PCR-RFLP assay. The NQO1 gene status was evaluated in respect to patient characteristics, chromosome abnormalities and IPSS cytogenetic classification. The NQO1 genotype was also investigated in 143 MDS/AML patients with -5/del(5q) and in 87 MDS/AML patients with chromosome 7 abnormalities. Cytogenetic analysis of bone marrow samples was performed at diagnosis in all groups of patients.

Results: The distribution of the NQO1 genotypes did not differ significantly between MDS patients and controls (homozygous wild type (C/C) 65.1 vs. 61.2%; heterozygotes (C/T) 33 vs. 37%; homozygous mutant (T/T) 1.9 vs. 1.8%). Stratification of patients according to gender, cytogenetic subgroups and IPSS classification revealed no

Flow cytometry-based quantification of cytokine levels in plasma and cell culture supernatants – study application of the bone marrow (BM) microenvironment in acute myeloid leukemia (AML)

- Rev. Med. Chir. Soc. Med. Nat., Iasi-

- Vol. 112(1) (2008): 196-202-

In this article, we bring compelling evidence that BM MSC from both, AML patients and healthy subjects, conferred a substantial beneficial effect on AML cells throughout the HPC-BM MSC co-culture system. Herein, we investigated the influence of BM MSCs on *in vitro* modulation of cytokine secretion (IL-1b, TNF-a, IL-10, IFN-g, IL-4, IL-5, and IL-2) by AML cells, as well as, the supportive capacity of soluble factors synthesized by BM MSCs on AML cells. Significant differences were observed between AML-BM MSC and normal-BM MSC with respect to IL1b secretion that was upregulated in AML cell cultures, both after 24 and 72 hours.

FLOW CYTOMETRY-BASED QUANTIFICATION OF CYTOKINE LEVELS IN AML PATIENTS PLASMA AND CELL CULTURE SUPERNATANTS

Angela Dăscălescu¹, Mihaela Zlei², Carmen Aanei¹,
Didona Ungureanu¹, Maria Tepeșu², Cristina Burcoveanu¹, C. Dănăilă¹
"Gr. T. Popa" University of Medicine and Pharmacy Iași

School of Medicine

¹ Department of Hematology

"Sf. Spiridon" University Hospital Iași

² Tumor Immunology Laboratory

FLOW CYTOMETRY-BASED QUANTIFICATION OF CYTOKINE LEVELS IN ACUTE MYELOBLASTIC LEUKEMIA (AML) PATIENTS PLASMA AND CELL CULTURE SUPERNATANTS (Abstract): **Aim**: Bone marrow stromal cells (BMSCs) have been found to support leukemic cell survival; however, the mechanisms responsible are far from being elucidated yet. The main aim of the current study is to identify particular cytokine/chemokine patterns of acute myeloid leukemia (AML) cells, and, on a longer term, to correlate them with the patient outcome and response to therapy. Therefore, the influence of BMSCs on *in vitro* modulation of cytokine secretion (IL-1 β , TNF- α , IL-10, IFN- γ , IL-4, IL-5, and IL-2) by AML cells as well as the AML cells supportive capacity of BMSCs-derived soluble factors was investigated. **MATERIAL AND METHODS**: With this purpose, we used an *in vitro* experimental model consisting in the evaluation of the effect of BMSC confluent layers-conditioning medium (BMSC-CM) on M4/5 AML cell cultures. **Results**: Our results show that BMSC-CM from both AML patients and healthy subjects conferred a substantial beneficial effect on AML cells throughout the culture ($p=0.0002$ and 0.0020 respectively at 24 hours and $p=0.0013$ and 0.0030 respectively at 72 hours), with a temporary increase in AML cell viability conferred by BM plasma from AML patients. Significant differences were observed with respect to IL1 b secretion which was upregulated in AML cell cultures both after 24 and 72 hours following the addition of AML-BMSC-CM, in contrast to control-BMSC-CM. **Conclusion**: Our results suggest the contribution of BMSCs from AML patients to the generation of particular factors which may be key players involved in the *in vivo* maintenance of the malignant clone. **Key words**: BONE MARROW STROMAL CELLS, CYTOKINES, ACUTE MYELOID LEUKEMIA

INTRODUCTION

Cytokines form a network that regulates proliferation and differentiation in various hematopoietic compartments (1). Cytokines are important regulators of acute myelogenous leukemia (AML) blast proliferation. For a subset of patients the AML blasts show constitutive cytokine secretion and can undergo autonomous proliferation *in vitro*, whereas for other patients the blasts are dependent on exogenous cytokines for proliferation. The capability of autocrine proliferation is an adverse prognostic factor in AML. The three cytokines, interleukin (IL)-4, IL-10 and IL-13 modulate *in vitro* blast proliferation, but the final effect of each cytokine (enhancement/inhibition/no effect) depends on differences between individual patients as well as the presence of other exogenous cytokines (2).

In one study, they observed that a high proliferative response to IL-1 beta in the cells of AML patients may indicate a poor prognosis (3). These growth factors are additionally involved in the control of immune modulation (IL-10, TGF- β), tumor neovascularization (IL-15, IL-18, VEGF) as well as prevention of apoptosis of tumor cells and stimulation of cell proliferation (IL-7, IL-10, IL-15) via autocrine or paracrine pathways (4,5). In addition to stromal cells, malignant cells, mainly B chronic lymphocytic leukemia (CLL) cells (6,7), leukemic blasts in acute myeloid leukemia (AML) (8) and lymphoma cells (9) have been shown to express a broad range of cytokines, i.e. IL-1a, IL-1b, IL-6, IL-7, IL-8, IL-13, IL-15, IFN- γ , TNF- α , G-CSF, TGF- β 1 and GM-CSF.

The hypothesis behind our project is that the origin of the leukemic defect may be clarified only through the understanding of the composition of the malignant microenvironment, its relationship with the pathogeny of the disease and how the host, 'normal', non-leukemic cells interact with the leukemic ones.

Evaluation in comparative fashion of the interactions between primary AML cells from M4/5 AML patients with the tumor niches accessory cells and molecules may offer a basis for the identification of biological and clinical patterns of the tumor.

MATERIAL AND METHODS

BMSCs. BM aspirates from M4/5 AML patients (n=4) and healthy volunteers (n=3) were cultured at 37°C and 5% CO₂ in 75 cm² flasks (Nunc, Denmark) using RPMI medium (Sigma) and 10% Foetal bovine serum (FBS, Sigma). Confluent stroma layers were generated within 4 to 8 weeks. At the time of confluence, conditioning medium (BMSCS-CM) was collected, centrifuged and filtered and stroma cells were detached from the culture flasks using 0,25% trypsin-ethylenediamine tetraacetic acid (Sigma) and viably frozen for later use.

Primary AML cells. BM aspirates with around 90% leukemic cell infiltration were obtained from M4/5 AML patients at initial diagnosis (n =8). AML blast fraction was enriched in all samples, by density gradient centrifugation (Ficol, Sigma) according to manufacturer's

instructions. 5×10^5 AML cells/mL/well were cultured in 24-well plates; culture medium consisted of RPMI-1640 with 10% FBS (standard culture conditions) with or without 20% BMSC-CM or BM plasma from M4/5 AML patients/ healthy controls.

Measurement of cell viability. 24 and 72 hours following BMSC-CM or BM plasma addition AML percentages of viable AML cells were calculated by flow-cytometry (FACSCalibur machine, Becton Dickinson, CellQuest software), using a gating strategy on CD45 (monoclonal antibody anti-human CD45-FITC, BD), HLA/DR (monoclonal antibody anti-human HLA/DR-PE, BD) double positive/Propidium iodide (PI) negative cells. Control cultures consisted of confluent layers of BMSCs, on one hand, and of AML cell cultures without BMSC-CM or plasma (standard culture conditions), on the other, were comparatively assessed.

Measurement of cytokine production in the culture supernatant. The level of the following 7 cytokines was evaluated in the culture supernatant at both culture time points (24 and 72 hours): IL-1b (by ELISA, Quantikine, R&D Systems) and TNF-a, IL-10, IFN-g, IL-4, IL-5, IL-2 (by flow cytometry, BD™ Cytometric, a FACS-based cytokine array kit using capture beads and fluorescent conjugated detection antibodies). 56 duplicated experiments were performed in total, representing co-cultures of AML cells with BMSC-CM or BM-plasma from AML patients or BMSC-CM from healthy controls.

RESULTS AND DISCUSSIONS

The assessment of BMSC-CM on AML cell viability. The comparative analysis of AML cell viability in different culture conditions: standard (RPMI+10% FBS), AML-BMSC-CM (20%), control-BMSC-CM (20%) and AML-BM-plasma (20%) has been carried out by calculation of propidium iodure (PI) negative (viable) cell fraction by flow cytometry (Fig. 1). Although the patients inclusion into the study group was carried out on the criterion of more than 90% BM infiltration with AML cells, the mononuclear cell fraction separated by density gradient centrifugation also contained small proportions of lymphocytes and erythrocytes (Fig.1).

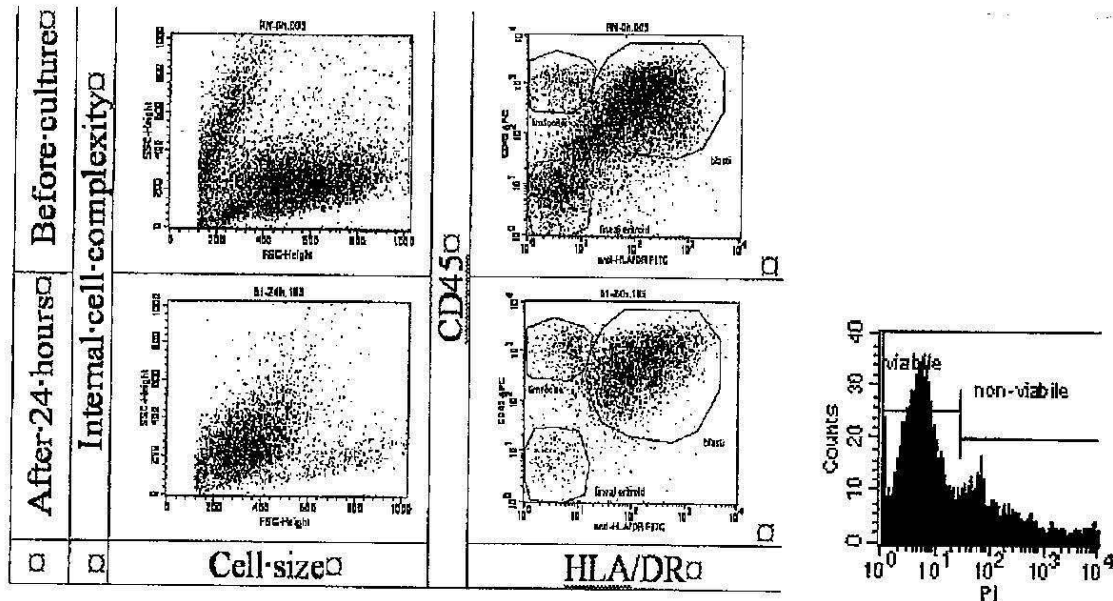


Fig. 1. The gating strategy used for the evaluation of the viability of AML cells (flow cytometry, FACSCalibur, CellQuest software, Becton Dickinson)

Therefore, we consider to use a gating strategy which allowed us to focus the analysis of PI expression within the cell population of interest. As leukemic cells in M4/5 AML are heterogeneous with respect to their expression of particular markers (CD14, CD64, CD4, CD34, CD117), the interest gate was design to contain CD45 (intermediate expression) HLA/DR double positive cells. Of note, the proportion between the mention cell populations within the AML specimens was preserved during culture progress (Fig. 1)

Soluble factors released by BMSC cultures from both AML patients (AML-BMSC-CM) and healthy subjects (control-BMSC-CM) conferred a significant higher viability to AML cells when compared to standard culture conditions, at both 24 h ($p=0.0002$ and 0.0020 respectively) and 72 hours ($p=0.0013$ and 0.0030 respectively) (Fig. 2). At 72 hours, both types of BMSC-CM proved to have a superior supportive effect when compared to BM-AML-plasma ($p=0.0059$ and 0.007 respectively). There were no significant differences between AML-BMSC-CM and control-BMSC-CM at either time point assessed. Bone marrow plasma from AML patients (AML-BM-plasma) had a significant supportive effect only in the first 24 hours ($p=0.0056$). The limited efficiency of BM plasma from AML patients in preserving AML cell viability reflects a stroma-dependent phenomenon, which are specific to the BM microenvironment. This context suggests *in vivo* events.

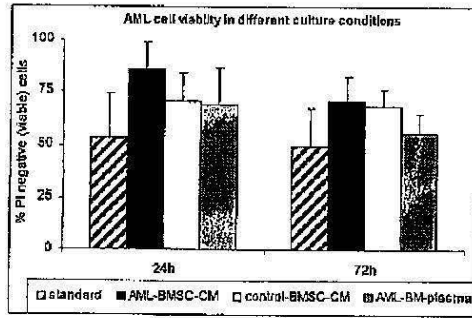


Fig. 2. The comparison of *in vitro* AML cell viability upon different culture conditions.

Assessment of the cytokine profile within BM plasma of AML patients. Recently developed human cytokine array kits combine the individual assets of flow cytometry and solid phase (microbeads)-cytokine capturing systems in order to detect multiple plasma cytokines simultaneously. We used such a system to evaluate the presence and quantity of 6 different cytokines in the plasma of 4 patients with M4/5 AML that were not on active therapy. BM plasma from 8 M4/5 AML patients was additionally assessed for the presence and concentration of IL1 b by ELISA (Quantikine, R&D Systems). The detectable plasma levels of the tested cytokines were very low, with a slightly higher production of IL-10 (Fig. 3).

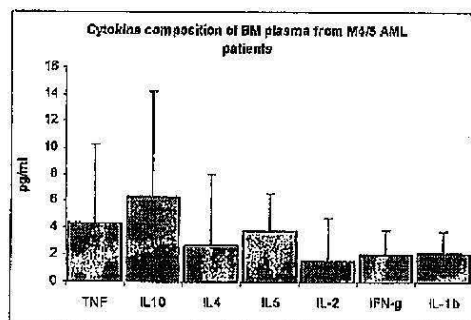


Fig. 3. Cytokine composition of BM plasma from M4/5 AML patients (n=8 for IL1b and n=4 for the others)

IL-10 production is known to be restricted to cells within the hematopoietic lineage. There are no data on IL-10R expression on AML cells, however, it has been shown by others that IL-10 stimulates cancer cell proliferation through secondary signals via oncostatin M and IL-11 (10). Our finding, alongside with the known contribution of IL-10 to inducing a state of immune tolerance against tumors (by suppressing function and differentiation ability of DCs) suggest that IL-10 production may be a key event within the BM microenvironment in AML (11). However, its level in the BM plasma of the tested patient was not significant.

The assessment cytokine production in the culture supernatant. We evaluated 7 cytokines levels in AML patients culture supernatants (CM1): IL-1b (ELISA, Quantikine, R&D Systems) and TNF-a, IL-10, IFN-g, IL-4, IL-5, IL-2 (flow cytometry, BD CBA Cytokine Detection kit, Becton Dickinson). More, we measured IL1b level in healthy subjects culture

supernatants (CM1 and CM2). We found very low cytokines levels in culture supernatants (Fig 4 a) but, with high level of IL-1b in CM1 up to 130 pg/ml (Fig 4b). In healthy subjects culture supernatants (CM2) we note significantly low levels than patients culture supernatants (CM1).

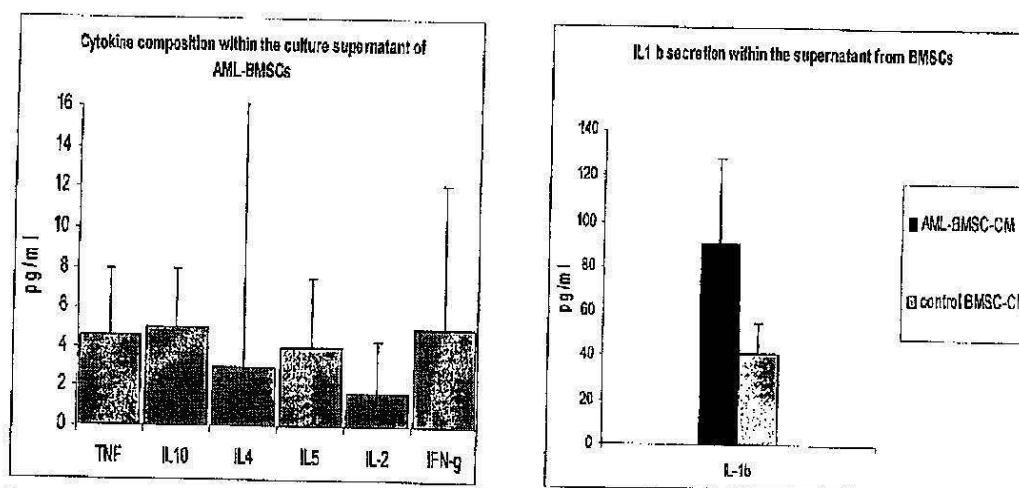


Fig. 4. a. Cytokine composition of the culture supernatant (conditioning medium, CM) of BMSC from M4/M5 AML patients (AML BMSC CM) and healthy subjects (control BMSCs CM) b. IL-1b secretion within the supernatants from AML- BMSC CM and control BMSCs CM.

The comparative analysis of the cytokine expression levels in the BM plasma from M4/M5 AML patients, in the culture supernatant from BMSC of AML patients and healthy subjects and in the culture supernatants of AML cells with or without the influence of stroma, revealed the following facts: with the exception of IL-1b, none of the assessed cytokine was elevated within the mixed cultures (Fig. 5 a to f). On the contrary, it seems that at least in the case of TNF α (Fig 5a), and, to a lesser extent, IL-10 (Fig 5b) a slight decrease of their levels has been observed. Significant differences were noted in the case of IL-1b within the mixed cultures of AML cells with AML-BMSC-CM, both at 24 hours and 72 hours (Fig 5g). Of note was the absence of this phenomenon in the presence of control BMSC-CM, which suggests the contribution of BMSCs from AML patients to the generation of particular factors which may be key players involved in the *in vivo* maintenance of the malignant clone. In order to confirm the current results the level of IL-1b needs to be assessed on extended study groups.

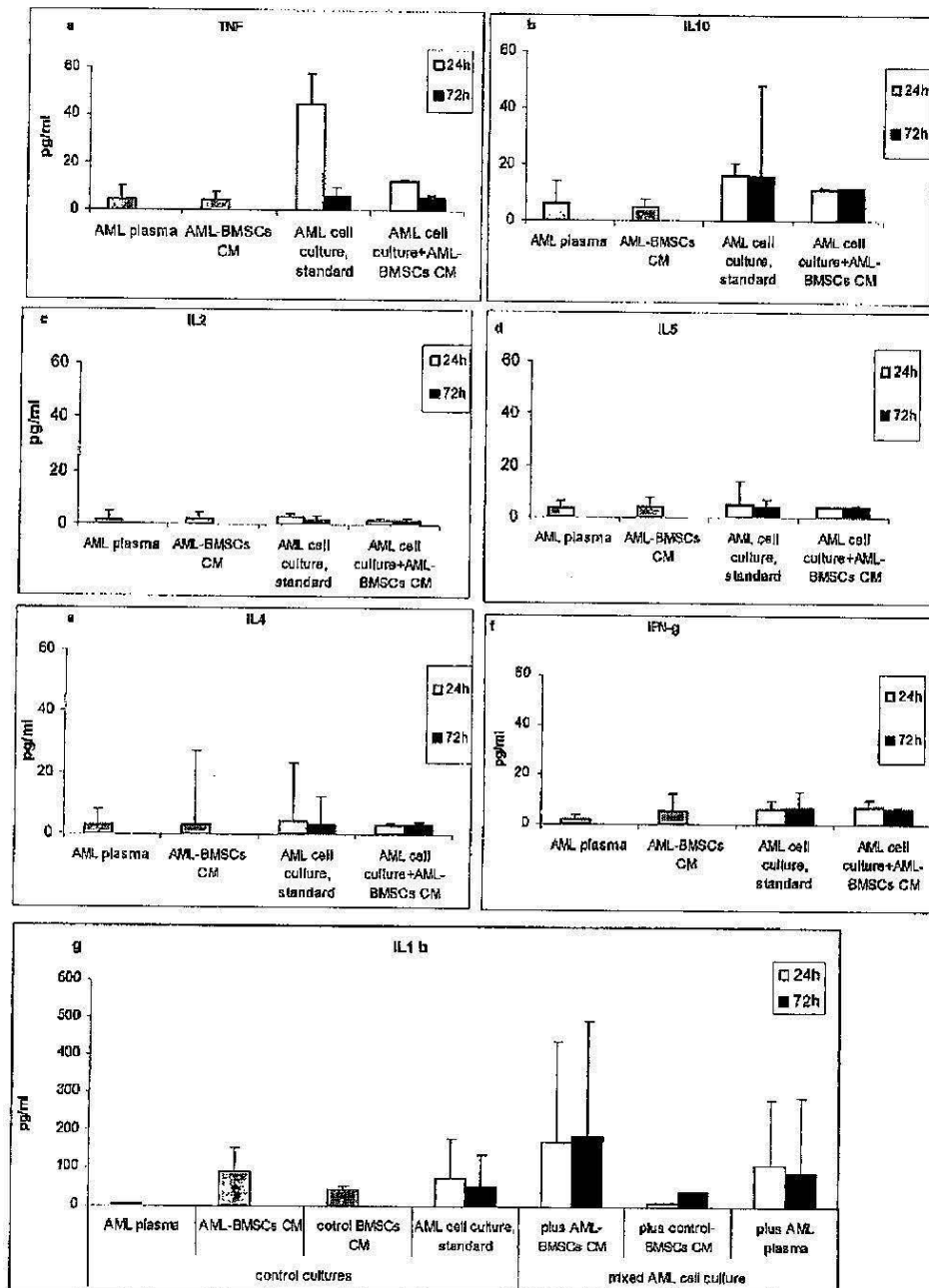


Fig 5. Cytokine expression levels in plasma and culture supernatants of patients stromal cells (CM1), healthy subjects stromal cells (CM2), leukemia cells in standard conditions (RPMI+10%FCS) and in mixed culture (with CM1 or CM2)

CONCLUSIONS

Particularities in the cytokine network may be directly involved in many types of leukemia and autocrine and paracrine activities by leukemic and normal cells represent largely the mechanisms of survival for these cells. Therefore, a successful therapy for leukemia should deprive leukemic cells of the cytokine(s) necessary for their survival with minimal effect on normal cells. Such treatment may be difficult in vivo because (i) many cell types in the body may produce any type of cytokine(s), (ii) the cytokine(s) produced is/are likely to be

necessary for growth and function of normal hematopoietic cells, and (iii) malignant cells survival may not be strictly depending on one specific cytokine. Therefore, a successful therapeutic approach should determine the cytokines that are necessary for the initiation or progression of a given disease. Consequently, the therapeutic combination, which results in maximum cytotoxicity to leukemic cells and minimal effect on normal cells, may be, on a long term, determined.

AKNOWLEDGMENTS

This study was performed by support of CNCSIS grants program 1149/2007.

REFERENCES

1. Moqattash S, Lutton J. Leukemia Cells and the Cytokine Network: Therapeutic Prospects. *Exp Biol Med* 2004; 229:121-137.
2. Bruserud O. IL-4, IL-10 and IL-13 in acute myelogenous leukemia. *Cytokines Cell Mol Ther* 1998 Sep;4 (3):187-98.
3. Ezaki K, Tsuzuki M, Katsuta I. Interleukin-1 beta (IL-1 beta) and acute leukemia: in vitro proliferative response to IL-1 beta, IL-1 beta content of leukemic cells and treatment outcome. *Leuk Res* 1995 Jan; 19(1): 35-41.
4. Wu S, Korte A, Kebelmann-Betzing C, Gessner R, Henze G, Seeger K. Interaction of bone marrow stromal cells with lymphoblasts and effects of prednisolone on cytokine expression. *Leuk Res* 2005; 29: 63-72.
5. Manakova TE, Tsvetaeva NV, Levina AA, Momotyuk KS, Sarkisyan GP, Khoroshko ND, Gerasimova LP. In vivo production of cytokines by BM stromal cells and macrophages from patients with myelodysplastic syndrome. *Bull Exp Biol Med* 2001;132(1):633-6.
6. Ghia P, Granziero L, Chilosi M, Caligaris-Cappio F. Chronic B cell malignancies and bone marrow microenvironment. *Semin Cancer Biol* 2002; 12: 149-155.
7. Ghia P, Caligaris-Cappio F. The indispensable role of microenvironment in the natural history of low-grade B cell neoplasms. *Adv Cancer Res* 2000 ; 79:157-173.
8. de Bont ES, Vellenga E, Molema G, van Wering E, de Leij LF, Kamps WA. A possible role for spontaneous interleukin-8 production by acute myeloid leukemic cells in angiogenesis related processes: work in progress. *Med Pediatr Oncol* 2001 Dec;37(6):511-7.
9. Benjamin D, Knobloch TJ, Dayton MA. Human B-cell interleukin-10 B-cell lines derived from patients with acquired immunodeficiency syndrome and Burkitt's lymphoma constitutively secrete large quantities of interleukin-10. *Blood* 1992;80:1289-98. 72 S.

10. Buggins AG, Milojkovic D, Arno MJ et al. Microenvironment Produced by Acute Myeloid Leukemia Cells Prevents T Cell Activation and Proliferation by Inhibition of NF- κ B, c-Myc and pRb Pathways. *J Immunol* 2001, 167: 6021-6030
11. Kiertscher SM, Luo J, Dubinett SM, Roth MD. Tumors Promote Altered Maturation and Early Apoptosis of Monocyte-Derived Dendritic Cells. *J Immunol* 2000, 164: 1269-1276

**Congenital Acute Leukemia with Initial Indolent Presentation—
A Case Report**

- Cytometry B Clinical Cytometry-

- Vol. 80(2) (2011):130-133-

In this brief communication, we present a case report of a congenital acute leukemia at a child. This entity is a challenge in terms of diagnosis, disease monitoring, and therapeutic decisions due of scarcity of the literature data, and due their unpredictable evolution, occasionally even to spontaneous remission.

In this case, we noticed a blast population without lineage assignment, expressing CD123 (hIL-3-R), normal karyotype, and displaying a resistant phenotype at conventional chemotherapy and to the gemtuzumab ozogamicin therapy. The allogeneic cord blood cell transplantation allowed the achievement of cytological and immunocytometric complete remission.

Brief Communication: Case Report

Congenital Acute Leukemia with Initial Indolent Presentation—A Case Report

Lydia Campos,^{1*} Nathalie Nadal,¹ Pascale Flandrin-Gresta,¹ Christian Vasselon,¹ Carmen Aanei,¹ Claire Berger,² and Jean Louis Stephan²

¹Laboratoire d'Hématologie, Hôpital Nord, Centre Hospitalier Universitaire, Saint Etienne, France

²Service d'Oncologie Pédiatrique, Institut de Cancérologie de la Loire, Saint Priest en Jarez, France

Background: Congenital acute leukemia is a rare event, presenting usually as an aggressive disease with a poor prognosis. A differential diagnosis is the transient myeloproliferative disorder observed in Down syndrome. We describe the case of an apparently healthy newborn male child presenting with normal peripheral blood (PB) counts but with a blast population on differentials. The child's condition and the blast population remained unchanged during the first year of life.

Methods: Bone marrow and PB were morphologically analyzed. Multiparametric flow cytometry was performed at the time of diagnosis and repeated at 1 year. These studies were completed by cytogenetic and molecular analyses.

Results: Bone marrow contained 40% of undifferentiated blasts. Multiparametric flow cytometry showed low expression of CD38, HLA-DR, and CD33 markers. All other markers were negative. Constitutional and blast cell karyotypes were normal. Fluorescence *in situ* hybridization analysis showed no rearrangement. Molecular studies were negative. The blast percentage remained stable during several months. After 1 year, the PB counts showed thrombocytopenia, with an increase of blast cells exhibiting the same phenotype. Clinically, an enlarged spleen was found. The child did not respond to chemotherapy and only partially to gemtuzumab ozogamicin. A cord blood cell transplantation was finally performed. With a follow-up of 12 months, the child is doing well.

Conclusions: To our knowledge, this is the first case of congenital acute leukemia with initially indolent course in a newborn without Down syndrome. This observation emphasizes the importance of a careful follow-up. © 2010 International Clinical Cytometry Society

Key terms: congenital acute leukemia; transient myeloproliferative disorder; cord blood transplantation

How to cite this article: Campos L, Nadal N, Flandrin-Gresta P, Vasselon C, Aanei C, Berger C, Stephan J.L. Congenital acute leukemia with initial indolent presentation—A case report. *Cytometry Part B* 2010; 00B: 000–000.

Although acute leukemia is the most common malignancy in childhood, congenital acute leukemia (CAL), manifesting within the first weeks of life, is a rare disease. Its frequency is less than 1% of all pediatric leukemias. Acute leukemia is derived from an abnormal immature hematopoietic precursor cell that has the capacity to expand and, nevertheless, shows characteristics of limited differentiation. Thus, acute myeloid leukemias (AMLs) retain many of the molecular and cellular phenotypic characteristics of their normal hematopoietic counterparts.

CAL is a rare event, and, even though a few cases with spontaneous remission have been described (1), the prognosis is generally very poor. The literature on

CAL is rather limited, most publications being single case reports. Bresters et al. (1), reviewed 117 CAL cases and showed that they differ from leukemia in older children because they are more often of the myeloid lineage and have a worse prognosis. Moreover, congenital acute lymphoblastic leukemia (ALL) constitutes a clinically and

*Correspondence to: Lydia Campos, Laboratoire d'Hématologie, Hôpital Nord, Centre Hospitalier Universitaire, 42055 Saint Etienne, France. E-mail: lydia.campos@chu-st-etienne.fr

Received 9 June 2010; Revision 29 September 2010; Accepted 30 September 2010

Published online in Wiley Online Library (wileyonlinelibrary.com). DOI: 10.1002/cyto.b.20578

biologically distinct entity from ALL diagnosed in older children (2). Van der Linden et al. (3) recently reported on a series of 30 patients with congenital ALL uniformly treated. They concluded that congenital ALL should be treated in a curative intent. However, the poor outcome makes it appropriate to test newer approaches to achieve higher remission rates and longer disease-free survival.

Extensive investigations are needed to distinguish between congenital AML and transient myeloproliferative disorder (TMD). TMD is a leukemia-like syndrome described in 10% of newborns with Down syndrome (DS). Leukocytosis and thrombocytopenia are common. TMD blasts typically express platelet-specific surface markers. It remains a poorly understood entity, and the frequency might be underestimated because it can occur in asymptomatic neonates and because blood counts are not routinely performed in newborns with DS (4). This condition resolves without treatment in most cases within 3–6 months after birth. However, 20–30% of these children subsequently develop acute megakaryoblastic leukemia usually in the first 4 years of life. The differential diagnosis with CAL can be a real challenge because TMD has been described in a few non-DS infants with clonal trisomy 21 limited to hematopoietic lineage (5).

To our knowledge, we present the first case of congenital acute undifferentiated leukemia in a full-term male newborn without DS. A fortuitous peripheral blood count (PBC) revealed a white blood cell count of $25 \times 10^9 \text{ L}^{-1}$ (normal between 7 and $26 \times 10^9 \text{ L}^{-1}$) with 17% blasts, a platelet count of $135 \times 10^9 \text{ L}^{-1}$ ($n = 150$ – 400), and a hemoglobin level of 185 g/L ($n = 160$ – 200). Physical examination showed no particularities. The bone marrow (BM) aspiration revealed 40% large blasts with high nucleocytoplasmic ratio, which were morphologically undifferentiated. Particularly, no features of megakaryoblastic differentiation were observed. Cytochemical stains (myeloperoxidase and esterases) were negative in blast cells. Nonblast cells were morphologically normal.

Multiparametric flow cytometry was performed on erythrocyte-lysed whole BM at the time of the diagnosis (Fig. 1). Using a CD45 gating strategy the blast gate represented 22% of cells. Blast cells were CD34 and CD123 (IL3RA, membrane low affinity receptor)-positive. A minor subset (10–15%) of blasts expressed the following surface markers: HLA-DR, CD33^{low}, CD65^{low}, CD38^{low}, and CD4^{low}. Other immaturity-related antigens (CD117 and CD133) were lacking. Lineage markers such as CD2, CD3, CD5, and CD7 for T-lymphoid lineage, CD19, CD22, and CD20 for B-lymphoid lineage, CD11b, CD13, CD15, CD16, and MPO for granulocytic lineage, CD14, CD36, and CD64, for monocytic lineage, and CD61 for megakaryocytic lineage were negative. CD56 (N-CAM) was also negative.

Cytogenetic analyses showed a normal male karyotype (46,XY) in all 40 metaphases. Fluorescence *in situ* hybridization analyses using *MLL* split signal and *LSI ETO/AML* probes showed no rearrangement at bands

11q23, 8q22, and 21q22. The molecular analyses by real-time polymerase chain reaction to test for *BCR-ABL*, *AML/ETO*, *CBFB/MYH11* fusion genes, and *FLT3-ITD* and *NPM1* mutations were negative.

At this time, the child was not treated because he had no clinical manifestations. A follow-up was instituted, and repeated blood counts and BM examinations were performed. After 4 months, the blast count decreased in peripheral blood to 5% and remained stable over the next 6 months. At 1 year of age, the child presented with splenomegaly. PBC showed thrombocytopenia ($40 \times 10^9 \text{ L}^{-1}$) and 5% blasts. The BM aspiration revealed the presence of 29% blasts. Immunophenotypic studies showed blast cells expressing the same markers as found at birth. In addition, CD41 and CD42 were assessed and were negative. Cytogenetic and molecular analyses were still normal. The patient was treated with cytarabine, mitoxantrone, and ansacrine according to the standard AML protocol, ELAM 02. Remission was not obtained after two induction courses. At day 40, BM phenotyping showed the persistence of 14% CD45^{dim} cells and 2.5% blast cells exhibiting the phenotype described at diagnosis. A rescue treatment was started with gemtuzumab ozogamicin (chaliceamycin-conjugated anti-CD33 monoclonal antibody) and cytarabine. Cytological complete remission finally occurred, but immunophenotypic studies showed the persistence of 1.2% blasts. The child underwent allogeneic cord blood cell transplantation. With a follow-up of 12 months, the child is well and with no evidence of disease, as seen by flow cytometry analysis.

The course of this disease is rather unusual. Typically, CAL presents as an aggressive disorder manifesting within the first 4 weeks of life and with a high leukemic cell load. However, a limited number of spontaneous remissions have been described (1). In our case, physical symptoms did not appear before 1 year of age, and the diagnosis would not have been done at birth if a PBC had not been performed. The possibility of TMD was, therefore, raised, but the diagnosis was ruled out because the infant presented neither constitutional trisomy 21 nor acquired trisomy 21 in the blast cells. In addition, megakaryocytic markers were negative and blasts never disappeared.

This case was difficult to diagnose because immunophenotyping did not show a lineage assignment. Although two myeloid markers were weakly positive (CD33 and CD65), this case was considered myeloid-negative (score < 2 based on the system of the European Group for the Immunological Characterization of Leukemias) (6). Morphological aspect and lack of CD56 also ruled out dendritic cell leukemia. An aberrant CD13–CD33+ pattern and a variable expression of CD34 are frequently encountered in AML with minimal maturation (7). Venditti et al. (8) compared the immunophenotypic and karyotypic features of 25 cases of minimally differentiated acute myeloid (AML-M0) with those of 247 cases, including all other French-American-British subtypes. AML-M0 expressed more frequently low levels

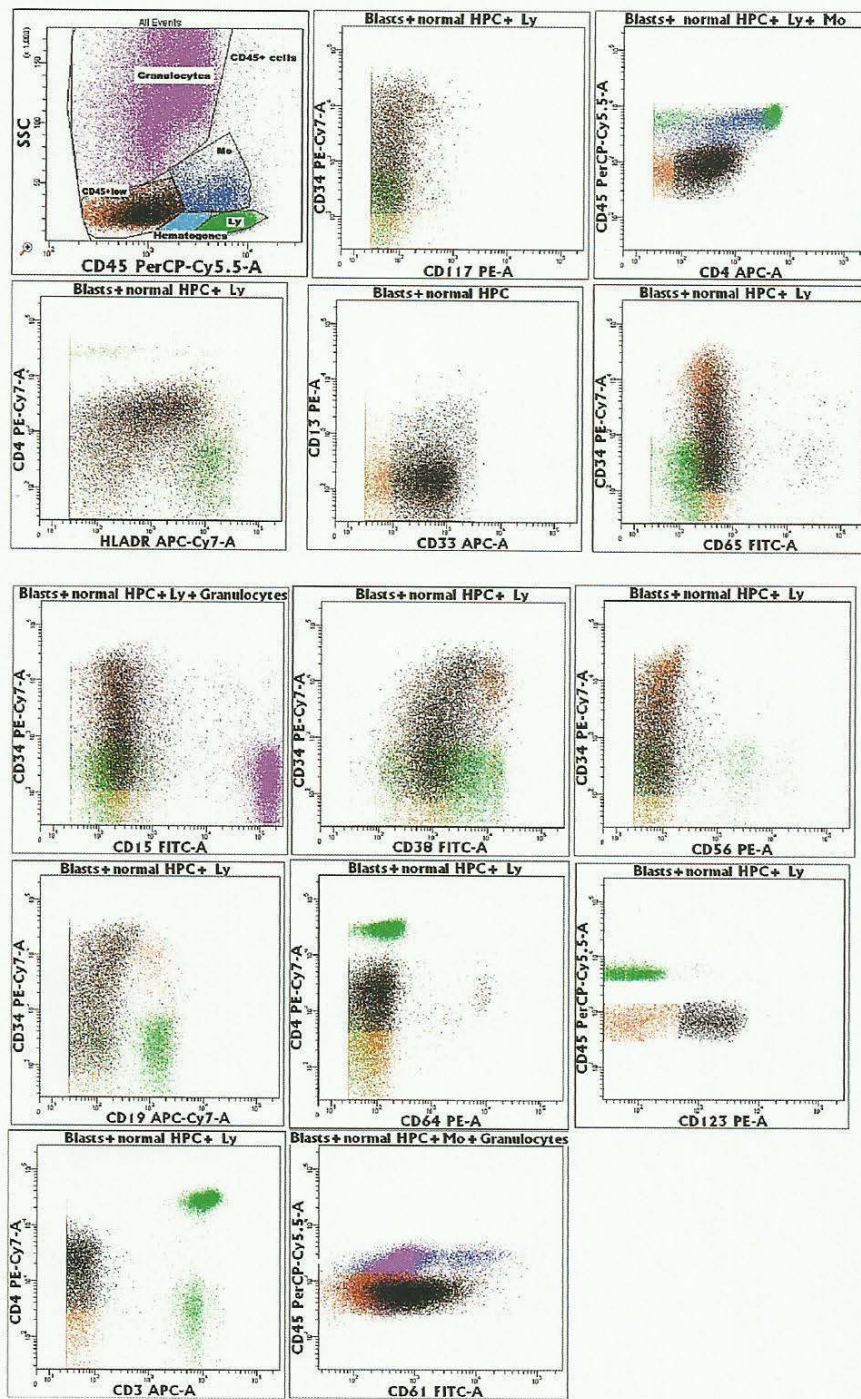


Fig. 1. FCM acquisition was performed with a Canto II cytometer, and the data analysis with Diva software 6.2.1. CD45-side scatter (SSC) gating is displayed. Gating is based on the expression of CD45 in combination with the SSC (left) (a), which allows a clear separation of CD45^{low} cells (orange) and pathological blasts (black) from lymphocytes (green), lymphoid precursors (turquoise), monocytes (blue), and granulocytes (pink). The pathological blast gate (b–n) was drawn around the CD34⁺ CD4^{low} cells cluster. Blast gate shows the following markers: CD34^{variable}, HLA-DR, CD33^{low}, CD65^{low}, CD38^{low}, and CD4^{low}. HPC, hematopoietic precursor cells; Ly, lymphocytes, Mo, monocytes.

of CD4. The CD2, CD5, CD10, and CD19 markers were similarly expressed in all AML types.

This observation emphasizes that CAL is not always associated with aggressive presentation. Postponing treatment in the absence of clinical symptoms may give time to differentiate leukemoid reaction or TMD from CAL, or even to observe a spontaneous remission. In this setting, a careful monitoring for disease progression, including flow cytometry analysis, is mandatory.

LITERATURE CITED

1. Bresters D, Reus ACW, Veerman AJP, Van Wering ER, Van Der Does-Van Den Berg A, Kaspers GJL. Congenital leukemia: The Dutch experience and review of the literature. *Br J Haematol* 2002;117:513-524.
2. Sande JE, Arceci RJ, Lampkin BC. Congenital and neonatal leukemias. *Semin Perinatol* 1999;23:274-285.
3. Van der Linden MH, Valsecchi MG, De Lorenzo P, Mörcke A, Janka G, Leblanc TM, Felice M, Biondi A, Campbell M, Hann I, Rubnitz JE, Stary J, Szczepanski T, Vora A, Ferster A, Hovi L, Silverman LB, Pieters R. Outcome of congenital acute lymphoblastic leukemia treated on the Interfant-99 protocol. *Blood* 2009;114:3764-3768.
4. Roy A, Roberts I, Norton A, Vyas P. Acute megakaryoblastic leukaemia (AMKL) and transient myeloproliferative disorder (TMD) in Down syndrome: A multi-step model of myeloid leukaemogenesis. *Br J Haematol* 2009;117:3-12.
5. Apollonsky N, Shende A, Ouansafi I, Brody J, Atlas M, Aygun B. Transient myeloproliferative disorder in neonates with and without Down syndrome. A tale of 2 syndromes. *J Pediatr Hematol Oncol* 2008;30:860-864.
6. Béné MC, Castoldi G, Krapp W, Ludwig WD, Matutes E, Orfao A, van't Veer MB. Proposals for the immunological classification of acute leukemias (EGIL). *Leukemia* 1995;9:1783-1786.
7. Nguyen D, Diamond LW, Braylan RC. *Flow Cytometry in Hematopathology: A Visual Approach to Data Analysis and Interpretation*. Totowa, NJ: Humana Press, 2003; pp 48-189.
8. Venditti A, Del Poeta G, Buccisano F, Tamburini A, Cox MA, Stasi R, Bruno A, Aronica G, Maffei L, Sappo G, Maria Simone MD, Forte L, Cordero V, Postorino M, Tufilli V, Isacchi G, Masti M, Papa G, Amadori S. Minimally differentiated acute myeloid leukemia (AML-M0): Comparison of 25 cases with other French American-British subtypes. *Blood* 1997;89:621-629.